

**MIMO-OFDM CHANNEL AND CARRIER FREQUENCY  
OFFSET ESTIMATION FOR MOBILE  
BROADBAND ACCESS**

**Nattaphat Promsuwanna**

**A Thesis Submitted in Partial Fulfillment of the Requirements for the  
Degree of Doctor of Philosophy in Telecommunication Engineering**

**Suranaree University of Technology**

**Academic Year 2012**

การประมาณช่องสัญญาณและค่าออฟเซตความถี่คลื่นพาห์ของ  
MIMO-OFDM สำหรับการเข้าถึงแถบกว้างเคลื่อนที่

นายณัฐพัชร์ พรหมสุวรรณ

วิทยานิพนธ์นี้เป็นส่วนหนึ่งของการศึกษาตามหลักสูตรปริญญาวิศวกรรมศาสตรดุษฎีบัณฑิต  
สาขาวิชาวิศวกรรมโทรคมนาคม  
มหาวิทยาลัยเทคโนโลยีสุรนารี  
ปีการศึกษา 2555

# MIMO-OFDM CHANNEL AND CARRIER FREQUENCY OFFSET ESTIMATION FOR MOBILE BROADBAND ACCESS

Suranaree University of Technology has approved this thesis submitted in partial fulfillment of the requirements for the Degree of Doctor of Philosophy.

Thesis Examining Committee

---

(Asst. Prof. Dr. Somsak Vanit-Anunchai)

Chairperson

---

(Asst. Prof. Dr. Peerapong Uthansakul)

Member (Thesis Advisor)

---

(Asst. Prof. Dr. Monthippa Uthansakul)

Member

---

(Asst. Prof. Dr. Chanchai Thaijiam)

Member

---

(Dr. Dheerasak Anantakul)

Member

---

(Prof. Dr. Sukit Limpijumnong)

Vice Rector for Academic Affairs

---

(Assoc. Prof. Flt. Lt. Dr. Kontorn Chamniprasart)

Dean of Institute of Engineering

ณัฐพัชร พรหมสุวรรณ : การประมาณช่องสัญญาณและค่าออฟเซตความถี่คลื่นพาห်ของ MIMO-OFDM สำหรับการเข้าถึงแถบกว้างเคลื่อนที่ (MIMO-OFDM CHANNEL AND CARRIER FREQUENCY OFFSET ESTIMATION FOR MOBILE BROADBAND ACCESS) อาจารย์ที่ปรึกษา : ผู้ช่วยศาสตราจารย์ ดร.พีระพงษ์ อุฑารสกุล, 153 หน้า.

การรวมกันระหว่างโมโม่และ OFDM ได้ถูกพิจารณาว่าเป็นวิธีการแห่งความหวังสำหรับการสื่อสารไร้สายในอนาคต อย่างไรก็ตาม ประสิทธิภาพของ MIMO-OFDM มีความอ่อนไหวต่อออฟเซตความถี่คลื่นพาห်ได้ง่าย โดยที่ค่าออฟเซตความถี่คลื่นพาห်ทำให้เกิดการแทรกสอดระหว่างคลื่นพาห် ดังนั้นค่าออฟเซตความถี่คลื่นพาห်จึงควรถูกทำการประมาณและทำการชดเชย ในช่องสัญญาณแถบกว้างเคลื่อนที่นั้น ช่องสัญญาณและออฟเซตความถี่คลื่นพาห်มีรูปแบบเป็นเปลี่ยนแปลงตามเวลาอันเนื่องจากการเคลื่อนที่และสภาพแวดล้อมรอบๆการสื่อสาร ดังนั้น ช่องสัญญาณและค่าออฟเซตความถี่คลื่นพาห်จึงควรถูกติดตามเพื่อรักษาประสิทธิภาพของระบบ โดยวิทยานิพนธ์นี้เสนอรูปแบบของสัญญาณนำที่ถูกแทรกในการส่งข้อมูลเพื่อติดตามความเปลี่ยนแปลงของช่องสัญญาณและออฟเซตความถี่คลื่นพาห်ในระบบ MIMO-OFDM โดยรูปแบบของสัญญาณนำสำหรับการประมาณค่าออฟเซตความถี่คลื่นพาห်ที่ออกแบบนั้นมีพื้นฐานมาจากวิธีการแทรกคลื่นพาห်ย่อยที่เป็นศูนย์ แต่ให้ประสิทธิภาพการประมาณเหนือกว่าอันเนื่องจากการเพิ่มขึ้นของอัตราส่วนระหว่างกำลังของสัญญาณต่อสัญญาณรบกวน นอกจากนี้ การประมาณโดยรูปแบบของสัญญาณนำที่ได้ออกแบบสามารถติดตามความเปลี่ยนแปลงของช่องสัญญาณและค่าออฟเซตความถี่คลื่นพาห်ได้โดยใช้เพียง OFDM สัญลักษณ์เดียวเท่านั้น

NATTAPHAT PROMSUWANNA : MIMO-OFDM CHANNEL AND  
CARRIER FREQUENCY OFFSET ESTIMATION FOR MOBILE  
BROADBAND ACCESS. THESIS ADVISOR : ASST. PROF. PEERAPONG  
UTHANSAKUL, Ph.D., 153 PP.

MIMO-OFDM/CHANNEL ESTIMATION/CARRIER FREQUENCY OFFSET  
ESTIMATION/MOBILE

The combination of Multi-Input Multi-Output (MIMO) with Orthogonal Frequency Division Multiplexing (OFDM) is regarded as a promising technique for the future wireless communications. However, the performance of MIMO-OFDM systems is very sensitive to carrier frequency offset (CFO), which introduces inter-carrier-interference (ICI), hence CFO should be estimated and compensated. In mobile broadband channel, the channel and CFO act as time-varying parameter due to the mobility and the surrounding environment. Thus the channel and CFO have to be tracked in order to maintain system performance. This thesis proposes a pilot scheme which is inserted in data transmission in order to track the variations of channel and CFO for MIMO-OFDM. The proposed pilot scheme for CFO estimation is based on null subcarrier insertion but provides more estimation efficiency due to the increasing of signal to noise ratio. In addition, the estimations from proposed pilot scheme can track the variations of channel and CFO by using only one OFDM symbol.

School of Telecommunication Engineering Student's Signature \_\_\_\_\_

Academic Year 2012

Advisor's Signature \_\_\_\_\_

## **ACKNOWLEDGEMENTS**

The author wishes to acknowledge the funding support from Telecommunications Research and Industrial Development Institute (TRIDI).

The grateful thanks and appreciation are given to the thesis advisor, Asst. Prof. Dr. Peerapong Uthansakul for his consistent supervision and thoughtfully comment on several drafts and advice towards the completion of this study.

My thanks go to Asst. Prof. Dr. Monthippa Uthansakul, Asst. Prof. Dr. Somsak Vanit-Anunchai, Asst. Prof. Dr. Chanchai Thaijiam and Dr. Dheerasak Anantakul for their valuable suggestion and guidance given as examination committees.

The author is also grateful to the financial support from Suranaree University of Technology (SUT).

Finally, I would also like to express my deep sense of gratitude to my parents for their support and encouragement me throughout the course of this study at the Suranaree University of Technology.

Nattaphat Promsuwanna

# TABLE OF CONTENTS

	<b>Page</b>
ABSTRACT (THAI) .....	I
ABSTRACT (ENGLISH) .....	II
ACKNOWLEDGMENTS .....	III
TABLE OF CONTENTS .....	IV
LIST OF TABLES .....	VIII
LIST OF FIGURES .....	IX
<b>CHAPTER</b>	
<b>I INTRODUCTION</b> .....	1
1.1 Background of problems .....	1
1.2 Research objectives.....	4
1.3 Scope and limitation of the study.....	5
1.4 Contributions.....	5
1.5 Thesis organization .....	5
<b>II LITERATURE REVIEW</b> .....	7
2.1 Introduction.....	7
2.2 Channel estimation in OFDM system.....	7
2.3 CFO estimation and compensation .....	10
2.4 Channel and CFO estimation for MIMO-OFDM system .....	14
2.5 Chapter Summary .....	15

## TABLE OF CONTENTS (Continued)

	Page
<b>III INTRODUCTION TO OFDM TECHNOLOGY .....</b>	<b>17</b>
3.1 Introduction.....	17
3.2 Background of OFDM technology .....	17
3.3 Conventional OFDM system .....	19
3.3.1 Modulation.....	19
3.3.2 Orthogonality property.....	20
3.3.3 Demodulation.....	21
3.4 Modern OFDM system .....	22
3.4.1 Orthogonality property.....	22
3.4.2 Modulation and demodulation .....	23
3.5 Intersymbol interference (ISI).....	24
3.5.1 Multipath fading.....	24
3.5.2 CP guard interval .....	26
3.6 Chapter summary .....	29
<b>IV CFO AND CHANNEL ESTIMATION .....</b>	<b>31</b>
4.1 Introduction.....	31
4.2 CFO effect.....	31
4.2.1 The effect of integer CFO .....	34
4.2.2 The effect of fractional CFO .....	35
4.3 CFO estimation techniques .....	37
4.3.1 CFO estimation by exploiting CP .....	37

## TABLE OF CONTENTS (Continued)

	<b>Page</b>
4.3.2 CFO estimation by using training symbol .....	38
4.3.3 CFO estimation by using pilot tone in frequency domain.....	39
4.4 Channel estimation in OFDM system.....	41
4.4.1 Pilot tones for channel estimation.....	41
4.4.2 Channel estimation technique in OFDM system .....	44
4.4.3 Channel estimation technique in MIMO-OFDM System.....	46
4.5 Chapter summary .....	49
<b>V THE PROPOSED PILOT SCHEME.....</b>	<b>50</b>
5.1 Introduction.....	50
5.2 Pilot design for OFDM system .....	50
5.2.1 Null subcarriers for CFO estimation.....	50
5.2.2 Proposed clustered pilot tones for CFO estimation .....	56
5.2.3 Proposed channel estimation technique.....	60
5.2.4 Simulation results.....	62
5.3 Pilot design for MIMO-OFDM system.....	69
5.3.1 Clustered pilot tones for CFO estimation .....	69
5.3.2 Pilot tones for channel estimation.....	74
5.3.3 Simulation results.....	76
5.4 Chapter summary .....	80



## TABLE OF CONTENTS (Continued)

	<b>Page</b>
APPENDICES	
APPENDIX A. TECHNICAL PUBLICATIONS .....	122
BIOGRAPHY .....	153



## LIST OF TABLES

Table	Page
4.1 Effect of CFO on the received signal. ....	34
6.1 Summary of specification of Altera cyclone III development boards.....	83



## LIST OF FIGURES

Figure	Page
1.1 (a) FDM subchannel allocation (b) OFDM subchannel allocation.....	2
2.1 Training schemes (a) block type (b) comb type.....	8
3.1 Subchannel allocation (a) FDM system (b) OFDM system.....	18
3.2 Signal modulation in OFDM .....	19
3.3 Signal demodulation in OFDM.....	21
3.4 The modern OFDM system configuration.....	22
3.5 Spectrum of OFDM signals.....	23
3.6 Channel impulse response and its effect in frequency domain.....	25
3.7 ISI effect in OFDM system.....	26
3.8 ISI effect with CP guard interval.....	27
3.9 ISI effect when CP length is less than maximum delay.....	28
3.10 Effect of timing offset.....	28
4.1 ICI due to $\varepsilon$ .....	32
4.2 Effect of CFO on the received signal in time domain .....	33
4.3 Effect of integer CFO.....	34
4.4 Effect of fractional CFO. ....	37
4.5 Block type pilot arrangement.....	41
4.6 Comb type pilot arrangement.....	43
4.7 MIMO system. ....	46
4.8 Orthogonal pilot scheme .....	48

## LIST OF FIGURES (Continued)

Figure	Page
5.1 MCRLB versus $\Delta$ .....	55
5.2 ICI improvement for any values of $\Delta$ .....	59
5.3 Variance of estimation errors versus SNR ( $\varepsilon = 0.2$ ).....	63
5.4 Variance of estimation errors versus SNR ( $\varepsilon = 0.4$ ).....	64
5.5 Variance of estimation errors versus SNR ( $\varepsilon = 0.7$ ).....	64
5.6 Received signal constellations .....	65
5.7 Variance of CFO estimation errors versus subcarrier spacing ( $\Delta f$ ).....	66
5.8 Variance of channel estimation errors versus SNR ( $\varepsilon = 0.2$ ).....	66
5.9 Example of channel response.....	67
5.10 BER versus SNR ( $\varepsilon = 0.15$ ).....	68
5.11 Proposed pilot scheme for $2 \times 2$ MIMO-OFDM channel estimation. ....	74
5.12 Proposed pilot scheme for $2 \times 2$ MIMO-OFDM system .....	75
5.13 a) Conventional pilot scheme b) Proposed pilot scheme.....	76
5.14 Variance of estimation errors versus SNR ( $\varepsilon = 0.2$ ).....	77
5.15 Variance of estimation errors versus SNR ( $\varepsilon = 0.4$ ).....	78
5.16 Variance of estimation errors versus SNR ( $\varepsilon = 0.7$ ).....	78
5.17 Variance of channel estimation errors versus SNR ( $\varepsilon = 0.3$ ).....	79
5.18 BER versus SNR ( $\varepsilon = 0.2$ ).....	79
6.1 Testbed diagram.....	82
6.2 Photograph of Altera cyclone III development board.....	83

## LIST OF FIGURES (Continued)

<b>Figure</b>	<b>Page</b>
6.3 Photograph of data conversion HSMC board. ....	84
6.4 Photograph of the processing unit connected with data conversion board via HSMC connector. ....	84
6.5 Block diagram of RF unit. ....	85
6.6 Schematic of IF amplifier. ....	86
6.7 Photograph of IF amplifier.....	86
6.8 Input and output signal from IF amplifier.....	87
6.9 Photograph of mixer. ....	87
6.10 Photograph of RF amplifier. ....	88
6.11 Photograph of monopole antenna. ....	88
6.12 Photograph of Hewlett Packard 83620B signal generator.....	89
6.13 Block diagram of transmitter unit.....	90
6.14 IQ modulation diagram. ....	91
6.15 Example of IQ signal from DAC.....	91
6.16 Power spectrum of the transmitted signal.....	92
6.17 Block diagram of receiver unit .....	93
6.18 IQ demodulation diagram. ....	93
6.19 Block diagram of Matlab programming .....	94
6.20 Photograph of testbed. ....	95
6.21 A photograph of the measurement area. ....	96
6.22 Received signal in frequency domain of the proposed pilot scheme.....	98

## LIST OF FIGURES (Continued)

<b>Figure</b>	<b>Page</b>
6.23 Received signal in frequency domain of null subcarrier technique .....	98
6.24 Received signal constellation when transmitted power is 0 dBm.....	99
6.25 Received signal constellation when transmitted power is -5 dBm. ....	99
6.26 Received signal constellation when transmitted power is -10 dBm. ....	100
6.27 Estimated channel response (time 1) .....	100
6.28 BER versus Transmitted power. ....	101
6.29 Block diagram for testing IF signal .....	102
6.30 Block diagram for testing RF amplifier .....	103
6.31 Received power spectrum. ....	104
6.32 Block diagram for testing mixer .....	104
6.33 FFT signal from receiver .....	105
6.34 The same source of signal generator test. ....	106
6.35 FFT output of received signal. ....	107
6.36 Signals constellation when carrier power is 9 dBm.....	108
6.37 Signals constellation when carrier power is 7 dBm.....	108
6.38 BER versus carrier power .....	109
6.39 Signals constellation of $s_I$ when carrier power is 7dBm.....	110
6.40 Experimental results versus the calculated $E_b/N_0$ from simulation .....	111
6.41 BER performance for experimental and simulation results .....	112

# CHAPTER I

## INTRODUCTION

### 1.1 Background of problems

Recently, OFDM (Orthogonal Frequency Division Multiplexing) has become one of the modern technologies and it plays a significant role in the development of wireless communication system performance. OFDM is a type of multicarrier transmission techniques where the serial data is transformed into parallel form, then it is modulated with subcarriers. Multicarrier transmission reduces the effect of frequency selective fading channel by transforming frequency selective fading channel into summation of flat fading channels thus this technique is an effective technique especially for broadband communications. In addition, OFDM can improve bandwidth efficiency compared with FDM (Frequency Division Multiplexing), where subchannel bandwidth of FDM has to be placed separately from another subchannel in order to avoid aliasing effect which produces interchannel interference, but OFDM allows the overlay of subchannel bandwidth without interfering with another subchannel due to the orthogonal property (as indicated in Figure 1.1). Moreover, with the emergence of digital signal processing in the present, OFDM can be applied to a wide range of other communication systems hence it has been added into many communication standards such as IEEE 802.11n, IEEE 802.16, IEEE 802.20 (Li and Stüber, 2006) digital terrestrial video broadcasting (DVB) and digital audio broadcasting (DAB) (ETSI EN300, 2001).

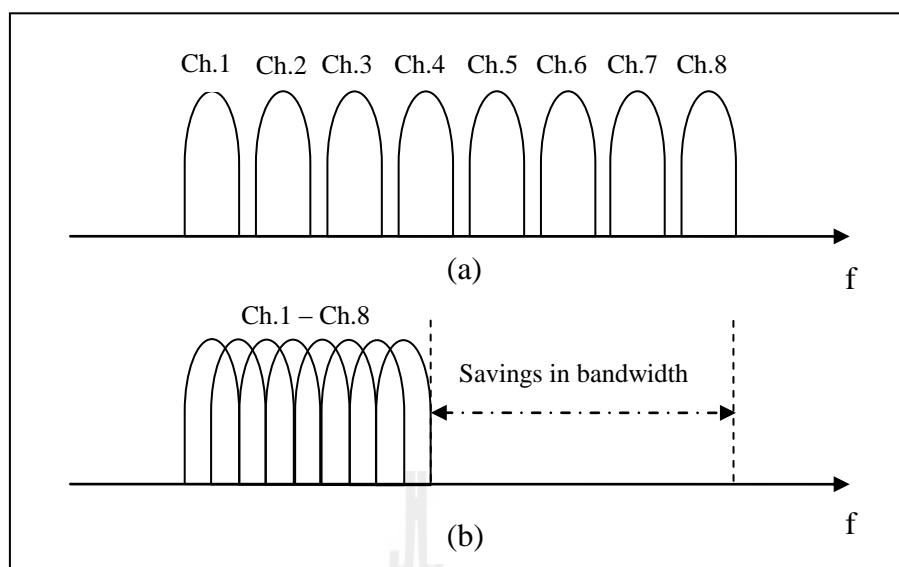


**Figure 1.1** (a) FDM subchannel allocation (b) OFDM subchannel allocation

For many years, MIMO (Multiple Input Multiple Output) has been the technology that becomes the focus of extensive research. It proposes an extensive improvement over conventional smart antenna systems in both Quality of Service (QoS) and transfer rate (Telatar, 1995). For this reason, the integration between MIMO and OFDM technologies to improve the quality and speed of data transmission has been created and named as MIMO-OFDM. MIMO-OFDM has been added in future broadband communication standards such as Mobile WiMAX (IEEE802.16e) and LTE (Long Term Evolution), and there are several works related with MIMO-OFDM such as Sampath, Talwar, Tellado, Erceg and Paulraj, (2002); [6] Zelst, Schenk and Tim, (2004). However, channel estimation is the important factor for data detection in MIMO system where the performance of channel estimation is depended on channel estimation technique and the characteristic of wireless channel. Based on previous works, channel estimation when the channel is rapidly changing due to the mobility of users or the environment of the channel challenges many researchers to do

the channel estimation to keep track of the channel variations.

In addition, even if overlapping between subchannels in OFDM technique improves bandwidth efficiency but the error from synchronization between transmitter and receiver causes the loss of orthogonal property in OFDM system which produces intercarrier interference (ICI). Where the effect of synchronization error can cause failing in communication. Frequency synchronization is one of synchronization parameters which is important for OFDM system. The carrier frequency between transmitter and receiver may be miss matched due to the stability of local oscillators between transmitter and receiver, and the Doppler effect from the mobility of user is also included. Where the normalization of frequency offset by subcarrier spacing in OFDM is so called Carrier Frequency Offset (CFO). Thus, CFO has to be estimated and compensated in order to keep orthogonality between subchannels and the performance of data detection in OFDM system.

From above problems, authors have realized the relation between channel estimation and CFO estimation which can be said that if we cannot compensate the effect of CFO thus the performance of channel estimation is degraded. From previous works, CFO and channel can be estimated according to two categorizes of pilot signal, the first one is using training symbol and the second one is inserting pilot tone. Based on using training symbol, the training symbol is inserted in the front of information data before transmitting into wireless channel. The information from training symbol is used for both channel and CFO estimations at the receiver. The estimated CFO and channel are used for CFO compensation and data detection for next incoming OFDM symbols. However, if wireless channel acts as a fast fading, it will cause channels on each OFDM symbol to be different. Thus this leads to performance degradation in

data detection. For CFO and channel estimation based on inserting pilot tone, the number of pilot subcarrier are inserted along subcarrier axis in every OFDM symbols where these pilot subcarriers are used for both CFO and channel estimation. The aim of this technique is to reduce pilot overhead but providing ability to keep track the variations of both channel and CFO even if some estimation performance are lost. Thus, pilot tone technique is more suitable for mobile broadband communication than training symbol technique. However, the estimation performance of inserting pilot tone technique is lower than training symbol technique due to less pilot information.

Therefore, in this thesis, I am interested to design pilot tones in order to enhance the performance of CFO and channel estimation for mobile broadband MIMO-OFDM system. By inserting the designed pilot tones in every OFDM symbol, it can not only help the estimation to keep track of the variation of channel but also improving the estimation performance for both channel and CFO estimations. In this work, Mobile WiMAX standard (IEEE802.16e) is used to be the standard that we are interested.

## **1.2 Research objectives**

The objectives of this research are as follows:

1.2.1 To study and develop pilot tones for CFO and channel estimations for mobile broadband OFDM and MIMO-OFDM systems.

1.2.2 To study the performance of channel and CFO estimations of designed pilot tones when mobile broadband channel is considered.

1.2.3 To design and construct a testbed in order to validate the proposed technique in the practical system.

### **1.3 Scope and limitation of the study**

1.3.1 The operating frequency of testbed is ranged from 2.4 to 2.6 GHz.

1.3.2  $2 \times 2$  antenna configuration is considered in order to reduce the system complexity and cost.

1.3.3 The performance of testbed is considered in the case that there is only one user. Therefore, the whole subcarriers are used for one user.

1.3.4 The experimental results are based on static user and small scale environment.

### **1.4 Contributions**

1.4.1 To obtain a designed pilot tones and the estimation technique which are useful and suitable for mobile broadband MIMO-OFDM system.

1.4.2 To obtain knowledge that can be applied for future MIMO-OFDM research.

### **1.5 Thesis organization**

The remainder of this thesis is organized as follows. Chapter 2 presents a literature review that relates to this work including channel estimation and CFO estimation from the basic OFDM system to MIMO-OFDM system.

Chapter 3 is an introduction to the OFDM technology where the principle and mathematical model of OFDM system are presented. In addition, the development from a conventional OFDM system to a present OFDM system and the investigation on ICI effect are also explained.

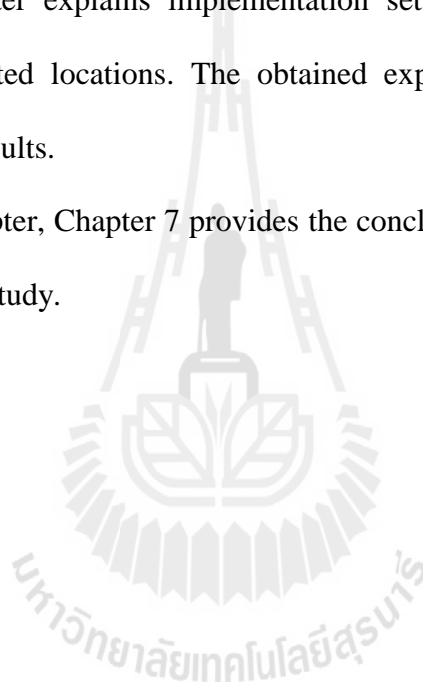
Chapter 4 presents the effect of carrier frequency offset in OFDM system including techniques for compensating this effect. Furthermore, the channel estimation

techniques for both OFDM and MIMO-OFDM are also presented.

Chapter 5 describes the proposed pilot tones for both channel and CFO estimation which can be used in either OFDM or MIMO-OFDM system. The performance analysis of the proposed pilot scheme including its simulation results is presented.

In chapter 6, the practical implementation setup and experimental results are presented. This chapter explains implementation setup including transmitter unit, receiver unit and tested locations. The obtained experimental results are used to validate simulation results.

In the last chapter, Chapter 7 provides the conclusion of the research work and suggestion for future study.



## **CHAPTER II**

### **LITERATURE REVIEW**

#### **2.1 Introduction**

The channel estimation and CFO estimation are paid attention by researchers for a long time where these parameters need to be estimated and compensated in order to maintain the performance of data detection at receiver. In case that channel and CFO change by time, the technique that can keep track these variations becomes a challenge to researchers. Hence the main object of this research is to design the pilot tones and the estimation technique that can keep tracking the variations of channel and CFO for mobile broadband communications. Therefore, it is necessary to do a survey and literature review of related works in order to study previous works, to verify problems, to set methodology and finally to achieve research objectives.

This chapter describes literature review and related works including channel estimation and CFO estimation from the basic OFDM system to MIMO-OFDM system. In addition, the works related with designing pilot tone for channel and CFO estimations are also included.

#### **2.2 Channel estimation in OFDM system**

The channel estimations for OFDM system can be performed by inserting a training signal in each OFDM symbol. Then receiver uses training data for channel estimation. We can categorize the type of training signal insertion into two types which are block type (Hou, Zhao, Yin and Yue, 2005) and comb type (Edfors,

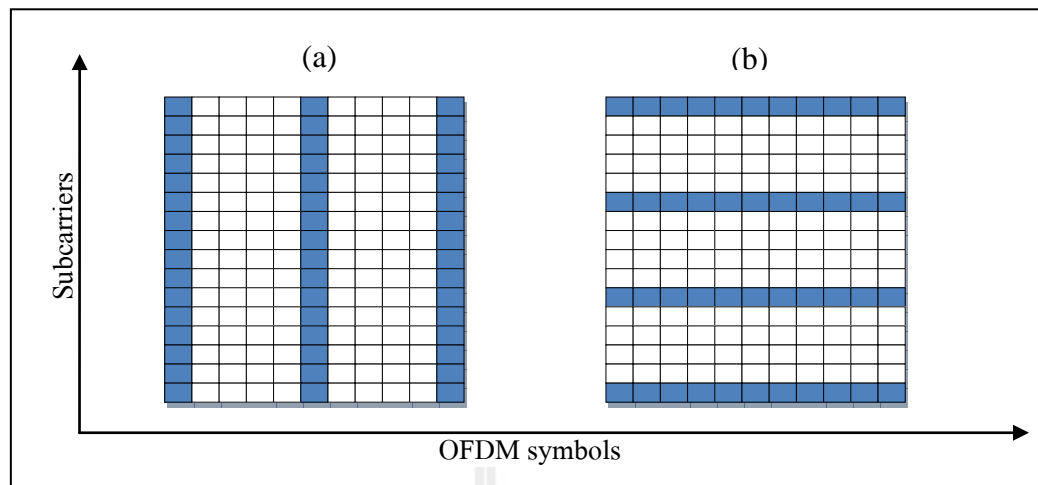


**Figure 2.1** Training schemes (a) block type (b) comb type.

Van de Beek, Wilson and Borjesson, 1998) which can be shown in Figure 2.1. The block type inserts a training data in every subcarrier, thus this OFDM symbol contains only training data where this OFDM symbol can be named as training symbol. Training symbol is inserted in front of data symbol group where the distances of inserting training symbol are different which depends on type of communication. By using training symbol, it provides a good performance on channel estimation due to many of training data. However, in the case that channel is changing rapidly, more frequently inserting a training symbol should be performed in order to keep track of the variation of channel. It means that system loses some of data symbols for training symbol hence it reduces bandwidth efficiency. Unlike comb type, only some of subcarriers are modulated with training data which are called pilot tones. These pilot tones are inserted in every OFDM symbol thus it provides system to keep track the variations of its channel, thus it improves robustness to fast fading channel. However, by inserting some pilot tones in comb type, it is necessary to do a channel interpolation for data subcarriers. From the previous works, there are many

interpolation techniques such as linear interpolation, low-pass interpolation and spline interpolation (Rinne and Renfors, 1996).

The techniques of training data insertion for MIMO-OFDM system are similar to OFDM system which are both training symbol and pilot tone. However, channel estimations in MIMO-OFDM system have more complexity due to the increasing of input and output parameters. There are many techniques for MIMO channel estimation such as least square estimation (LSE), minimum mean square error (MMSE) and maximum likelihood estimation (MLE) (Cho, 2010). In addition, MIMO channel estimation is necessary to transmit a training symbols at least  $N_T$  (the number of transmitted antennas) symbols in order to perform a channel estimation thus it is hard to keep track of the channel if fast fading channel is considered. There are many works related with using training symbol for MIMO-OFDM channel estimation such as He Zhong Tang and Cen Zi Li (2005) which have proposed a training scheme that reduces the effect of intersymbol interference (ISI). In addition, this technique can reduce the complexity of channel estimation. Delestre and Sun (2010) have proposed the design of training symbol that reduces the complexity of channel estimation when STBC (Space Time Block Code) is used. For the works that related with pilot tone for channel estimation, Bahumi, Leus and Moonen (2003) have showed that pilot tones should have equal power and should be placed with equal distance. Moreover, the training data on pilot tones should be phase shift orthogonal in order to achieve the best channel estimation performance in term of MSE (Mean Square Error). In addition, Wang, Zhu and Hu (2004) have proposed a pilot scheme that minimizes channel estimation error based on LSE technique. However, the above techniques are under the assumption that the channel is not changing during  $N_T$  (or during channel

estimation process). Thus, it is not suitable for mobile broadband channel when channel changes all the time. Based on this problem, Qiao, Yu, Su and Zhang (2004) have proposed the orthogonal pilot scheme where this technique reduces the complexity of MIMO channel estimation into SISO (Single Input Single Output) channel estimation. The estimation process of this technique can be done with only one OFDM symbol thus this is a useful technique especially for mobile broadband communications. However, this technique has been designed for channel estimation only while CFO is one of the important parameters which should be estimated and compensated. Therefore, the candidate is interested in the design of the pilot scheme for both channel and CFO estimation, where the designed pilot scheme still provides the same channel estimation benefit as orthogonal pilot scheme and it also keeps track of the variations of CFO.

### **2.3 CFO estimation and compensation**

There are two methods to compensate the effect of CFO, the first one is technique that reduces the effect of CFO (ICI effect) and the second is CFO estimation. Works related with reducing the effect of CFO are such as, Zhao and Haggman (1996) have proposed self ICI cancellation by sending the same data on consecutive subcarrier. These data are antipodal to each other which is described by  $a_k = -a_{k+1}$  where subscript  $k$  refers to subcarrier position index thus half of bandwidth efficiency is lost. Furthermore, Gudmunson and Anderson (1998) have showed that the effect of ICI can be reduced by using Hanning window for time domain baseband filter. However, using Hanning window reduces signal to noise ratio (SNR) of signal which is located on edge of symbol thus it may degrade the overall system

performance. The above techniques can reduce some of ICI effect caused by CFO but the effect of CFO still exists. In order to achieve a better performance, CFO estimation should be performed.

Based on CFO estimation, CFO is estimated and compensated at receiver. There are many works that are developed and based on work presented by Moose (1984). Moose has proposed a maximum likelihood for CFO estimation based on frequency domain where this technique requires the transmitting duplicate OFDM symbols. The estimated CFO is achieved by measuring a phase difference between consecutive and duplicate OFDM symbols thus a half of bandwidth efficiency is lost due to sending duplicate symbols. In addition, this technique may increase CFO estimation errors if channel is changed during sending two duplicated symbols. Moreover, the range of estimation from this technique is limited by  $\pm 0.5$  of subcarrier spacing. Work in (Van de Beek, Sandell and Borjesson, 1997) has proposed CFO estimation by using the same idea as Moose but the estimation is based on time domain. The estimated CFO is obtained by using CP (Cyclic Prefix). CP is some identical data of the front section of OFDM symbol but it is placed at the last section of symbol. Hence CFO can be estimated by measuring phase difference between copied data in CP and original data. This technique offers the same estimation range as Moose but provides higher bandwidth efficiency than Moose's technique. The estimation performance depends on the length of CP where more data in CP should provide a better performance. However, the aim of CP is to prevent ISI. Therefore, if there is ISI in system, the estimation performance of this technique is degraded. In order to increase the estimation range, the work of Morelli and Mengali in 1999 has proposed a training symbol which compounds by duplicate data within one OFDM

symbol where  $M$  is the number of duplicate data. This technique extends estimation range of CFO up to  $\pm M$  of subcarrier spacing. However, even this technique is a useful and effective technique due to wide range of CFO estimation and high performance due to using training symbol, it is not suitable for mobile broadband communications. At this point, Schmidl and Cox (1997) have proposed CFO estimation which is able to keep track of the variations of CFO. Schmidl and Cox have divided CFO into two parts which are integer and fractional. The integer CFO can be estimated by calculating the CFO which causes maximum correlation of pilot tones between consecutive symbols. Then this estimated integer CFO is used to compensate a received signal. After that, the compensated signal is used to calculate the fractional CFO by using the technique proposed by Moose. However, work in (Shim, Kim, Song and You, 2007) has shown that the technique which was presented by Schmidl and Cox can cause estimation error when frequency selective channel is considered. Furthermore, (Fu and Minn, 2007) and (Zhang, Xia and Ching, 2007) have presented technique that improves the estimation performance when pilot tones are used. Work in (Fu and Minn, 2007) has proposed data-interference to pilot tone reduction by inserting null data or correlated data on the adjacent subcarrier at the left and the right of pilot subcarrier, thus the dominant ICI affects pilot tone to be decreased. Zhang, Xia and Ching (2007) have proposed clustered pilot tones where two pilot tones are clustered into a group. The pilot data on the left and the right are antipodal to each other. Zhang, Xia and Ching have shown that pilot signal to data-interference ratio is increased by using this technique. From above techniques which use pilot tone for CFO estimation, these techniques are based on the basis of Moose's technique which requires resending duplicate data on consecutive symbol. Thus, it

reduces the estimation performance if channels on consecutive symbols are different.

From above problem, candidate aims to develop CFO estimation technique where the estimation process can be done by using only one OFDM symbol. The estimation can keep track of the variations of CFO and robust to frequency selective fading. Based on the previous works, there are two methods that can solve this problem which are adaptive algorithm and searching algorithm. For adaptive algorithm, Yang, Li and The (2005) have proposed LMS-like algorithm by adjusting compensated CFO with received signal until the compensated signal is the same as reference signal (training symbol). However, this technique does not consider channel thus it reduces the estimation performance. Moreover, Jian and Chunn (2009) have presented CFO estimation by using Kalman filter. For searching algorithm, candidate is interested in the technique called null subcarrier insertion. Null subcarrier insertion was first proposed by Liu and Tureli (1998) by exploiting structure of OFDM symbol which has virtual subcarriers at the frequency edge on each OFDM symbol. These virtual subcarriers are usually used for preventing the effect from roll-off region of filter. In general, these virtual subcarriers are not used to transmit any data (0 or null) thus if there is ICI which is caused by CFO then the signal on virtual subcarriers will not be 0. Based on this fact, CFO can be estimated by searching compensated CFO which minimizes signal power on virtual subcarriers and set it to be the estimated CFO. After that, Ma, Tepedelenlioglu, Giannakis and Barbarossa (2001) have shown that estimation performance of Liu and Tureli (1998) is reduced when frequency selective fading is considered. In addition, Ma, Tepedelenlioglu, Giannakis and Barbarossa have also proposed null insertion technique to overcome this problem where null subcarriers are inserted along data subcarriers in order to compensate the

effect from frequency selective fading. Moreover, there are several works related with null subcarriers for CFO estimation such as Huang and Lataef (2006) and Lin, Nakao, Lu and Yamashita (2007).

As mentioned above, candidate is interested in CFO estimation by using null subcarrier. This technique does not require a known reference signal or any training data at receiver. In addition, this technique does not require channel information thus it gives less complexity than other techniques. However, from previous works this technique has been studied and based on SISO system. Due to the insertion of these null subcarriers, it causes these subcarriers to be used for CFO estimation only. In this work, candidate aims to design pilot scheme and the estimation technique which can be used for both channel and CFO estimation while still provide the same benefit of CFO estimation as null subcarrier technique.

## **2.4 Channel and CFO estimation for MIMO-OFDM system**

The previous works that have dealt with channel and CFO estimation for MIMO-OFDM system are almost based on training symbol such as Zhen and Jianhua (2006); He (2008) and Simon, Ross, Hijazi, Jin, Gaillot and Berbineau (2011). However, in order to improve the performance for mobile broadband communications, it is necessary to keep track the variations of channel and CFO for every OFDM symbol. Hung, Tho and Chi (2007) have proposed pilot tones to overcome with this problem but this work gives high complexity due to channel estimation for both frequency and time domains. In addition, the performance of this technique is reduced if channels on each symbol are different. Wu, Samir and Bergmans (2007) have presented a training symbol for channel and CFO estimation where the estimation

process can be carried out with only one OFDM symbol. This work realizes channel estimation complexity in MIMO system where it requires to send the training symbol at least  $N_T$  symbols in order to estimate channel. However, this work is based on using training symbol thus it is not suitable for mobile broadband applications.

In addition, there is a technique that differs from pilot tone and training symbol where it does not require any training data and it is called blind estimation. This technique exploits statistic information of received signal for channel and CFO estimation without any help from training data. Thus, it provides the best in bandwidth efficiency. However, the estimation performance of this technique is based on the number of collecting the received data. The more data is collected, the more estimation performance can be improved. Thus this technique is not suitable for mobile broadband communications and candidate does not include this technique in this thesis for next section.

## 2.5 Chapter summary

The channel and CFO estimations for mobile broadband communications should not be limited with using training symbol. Thus, it is necessary to keep track of the variations of channel and CFO due to mobility or environments surrounding user in order to maintain the system performance. This work focuses on channel estimation by using orthogonal pilot scheme and CFO estimation by using null subcarriers where these techniques exploit the benefit of pilot tone. In addition, these techniques are able to keep track of the variations of the estimated parameters where the estimation process can be carried out with only one OFDM symbol. Thus they are the useful techniques especially for mobile broadband communications. However, the above

techniques require null subcarriers for CFO estimation where these null subcarriers are inserted along data subcarrier axis and these pilot tones cannot be reused for other purposes. Hence, this work proposes pilot scheme which provides the same benefits as null subcarrier and orthogonal subcarrier. Furthermore, the proposed pilot scheme can be used for both channel and CFO estimation and it also improve the estimation performance.



## **CHAPTER III**

### **INTRODUCTION TO OFDM TECHNOLOGY**

#### **3.1 Introduction**

This chapter describes an introduction of OFDM technology where the principles and mathematical model are presented in order to understand the fundamental of OFDM system. In addition, the development of the conventional OFDM system to the modern OFDM system and the effect of ISI are also presented.

#### **3.2 Background of OFDM technology**

The OFDM technology is classified in a group of spread spectrum. This technique uses multiple subcarriers modulation where the transmission channel is divided into multiple subchannels which are independent to each other. FDM (Frequency Division Multiplexing) is one of the most well known techniques. FDM divides serial data into parallel data then modulates into subchannels where each subchannel bandwidth must not overlap by other subchannel in order to prevent ICI. Therefore, this technique requires guard band to avoid such problem. However, even if guard band is a good technique for ICI avoidance in FDM systems but it reduces bandwidth efficiency due to bandwidth requisition for guard band. The subchannel allocation in FDM system can be shown in Figure 3.1 (a). OFDM was discovered in order to improve bandwidth efficiency and it was firstly proposed by Chang (Chang, 1996). Chang has proposed the orthogonal signal synthesis for multiple subchannel transmission with limited bandwidth. This technique uses orthogonal subcarriers for

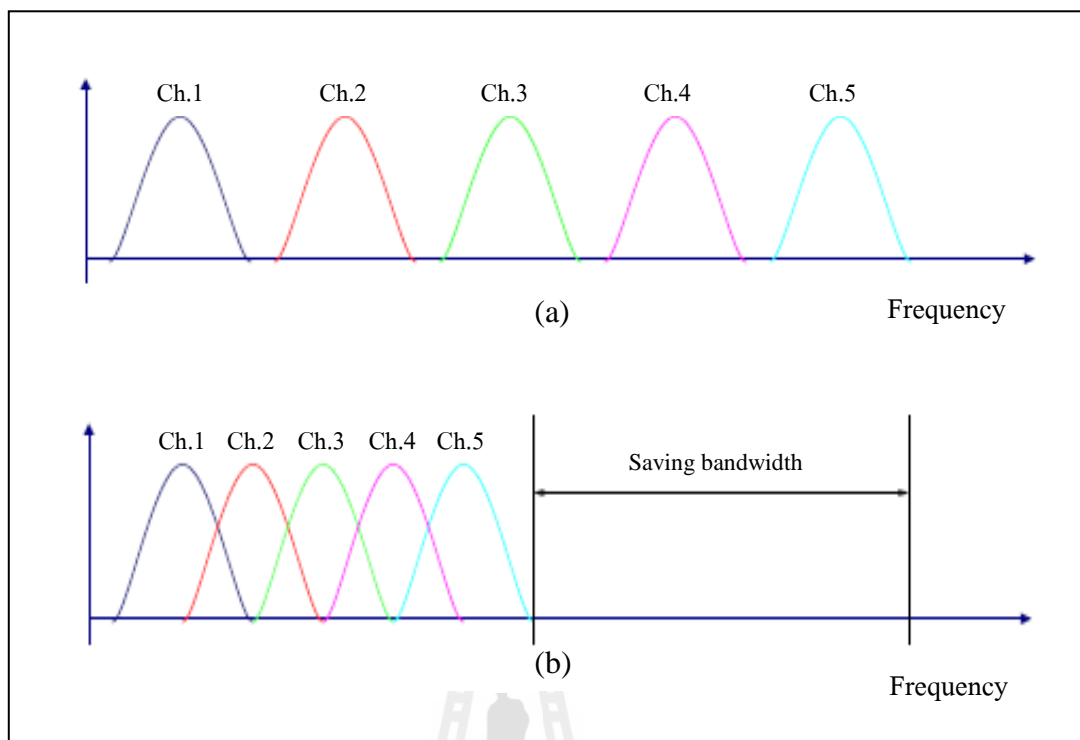


**Figure 3.1** Subchannel allocation (a) FDM system (b) OFDM system.

subchannel modulation where subchannels can be placed closer than the conventional FDM system therefore it increases bandwidth efficiency and transmission rate. The subchannel allocation in OFDM system can be shown in Figure 3.1 (b).

In the past, the orthogonal subcarrier generation in OFDM system is very complicated. The conventional OFDM system is based on analog configurations where there are a lot of frequency oscillators. Thus, OFDM system becomes a large system and it is difficult to apply to other communication systems. However, with the help of high-speed digital ICs and FFT (Fast Fourier Transform), OFDM can be utilized for various communication system standards such as IEEE8.2.11n (Wireless LAN), IEEE802.16e (mobile WiMAX) and 4<sup>th</sup> generation of communication (4G).

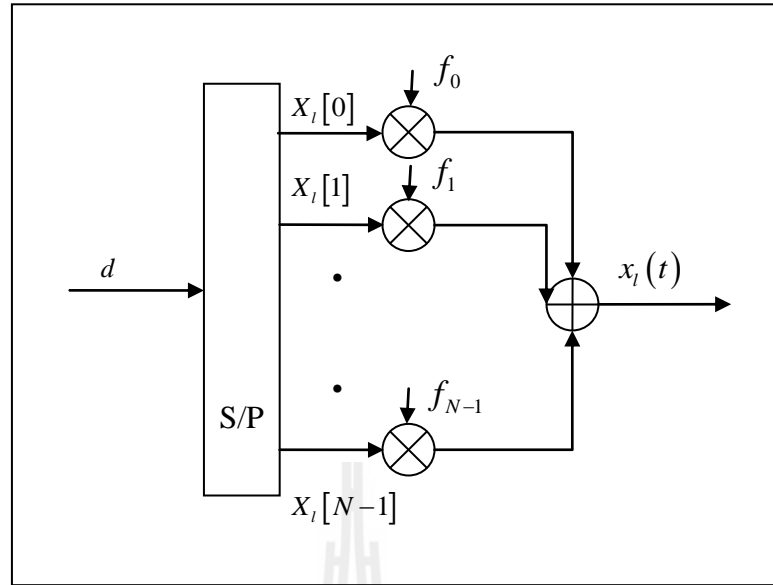


**Figure 3.2** Signal modulation in OFDM.

### 3.3 Conventional OFDM system

#### 3.3.1 Modulation

The signals modulation scheme in OFDM system can be shown in Figure 3.2. The high speed serial digital data  $d$  is divided into groups of low speed parallel data then these parallel data are modulated with subcarrier  $f_k$  where the modulation types are such as QAM, 16QAM and 64QAM.  $X_i[k]$  is the modulation symbol of QAM, 16QAM or 64QAM modulations for the  $k^{\text{th}}$  subcarrier and the  $l^{\text{th}}$  OFDM symbol. After that, the modulated data are mixed with subcarrier then these signals are summarized and then it is transformed into passband signal by using frequency up converter. The  $k^{\text{th}}$  subcarrier signal with frequency  $f_k$  can be given by

$$\psi_{l,k}(t) = \begin{cases} e^{j2\pi f_k(t-lT_{sym})}, & 0 < t \leq T_{sym} \\ 0, & \text{else} \end{cases} \quad (3.1)$$

where  $T_{sym}$  is the OFDM symbol time. Then the baseband OFDM signal in time domain can be shown by

$$x_l(t) = \sum_{l=0}^{\infty} \sum_{k=0}^{N-1} X_l[k] e^{j2\pi f_k(t-lT_{sym})} \quad (3.2)$$

Then the baseband signal  $x_l(t)$  is transformed into passband signal which will be sent to wireless channel.

### 3.3.2 Orthogonality property

From Figure 3.2, after groups of parallel data  $X_l[k]$  are generated, these parallel data will be modulated with different subcarriers which are  $f_0, f_1, f_2, \dots, f_{N-1}$  as same as FDM but these subcarriers must be orthogonal to each other.

By assuming that, OFDM subcarrier signal is in exponential form which is  $\{e^{j2\pi f_k t}\}_{k=0}^{N-1}$  with subcarrier frequency  $f_k$  and  $0 \leq t \leq T_{sym}$ . These subcarriers are considered to be orthogonal if

$$\begin{aligned} \frac{1}{T_{sym}} \int_0^{T_{sym}} e^{j2\pi f_k t} e^{-j2\pi f_i t} dt &= \frac{1}{T_{sym}} \int_0^{T_{sym}} e^{j2\pi \frac{k}{T_{sym}} t} e^{-j2\pi \frac{i}{T_{sym}} t} dt \\ &= \frac{1}{T_{sym}} \int_0^{T_{sym}} e^{j2\pi \frac{(k-i)}{T_{sym}} t} dt \\ &= \begin{cases} 1, & k = i \\ 0, & \text{otherwise} \end{cases} \end{aligned} \quad (3.3)$$

The orthogonal subcarrier frequency can be given by  $f_k = k/T_{sym}$  or  $f_k = k\Delta f$  where  $\Delta f$  is the subcarrier spacing and it can be written by

$$\Delta f = 1/T_{sym} = B/N \quad (3.4)$$

where  $B$  is the system bandwidth.

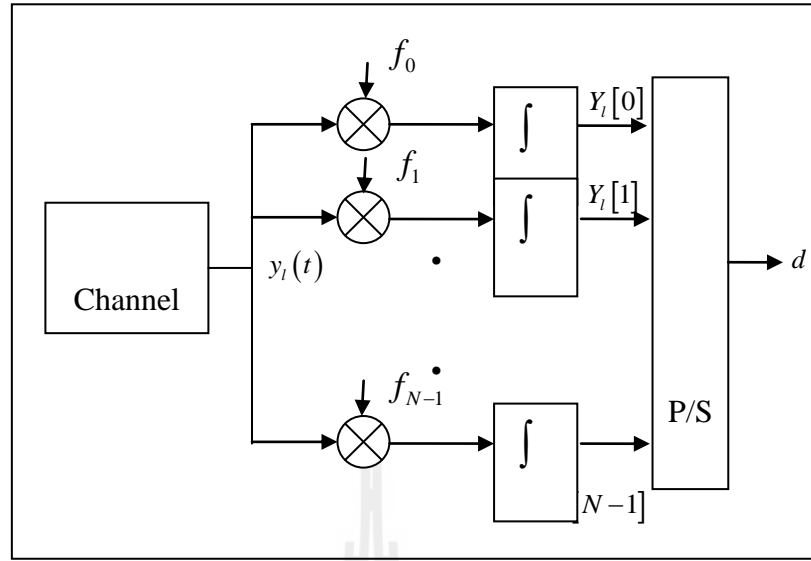


**Figure 3.3** Signal demodulation in OFDM.

### 3.3.3 Demodulation

After that baseband signal (3.2) is transformed into passband signal and sent through wireless, then receiver will transform the received signal into baseband signal by using frequency down converter. This signal is cleaned by low pass filter in order to reduce the interference. Then each subchannel is separated by demodulation with its subcarrier. By using the integration operation as shown in Figure 3.3, the signals demodulated in an OFDM system can be given by

$$\begin{aligned}
 Y_l[k] &= \frac{1}{T_{sym}} \int_{-\infty}^{\infty} y_l(t) e^{j2\pi f_k(t-IT_{sym})} dt \\
 &= \frac{1}{T_{sym}} \int_{-\infty}^{\infty} \left\{ \sum_{i=0}^{N-1} X_l[i] e^{j2\pi f_i(t-IT_{sym})} \right\} e^{-j2\pi f_k(t-IT_{sym})} dt \\
 &= \sum_{i=0}^{N-1} X_l[i] \frac{1}{T_{sym}} \int_{-\infty}^{\infty} e^{j2\pi(f_i-f_k)(t-IT_{sym})} dt = X_l[k]
 \end{aligned} \tag{3.5}$$

where  $Y_l[k]$  is the received data of the  $k^{\text{th}}$  subcarrier and the  $l^{\text{th}}$  OFDM symbol.

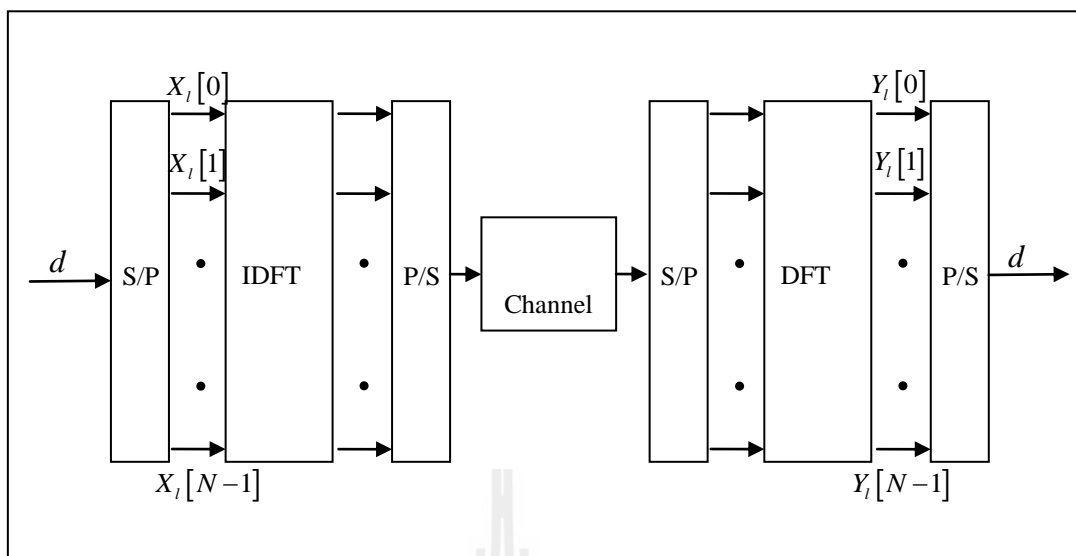


**Figure 3.4** The modern OFDM system configuration.

From (3.5), it shows an OFDM signal demodulation where the effect of channel is not considered. The system with channel effect is described in the next chapter.

### 3.4 Modern OFDM system

#### 3.4.1 Orthogonality property

Today, electronic ICs and digital signal processing are developed rapidly which causes modern communication systems become almost digital communication. OFDM as well, the complexity of OFDM system is greatly reduced where discrete fourier transform (DFT) and inverse discrete fourier transform (IDFT) can be used for orthogonal subcarrier synthesis. Therefore, the investigation of orthogonal property of OFDM signal can be performed by sampling the continuous signal from (3.3) at time  $t = nT_s = nT_{sym}/N$  where  $n = 0, 1, 2, \dots, N-1$  and  $T_s$  is sampling period. Then the discrete form of (3.3) can be written by

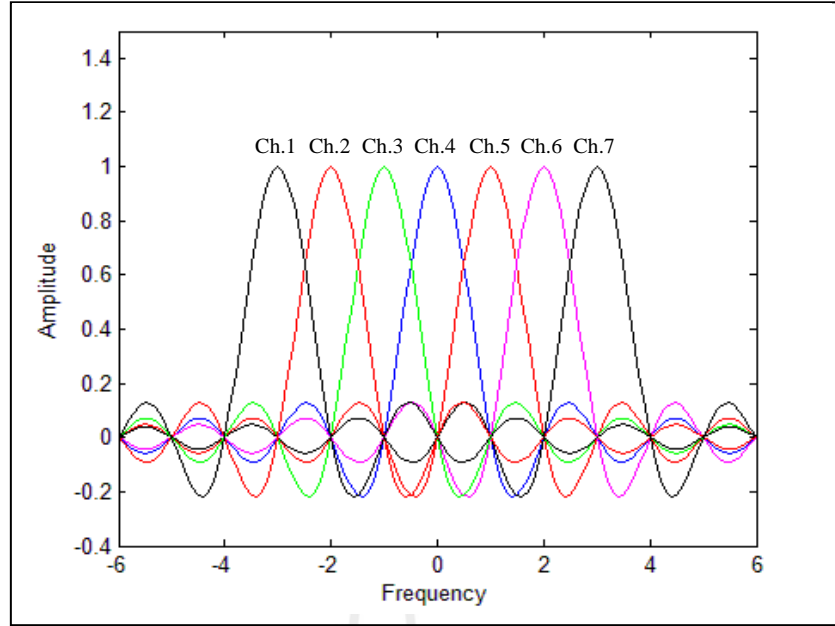


**Figure 3.5** Spectrum of OFDM signals.

$$\begin{aligned}
 \frac{1}{N} \sum_{n=0}^{N-1} e^{j2\pi \frac{k}{T_{sym}} n T_s} e^{-j2\pi \frac{i}{T_{sym}} n T_s} &= \frac{1}{N} \sum_{n=0}^{N-1} e^{j2\pi \frac{k}{T_{sym}} n \frac{T_{sym}}{N}} e^{-j2\pi \frac{i}{T_{sym}} n \frac{T_{sym}}{N}} \\
 &= \frac{1}{N} \sum_{n=0}^{N-1} e^{j2\pi \frac{(k-i)}{N} n} \\
 &= \begin{cases} 1, & k = i \\ 0, & \text{otherwise} \end{cases}
 \end{aligned} \tag{3.6}$$

As seen in (3.6), the result is the same as (3.3)

### 3.4.2 Modulation and demodulation

The configuration signal modulation and demodulation in modern OFDM system can be shown in Figure 3.4. As seen in figure, transmitter uses IDFT to create time domain baseband signal while receiver uses DFT operation. The transmitted signal can be shown by sampling the continuous baseband signal from (3.2) at time  $t = nT_s = nT_{sym}/N$  where  $n = 0, 1, 2, \dots, N-1$  and  $T_s$  is sampling period.

Then the transmitted signal can be written by

$$x_l[n] = \frac{1}{\sqrt{N}} \sum_{k=0}^{N-1} X_l[k] e^{j\frac{2\pi kn}{N}} \quad (3.7)$$

where  $n = 0, 1, 2, \dots, N-1$ .

From equation (3.7), it refers to  $N$ -point IDFT operation. The example of spectrum of transmitted signal from (3.7) can be shown in Figure 3.5 and we can see that there is no interference from another subchannel at the center of each subcarrier.

For signal demodulation, as same as modulation but in the contrary, the demodulated signals can be archived by using DFT operation which can be given by

$$\begin{aligned} Y_l[k] &= \frac{1}{\sqrt{N}} \sum_{n=0}^{N-1} y_l[n] e^{-j\frac{2\pi kn}{N}} \\ &= \sum_{n=0}^{N-1} \left\{ \frac{1}{\sqrt{N}} \sum_{i=0}^{N-1} X_l[i] e^{j\frac{2\pi in}{N}} \right\} e^{-j\frac{2\pi kn}{N}} \\ &= \frac{1}{N} \sum_{n=0}^{N-1} \sum_{i=0}^{N-1} X_l[i] e^{j\frac{2\pi(i-k)n}{N}} = X_l[k] \end{aligned} \quad (3.8)$$

### 3.5 Intersymbol interference (ISI)

#### 3.5.1 Multipath fading

The  $l^{\text{th}}$  OFDM symbol,  $x_l(t) = \frac{1}{\sqrt{N}} \sum_{k=0}^{N-1} X_l[k] e^{j2\pi f_k(t - IT_{\text{sym}})}$ , pass through wireless channel with channel impulse response  $h_l(t)$ . Then the received signal can be given by

$$y_l(t) = x_l(t) * h_l(t) = \int_0^{\infty} h_l(\tau) x_l(t - \tau) dt + z_l(t) \quad (3.9)$$

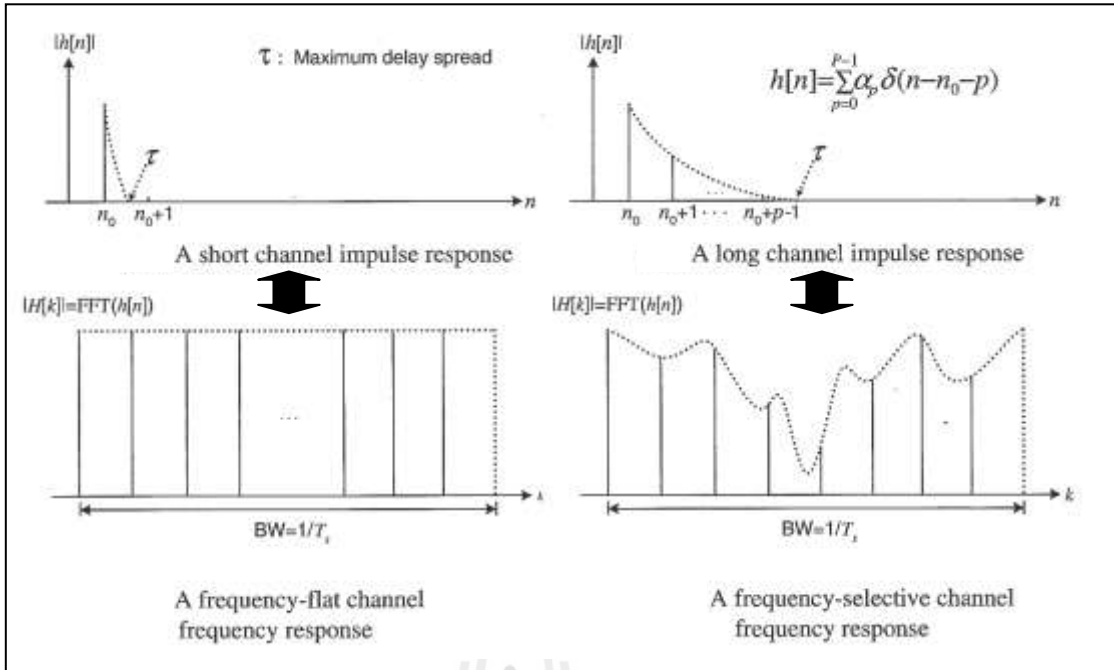


**Figure 3.6** Channel impulse response and its effect in frequency domain.

where  $z_l(t)$  is AWGN (additive white Gaussian noise). The discrete form of (3.9) can be performed by sampling (3.9) at  $nT_s$  where  $nT_s = nT_{sym}/N$ . Then (3.9) can be rewritten by

$$y_l[n] = x_l[n] * h_l[n] = \sum_{m=0}^{\infty} h_l[m] x_l[n-m] + z_l[n] \quad (3.10)$$

where  $x_l[n] = x_l(nT_s)$ ,  $y_l[n] = y_l(nT_s)$ ,  $h_l[n] = h_l(nT_s)$  and  $z_l[n] = z_l(nT_s)$ .

Figure 3.6 shows the discrete time channel impulse responses of two different channels where their frequency responses are also presented. In addition, Figure 3.7 shows the effect of multipath fading which affects on consecutive OFDM symbols in the time domain. As seen in both figures, multipath fading channel not only causes channel to act as frequency selective fading (as seen in Figure 3.6 when a long channel impulse response is assumed) but also produces ISI as shown in Figure

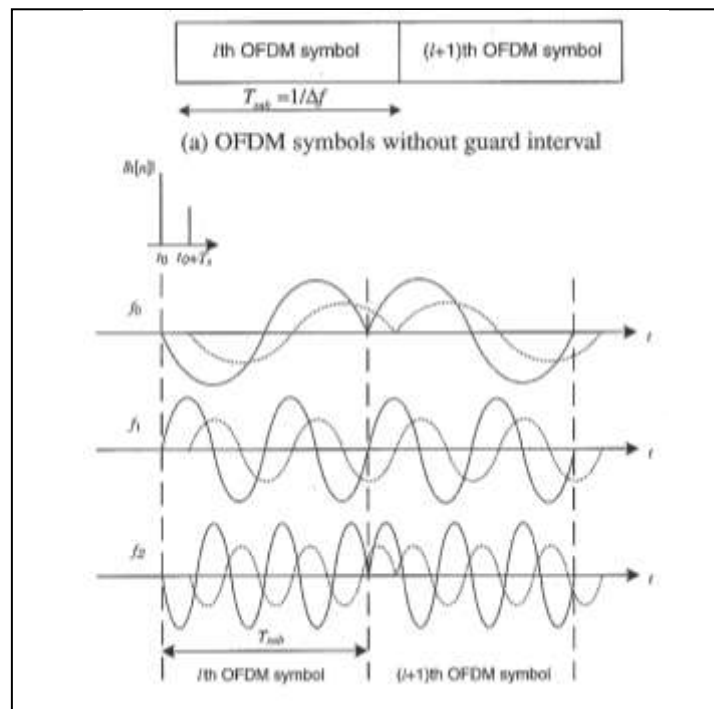


**Figure 3.7** ISI effect in OFDM system.

3.7. Even if OFDM technique can reduce the frequency selective effect due to multipath fading very well but ISI caused by multipath fading can destroy orthogonality property of OFDM signal. Thus, guard interval for preventing ISI in OFDM system is invented in order to maintain overall system performance. There are many guard time interval techniques such as CP (cyclic prefix), CS (cyclic suffix) and ZP (zero padding).

### 3.5.2 CP guard interval

CP can avoid the effect of ISI by extending OFDM symbol time where some of copied data at the end of each OFDM symbol is inserted at the front of symbol. Let  $T_G$  is the length of CP (number of copied sample data) then length of OFDM symbol with CP can be written by  $T_{sym} = T_{sub} + T_G$ . Figure 3.8 shows consecutive OFDM symbols with CP guard interval and its performance on ISI

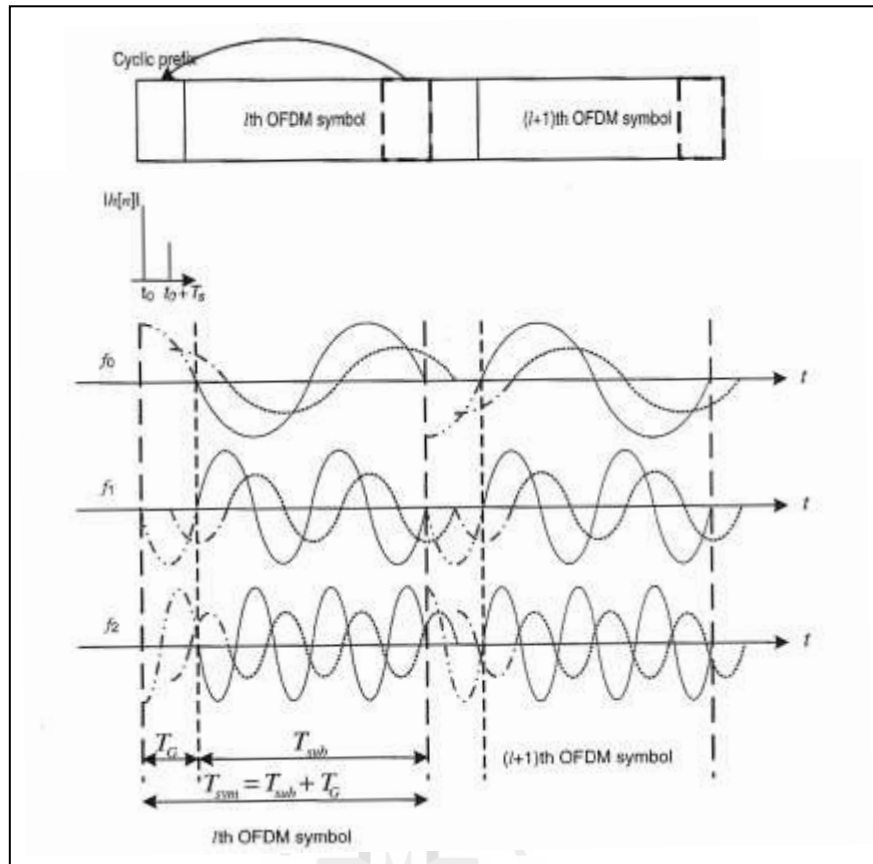


**Figure 3.8** ISI effect with CP guard interval.

avoidance. As seen in figure, the effect of ISI can be limited in CP interval if the length of CP is greater than the maximum delay of channel impulse response. Then the orthogonality of OFDM signal can be given by

$$\frac{1}{T_{sub}} \int_0^{T_{sub}} e^{j2\pi f_k(t-t_0)} e^{j2\pi f_i(t-t_0)} dt = 0, \quad k \neq i \quad (3.11)$$

for the OFDM symbol with delay  $t_0$  and

$$\frac{1}{T_{sub}} \int_0^{T_{sub}} e^{j2\pi f_k(t-t_0)} e^{j2\pi f_i(t-t_0-T_s)} dt = 0, \quad k \neq i \quad (3.12)$$

for the OFDM symbol with delay  $t_0 + T_s$ .

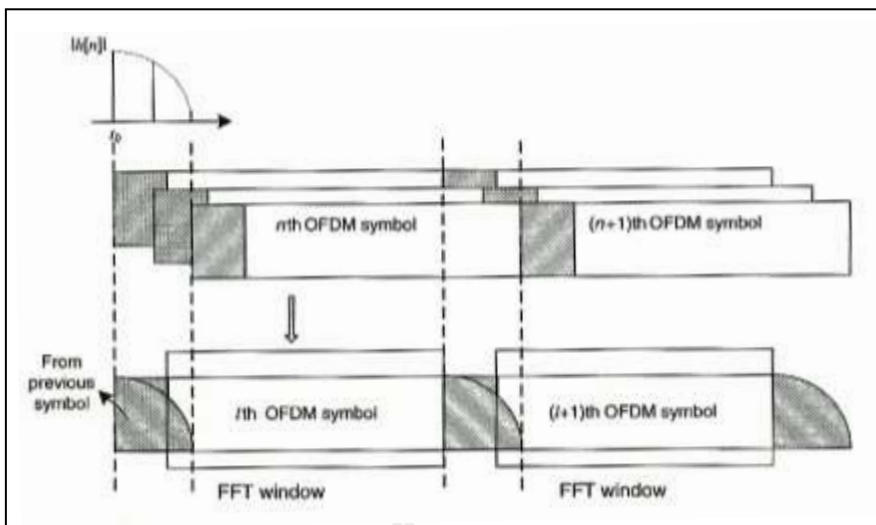


**Figure 3.9** ISI effect when CP length is less than maximum delay.

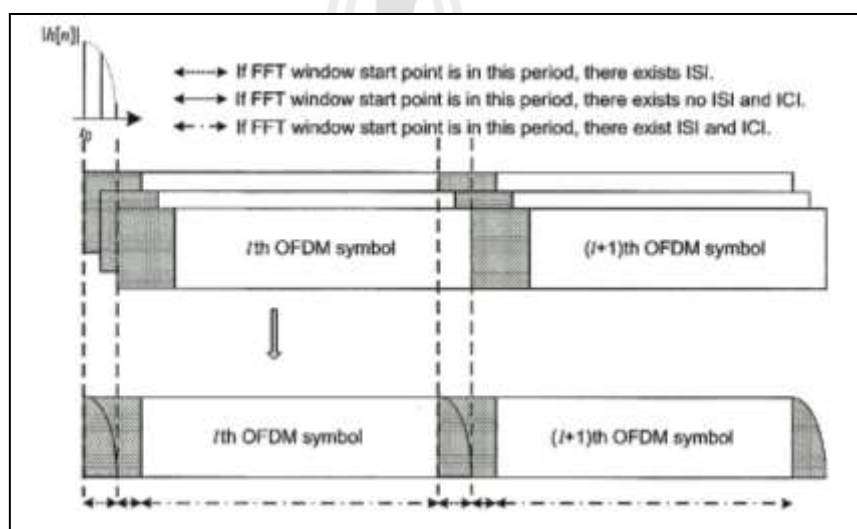


**Figure 3.10** The effect of timing offset.

Figure 3.9 shows OFDM signals with CP guard interval when length of CP is less than the maximum delay of channel impulse. As seen in figure, the ISI effect still exists due to the lack of CP length and thus more extension of CP should be used in order to improve the performance. In practical system, there is not only multipath fading that causes ISI in OFDM system but timing offset due to the error of

OFDM symbol synchronization is also considered. Figure 3.10 shows that even if length of CP is greater than the maximum delay of channel but ISI can exist. The existence of ISI depends on the starting point of FFT window where there still is ISI if the start point is less than maximum delay of channel impulse and if it is more than CP interval, it produces not only ISI but also ICI. Therefore, the start point of FFT should have value between maximum delay of channel impulse and the beginning of OFDM data symbol.

In the case that system can completely eliminate ISI with the help of CP and the starting point of FFT window in the appropriate position, then the frequency domain of the received signal can be written by

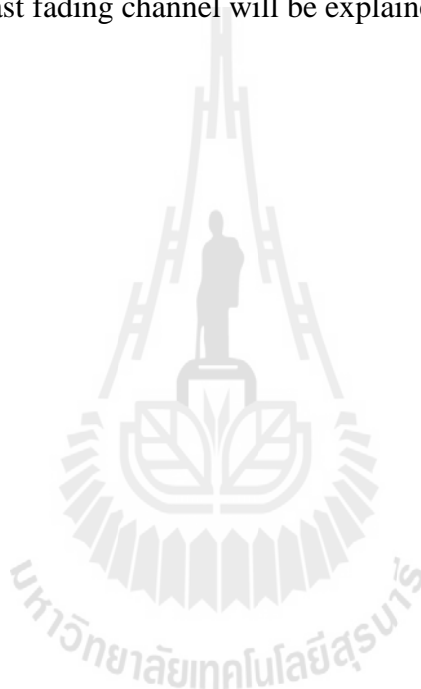
$$\begin{aligned}
Y_l[k] &= \frac{1}{\sqrt{N}} \sum_{n=0}^{N-1} y_l[n] e^{-j2\pi kn/N} \\
&= \frac{1}{\sqrt{N}} \sum_{n=0}^{N-1} \left\{ \sum_{m=0}^{\infty} h_l[m] x_l[n-m] + z_l[n] \right\} e^{-j2\pi kn/N} \\
&= \frac{1}{\sqrt{N}} \sum_{n=0}^{N-1} \left\{ \sum_{m=0}^{\infty} h_l[m] \left\{ \frac{1}{\sqrt{N}} \sum_{i=0}^{N-1} X_l[i] e^{j2\pi i(n-m)/N} \right\} \right\} e^{-j2\pi kn/N} + Z_l[k] \quad (3.13) \\
&= \frac{1}{N} \sum_{i=0}^{N-1} \left\{ \left\{ \sum_{m=0}^{\infty} h_l[m] e^{j2\pi im/N} \right\} X_l[i] \sum_{n=0}^{N-1} e^{j2\pi(i-k)n/N} \right\} + Z_l[k] \\
&= H_l[k] X_l[k] + Z_l[k]
\end{aligned}$$

where  $X_l[k]$ ,  $Y_l[k]$ ,  $H_l[k]$  and  $Z_l[k]$  are the transmitted data symbol, the received data symbol, the channel response in frequency domain and noise at the  $k^{\text{th}}$  subcarrier and the  $l^{\text{th}}$  OFDM symbol, respectively.

### 3.6 Chapter summary

The OFDM technology was found for a long time. By using orthogonal subcarriers, it improves bandwidth efficiency more than other types of multiple

subcarrier technique. In addition, with the help of CP and the transformation of system bandwidth into multiple subchannels, it makes OFDM signal to resist to ISI and frequency selective fading. Thus, it is a useful technique especially for broadband communications. However, the effect of frequency offset due to the difference between the transmitted local frequency and the received local frequency as well as the effect of fast fading channel are not considered in this chapter. The effect of frequency offset and fast fading channel will be explained in the next chapter.



# CHAPTER IV

## CFO AND CHANNEL ESTIMATION

### 4.1 Introduction

This chapter describes the effect of CFO due to the difference of carrier frequency between transmitter and receiver that reduces the performance in OFDM system. This chapter also presents some of popular techniques which are used to compensate CFO for both training scheme and pilot scheme. In addition, some background of channel estimation for OFDM and MIMO-OFDM systems are also presented.

### 4.2 CFO effect

The baseband signal is transformed into passband signal by modulating with carrier signal (high frequency signal). Then it is transmitted into the wireless channel. This signal is transformed back to baseband signal at receiver by demodulating with the same frequency of carrier signal. Normally, there are some carrier frequency errors between transmitter and receiver. The difference of carrier frequency can be caused by phase noise of local oscillator, frequency Doppler  $f_d$  and the physical properties of crystal in crystal oscillator. Frequency offset due to frequency Doppler can be given by

$$f_d = \frac{\Delta v \cdot f_c}{c} \quad (4.1)$$

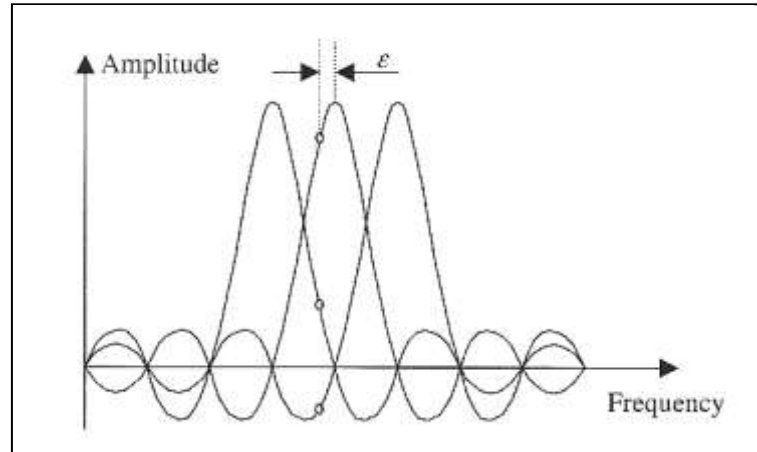


**Figure 4.1** ICI due to  $\varepsilon$ .

where  $f_c$  is carrier frequency,  $c$  is the velocity of light in the medium and  $\Delta v$  is the velocity of the receiver relative to the source. It is positive when the source and the receiver are moving towards each other. Assuming that  $f_{offset}$  is the difference of carrier frequency  $f_{offset} = f_c - f'_c$  then based on (3.13), we can write the received OFDM signal in time domain with the effect of CFO by

$$y[n] = e^{j2\pi f_{offset} t} \cdot \frac{1}{\sqrt{N}} \sum_{k=0}^{N-1} H[k] X[k] e^{j2\pi kn/N} + z[n] \quad (4.2)$$

By replacing  $t$  in (4.2) with sampling time  $nT_s$  where  $T_s = \frac{1}{N \cdot \Delta f}$ , then (4.2) can be

rewritten by

$$\begin{aligned} y[n] &= \frac{1}{\sqrt{N}} \sum_{k=0}^{N-1} H[k] X[k] e^{j2\pi \left( k + \frac{f_{offset}}{\Delta f} \right) n/N} + z[n] \\ &= \frac{1}{\sqrt{N}} \sum_{k=0}^{N-1} H[k] X[k] e^{j2\pi (k + \varepsilon) n/N} + z[n] \end{aligned} \quad (4.3)$$

where  $\varepsilon$  is the normalized carrier frequency offset,  $T_s$  is the sampling period and  $\Delta f$  is a subcarrier spacing.

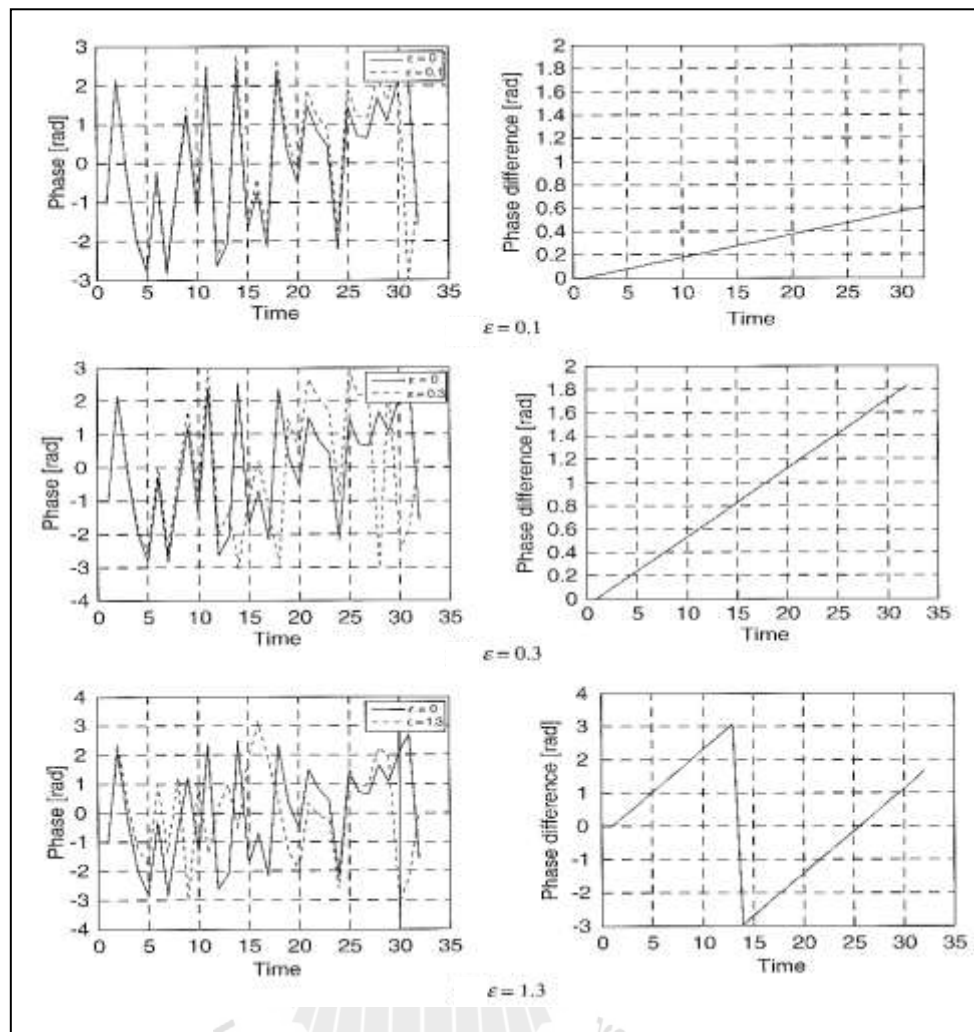


**Figure 4.2** Effect of CFO on the received signal in time domain.

Actually, CFO can be separated into two parts which are integer CFO  $\varepsilon_i$  and fractional CFO  $\varepsilon_f$  where  $\varepsilon = \varepsilon_i + \varepsilon_f$ . As shown in (4.3), CFO causes phase offset by  $2\pi n\varepsilon$  for each sampled index  $n$  thus it causes frequency shifting in frequency domain by  $\varepsilon$  which can be shown in table 4.1.

Figure 4.1 shows the effect of CFO for frequency domain signal  $X[k]$ . As seen in figure, CFO produces ICI due to the discrepancy of signal sample in frequency domain by  $\varepsilon$ .

**Table 4.1** Effect of CFO on the received signal.

Domain	Received signal	Effect of CFO on the received signal
Time	$y[n]$	$e^{j2\pi n\epsilon/N} x[n]$
Frequency	$Y[k]$	$X[k - \epsilon]$

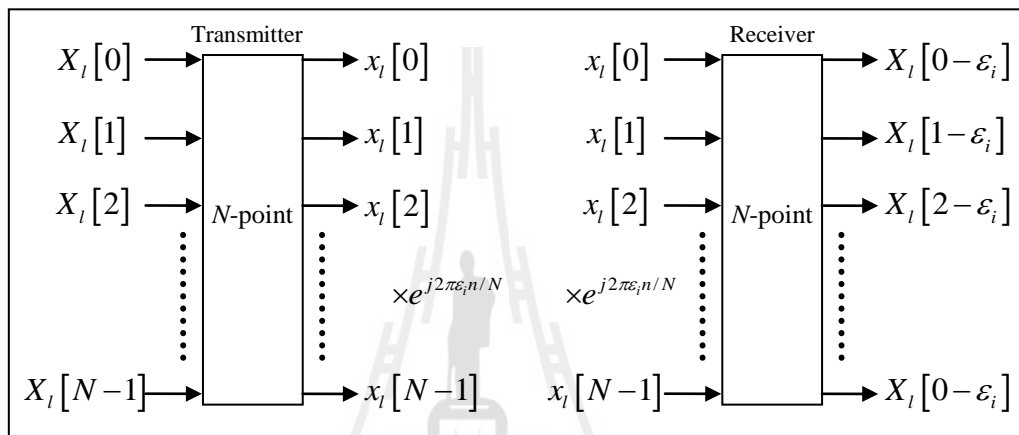
**Figure 4.3** Effect of integer CFO.

Figure 4.2 shows phase shifting of received signal in time domain by using 32 points FFT, QAM modulation and assuming that there is no noise in system. The solid line and the dot line present system without CFO ( $\epsilon = 0$ ) and system with CFO respectively. As seen in figure, phase of received signal goes faster if CFO becomes larger where the phase transition is linear and its slope is depended on CFO value.

#### 4.2.1 The effect of integer CFO

The effect of integer CFO can be shown in figure 4.3. As seen in the figure, the time domain transmitted signal  $\{x[n]\}_{n=0}^N$  affects by integer CFO  $\epsilon_i$ . This integer CFO causes phase shifting in the received signal  $e^{j2\pi\epsilon_i n/N} x[n]$  where channel

effect is not considered. It causes frequency shifting by  $\varepsilon_i$  of the frequency domain signal which is  $X[k - \varepsilon_i]$ . For example, if  $\varepsilon_i = 1$  then  $X[1]$  will be moved to the second subcarrier index and  $X[2]$  will be moved to the third subcarrier index. Thus, the integer CFO can significantly reduce the BER performance. However, the integer CFO does not produce ICI.

#### 4.2.2 The effect of fractional CFO

The effect of fractional CFO can be described by taking FFT operation with (4.3) and replacing  $\varepsilon$  with  $\varepsilon_f$ . Then the received signal in frequency domain can be given by

$$\begin{aligned}
Y_l[k] &= \text{FFT} \{y_l[n]\} = \sum_{n=0}^{N-1} y_l[n] e^{-\frac{j2\pi kn}{N}} \\
&= \sum_{n=0}^{N-1} \frac{1}{N} \sum_{m=0}^{N-1} H_l[m] X_l[m] e^{\frac{j2\pi(m+\varepsilon_f)n}{N}} e^{-\frac{j2\pi kn}{N}} + \sum_{n=0}^{N-1} z_l[n] e^{-\frac{j2\pi kn}{N}} \\
&= \frac{1}{N} \sum_{m=0}^{N-1} H_l[m] X_l[m] \sum_{n=0}^{N-1} e^{\frac{j2\pi(m-k+\varepsilon_f)n}{N}} + Z_l[k] \\
&= \frac{1}{N} H_l[k] X_l[k] \sum_{n=0}^{N-1} e^{\frac{j2\pi\varepsilon_f n}{N}} + \frac{1}{N} \sum_{\substack{m=0, \\ m \neq k}}^{N-1} H_l[m] X_l[m] \sum_{n=0}^{N-1} e^{\frac{j2\pi(m-k+\varepsilon_f)n}{N}} + Z_l[k] \\
&= \frac{1}{N} \frac{1 - e^{j2\pi\varepsilon_f}}{1 - e^{\frac{j2\pi\varepsilon_f}{N}}} H_l[k] X_l[k] + \frac{1}{N} \sum_{\substack{m=0, \\ m \neq k}}^{N-1} H_l[m] X_l[m] \frac{1 - e^{j2\pi(m-k+\varepsilon_f)}}{1 - e^{\frac{j2\pi(m-k+\varepsilon_f)}{N}}} + Z_l[k] \\
&= \frac{1}{N} \frac{e^{j\pi\varepsilon_f} (e^{-j\pi\varepsilon_f} - e^{j\pi\varepsilon_f})}{e^{j\pi\varepsilon_f/N} \left( e^{\frac{-j\pi\varepsilon_f}{N}} - e^{\frac{j\pi\varepsilon_f}{N}} \right)} H_l[k] X_l[k] \\
&\quad + \frac{1}{N} \sum_{\substack{m=0, \\ m \neq k}}^{N-1} H_l[m] X_l[m] \frac{e^{j\pi(m-k+\varepsilon_f)} (e^{-j\pi(m-k+\varepsilon_f)} - e^{j\pi(m-k+\varepsilon_f)})}{e^{\frac{j\pi(m-k+\varepsilon_f)}{N}} \left( e^{\frac{-j\pi(m-k+\varepsilon_f)}{N}} - e^{\frac{j\pi(m-k+\varepsilon_f)}{N}} \right)} + Z_l[k]
\end{aligned}$$

$$\begin{aligned}
&= e^{\frac{j\pi\varepsilon_f(N-1)}{N}} \left\{ \frac{\sin(\pi\varepsilon_f)}{N \sin(\pi\varepsilon_f/N)} \right\} H_l[k] X_l[k] \\
&+ e^{\frac{j\pi\varepsilon_f(N-1)}{N}} \sum_{\substack{m=0, \\ m \neq k}}^{N-1} \frac{\sin(\pi(m-k+\varepsilon_f))}{N \sin(\pi(m-k+\varepsilon_f)/N)} H_l[m] X_l[m] e^{\frac{j\pi(m-k)(N-1)}{N}} + Z_l[k] \\
&= \frac{\sin(\pi\varepsilon_f)}{N \sin(\pi\varepsilon_f/N)} e^{\frac{j\pi\varepsilon_f(N-1)}{N}} H_l[k] X_l[k] + I_l[k] + Z_l[k] \tag{4.4}
\end{aligned}$$

where

$$I_l[k] = e^{\frac{j\pi\varepsilon_f(N-1)}{N}} \sum_{\substack{m=0, \\ m \neq k}}^{N-1} \frac{\sin(\pi(m-k+\varepsilon_f))}{N \sin(\pi(m-k+\varepsilon_f)/N)} H_l[m] X_l[m] e^{\frac{j\pi(m-k)(N-1)}{N}} \tag{4.5}$$

The first term in (4.4) refers to the desired signal with phase distortion and amplitude attenuation due to the fractional CFO where  $I[k]$  refers to ICI from another subchannel. From (4.4), if the fractional CFO exists, it destroys the orthogonal property of an OFDM system whether the integer CFO is considered in system or not. Figure 4.4 shows the frequency response of the received signal  $Y[k]$  where  $k=5$ ,  $N=16$  and assuming that  $H[k]=1$ . As seen in figure, the frequency responses for  $k \neq 5$  are equal to 0 in case that  $\varepsilon_f = 0$ . Thus there is no ICI in system. But for  $\varepsilon_f \neq 0$ , it produces ICI in system where ICI power increases as the fractional CFO increases. The increasing in ICI power can reduce BER performance so the effect of fractional CFO should be compensated.

From above descriptions, the BER performance from both integer CFO and fractional CFO can be reduced significantly. Therefore, these parameters should be estimated and compensated in order to maintain the required system performance.

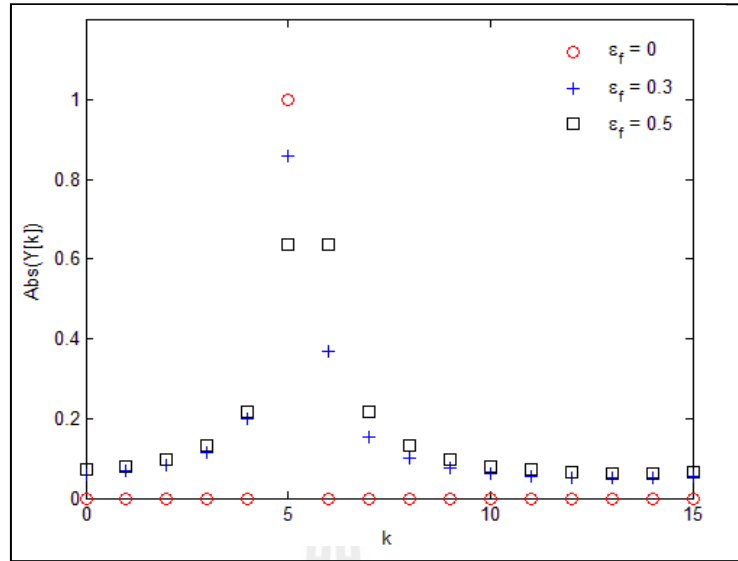


**Figure 4.4** Effect of fractional CFO.

In the next section, techniques for CFO estimation are described for both training aided and pilot aided.

### 4.3 CFO estimation techniques

#### 4.3.1 CFO estimation by exploiting CP

In the case that there is no time offset, CFO causes phase shifting to the received signal sample  $y[n]$  by  $2\pi n\varepsilon / N$  as indicated in Table 4.1. Based on using CP, CP is the guard interval which is used for preventing ISI. The information in CP is the copied data of the beginning of the symbol. The spacing between the copied data in CP and the original data is  $N$  samples. It causes phase difference by  $2\pi N\varepsilon / N = 2\pi\varepsilon$ . Therefore, CFO can be estimated by measuring phase difference between CP and its original data which can be written by  $\varepsilon = (1/2\pi) \arg \{ y_l^*[n] y_l[N+n] \}$  ( $n = 0, 2, \dots, N_{CP} - 1$ ). By using all CP data, the estimated CFO for each OFDM symbol using CP can be given by

$$\varepsilon = \frac{1}{2\pi} \angle \sum_{n=1}^{N_{CP}} \{y_l^*[n] y_l[N+n]\} \quad (4.6)$$

where  $\angle$  refers to phase calculation of the complex number. Therefore, the estimation range of (4.6) is  $[-\pi, \pi) / 2\pi = [-0.5, 0.5)$  which is  $|\varepsilon| \leq 0.5$ . However, this technique is not suitable for the case that  $|\varepsilon|$  is greater than 0.5.

### 4.3.2 CFO estimation by using training symbol

Based on using CP for CFO estimation, CP can be used to estimate CFO without any loss in bandwidth efficiency where its estimation range is  $|\varepsilon| \leq 0.5$ . But in the practical system, CFO can be any value and it can exceed this estimation range. Thus the technique which offers more estimation range is necessary. As the same idea as CFO estimation by using CP, phase difference in CP technique is  $2\pi N\varepsilon / N = 2\pi\varepsilon$  due to the distance between duplicate data by  $N$  samples. Therefore, if we design an OFDM symbol with less duplicate distance than CP technique, the estimation range should be increased. Assuming that  $D$  is an integer which refers to the ratio between FFT points ( $N$ ) and the number of times of duplicate data. The OFDM symbol that its time domain signal has  $D$  times of duplicate data can be generated by inserting pilot tones in frequency domain. Where pilot tone on each subcarrier can be given by

$$X_l[k] = \begin{cases} A_m, & k = D \cdot i, i = 0, 1, \dots, (N/D - 1) \\ 0, & \text{otherwise} \end{cases} \quad (4.7)$$

Where  $A_m$  is data symbol on each subcarrier which its modulation type is M-ary and  $N/D$  is an integer where  $x_l[n]$  and  $x_l[n + N/D]$  are the same. Then the estimated CFO

by using this technique can be written by

$$\varepsilon = \frac{D}{2\pi} \arg \sum_{n=1}^{N/D-1} \{y_l^*[n] y_l[N/D+n]\} \quad (4.8)$$

As seen in (4.8), the estimation range of this technique is extended to  $|\varepsilon| \leq D/2$  where its estimation range is depended on the number of times of duplicate data  $D$ . However, (4.8) reduces the number of signal sample by  $1/D$  thus it reduces the estimation performance if noise is considered (MSE performance reduction). Thus, the duplicate data for every group in an OFDM symbol should be used in order to maintain the estimation performance where the estimated CFO from (4.8) can be rewritten by

$$\varepsilon = \frac{D}{2\pi} \arg \sum_{m=0}^{D-2} \sum_{n=1}^{N/D-1} \{y_l^*[n+mN/D] y_l[(m+1)N/D+n]\} \quad (4.9)$$

### 4.3.3 CFO estimation by using pilot tone in frequency domain

In the case that, transmitter transmits two consecutive OFDM symbols where these symbols are same. If noise is not considered in system,  $2N$  samples of the received signal in time domain can be given by

$$r[n] = \frac{1}{N} \sum_{k=0}^{N-1} X_l[k] H_l[k] e^{j2\pi(k+\varepsilon)n/N} \quad (4.10)$$

where  $n=0, 2, \dots, 2N-1$ . By taking FFT operation, the received signal in frequency domain of the first OFDM symbol when  $n=0, 2, \dots, N-1$  can be written by

$$R_1[k] = \sum_{n=0}^{N-1} r[n] e^{-j2\pi nk/N} \quad (4.11)$$

where  $k = 0, 1, 2, \dots, N-1$ . Then as same as (4.11), the received signal in frequency domain of the second OFDM symbol when  $n = N, 2, \dots, 2N-1$  can be written by

$$\begin{aligned} R_2[k] &= \sum_{n=N}^{2N-1} r[n] e^{-j2\pi nk/N} \\ &= \sum_{n=0}^{N-1} r[n+N] e^{-j2\pi nk/N} \end{aligned} \quad (4.12)$$

Based on (4.11) and (4.12), the relationship between time domain signal and frequency domain signal with the effect of CFO can be shown by

$$r[n+N] = r[n] e^{j2\pi \varepsilon} \xrightarrow{FFT} R_2[k] = R_1[k] e^{j2\pi \varepsilon} \quad (4.13)$$

If there is noise in system, then (4.13) can be rewritten by

$$\begin{aligned} Y_1[k] &= R_1[k] + Z_1[k] \\ Y_2[k] &= R_1[k] e^{j2\pi \varepsilon} + Z_2[k] \end{aligned} \quad (4.14)$$

From (4.14), the estimated CFO can be performed by measuring the phase shift of pilot tone in consecutive OFDM symbols and it can be written by

$$\varepsilon = \frac{1}{2\pi} \tan^{-1} \left\{ \frac{\sum_{k=0}^{N-1} \text{Im} [Y_1^*[k] Y_2[k]]}{\sum_{k=0}^{N-1} \text{Re} [Y_1^*[k] Y_2[k]]} \right\} \quad (4.15)$$

From (4.15), it is a popular technique which was firstly proposed by Moose (1994) and there are many works which are developed based on this technique. However, the estimation range of this technique is  $|\varepsilon| \leq 0.5$  and it reduces half of bandwidth efficiency due to transmitting the duplicate OFDM symbol. Therefore, to improve bandwidth efficiency, this technique is usually inserted at the beginning before

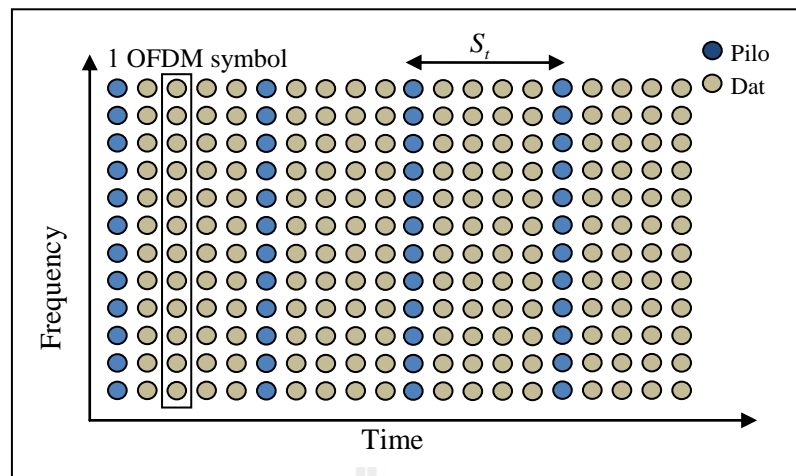


**Figure 4.5** Block type pilot arrangement.

transmitting data in order to reduce the number of duplicate symbols. In addition, by using frequency domain signal for CFO estimation, it is possible to choose or use some pilot tones for CFO estimation where the estimation can be performed by measuring the phases on pilot tones. Therefore, the estimation can be continued due to the insertion of pilot tones in every OFDM symbols and it also improves bandwidth efficiency. Furthermore, the use of pilot tone for CFO estimation can improve bandwidth efficiency but this technique requires the channels on consecutive OFDM symbols to be unchanged (the consecutive symbols which are used for measuring phase). Thus it gives a significant estimation error if channels on each OFDM symbol are different.

## 4.4 Channel estimation in OFDM system

### 4.4.1 Pilot tones for channel estimation

#### *Block type*

The channel estimation based on block type pilot arrangement can be shown in Figure 4.5. As seen in the figure, the pilot tones are inserted in all subcarriers

for each OFDM symbol but not all OFDM symbols where these symbols are used for channel estimation. The block type pilot arrangement can be called as training symbol where all subcarriers in an OFDM symbol are used for channel estimation. These training symbols are inserted continuously along time axis in order to track channel variations. The OFDM symbol which does not contain pilot tones uses the previous estimated channel from training symbol to be its estimated channel or by interpolating the estimated channels from the right side and the left side training symbol. From Figure 4.5,  $S_t$  is the period of training symbol insertion and thus  $S_t$  should be less than channel coherence time in order to keep track of the variations of channel where channel coherence time is the inversion of frequency Doppler  $f_d$ . Then the period of training symbol insertion  $S_t$  should be valid by

$$S_t \leq \frac{1}{f_d} \quad (4.16)$$

The block type pilot arrangement is the effective channel estimation technique especially for frequency selective channel where it reduces estimation error due to the used of large number of pilot tones. However, if channel acts as fast fading and causes the different channel response on each OFDM symbol, thus more frequent training symbol should be adopted in order to track the channel.

### ***Comb type***

The channel estimation based on comb type pilot arrangement can be shown in Figure 4.6 where  $S_f$  is the pilot tone insertion period in frequency domain. As seen in the figure, the pilot tones are inserted in every OFDM symbol but not all subcarriers. The whole estimated channel for each OFDM symbol including estimated channel on data subcarrier can be performed by using channel estimation on pilot tone

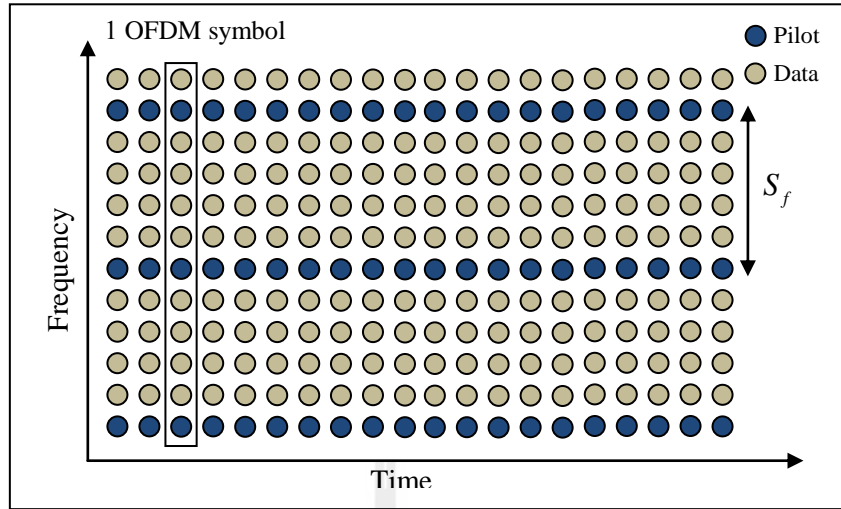


**Figure 4.6** Comb type pilot arrangement.

and interpolation technique for non-pilot subcarrier. Therefore, the pilot tones should be placed with distance at least equal to coherence bandwidth in order to avoid channel estimation error from the lack of pilot tone. Then pilot frequency spacing  $S_f$  can be written by

$$S_f \leq \frac{1}{\sigma_{\max}} \quad (4.17)$$

where  $\sigma_{\max}$  is the maximum delay of channel impulse response and it is an inversion of coherence bandwidth.

The comb type offers ability to track channel when channel acts as fast fading due to the insertion of pilot tones in every OFDM symbol. However, by using some of pilot tones for channel estimation, the estimation performance is not only depended on the number of pilot tones but the interpolation technique should be considered. There are many interpolation techniques such as linear interpolation, spline interpolation and lowpass interpolation.

#### 4.4.2 Channel estimation technique in OFDM system

If training symbol is used for channel estimation in an OFDM system, then the transmitted pilot matrix can be given by

$$\mathbf{X} = \begin{bmatrix} X[0] & 0 & \dots & 0 \\ 0 & X[1] & & \vdots \\ \vdots & & \ddots & 0 \\ 0 & \dots & 0 & X[N-1] \end{bmatrix} \quad (4.18)$$

where  $X[k]$  is the pilot symbol at the  $k^{\text{th}}$  pilot subcarrier with  $E\{X[k]\} = 0$  and  $\text{Var}\{X[k]\} = \sigma_x^2$  ( $E\{\}$  refers to expectation and  $\text{Var}\{\}$  refers to variance). If there is no time offset and frequency offset, the received signal matrix can be written by

$$\begin{bmatrix} Y[0] \\ Y[1] \\ \vdots \\ Y[N-1] \end{bmatrix} = \begin{bmatrix} X[0] & 0 & \dots & 0 \\ 0 & X[1] & & \vdots \\ \vdots & & \ddots & 0 \\ 0 & \dots & 0 & X[N-1] \end{bmatrix} \begin{bmatrix} H[0] \\ H[1] \\ \vdots \\ H[N-1] \end{bmatrix} + \begin{bmatrix} Z[0] \\ Z[1] \\ \vdots \\ Z[N-1] \end{bmatrix} \quad (4.19)$$

which can be reduced into

$$\mathbf{Y} = \mathbf{XH} + \mathbf{Z} \quad (4.20)$$

Where  $\mathbf{H}$  and  $\mathbf{Z}$  are the channel vector and the noise vector with  $E\{Z[k]\} = 0$  and  $\text{Var}\{Z[k]\} = \sigma_z^2$ , respectively.

#### *Least square channel estimation (LSCE) technique*

The objective of least square estimation is to minimize the sum of the squares of the errors made in the results of every single equation. From (4.20), the objective function of least square estimation can be given by

$$\begin{aligned}
J(\mathbf{H}) &= \|\mathbf{Z}\|^2 \\
&= \|\mathbf{Y} - \mathbf{X}\mathbf{H}\|^2 \\
&= (\mathbf{Y} - \mathbf{X}\mathbf{H})^H (\mathbf{Y} - \mathbf{X}\mathbf{H}) \\
&= \mathbf{Y}^H \mathbf{Y} - \mathbf{Y}^H \mathbf{X}\mathbf{H} - \mathbf{H}^H \mathbf{X}^H \mathbf{Y} + \mathbf{H}^H \mathbf{X}^H \mathbf{X}\mathbf{H}
\end{aligned} \tag{4.21}$$

where  $\mathbf{H}$  is the estimated channel and  $( )^H$  refers to conjugate transpose. Then we can show  $\mathbf{H}$  that minimizes the objective function from (4.21) by

$$\frac{\partial J(\mathbf{H})}{\partial \mathbf{H}} = -2(\mathbf{X}^H \mathbf{Y}) + 2(\mathbf{X}^H \mathbf{X}\mathbf{H}) = 0 \tag{4.22}$$

The result from (4.22) can be given by  $\mathbf{X}^H \mathbf{X}\mathbf{H} = \mathbf{X}^H \mathbf{Y}$ . Then the estimated channel from LSCE can be written by

$$\mathbf{H}_{LS} = (\mathbf{X}^H \mathbf{X})^{-1} \mathbf{X}^H \mathbf{Y} = \mathbf{X}^{-1} \mathbf{Y} \tag{4.23}$$

From (4.23),  $\mathbf{X}$  is the diagonal matrix and there is no ICI in system then channel estimation (4.23) can be rewritten for subcarrier channel estimation by

$$H_{LS}[k] = \frac{Y[k]}{X[k]} \tag{4.24}$$

From (4.24), it is used to estimate the channel when comb type pilot arrangement is considered. The MSE (mean square error) of LSCE can be written by

$$\begin{aligned}
MSE_{LS} &= E \left\{ (\mathbf{H} - \mathbf{H}_{LS})^H (\mathbf{H} - \mathbf{H}_{LS}) \right\} \\
&= E \left\{ (\mathbf{H} - \mathbf{X}^{-1} \mathbf{Y})^H (\mathbf{H} - \mathbf{X}^{-1} \mathbf{Y}) \right\}
\end{aligned}$$

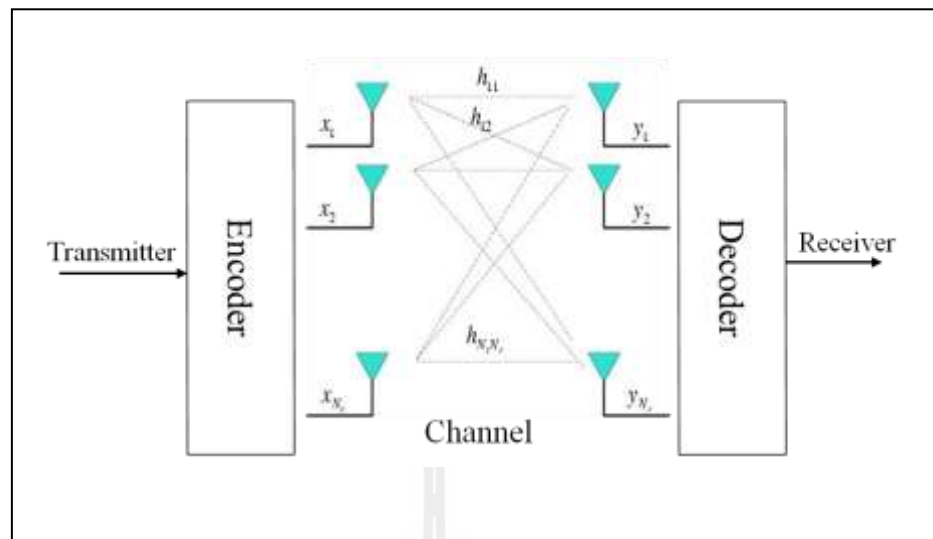


Figure 4.7 MIMO system.

$$\begin{aligned}
 &= E \left\{ (\mathbf{X}^{-1} \mathbf{Z})^H (\mathbf{X}^{-1} \mathbf{Z}) \right\} \\
 &= E \left\{ \mathbf{Z}^H (\mathbf{X} \mathbf{X}^H)^{-1} \mathbf{Z} \right\} \\
 &= \frac{\sigma_z^2}{\sigma_x^2} \mathbf{I}_N
 \end{aligned} \tag{4.25}$$

where  $\mathbf{I}_N$  is  $N \times N$  identity matrix. From (4.25), the estimation performance of LSCE depends on the ratio of noise power and signal power where a higher signal power gains a better estimation performance.

#### 4.4.3 Channel estimation technique in MIMO-OFDM system

Even MIMO is merged to OFDM for improving QOS and transmission rate effectively but MIMO increases the complexity of system due to many numbers of inputs and outputs. The channel estimation in MIMO system is complex as the number of unknown subchannel  $h_{ij}$  where MIMO system can be shown in Figure 4.7. The channel matrix for any  $k^{\text{th}}$  subcarrier in MIMO-OFDM system can be written by

$$\mathbf{H}_k = \begin{bmatrix} h_{1,1}^k & h_{1,2}^k & \cdots & h_{1,N_T}^k \\ h_{2,1}^k & h_{2,2}^k & \cdots & h_{2,N_T}^k \\ \vdots & \vdots & \ddots & \vdots \\ h_{N_R,1}^k & h_{N_R,2}^k & \cdots & h_{N_R,N_T}^k \end{bmatrix} \quad (4.26)$$

where  $N_T$  and  $N_R$  are the number of transmitted antennas and the number of received antennas respectively. In order to estimate channel matrix in (4.26), transmitter has to transmit at least  $N_T$  consecutive pilot tone (training sequence). The training sequence for any  $k^{\text{th}}$  subcarrier can be given by

$$\mathbf{X}_k = \begin{bmatrix} X_{1,1}[k] & X_{1,2}[k] & \cdots & X_{1,N_T}[k] \\ X_{2,1}[k] & X_{2,2}[k] & \cdots & X_{2,N_T}[k] \\ \vdots & \vdots & \ddots & \vdots \\ X_{N_T,1}[k] & X_{N_T,2}[k] & \cdots & X_{N_T,N_T}[k] \end{bmatrix} \quad (4.27)$$

where  $X_{i,j}[k]$  refers to pilot symbol on the  $k^{\text{th}}$  subcarrier of the  $i^{\text{th}}$  transmitted antenna and the  $j^{\text{th}}$  OFDM symbol. From (4.26) and (4.27), the received signal matrix on the  $k^{\text{th}}$  subcarrier can be given by

$$\mathbf{Y}_k = \mathbf{H}_k \mathbf{X}_k + \mathbf{Z}_k \quad (4.28)$$

where

$$\mathbf{Y}_k = \begin{bmatrix} Y_{1,1}[k] & Y_{1,2}[k] & \cdots & Y_{1,N_T}[k] \\ Y_{2,1}[k] & Y_{2,2}[k] & \cdots & Y_{2,N_T}[k] \\ \vdots & \vdots & \ddots & \vdots \\ Y_{N_R,1}[k] & Y_{N_R,2}[k] & \cdots & Y_{N_R,N_T}[k] \end{bmatrix} \quad (4.29)$$

$$\mathbf{Z}_k = \begin{bmatrix} Z_{1,1}[k] & Z_{1,2}[k] & \cdots & Z_{1,N_T}[k] \\ Z_{2,1}[k] & Z_{2,2}[k] & \cdots & Z_{2,N_T}[k] \\ \vdots & \vdots & \ddots & \vdots \\ Z_{N_R,1}[k] & Z_{N_R,2}[k] & \cdots & Z_{N_R,N_T}[k] \end{bmatrix} \quad (4.30)$$

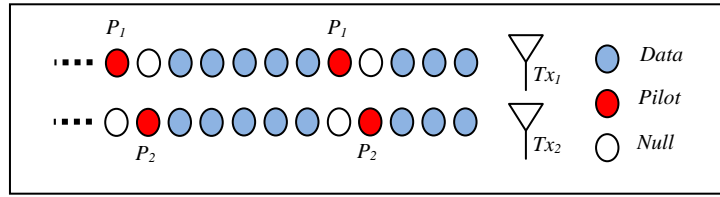


**Figure 4.8** Orthogonal pilot scheme.

Where  $\mathbf{Y}_k$  and  $\mathbf{Z}_k$  are the received signal matrix and the noise matrix on the  $k^{\text{th}}$  subcarrier respectively. From (4.28), the channel estimation based on least square technique can be written by

$$\mathbf{H}_{k,LS} = (\mathbf{X}_k^H \mathbf{X}_k)^{-1} \mathbf{X}_k^H \mathbf{Y}_k = \mathbf{X}_k^\dagger \mathbf{Y}_k \quad (4.31)$$

where  $(\ )^\dagger$  is the pseudo-inverse and  $\mathbf{X}_k^\dagger = (\mathbf{X}_k^H \mathbf{X}_k)^{-1} \mathbf{X}_k^H$ .

In MIMO-OFDM system, it is necessary to transmit pilot tones at least  $N_T$  OFDM symbol in order to perform (4.31). Therefore, if channel changes during transmitting  $N_T$  OFDM symbol, it may give an excessive estimation error and lead to BER performance reduction.

Furthermore, Qiao (2004) has proposed the pilot scheme for channel estimation in a MIMO-OFDM system in order to reduce the estimation complexity. This pilot scheme can be shown in Figure 4.8 and it is called as orthogonal pilot scheme. As seen in the figure, the pilot tones are placed orthogonally over frequency axis and space axis where there is no interference on each pilot tone from other antennas. Therefore, the complexity of MIMO-OFDM channel estimation can be reduced to OFDM channel estimation which provides less complexity and faster estimation process. In addition, the estimation process of this technique can be carried out with only one OFDM symbol and this pilot scheme can be inserted in every

OFDM symbol. Thus it is an effective technique for mobile broadband communications.

#### 4.5 Chapter summary

From this chapter, we can see that CFO estimation and channel estimation are very important because the better estimation can improve the performance of data recovery at receiver. The performance of channel estimation is also based on CFO estimation in which it can be improved by increasing the accuracy of CFO estimation. CFO estimation can be performed in both time and frequency domains where in time domain CFO can be estimated by using CP and training symbol. Based on using CP, this technique can save system bandwidth efficiency as well. But it may cause an estimation error if there is ISI in system and its estimation range is limited by  $\pm 0.5$ . Based on training symbol, not only the estimation range but also the estimation performance due to large number of training data are improved. However, if CFO is a time-varying parameter, the system bandwidth is lost due to the use of many training symbol for CFO tracking. By using pilot tones based on frequency domain estimation, CFO can be estimated and tracked by inserting pilot tones in every OFDM symbol. Thus it is a useful technique especially for mobile broadband systems. However, this technique requires channels on consecutive OFDM symbols to be constant hence this technique may produce an unexpected estimation error if channels on each OFDM symbols are different.

# CHAPTER V

## THE PROPOSED PILOT SCHEME

### 5.1 Introduction

This chapter presents an analysis and design of the proposed pilot tone for CFO and channel estimations in both OFDM and MIMO-OFDM systems. The proposed pilot tones not only can track the variations of channel and CFO but also can improve the estimation performance. This leads to BER performance enhancement. In addition, the proposed pilot scheme and its estimation technique are suitable for mobile broadband communication systems where the estimation process can be carried out with only one OFDM symbol.

### 5.2 Pilot design for OFDM system

#### 5.2.1 Null subcarriers for CFO estimation

In the OFDM system with  $N$  subcarriers, we denote  $\mathbf{X}(m) = [X_1(m) X_2(m) \cdots X_N(m)]^T$  where  $\mathbf{X}(m)$  is the transmitted signal vector in the frequency domain of the  $m^{\text{th}}$  OFDM symbol,  $N_{cp}$  is the cyclic prefix (CP) length to prevent intersymbol interference,  $\mathbf{z}(m)$  is the additive white Gaussian noise (AWGN) and  $\mathbf{H}_D$  is the channel frequency response matrix. The received signal vector in the time domain is effected by the normalized CFO ( $\varepsilon$ ) which is given by

$$\mathbf{y}(m) = \text{diag} \left[ 1, e^{\frac{j2\pi\varepsilon}{N}}, \dots, e^{\frac{j2\pi\varepsilon(N-1)}{N}} \right] e^{j\phi_m} \mathbf{V} \mathbf{H}_D \mathbf{X}(m) + \mathbf{z}(m) \quad (5.1)$$

where  $\phi_m = 2\pi\epsilon m(N + N_{cp})/N$ ,  $\mathbf{H}_D = \text{diag}[H_1, H_2, \dots, H_N]$  and  $\mathbf{V}$  is the inverse DFT matrix  $\mathbf{V} = [\mathbf{v}_1 \ \mathbf{v}_2 \ \dots \ \mathbf{v}_N]$

$$\mathbf{v}_i = (1/\sqrt{N}) \left[ 1 \ e^{j2\pi i/N} \ e^{j2\pi(2i)/N} \ \dots \ e^{j2\pi((N-1)i)/N} \right]^T \quad (5.2)$$

Note that  $e^{j\phi_m}$  is a constant for each OFDM block and can be absorbed into  $\mathbf{H}_D$ . For the sake of simplicity, we drop  $e^{j\phi_m}$  in the following equations.

From previous chapter, CFO estimation based on the pilot tone insertion can be achieved by using Moose's technique. However, this technique requires pilot tones from the consecutive OFDM symbols in order to perform the estimation. Thus it causes an estimation error if the channel responses on each OFDM symbol are different. In addition, the estimation range of this technique is limited by  $\pm 0.5$  where it can exceed this range in the practical system. Huang and Letaef (2006) proposed CFO estimation technique by using null subcarrier insertion where the estimated CFO can be obtained by searching the estimated CFO to minimize the objective function. The estimated CFO by using null subcarrier insertion can be given by

$$\epsilon = \arg \min_{\epsilon} \sum_{i \in \Gamma} |\mathbf{v}_i^H \mathbf{D}_{\epsilon}^H \mathbf{y}|^2 \quad (5.3)$$

where  $\Gamma$  is the set of null subcarrier indexes,  $\mathbf{D}_{\epsilon} = \text{diag} \left[ 1, e^{j2\pi\epsilon/N}, \dots, e^{j2\pi\epsilon(N-1)/N} \right]$  and

$(\cdot)^H$  denotes conjugate transpose. From (5.3), the estimated normalized CFO ( $\epsilon$ ) can be obtained by searching  $\epsilon$  that minimizes signal power on null subcarriers. This technique can estimate CFO by using one OFDM symbol where its estimation range

can be extended to  $\pm 1$  for fractional CFO estimation and it also can be used for integer CFO estimation (Sameer and Kumar, 2008). This technique is an effective technique for both fractional and integer CFO but only fractional CFO is considered in this work where the integer part is assumed to be compensated by training symbol in preamble.

### ***Performance analysis***

The modified Cramér-Rao lower bound (MCRLB) is used in this work in order to investigate the performance of (5.3), where the observed data at null subcarrier position can be given by

$$Y_i = X_i H_i e^{j\pi\epsilon(N-1)/N} \cdot \left[ \frac{\sin(\pi\epsilon)}{N \cdot \sin(\pi\epsilon/N)} \right] + I_i + Z_i \quad (5.4)$$

$$I_i(\epsilon) = \sum_{\substack{m=0 \\ m \neq i}}^{N-1} X_m H_m e^{j\pi(m+\epsilon-i)(N-1)/N} \cdot \left[ \frac{\sin(\pi(m+\epsilon-i))}{N \cdot \sin(\pi(m+\epsilon-i)/N)} \right] \quad (5.5)$$

where  $Y_i$  is the received signal in the frequency domain,  $I_i$  is the ICI caused by the frequency offset,  $X_i$ ,  $H_i$  and  $Z_i$  are the modulation symbol, channel frequency response and noise at the  $i^{\text{th}}$  subcarrier respectively. From (5.4), when  $X_i$  is represented by null subcarrier ( $X_i=0$ ) then (5.4) can be rewritten by

$$Y_i = I_i + Z_i \quad (5.6)$$

Assuming that  $Z_i$  is independent from  $X_i$  where  $E\{Z_i\}=0$ ,  $Cov(Z_m Z_n^H) = 0$  and its variance is  $\sigma^2$ . Then the joint probability density function of received signal on null subcarriers  $\mathbf{Y} = [Y_1, Y_2, \dots, Y_{N_{null}}]$  for unknown parameters  $\mathbf{X}$ ,  $\mathbf{H}$  and  $\epsilon$  can be given by

$$p(\mathbf{Y}|\mathbf{X}, \mathbf{H}, \varepsilon) = \frac{1}{(\pi\sigma^2)^{N_{null}}} \exp\left(\frac{-1}{\sigma^2} \sum_{i=1}^{N_{null}} |Y_i - I_i(\mathbf{X}, \mathbf{H}, \varepsilon)|^2\right) \quad (5.7)$$

where  $\mathbf{X} = [X_1, X_2, \dots, X_N]$ ,  $\mathbf{H} = [H_1, H_2, \dots, H_N]$ ,  $N_{null}$  is the number of null subcarriers and  $|\cdot|$  stands for  $l_2$  norm. Then the MCRLB of  $\varepsilon$  is obtained by the inverse of the modified Fisher information which is defined as

$$MCRLB(\varepsilon) = \frac{1}{I_{\varepsilon\varepsilon}} = 1 / -E \left\{ \frac{\partial^2 \ln p(\mathbf{Y}|\mathbf{X}, \mathbf{H}, \varepsilon)}{\partial \varepsilon^2} \right\} \quad (5.8)$$

where the modified Fisher information from (5.8) is given by

$$\begin{aligned} I_{\varepsilon\varepsilon} &= -E \left\{ \frac{\partial^2 \ln p(\mathbf{Y}|\mathbf{X}, \mathbf{H}, \varepsilon)}{\partial \varepsilon^2} \right\} \\ &= -E \left\{ \frac{\partial}{\partial \varepsilon^2} \left\{ -\ln \left( (\pi\sigma^2)^{N_{null}} - \frac{1}{\sigma^2} \sum_{i=1}^{N_{null}} (Y_i - I_i(\mathbf{X}, \mathbf{H}, \varepsilon))^* (Y_i - I_i(\mathbf{X}, \mathbf{H}, \varepsilon)) \right) \right\} \right\} \\ &= -E \left\{ \frac{\partial}{\partial \varepsilon^2} \left\{ -\frac{1}{\sigma^2} \sum_{i=1}^{N_{null}} \left[ Y_i^* Y_i - Y_i^* I_i(\mathbf{X}, \mathbf{H}, \varepsilon) - I_i^*(\mathbf{X}, \mathbf{H}, \varepsilon) Y_i + I_i^*(\mathbf{X}, \mathbf{H}, \varepsilon) I_i(\mathbf{X}, \mathbf{H}, \varepsilon) \right] \right\} \right\} \end{aligned} \quad (5.9)$$

where  $E\{Y_i\} = E\{I_i(\mathbf{X}, \mathbf{H}, \varepsilon)\} + E\{Z_i\} = E\{I_i(\mathbf{X}, \mathbf{H}, \varepsilon)\}$ . Then, (5.9) can be rewritten

by

$$\begin{aligned} I_{\varepsilon\varepsilon} &= \frac{1}{\sigma^2} \sum_{i=1}^{N_{null}} E \left\{ \frac{\partial}{\partial \varepsilon} I_i(\mathbf{X}, \mathbf{H}, \varepsilon) \frac{\partial}{\partial \varepsilon} I_i^*(\mathbf{X}, \mathbf{H}, \varepsilon) + \frac{\partial}{\partial \varepsilon} I_i^*(\mathbf{X}, \mathbf{H}, \varepsilon) \frac{\partial}{\partial \varepsilon} I_i(\mathbf{X}, \mathbf{H}, \varepsilon) \right\} \\ &= \frac{2}{\sigma^2} \sum_{i=1}^{N_{null}} E \left\{ \frac{\partial I_i(\mathbf{X}, \mathbf{H}, \varepsilon)}{\partial \varepsilon} \frac{\partial I_i^*(\mathbf{X}, \mathbf{H}, \varepsilon)}{\partial \varepsilon} \right\} \end{aligned} \quad (5.10)$$

The differential term,  $\frac{\partial I_i(\mathbf{X}, \mathbf{H}, \varepsilon)}{\partial \varepsilon}$ , in (5.10) can be given by

$$\frac{\partial I_i(\mathbf{X}, \mathbf{H}, \varepsilon)}{\partial \varepsilon} = \pi \left( \Lambda(\mathbf{X}, \mathbf{H}, \varepsilon) + j \left( \frac{N+1}{N} \right) I_i(\mathbf{X}, \mathbf{H}, \varepsilon) \right) \quad (5.11)$$

$$\Lambda(\mathbf{X}, \mathbf{H}, \varepsilon) = \sum_{\substack{m=0 \\ m \neq i}}^{N-1} X_m H_m e^{j\pi(\beta)\left(\frac{N-1}{N}\right)} \left[ \frac{N \sin\left(\frac{\pi\beta}{N}\right) \cos(\pi\beta) - \sin(\pi\beta) \cos\left(\frac{\pi\beta}{N}\right)}{\left(N \sin\left(\frac{\pi\beta}{N}\right)\right)^2} \right] \quad (5.12)$$

Additionally, it will be assumed that  $E\{H_m H_m^*\} = |H|^2$ ,  $E\{X_m\} = 0$ ,  $E\{X_m X_m^*\} = |X|^2$  where  $Cov_{m \neq n}(X_m X_n^*) = 0$  which is the condition when the modulation symbols are uncorrelated. The MCRLB from (5.8) can be shown as

$$MCRLB(\varepsilon) = \frac{\sigma^2}{2\pi^2 \sum_{i=1}^{N_{null}} \left[ A_i(\varepsilon) + \left(\frac{N-1}{N}\right)^2 P_i(\varepsilon) \right]} \quad (5.13)$$

$$A_i(\varepsilon) = |X|^2 |H|^2 \sum_{\substack{m=0 \\ m \neq i}}^{N-1} \left[ \frac{N \sin\left(\frac{\pi\beta}{N}\right) \cos(\pi\beta) - \sin(\pi\beta) \cos\left(\frac{\pi\beta}{N}\right)}{\left(N \sin\left(\frac{\pi\beta}{N}\right)\right)^2} \right]^2 \quad (5.14)$$

$$P_i(\varepsilon) = E\left\{ |I_i(\mathbf{X}, \mathbf{H}, \varepsilon)|^2 \right\} = |X|^2 |H|^2 \left\{ \sum_{\substack{m=0 \\ m \neq i}}^{N-1} \left[ \frac{\sin(\pi\beta)}{N \cdot \sin(\pi\beta/N)} \right]^2 \right\} \quad (5.15)$$

where  $\beta = m + \varepsilon - i$  and  $P_i(\varepsilon)$  is the ICI power appearing on the  $i^{\text{th}}$  null subcarrier.

Figure 5.1 shows MCRLB calculated by using (5.13) when  $N=256$ ,  $N_{null}=16$  and  $|X|^2 |H|^2 / \sigma^2 = 1$ . The result shows that  $MCRLB(\varepsilon)$  decreases as  $\varepsilon$  increases or as the ICI power increases when  $N_{null}$  is fixed. The minimum MCRLB in (5.13) can be obtained when  $|\varepsilon| \rightarrow 1$ , so the lower bound of variance can be given by

$$\text{var}(\varepsilon) \geq MCRLB_{\min}(\varepsilon) = 1/2.464\pi^2 N_{null} \rho \quad |\varepsilon| < 1 \quad (5.16)$$

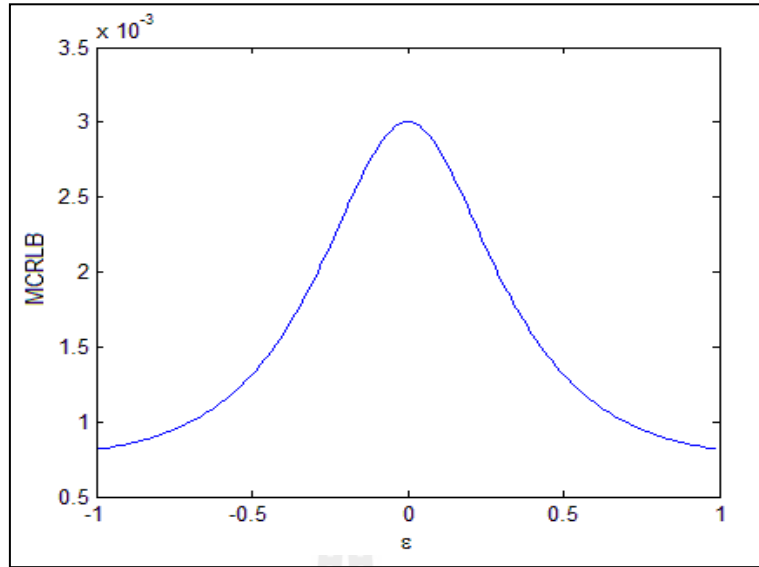


**Figure 5.1** MCRLB versus  $\Delta$  .

where  $\rho = \frac{|X|^2 |H|^2}{\sigma^2}$  is the average SNR. From (5.13) and (5.16), it can be concluded that the performance of optimal CFO estimation in (5.3) can be improved by the increasing of  $N_{null}$  and average  $P_i$  due to substituting  $\varepsilon$  in (5.3).

The cost function of (5.3) based on the ICI power consideration can be written by

$$F = \sum_{i \in \Gamma} |\mathbf{v}_i^H \mathbf{D}_\varepsilon^H \mathbf{y}|^2 = \sum_{i \in \Gamma} |I_i(\Delta) + Z_i|^2 \quad (5.17)$$

where  $\Delta = \varepsilon - \varepsilon$  . Then the expectation of (5.17) can be given by

$$E\{F\} = \sum_{i \in \Gamma} P_i(\Delta) + \sigma^2 \quad (5.18)$$

Based on  $P_i$ , when the fractional CFO estimation is performed ( $-1 < \varepsilon < 1$ ), the sufficient range of  $\Delta$  for the estimation can be given by  $-1 < \Delta < 1$  then we can write

the average of  $P_i(\Delta)_{|\Delta|<1}$  by

$$\overline{P_i(\Delta)_{|\Delta|<1}} = |X|^2 |H|^2 0.345 \quad (5.19)$$

Based on the method of null subcarriers, the subcarriers having null are inserted along frequency axis for the purpose of CFO estimation only. Hence, in order to estimate the channel, some additional pilot symbols have to be used. In next section, we propose the estimation in (5.3) by replacing null subcarriers with a pair of antipodal pilot tones in order to improve ICI power. These pilot tones can be used instead of nulls but these pilot tones still provide the same benefit as nulls because of the antipodal property. In addition, these antipodal subcarriers can be utilized for channel estimation which they become more useful than null subcarrier technique.

### 5.2.2 Proposed clustered pilot tones for CFO estimation

The method of clustered pilot tones was first proposed by Zhang, Xia and Ching (2007) to improve the signal to interference ratio for CFO estimation where its estimation is based on Moose's technique. Unlike Zhang's method, the proposed pilot scheme can improve the estimation performance by enhancing the ICI power. The proposed pilot scheme is designed and based on null subcarrier technique but it provides a better estimation performance due to ICI power improvement (as indicated in MCRLB). Two pilot tones are clustered as a group by letting  $-X_p$  and  $X_p$  be the pilot symbols on the left and the right pilot subcarriers. These pilots act as null subcarriers when they are combined. Then we rewrite the estimation equation based on (5.3) by

$$\varepsilon = \arg \min_{\varepsilon} \sum_{i \in \Gamma} \left| \mathbf{v}_i^H \mathbf{D}_{\varepsilon}^H \mathbf{y} + \mathbf{v}_{i+1}^H \mathbf{D}_{\varepsilon}^H \mathbf{y} \right|^2 \quad (5.20)$$

In order to investigate the performance of (5.20), the cost function of (5.20) can be written by

$$F = \sum_{i \in \Gamma} \left| -X_p H_i e^{j\pi\Delta(N-1)/N} \left[ \frac{\sin(\pi\Delta)}{N \cdot \sin(\pi\Delta/N)} \right] + I_i(\Delta) + Z_i + I_p^{i+1} \right. \\ \left. + X_p H_{i+1} e^{j\pi\Delta(N-1)/N} \left[ \frac{\sin(\pi\Delta)}{N \cdot \sin(\pi\Delta/N)} \right] + I_{i+1}(\Delta) + Z_{i+1} + I_p^i \right|^2 \quad (5.21)$$

where  $I_p^{i+1}$  and  $I_p^i$  are the ICI from the  $i+1^{\text{th}}$  pilot subcarrier affecting to the  $i^{\text{th}}$  pilot subcarrier and the ICI from the  $i^{\text{th}}$  pilot subcarrier affecting to the  $i+1^{\text{th}}$  pilot subcarrier respectively. From (19),  $I_p^{m+1}$  and  $I_p^m$  can be eliminated by utilizing  $I_p^{i+1}$  and  $I_p^i$  ( $m \neq i$ ) due to the concept of self ICI cancellation which was proposed by Zhao and Häggman (2001). The definition of  $I_p^{i+1}$  and  $I_p^i$  can be given by

$$I_p^{i+1} = X_p H \left[ \frac{\sin(\pi(\Delta+1))}{N \cdot \sin(\pi(\Delta+1)/N)} \right] \cdot e^{j\pi(\Delta+1)(N-1)/N} \quad (5.22)$$

$$I_p^i = -X_p H \left[ \frac{\sin(\pi(\Delta-1))}{N \cdot \sin(\pi(\Delta-1)/N)} \right] \cdot e^{j\pi(\Delta-1)(N-1)/N} \quad (5.23)$$

Normally,  $N$  is a large number,  $N \gg \pi(\Delta+1), \pi(\Delta-1)$ , and it causes  $\sin(\pi(\Delta+1)/N) \approx \pi(\Delta+1)/N$ ,  $\sin(\pi(\Delta-1)/N) \approx \pi(\Delta-1)/N$  and  $e^{\pm j\pi(N-1)/N} \approx -1$ .

Then the term of  $I_p^{i+1}$  and  $I_p^i$  can be written by

$$I_p^{i+1} = X_p H \cdot \text{sinc}(\Delta+1) \cdot e^{j\pi(\Delta+1)(N-1)/N} \quad (5.24)$$

$$I_p^i = -X_p H \cdot \text{sinc}(\Delta-1) \cdot e^{j\pi(\Delta-1)(N-1)/N} \quad (5.25)$$

From (5.24) and (5.25), it can be rewritten by

$$I_p^{i+1} + I_p^i = X_p H \cdot e^{j\pi\Delta(N-1)/N} \left[ \text{sinc}(\Delta+1) \cdot e^{j\frac{\pi(N-1)}{N}} - \text{sinc}(\Delta-1) \cdot e^{-j\frac{\pi(N-1)}{N}} \right] \quad (5.26)$$

where  $e^{\pm j\pi(N-1)/N} \approx -1$  then (5.26) can be rewritten by

$$I_{i,i+1} = X_p H \cdot e^{j\pi\Delta(N-1)/N} \left[ \text{sinc}(\Delta-1) - \text{sinc}(\Delta+1) \right] \quad (5.27)$$

To evaluate the performance of (5.20), some assumptions have been used in the preliminary study. I assume that the channel frequency response is flat during two neighboring subcarriers which cause  $H_i \approx H_{i+1} = H$  and the same assumptions on the modulation symbol  $X_m$  and noise  $Z_i$  as explained earlier are employed. Then the expectation of (5.21) can be written by

$$E\{F\} = \sum_{i \in \Gamma} P_{I_i, I_{i+1}}(\Delta) + 2\sigma^2 + \left( |I_{i,i+1}|^2 \right) \quad (5.28)$$

Where

$$\begin{aligned} P_{I_i, I_{i+1}}(\Delta) &= E\left\{ |I_i(\Delta) + I_{i+1}(\Delta)|^2 \right\} \\ &= |X|^2 |H|^2 \sum_{\substack{m=0 \\ m \neq i, i+1}}^{N-1} \left[ \frac{\sin(\pi(m+\Delta-i))}{N \cdot \sin(\pi(m+\Delta-i)/N)} \right. \\ &\quad \left. + \frac{\sin(\pi(m+\Delta-i-1))}{N \cdot \sin(\pi(m+\Delta-i-1)/N)} \right]^2 \end{aligned} \quad (5.29)$$

$$|I_{i,i+1}|^2 = |X|^2 |H|^2 \left[ \text{sinc}(\Delta-1) - \text{sinc}(\Delta+1) \right]^2 \quad (5.30)$$

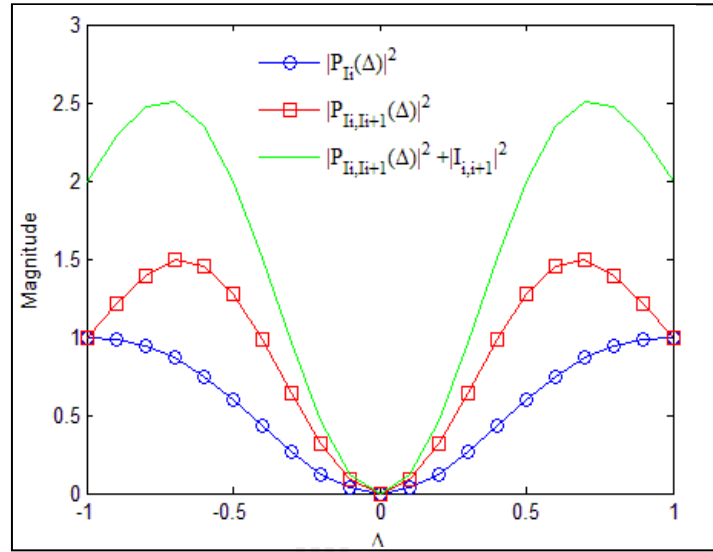


**Figure 5.2** ICI improvement for any values of  $\Delta$ .

By assuming that  $|X_p|^2 = |X|^2$ , the results using the proposed scheme in (5.28) show the ICI improvement when comparing with a conventional scheme in (5.18) as indicated in Figure 5.2, where the range of  $\Delta$  is  $-1 < \Delta < 1$  (the range of  $-1 < \Delta < 1$  is sufficient in order to estimate a fractional CFO that produces ICI when  $-1 < \varepsilon < 1$ ). As a result, we can rewrite (5.28) based on (5.18) in order to investigate the average performance of ICI improvement by

$$\begin{aligned}
 E\{F\} &= \sum_{i \in \Gamma} 2P_i + 2\sigma^2 + 1.1570P_i \\
 &= \sum_{i \in \Gamma} P_i + \sigma^2 + 0.5785P_i
 \end{aligned} \tag{5.31}$$

In (5.31), it can be clearly seen that the proposed scheme provides a better performance at 57.85% in an average ICI power enhancement when it is compared with a conventional scheme in (5.18). The ICI power enhancement of the proposed scheme is bounded by 0% to 90%. However, its performance is preliminarily based on the flat fading assumption where the channel gains on all

clustered pilot tones are assumed to be the same.

### 5.2.3 Proposed channel estimation technique

For channel estimation, by replacing null subcarriers with antipodal pilot subcarriers, these subcarriers can be utilized by any algorithms such as least square channel estimation. The channel estimation is based on the received signals on pilot subcarriers when there is no CFO can be given by

$$Y_{i,i \in \Gamma_p} = H_i X_p + Z_i \quad (5.32)$$

then we can write SNR at the  $i^{\text{th}}$  pilot subcarrier by

$$SNR = \frac{|H_i X_p|^2}{\sigma^2} \quad (5.33)$$

The estimated channel based on least square channel estimation can be written by

$$H_i = Y_i / X_p \quad (5.34)$$

The whole channel frequency response is obtained by the insertion of the pilot subcarriers along the frequency axis. Then some interpolation techniques such as linear interpolation can be employed in order to estimate the channel on subcarriers which are not inserted by antipodal pilot symbols.

In this thesis, the candidate also proposes the antipodal pilot tones for the purpose of channel estimation. Importantly, the estimation can be carried out by the same pilot scheme for CFO estimation. This is based on the assumption that, even if a channel acts as a frequency selective channel, the channel responses of the adjacent subcarriers can be slightly different from their neighbors. With this assumption, the

subtraction between the received pilot subcarriers on each pilot group can be written by

$$\begin{aligned}
 M_{i \in \Gamma_p} &= Y_{i+1} - Y_i \\
 &= H_i X_p - H_i (-X_p) + Z_i + Z_{i+1} \\
 &= 2H_i X_p + Z_i + Z_{i+1}
 \end{aligned} \tag{5.35}$$

The estimated channel on the  $i^{\text{th}}$  pilot subcarrier can be given by

$$H_i = \frac{M_i}{2X_p} \tag{5.36}$$

Where  $SNR$  of this technique can be written by

$$SNR = \frac{4|H_i X_p|^2}{2\sigma^2} = \frac{2|H_i X_p|^2}{\sigma^2} \tag{5.37}$$

From (5.37), the proposed pilot tones for channel estimation provide a better performance in  $SNR$  improvement when comparing with the conventional estimation in (5.33). In addition, by subtracting the adjacent received pilot signals on each pilot group, it is not only to improve the signal energy of antipodal pilot signals but also to reduce the ICI power on each group (Zhang, Xia and Ching, 2007). However, the performance of this technique is based on the specific assumption as mentioned earlier so the real performance in case of the severe frequency selective fading channel will provide more estimation errors. In next section, the performance of channel estimation based on the various conditions of frequency selective fading channels is investigated in order to clarify the real performance of the proposed technique.

#### 5.2.4 Simulation results

The simulation results are undertaken to investigate the performance of the proposed technique for both flat and frequency selective fading channels. The results are averaged by 5,000 random fading channels. The number of pilot subcarriers of the proposed technique and null subcarrier technique (including pilot tones for channel estimation) are the same in order to make a peer comparison between both techniques. The other simulation parameters are as follows:

- number of subcarriers ( $N$ ) = 256
- modulation = QPSK
- number of pilots ( $N_p$ ) = 48 (including  $N_{Null} = 16$  for null subcarrier technique)
- subcarrier spacing ( $\Delta f$ ) = 10.93kHz
- cyclic prefix length =  $N/8$
- step size of  $\varepsilon = 0.02$  (to keep signal-to-interference ratio less than 20dB Moose (1994))

The pilot and null subcarriers are placed with equal spacing along the subcarrier axis. There are 48 pilot tones for each OFDM symbol used for tracking channel gain and CFO where there are 32 isolated pilot tones used for channel estimation with 8 subcarriers spacing between two pilots. For null subcarrier technique, there are additional 16 null subcarriers used for CFO estimation where the spacing between null subcarrier is 16 subcarriers. For the proposed technique, there are 16 additional pilot tones and these pilot tones are placed next to the isolated pilot tones with antipodal symbol to the isolated pilot tone in order to make the proposed pilot scheme. Total pilot energy for both null subcarrier technique and the proposed technique is the same in order to make a peer comparison.

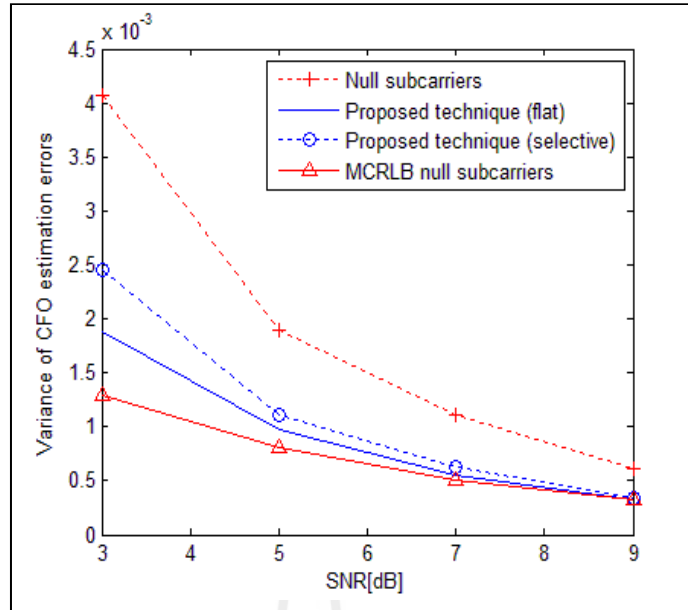


**Figure 5.3** Variance of estimation errors versus SNR ( $\varepsilon = 0.2$ ).

In order to investigate the estimation performance in frequency selective channel, this thesis adopts the ITU vehicular A to be a channel model where this model has been adopted in the WiMAX forum. The relative multipath delay ( $\tau$ ) and the normalized path gain ( $\alpha$ ) can be given by

$$\begin{aligned} \tau &= [0 \ 0.31 \ 0.71 \ 1.09 \ 1.73 \ 2.51] \mu s \\ \alpha &= [0 \ -1 \ -9 \ -10 \ -15 \ -20] \text{dB} \end{aligned} \quad (5.38)$$

Figure 5.3 shows the estimation performance in terms of variance of estimation errors versus OFDM symbol's SNR where  $\varepsilon$  is 0.2. As seen in the figure, the proposed technique provides a better estimation performance than the null subcarrier technique by reducing the variance of errors especially for low SNR cases. Also observed in this figure, the performances between flat and frequency selective fading channels are similar in which the flat channel result is slightly better. This confirms that the proposed technique can be effectively applied for either flat of

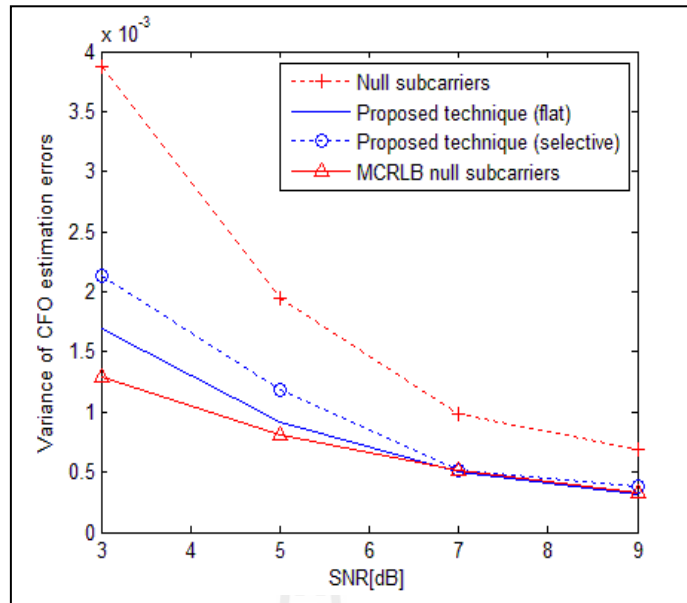


**Figure 5.4** Variance of estimation errors versus SNR ( $\varepsilon = 0.4$ ).

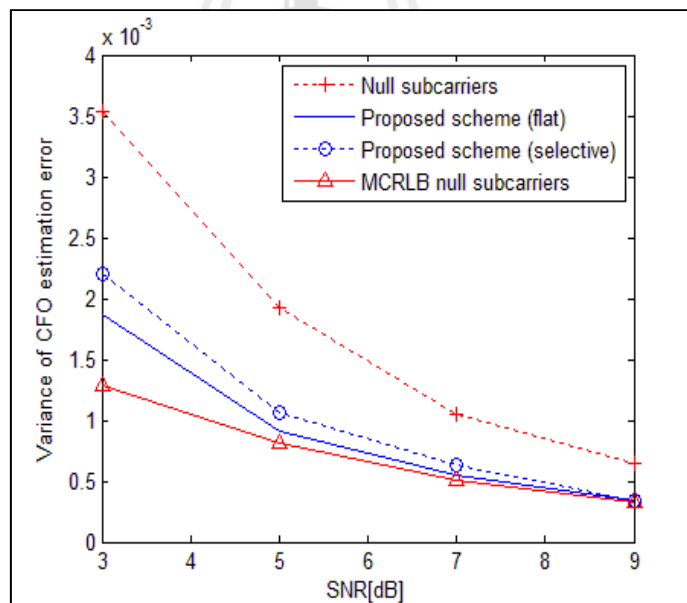


**Figure 5.5** Variance of estimation errors versus SNR ( $\varepsilon = 0.7$ ).

frequency selective fading channels. In addition, the performances of the proposed technique and null subcarrier technique are close to MCRLB if SNR is high.

Therefore, SNR is still the dominant parameter to indicate the performance of the

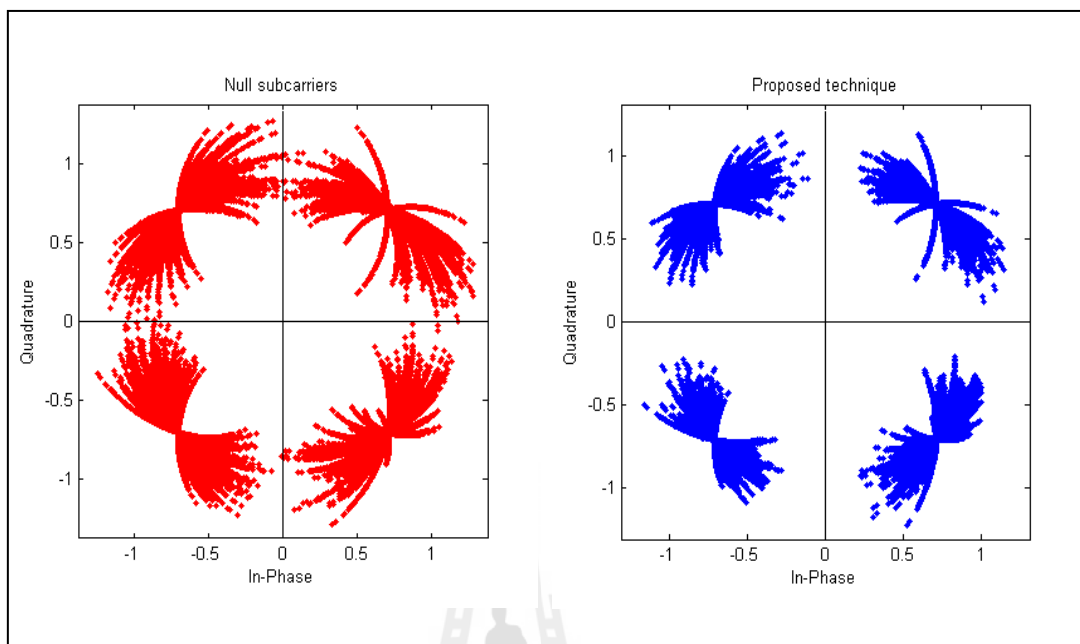


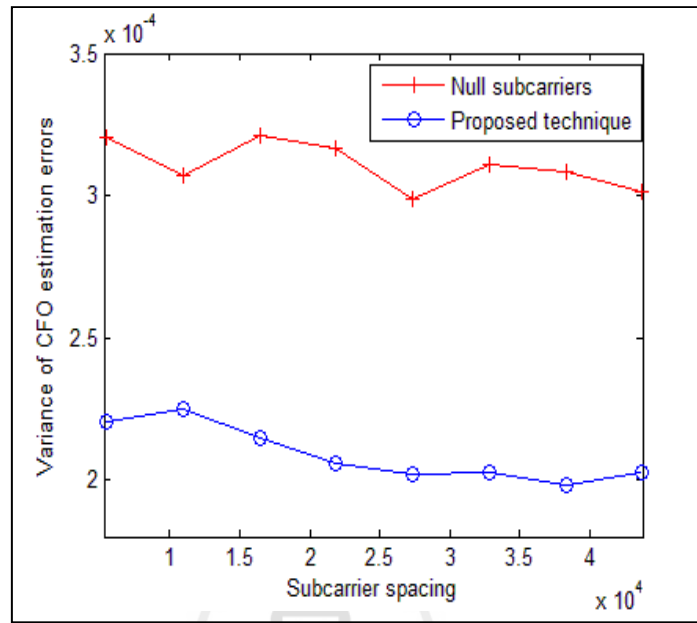
**Figure 5.6** Received signal constellations.

proposed technique or null subcarrier technique.

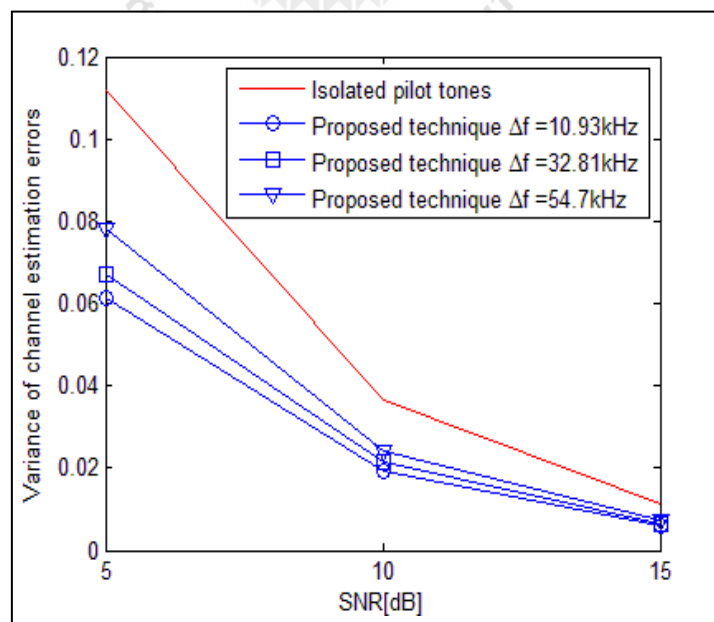
Figure 5.4 and 5.5 show the estimation performance in terms of variance of estimation errors versus OFDM symbol's SNR where  $\varepsilon$  are 0.4 and 0.7 respectively. The trend of the proposed and null subcarrier techniques is similar to the results in Figure 5.3. This confirms that the estimation range of the proposed technique covers all fractional CFO while the estimation range of pilot techniques based on Moose are limited by  $\pm 0.5$ .

Figure 5.6 shows the received signal constellations of the compensated signal from the null subcarrier technique and the proposed technique. This figure illustrates how the variance of CFO estimation errors affects to the received signals when the other effects from channels and noises are neglected. The variances of both

techniques are chosen from Figure 5.3 at SNR = 5dB. As seen in figure 5.6, the proposed technique provides a better performance than the null subcarrier



**Figure 5.7** Variance of CFO estimation errors versus subcarrier spacing ( $\Delta f$ ).



**Figure 5.8** Variance of channel estimation errors versus SNR ( $\varepsilon=0.2$ ).

technique by reducing the received signal dispersion. The results can imply to the improved BER performance obtained by the proposed technique.

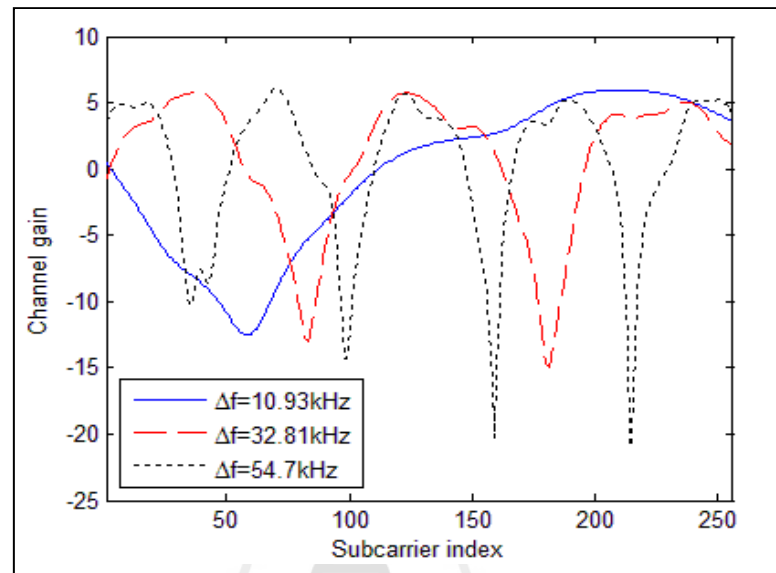


**Figure 5.9** Example of channel response.

In order to investigate the performance of the proposed technique when various type of frequency selective fading is considered, Figure 5.7 shows the variance of CFO estimation errors versus subcarrier spacing when  $\varepsilon$  is 0.2 and SNR = 10dB. This is because the increasing of the subcarrier spacing causes channel responses on adjacent subcarriers to be more separated. The result shows that the estimation performance of the proposed technique is better than the null subcarrier technique for all subcarrier spacing. Therefore, this benefit of the proposed technique can be applied in any OFDM applications.

Figure 5.8 shows the variance of channel estimation errors versus subcarrier spacing ( $\varepsilon$  is 0.2 and SNR = 5dB). The proposed clustered pilot tone in (5.36) is

compared with the conventional isolated pilot tone. As seen in the figure, the proposed technique provides a better channel estimation than the conventional technique for all subcarrier spacing. The increasing of the subcarrier spacing induces the slight growing in estimation errors because the increasing in subcarrier spacing causes

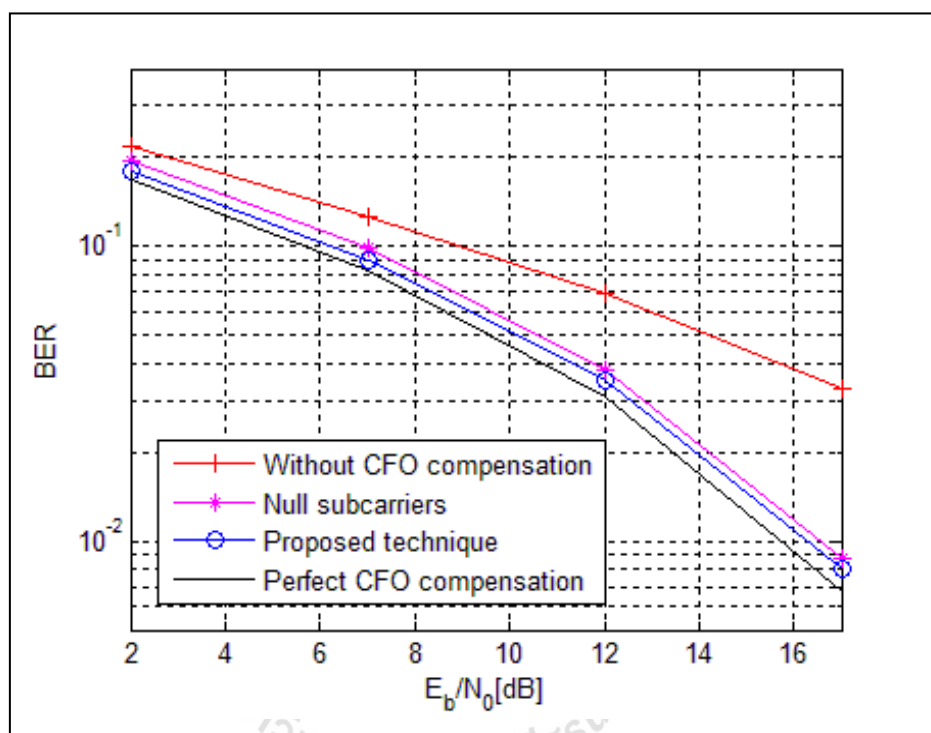


**Figure 5.10** BER versus SNR ( $\varepsilon=0.15$ ).

channel on adjacent subcarrier to be more uncorrelated. Thus it gains more channel estimation error for the proposed estimation technique. An example of the channel response for the simulated subcarrier spacing can be shown in Figure 5.9.

Figure 5.10 shows BER performance versus  $E_b/N_0$  of the proposed technique compared with the null subcarrier technique when  $CFO = 0.15$ . The results confirm that the proposed technique provides a better performance than the null subcarrier technique. For example at  $BER = 0.09$ , the proposed technique gains about

2.8 dB from a system without CFO compensation while the performance gain is about 0.5dB when comparing with the null subcarrier technique. The deviation between the system without CFO compensation and the perfect CFO compensation becomes larger when SNR is high. This is because BER performance of the system without CFO compensation is limited by ICI and thus higher CFO will extend this deviation. In addition, in order to reach the ideal BER performance shown as a system with perfect CFO compensation, the proposed technique requires more pilot tones for CFO estimation.

### **5.3 Pilot design for MIMO-OFDM system**

#### **5.3.1 Clustered pilot tones for CFO estimation**

##### *Null subcarriers*

In an OFDM system, the proposed technique has shown that it improves the performance of CFO estimation over the conventional null subcarrier technique due to the increasing of ICI power on pilot subcarriers. In an MIMO-OFDM system, CFO can be estimated by using technique based on OFDM system under the assumption that CFO on each MIMO's subchannel is the same. Actually, CFO on each MIMO's subchannel can be different or identical where there are many works based on the same CFO assumption such as (Zhen and Jianhua, 2006), (Hung, 2007) and (Sameer and Raja Kumar, 2008). In this work, CFO estimation in MIMO-OFDM with the same CFO assumption is considered. By using the same pilot scheme proposed in the previous section, the estimated CFO for MIMO-OFDM system by using null subcarriers can be given by

$$\varepsilon = \arg \min_{\varepsilon} \sum_{m=1}^{N_R} \left( \sum_{i \in \Gamma} \left| \mathbf{v}_i^H \mathbf{D}_{\varepsilon}^H \mathbf{y}_m \right|^2 \right) \quad (5.39)$$

where  $N_R$  is the number of received antennas. The cost function (5.39) based on ICI power consideration can be given by

$$F = \sum_{m=1}^{N_R} \left( \sum_{i \in \Gamma} \left| \sum_{n=1}^{N_T} X_n H_i^{m,n} e^{j\pi\Delta(N-1)/N} \cdot \left[ \frac{\sin(\pi\Delta)}{N \cdot \sin(\pi\Delta/N)} \right] + Z_i^m \right|^2 \right) \quad (5.40)$$

Where  $N_T$  is the number of transmitted antennas and  $I_i^{m,n}(\Delta)$  is ICI on the  $i^{\text{th}}$  subcarrier of the  $m^{\text{th}}$  received antenna which is produced by the  $n^{\text{th}}$  transmitted antenna.

$$I_i^{m,n}(\Delta) = \sum_{\substack{k=0 \\ k \neq i}}^{N-1} X_k^n H_k^{m,n} e^{j\pi(k+\Delta-i)(N-1)/N} \cdot \left[ \frac{\sin(\pi(k+\Delta-i))}{N \cdot \sin(\pi(k+\Delta-i)/N)} \right] \quad (5.41)$$

From (5.40), when  $X_i$  is represented by null subcarrier ( $X_i=0$ ) then (5.40) can be rewritten by

$$F = \sum_{m=1}^{N_R} \left( \sum_{i \in \Gamma} \left| \sum_{n=1}^{N_T} I_i^{m,n}(\Delta) + Z_i^m \right|^2 \right) \quad (5.42)$$

From (5.41), assuming that  $H_k^{m,n} = H_{l,l \neq k}^{m,n}$  (flat channel),  $E\{X_m^n\} = 0$ ,  $E\{|X_m^n|^2\} = |X|^2$

and data symbol  $X_k^n$  on each transmitted antenna are uncorrelated  $Cov\{X_i^n, X_j^m\} = 0$ .

Thus it causes  $E\{I_i^{m,n}(\Delta)\} = 0$  and

$$P_{I_i}^{m,n} = E \left\{ \left| I_i^{m,n}(\Delta) \right|^2 \right\} = |X|^2 |H^{m,n}|^2 \sum_{k=0}^{N-1} \left[ \frac{\sin(\pi(k+\Delta-i))}{N \cdot \sin(\pi(k+\Delta-i)/N)} \right] \quad (5.43)$$

For the sake of simplicity, we assume that  $|H^{m,n}|^2 = |H|^2$ , Then the expectation of (5.42) can be rewritten by.

$$E\{F\} = N_R \sum_{i \in \Gamma} N_T P_{I_i} + \sigma^2 = N_R \sum_{i \in \Gamma} P_{I_i}^T + \sigma^2 \quad (5.44)$$

By normalizing (5.44) with  $N_R$ , then (5.44) can be rewritten by

$$E\{F\}_{\text{norm}} = \sum_{i \in \Gamma} P_{I_i}^T + \sigma^2 \quad (5.45)$$

Where  $P_{I_i}^T$  is the summation of ICI from  $N_T$  transmitted antennas on the  $i^{\text{th}}$  subcarrier.

From (5.45), it can be concluded that the performances in ICI improvement of null subcarrier technique for both OFDM system in (5.18) and MIMO-OFDM system in (5.45) are identical if the same SNR is considered.

### ***Clustered pilot tones***

As same as clustered pilot tones for OFDM system from the previous section, the proposed clustered pilot tones for CFO estimation can improve the estimation performance due to ICI enhancement, the estimated CFO of the proposed technique can be written by

$$\varepsilon = \arg \min_{\varepsilon} \sum_{m=1}^{N_R} \left( \sum_{i \in \Gamma} \left| \mathbf{v}_i^H \mathbf{D}_{\varepsilon}^H \mathbf{y}_m + \mathbf{v}_{i+1}^H \mathbf{D}_{\varepsilon}^H \mathbf{y}_m \right|^2 \right) \quad (5.46)$$

When  $-X_p$  and  $X_p$  represent pilot symbol on the left ( $i^{\text{th}}$ ) and the right ( $(i+1)^{\text{th}}$ ) pilot subcarrier, then the cost function of (5.46) can be written by

$$F = \sum_{m=1}^{N_R} \sum_{i \in \Gamma} \left| \sum_{n=1}^{N_T} \left\{ \begin{aligned} &[-X_p H_i^{m,n} S(\Delta) + I_i^{m,n}(\Delta) + I_{p,i+1}^{m,n}] \\ &+ [X_p H_{i+1}^{m,n} S(\Delta) + I_{i+1}^{m,n}(\Delta) + I_{p,i}^{m,n}] \end{aligned} \right\} + Z_i^m + Z_{i+1}^m \right|^2 \quad (5.47)$$

where

$$S(\Delta) = e^{j\pi\Delta(N-1)/N} \left[ \frac{\sin(\pi\Delta)}{N \cdot \sin(\pi\Delta/N)} \right] \quad (5.48)$$

As same as (5.43), by assuming that channel is flat and all MIMO's subchannel gains are equal then (5.47) can be rewritten by

$$F = \sum_{m=1}^{N_R} \sum_{i \in \Gamma} \left| \sum_{n=1}^{N_T} \left\{ \begin{aligned} &[I_i^{m,n}(\Delta) + I_{p,i+1}^{m,n}] \\ &+ [I_{i+1}^{m,n}(\Delta) + I_{p,i}^{m,n}] \end{aligned} \right\} + Z_i^m + Z_{i+1}^m \right|^2 \quad (5.49)$$

Let  $I_i^{m,n}(\Delta) + I_{i+1}^{m,n}(\Delta) = I_{I_i, I_{i+1}}^{m,n}$  be the total ICI and  $I_{p,i+1}^{m,n} + I_{p,i}^{m,n} = I_{i,i+1}^{m,n}$  be the ICI which is produced by pilot tones. Then the expectation of (5.49) can be given by

$$\begin{aligned} E\{F\} &= \sum_{m=1}^{N_R} \sum_{i \in \Gamma} E \left\{ \left| \sum_{n=1}^{N_T} (I_{I_i, I_{i+1}}^{m,n} + I_{i,i+1}^{m,n}) + Z_i^m + Z_{i+1}^m \right|^2 \right\} \\ &= \sum_{m=1}^{N_R} \sum_{i \in \Gamma} \left\{ \sum_{n=1}^{N_T} E \left\{ \left| I_{I_i, I_{i+1}}^{m,n} \right|^2 \right\} + \left| \sum_{n=1}^{N_T} I_{i,i+1}^{m,n} \right|^2 + \sigma^2 + \sigma^2 \right\} \\ &= \sum_{m=1}^{N_R} \sum_{i \in \Gamma} \left\{ N_T P_{I_i, I_{i+1}} + \left| \sum_{n=1}^{N_T} I_{i,i+1}^{m,n} \right|^2 + 2\sigma^2 \right\} \end{aligned} \quad (5.50)$$

Where

$$\left| \sum_{n=1}^{N_T} I_{i,i+1}^{m,n} \right|^2 = |X_p|^2 \left[ \text{sinc}(\Delta-1) - \text{sinc}(\Delta+1) \right]^2 \left| \sum_{n=1}^{N_T} H^{m,n} \right|^2 \quad (5.51)$$

From (5.50) and (5.51), we can see that the estimation performance of the proposed technique depends on summation of MIMO's subchannel. Therefore, we have to categorize the cases of study into two cases which are the best case and the worst case given by

$$\sum_{n=1}^{N_T} H^{m,n} = N_T H \rightarrow \text{the best case when } H^{m,1} = H^{m,2} = \dots = H^{m,N_T} \quad (5.52)$$

$$\sum_{n=1}^{N_T} H^{m,n} = 0 \rightarrow \text{the worst case} \quad (5.53)$$

If the worst case is considered, the ICI improvement from (5.50) can be rewritten by

$$E\{F\} = N_R \sum_{i \in \Gamma} \left\{ N_T P_{I_i, I_{i+1}} + 2\sigma^2 \right\} \quad (5.56)$$

As seen in Figure 5.2, the performance of ICI from (5.56) can be given by

$$E\{F\} = N_R \sum_{i \in \Gamma} N_T (P_{I_i} + 0.4P_{I_i}) + 2\sigma^2 \quad (5.57)$$

$$E\{F\}_{\text{norm}} = \sum_{i \in \Gamma} 0.7P_{I_i}^T + \sigma^2 \quad (5.58)$$

Then if the best case is considered, the ICI improvement from (5.50) can be rewritten by

$$\begin{aligned} E\{F\} &= \sum_{m=1}^{N_R} \sum_{i \in \Gamma} \left\{ N_T P_{I_i, I_{i+1}} + \left| \sum_{n=1}^{N_T} I_{i,i+1}^{m,n} \right|^2 + 2\sigma^2 \right\} \\ &= N_R \sum_{i \in \Gamma} \left\{ N_T P_{I_i, I_{i+1}} + N_T |I_{i,i+1}|^2 + 2\sigma^2 \right\} \end{aligned} \quad (5.59)$$

As same as (5.31), (5.59) can be rewritten by

$$E\{F\} = N_R \sum_{i \in \Gamma} N_T (2P_{I_i} + 1.1570P_{I_i}) + 2\sigma^2 \quad (5.60)$$

$$\begin{aligned} E\{F\}_{\text{norm}} &= \sum_{i \in \Gamma} N_T (P_{I_i} + 0.5785P_{I_i}) + \sigma^2 \\ &= \sum_{i \in \Gamma} P_{I_i}^T + 0.5785P_{I_i}^T + \sigma^2 \end{aligned} \quad (5.61)$$

From (5.58) and (5.61), if we assume that MIMO's subchannels  $H^{m,n}$  are uniformly distribution between the worst case and the best case, the average performance of the proposed technique in MIMO-OFDM system can be approximated by averaging the performance of (5.58) and (5.61) which can be given by

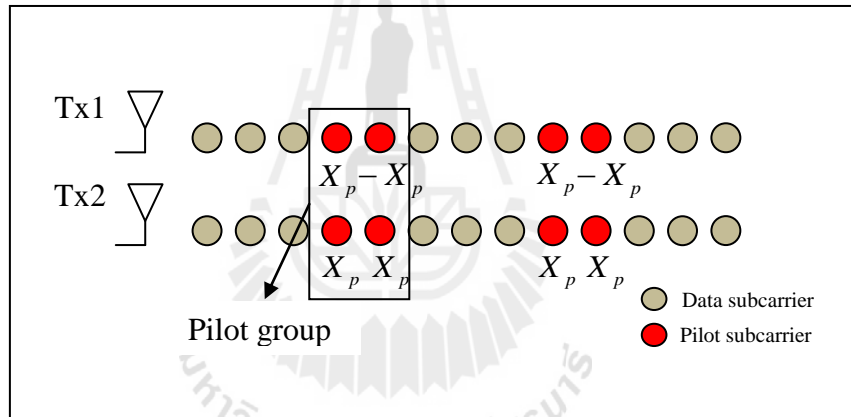


**Figure 5.11** Proposed pilot scheme for  $2 \times 2$  MIMO-OFDM channel estimation.

$$E\{F\}_{\text{norm}} = \sum_{i \in \Gamma} P_{I_i}^T + 0.2785P_{I_i}^T + \sigma^2 \quad (5.62)$$

From (5.62), the proposed technique shows that it improves estimation performance by increasing ICI power which is about 27.85% improvement when comparing with the conventional null subcarriers from (5.45). However, the performance from (5.62)

is based on flat assumption thus the investigation of the proposed technique when frequency selective channel should be considered.

### 5.3.2 Pilot tones for channel estimation

For MIMO-OFDM channel estimation, candidate also proposes pilot scheme for  $2 \times 2$  MIMO-OFDM system which can reduce the complexity of matrix inversion in MIMO channel estimation as the orthogonal pilot scheme. The proposed pilot scheme can improve MIMO channel estimation as the clustered pilot scheme which has been presented in section 5.2.3 and this pilot scheme can be shown in Figure 5.11. As seen in the figure, the candidate clusters two pilot tones as group for both transmitted antennas at the same pilot subcarrier where pilot tones in each group of the first antenna are antipodal but pilot tones from the second antenna are the same.

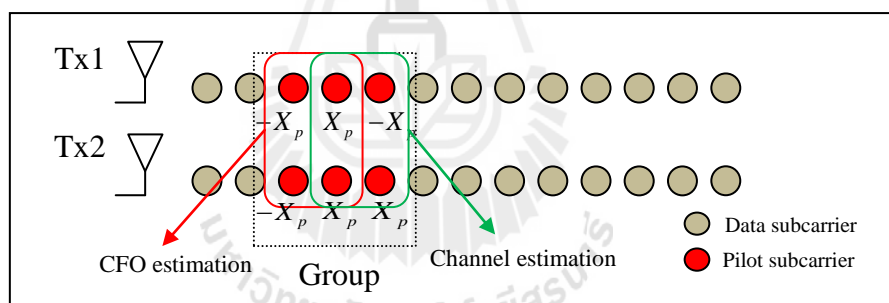


**Figure 5.12** Proposed pilot scheme for  $2 \times 2$  MIMO-OFDM system.

By using this pilot scheme, MIMO channel estimation can be performed by using deduction and summation on each pilot group from each received antenna, thus it can ignore the interference which is produced by pilot symbols from another antenna. If  $\Gamma_p$  is the set of the left pilot subcarrier indexes then we can write channel estimation for each received antenna by

$$H_i^{m,1} = \frac{Y_i^m - Y_{i+1}^m}{2X_p} \quad (5.63)$$

$$H_i^{m,2} = \frac{Y_i^m + Y_{i+1}^m}{2X_p} \quad (5.64)$$

where  $i \in \Gamma_p$  and  $Y_i^m$  is the received signal from the  $m^{\text{th}}$  received antenna on the  $i^{\text{th}}$  pilot subcarrier. The estimation performance of (5.63) and (5.64) are same as the proposed pilot tone for OFDM channel estimation which has been presented in 5.2.3.

The combination between the proposed pilot scheme for channel estimation and the proposed pilot scheme for CFO estimation can be shown in Figure 5.12. This pilot scheme is suitable for  $2 \times 2$  MIMO-OFDM configuration where this MIMO configuration is used in IEEE 802.16e standard (WiMAX forum, 2006). As seen in the figure, candidate divides pilot tones from each pilot group into two parts

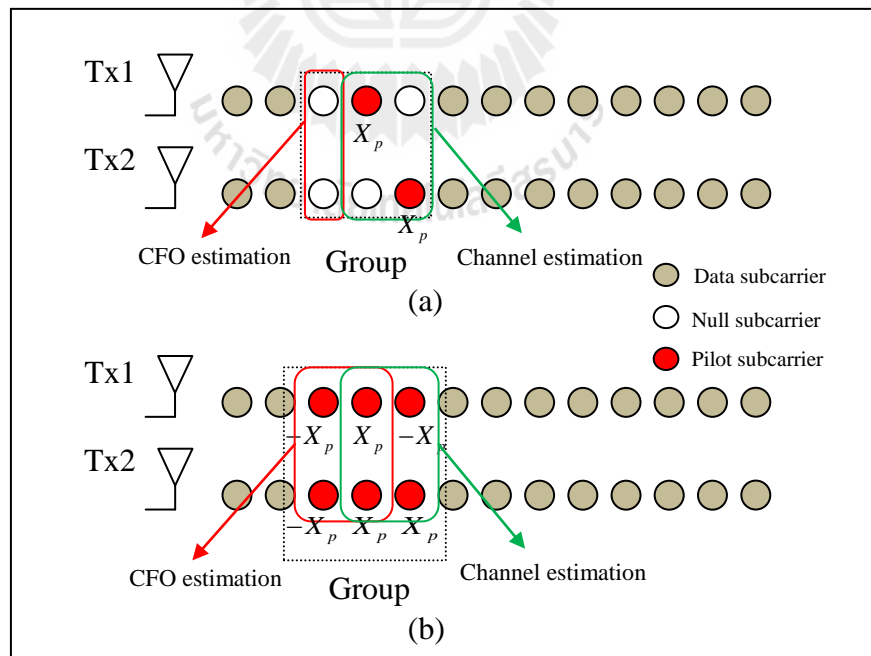


**Figure 5.13** a) Conventional pilot scheme b) Proposed pilot scheme.

where the first part is used for CFO estimation and the second part is used for channel estimation. The performance of this pilot scheme is investigated in the next section.

### 5.3.3 Simulation results

In order to investigate the performance of the proposed pilot scheme for  $2 \times 2$  MIMO-OFDM system, the same simulation parameters from section 5.2.4 are used to be our system configurations. The performance for both CFO estimation and channel estimation is averaged from 5,000 random channels where the ITU vehicular scheme A is used to be a channel model. The number of pilot tones for each transmitted antenna is 64 (56 subcarriers for channel estimation and 8 subcarriers for CFO estimation) for the proposed scheme and the conventional scheme. The comparison between the proposed pilot scheme and the conventional scheme can be shown in Figure 5.13, where the conventional pilot scheme is the combination between null subcarrier technique and orthogonal pilot technique. In addition,

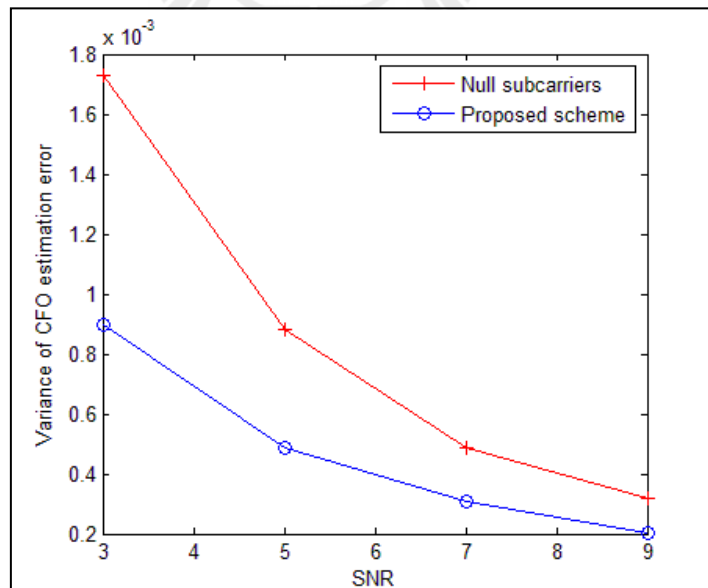


**Figure 5.14** Variance of estimation errors versus SNR ( $\varepsilon = 0.2$ ).

simulation results are based on the assumption that. The frequency offset of each MIMO subchannel is the same (this assumption has been acceptable in many works such as Zhen and Jianhua, (2006); Hung, Tho and Chi, (2007); Sameer and Raja Kumar, (2008)).

Figure 5.14 shows an error variance of CFO estimation versus SNR when  $\varepsilon = 0.2$ . As seen in the figure, the proposed scheme still provides a better estimation performance than the null subcarrier technique and it is about 45% on error variance reduction when SNR is 5dB. In addition, the deviation between the proposed scheme and the null subcarrier technique are similar to the proposed pilot scheme which has been presented in section 5.2.4. However, MIMO-OFDM system provides a better performance than OFDM system due to more number of pilot subcarriers (pilot subcarriers from all transmitted antennas are used for estimation). The performances for another value of  $\varepsilon$  are similar to the result from Figure 5.14 and they can be shown in Figure 5.15 and Figure 5.16.

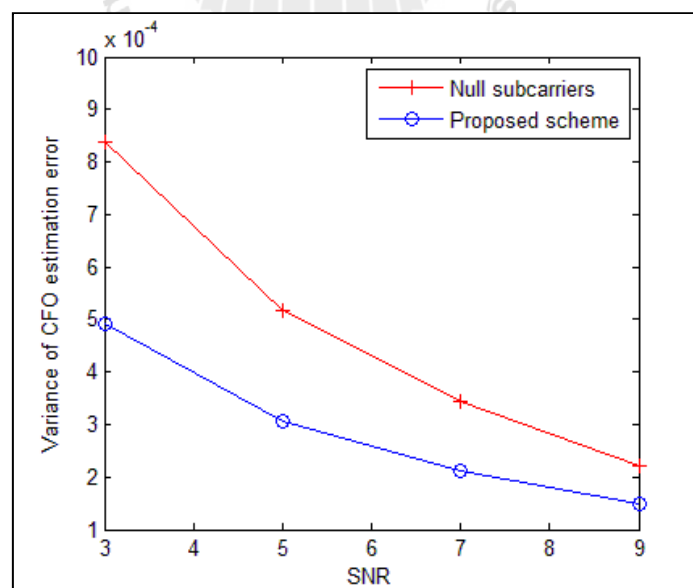


**Figure 5.15** Variance of estimation errors versus SNR ( $\varepsilon = 0.4$ ).

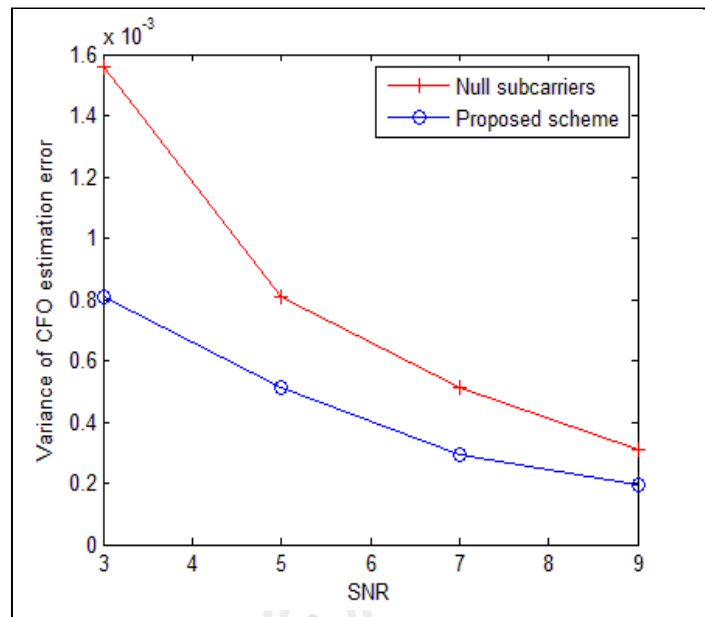


**Figure 5.16** Variance of estimation errors versus SNR ( $\varepsilon = 0.7$ ).

Figure 5.17 shows an example of the channel estimation performance of  $H_{11}$  in the view of error variance versus symbol's SNR. The result shows that the proposed pilot scheme provides better performance by reducing error variance over

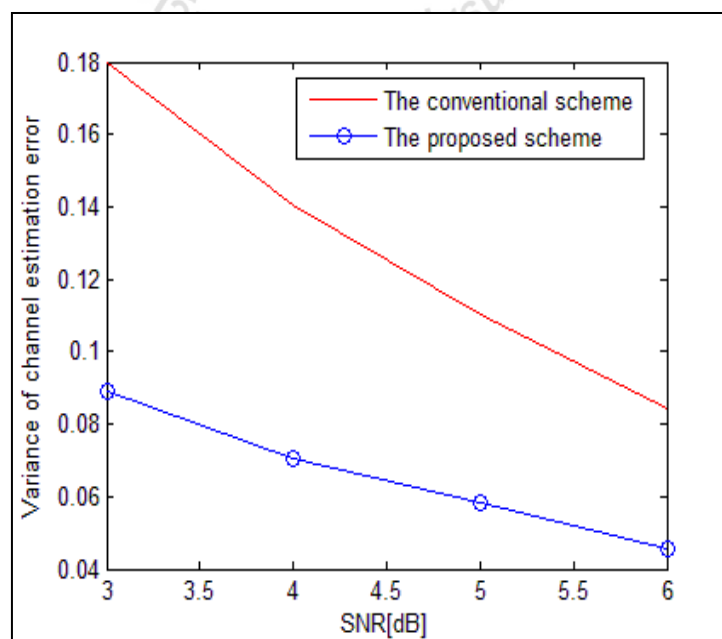


**Figure 5.17** Variance of channel estimation errors versus SNR ( $\varepsilon = 0.3$ ).

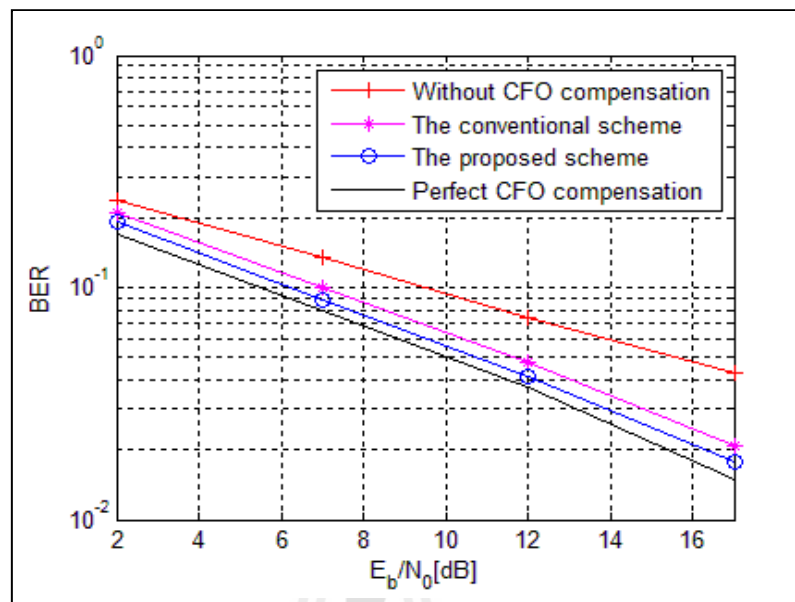


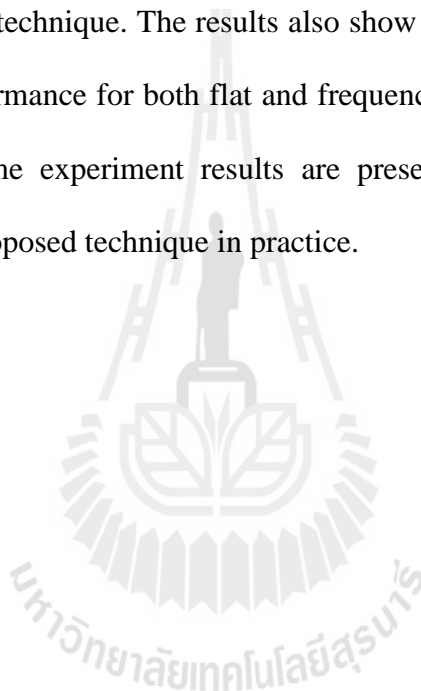
**Figure 5.18** BER versus SNR ( $\varepsilon = 0.2$ ).

the conventional orthogonal pilot scheme and it is about 50% on the average of error variance reduction.

Figure 5.18 shows the BER performance between the proposed pilot scheme and the conventional pilot scheme when  $\varepsilon = 0.2$ . As seen in the figure, the proposed scheme provides a better performance than the conventional scheme due to the improvement from both CFO and channel estimation performances. The result is similar to Figure 5.10 (BER performance of an OFDM system) but MIMO-OFDM provides a better BER performance due to better CFO estimation. For other values of  $\varepsilon$ , the results still provide similar benefits of the proposed pilot scheme as shown in Figure 5.18.

## 5.4 Chapter summary

This chapter presents the proposed pilot scheme design and its performance analysis for both OFDM system and MIMO-OFDM system. The  $2 \times 2$  MIMO configuration is used in this thesis where it is designed and based on IEEE 802.16 (Mobile WiMAX) standard. As we can see in simulation results, the proposed pilot scheme provides a better performance for both channel estimation and CFO estimation than the conventional technique. The results also show that the proposed pilot scheme provides a good performance for both flat and frequency selective fading channels. In the next chapter, some experiment results are presented in order to confirm the performance of the proposed technique in practice.



# **CHAPTER VI**

## **THE EXPERIMENTAL RESULTS**

### **6.1 Introduction**

The previous chapter has focused on the pilot scheme design and also the idea has been confirmed through simulation results. This chapter presents the design and construction of testbed in order to validate the proposed pilot scheme where the experimental results are also included. However, the testbed is based on an OFDM system configuration and the small area consideration is undertaken due to the limitation of hardware resource. The practical performance of the proposed pilot scheme for MIMO-OFDM system can be predicted from the results of OFDM system testbed where it should provide the same benefits as the simulation results from previous chapter.

### **6.2 Design of the testbed**

Figure 6.1 shows the diagram of testbed configuration. As seen in the figure, the testbed is divided into two parts which are transmitter unit and receiver unit. For the transmitter unit, this unit is consisted of processing unit, digital and analog conversion unit and RF unit. The responsibilities of these units are to create an OFDM signal and send to the receiver unit over wireless channel where the OFDM system parameters are the same as simulation parameters described in section 5.2.4. For the receiver unit, this unit is configured by the same components as the transmitter unit but in the inverse direction. This unit is responsible for OFDM signal

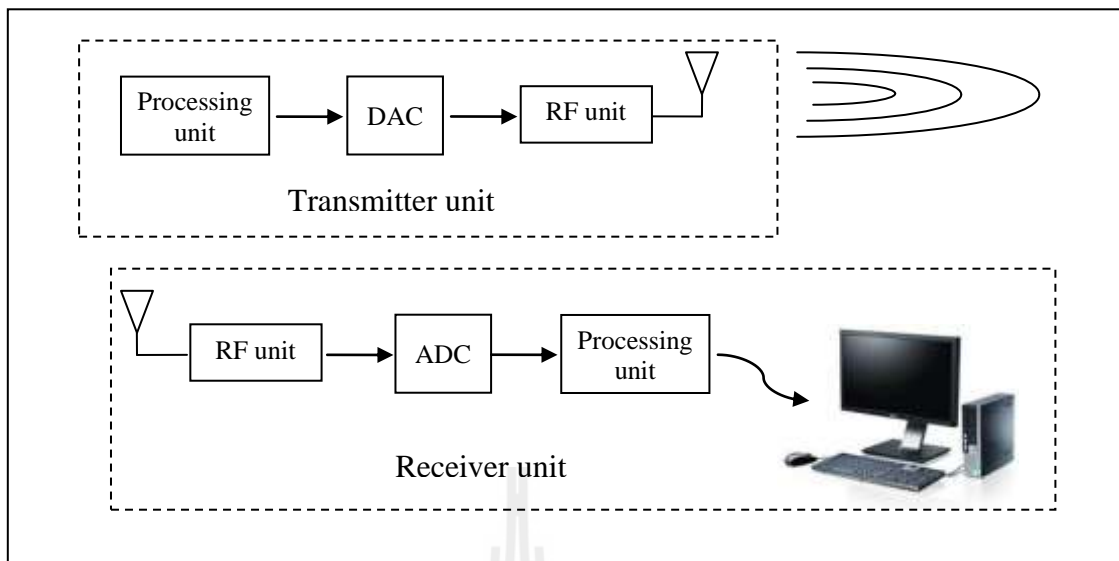


**Figure 6.1** Testbed diagram.

synchronization, CFO estimation, channel estimation and data detection. The performance of each technique can be measured by Matlab programming at the end of the receiver unit. In addition, this testbed is not fully wireless operation where it still requires the synchronized signal sent from transmitter unit to receiver unit over the synchronized wire.

### 6.2.1 Processing unit

The Altera cyclone III development boards are utilized to be the processing unit for both transmitter and receiver. The Altera cyclone III development board is a FPGA board designed especially for DSP (digital signal processing) works such as wireless, video and image processing and other high bandwidth applications. In addition, The Altera cyclone III development board can be future connected with a daughter board which provides 2 data conversions for both DAC (digital to analog conversion) and ADC (analog to digital conversion) thus this development boards can provide sufficient functions for our objectives. Figure 6.2 demonstrates a photograph



**Figure 6.2** Photograph of Altera cyclone III development board.

**Table 6.1** Summary of specification of Altera cyclone III development boards.

Parameters	Details
Cyclone III EP3C120F780 FPGA	- 119,088 logic elements - 4 PLLs
Memory	- 256 MB dual-channel DDR2 SDRAM - 8 MB SRAM - 64 MB flash memory
Communication ports	- 10/100/1000 Ethernet - USB 2.0
Clocking	- 50 MHz and 125 MHz on-board clock - SMA inputs/outputs
Display	- 128x64 graphic LCD
Connector	- 2 HSMC ports - USB type B
Cable and power	- 14 V to 20 V DC input

of Altera cyclone III development board. The summary of this development board can be described in Table 6.1.

### 6.2.2 Data and analog conversion

In order to generate baseband OFDM signal, a high speed clock data conversion for both DAC and ADC should be considered. A data and analog

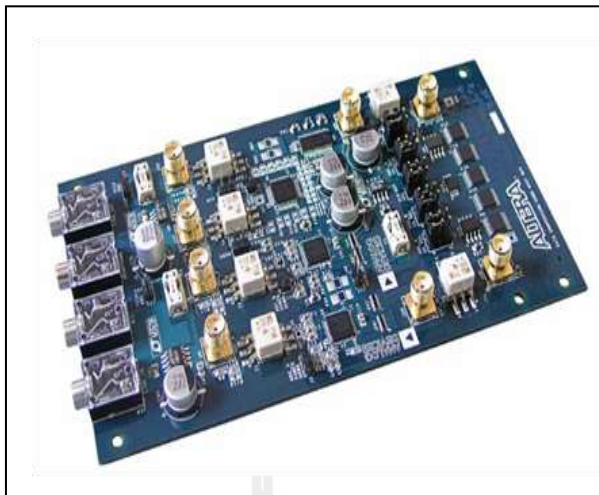


**Figure 6.3** Photograph of data conversion HSMC board.

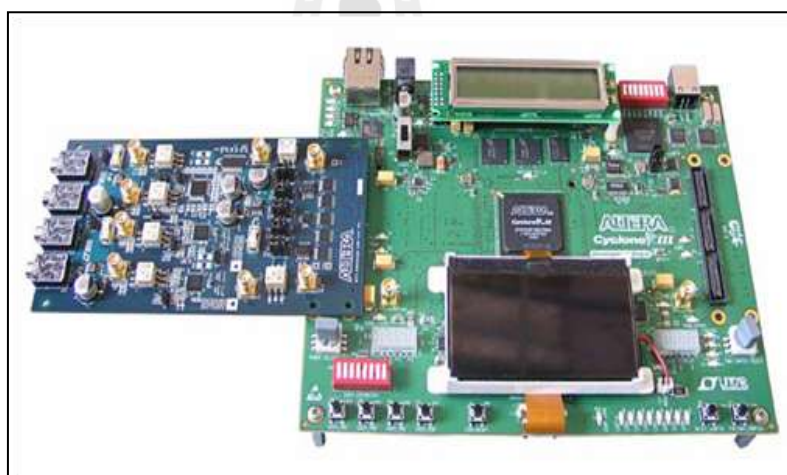


**Figure 6.4** Photograph of the processing unit connected with data conversion board via HSMC connector.

conversion unit is a significant part of any digital communication systems where its resolution and clock speed can be used to indicate the performance of its output signal. In this work, the data conversion HSMC boards are used for both transmitter and receiver where the photograph of this board is shown in Figure 6.3. Figure 6.4 shows a photograph when Altera cyclone III development boards is connected with data

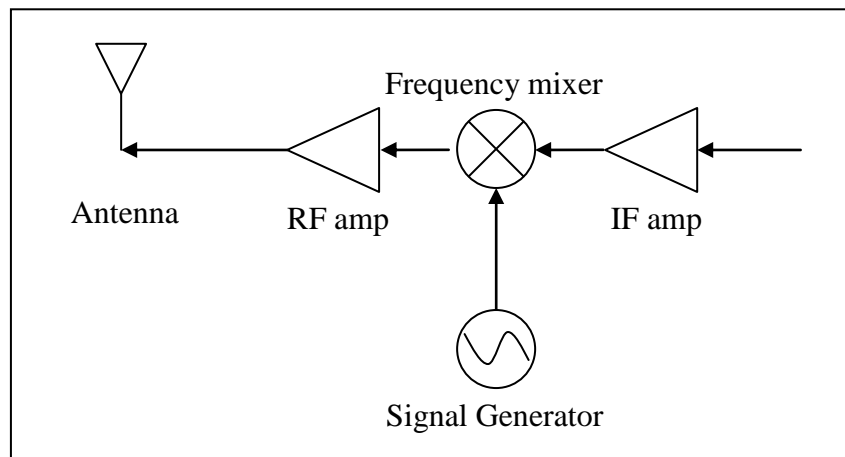


**Figure 6.5** Block diagram of RF unit.

conversion HSMC boards via HSMC connector. The features of data conversion HSMC board are as follow:

- Audio CODEC interface
- External Clock in interface
- External Clock out interface
- 2 ADC channels 14 bits 250 MS/s
- 2 DAC channels 14 bits 150 MS/s

### 6.2.3 RF unit

The RF unit is responsible for converting the baseband signal to the passband signal and increasing signal power that is sufficient for signal transmission between transmitter and receiver. Figure 6.5 shows detail of transmitter's RF unit design. As same as transmitter, receiver uses the same components of RF unit as the transmitter but in the inverse direction. As seen in the figure, RF unit is consisted of 5 components which are IF amplifier, frequency mixer, signal generator, RF amplifier and antenna. The detail of each component is shown as follows:

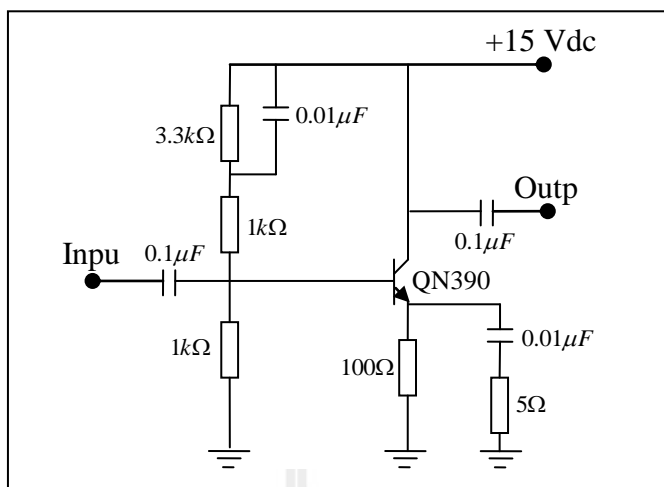


**Figure 6.6** Schematic of IF amplifier.



**Figure 6.7** Photograph of IF amplifier.

### ***IF amplifier***

The IF amplifier is used to amplify the IQ signal from data conversion for transmitter unit while it is used to amplify the received IQ signal before sending to ADC for receiver unit. Figure 6.6 shows the design schematic of IF amplifier. As seen in the figure, the IF amplifier is designed and based on common emitter amplifier where NPN transistor QN3904 is used in this work. A photograph of IF amplifier can

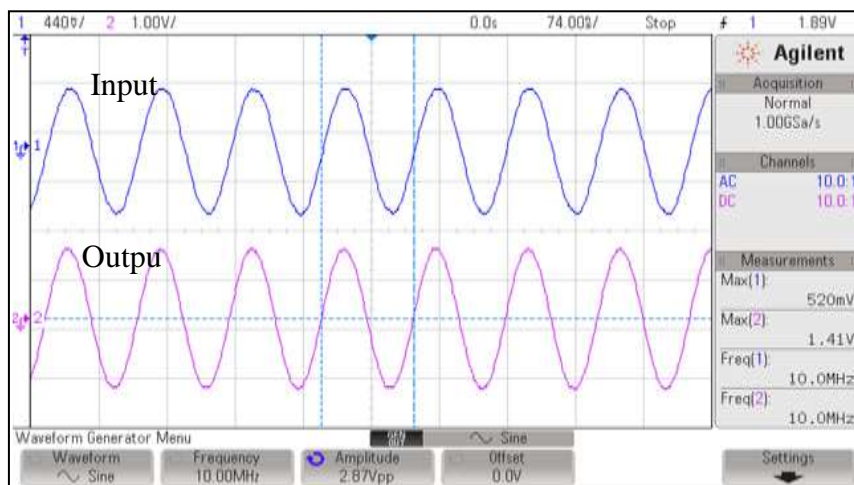


**Figure 6.8** Input and output signal from IF amplifier.

be shown in Figure 6.7. Figure 6.8 shows input and output comparison from IF amplifier when input signal is a sine wave with 10 MHz frequency. As seen in Figure 6.7, the IF amplifier voltage gain is about 3 which is 9.54 dB in power gain.



**Figure 6.9** Photograph of mixer.

### ***Frequency mixer***

The frequency mixer is used for frequency conversion and it is a critical component in modern communication systems. A frequency mixer combines RF power of one frequency with the power of another frequency to make signal processing easier and also inexpensive. Figure 6.9 shows a photograph of frequency



**Figure 6.10** Photograph of RF amplifier.

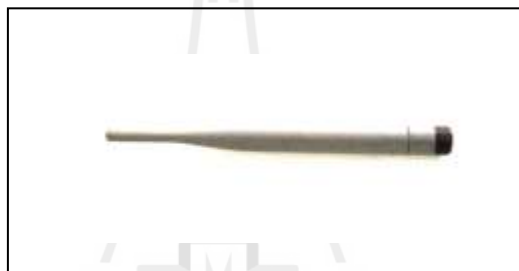


**Figure 6.11** Photograph of monopole antenna.

mixer used in this work which its model number is ZX05-73L+ from Minicircuit<sup>®</sup>. This model supports RF bandwidth from 2400 to 7000 MHz, IF bandwidth from DC to 3000 MHz with low conversion loss about 6.2 dB.

### ***RF amplifier***

Figure 6.10 shows a photograph of RF amplifier that is utilized in this work and its model number is ZQL-2700MLNW+ from Minicircuit<sup>®</sup>. This RF amplifier model has very low noise figure about 1.5 dB but provides high average RF gain about 30 dB for frequency range 2200 - 2700 MHz. RF amplifiers are placed in both transmitter unit and receiver unit in order to improve signal strength and ability to combat noise signal.



**Figure 6.12** Photograph of Hewlett Packard 83620B signal generator.

### *Antennas*

In this work, the omni-directional monopole antennas are used for both transmitter and receiver. Figure 6.11 shows a photograph of monopole antenna which is used in our testbed. A monopole antenna is designed for bandwidth range 2.4 - 2.5 GHz (ISM band) with 5 dBi gain.

### *Signal generator*

The signal generator is used to generate carrier frequency for both up and down conversions. There are two signal generators used in testbed, one for transmitter unit and another one for receiver unit. Hewlett Packard 83620B signal generators are used in this work where this model provides frequency range from 10 MHz to 20 GHz with a lot of signal functions such as AM modulation and FM modulation. A photograph of Hewlett Packard 83620B can be shown in Figure 6.12.

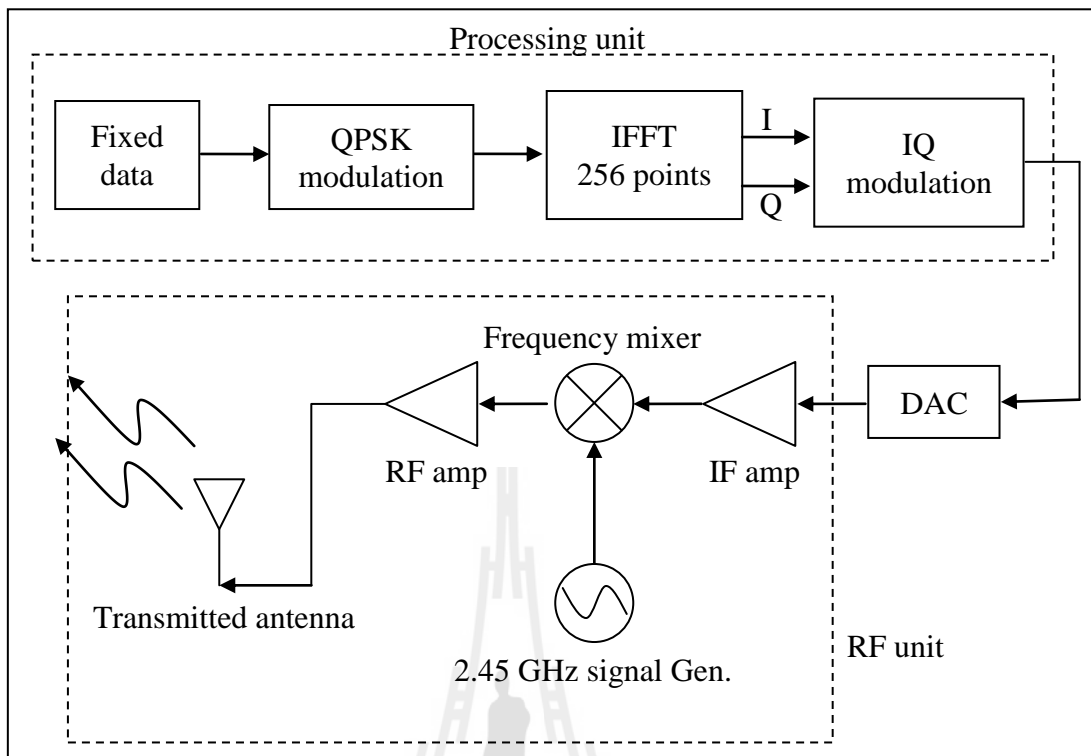


**Figure 6.13** Block diagram of transmitter unit.

## 6.3 Testbed implementation

### 6.3.1 Transmitter unit

The deep detail of the transmitter unit can be shown in Figure 6.13. As seen in the figure, the transmitter unit starts with fixed data sequence block where this block is used to generate the fixed binary data, and these data are transmitted for every OFDM symbol. These serial data will be modulated with QPSK modulation scheme and then these data symbols will be sent to IFFT block. The IFFT block is used to transform frequency domain signal to time domain signal where the transformation size used in this work is 256 points. The subcarrier spacing is designed to be 9.765 kHz in order to be similar to mobile WiMAX standard (mobile WiMAX standard is 10.94 kHz) and there is no guard interval insertion. The time domain signals

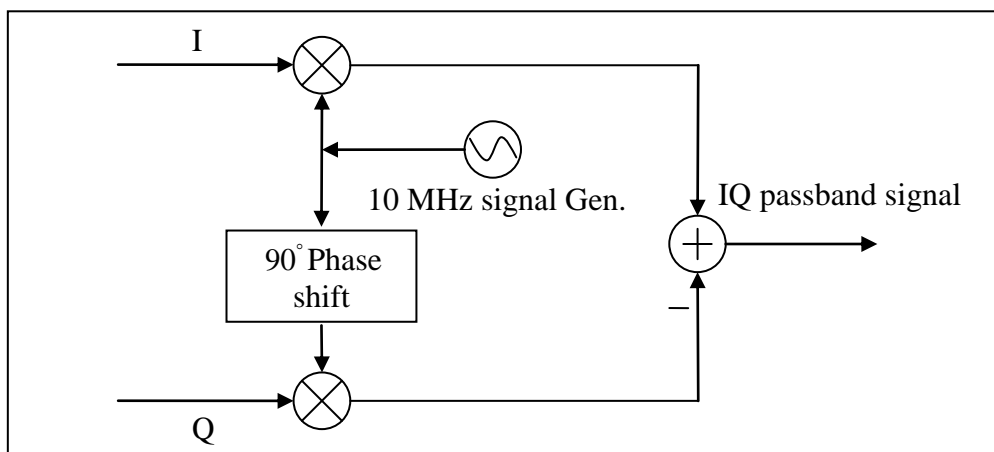


**Figure 6.14** IQ modulation diagram.

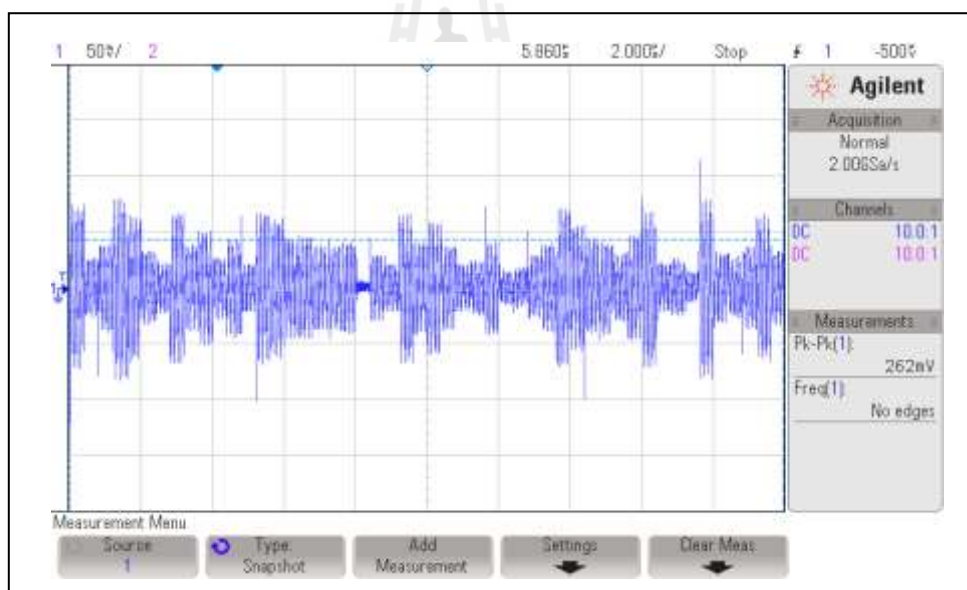


**Figure 6.15** Example of IQ signal from DAC.

for both real and imaginary from IFFT block will be modulated with IQ modulation where the block diagram of IQ modulation can be shown in Figure 6.14. The IQ modulation will modulate baseband signal with 10 MHz carrier frequency then send to DAC unit (digital to analog conversion) in order to create analog signal. The example of analog IQ signal from DAC can be shown in Figure 6.15. This analog signal will

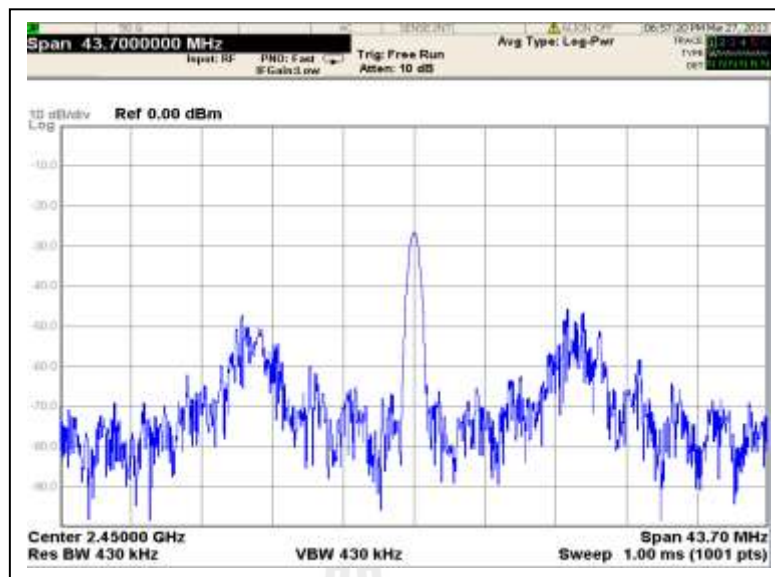


**Figure 6.16** Power spectrum of the transmitted signal.

be sent to the RF unit where RF unit is responsible for amplifying and converting the IF signal into the RF signal. The carrier frequency used in this work is 2.45 GHz. Then the RF signal will be sent to wireless channel via the transmitted antenna where an example of RF spectrum can be shown in Figure 6.16.

### 6.3.2 Receiver unit

As seen in Figure 6.17, the receiver unit starts with RF unit where this unit contains the same components as transmitter unit but in the inverse direction. Then the analog IQ signal from IF amplifier is converted to digital signal type by ADC and sent to the processing unit. The receiver's processing unit controls the different responsibility to the transmitter's processing unit. The receiver's processing unit is responsible for IQ demodulation so the demodulated IQ signal will be sent to Matlab programming. The diagram of IQ demodulation can be shown in Figure 6.18.

The Matlab programming is used in order to make receiver unit become easier than just using only processing unit. The responsibility of Matlab

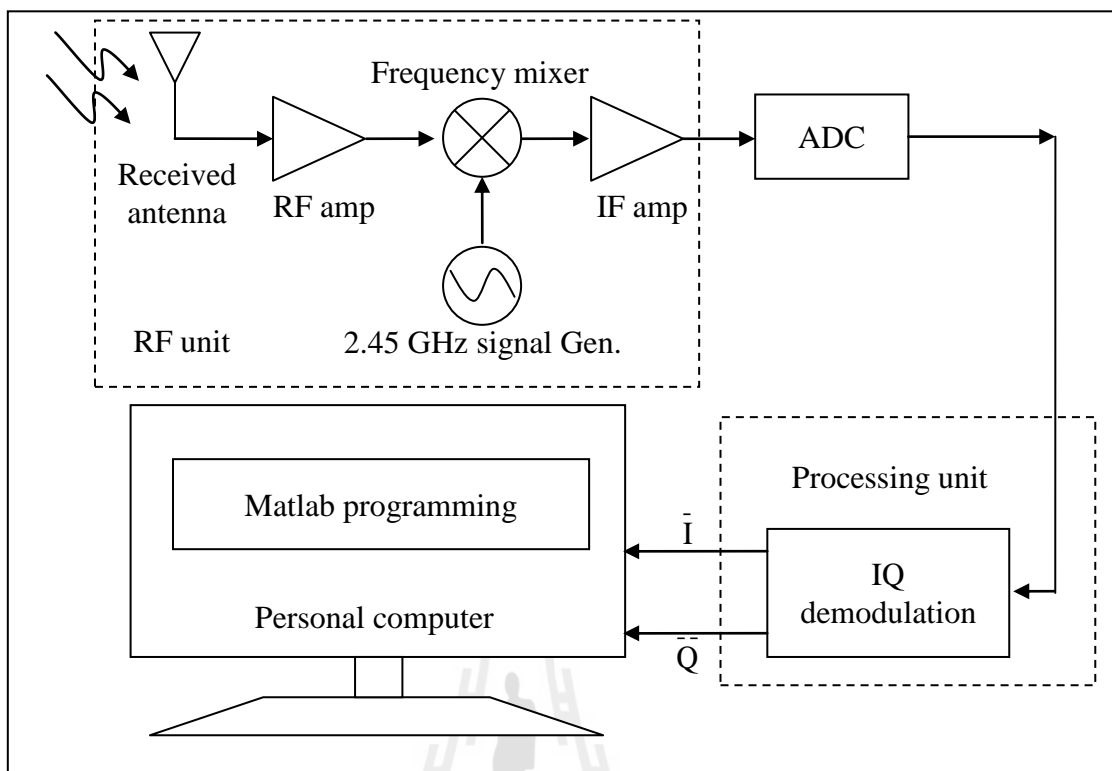


**Figure 6.17** Block diagram of receiver unit.

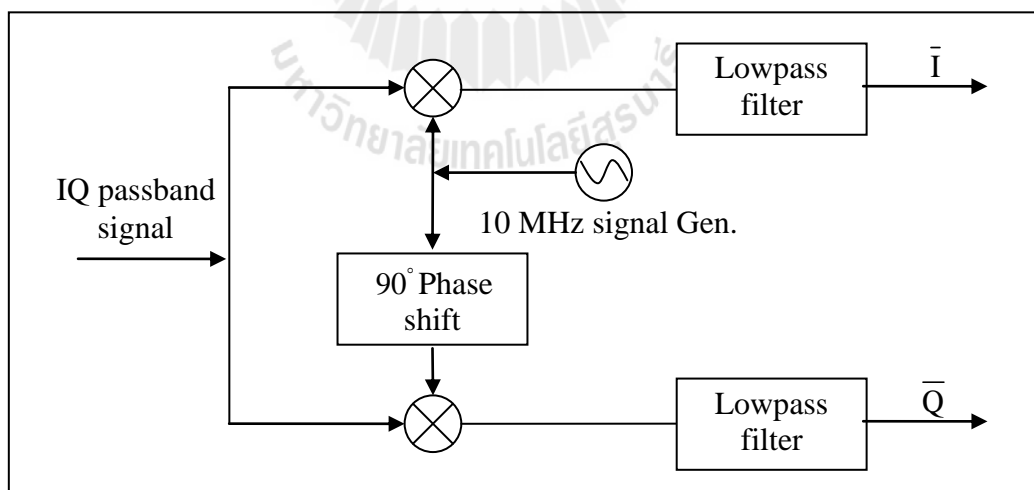


**Figure 6.18** IQ demodulation diagram.

programming can be shown in Figure 6.19. As seen in the figure, the received demodulated I and Q signals for each OFDM symbol are firstly converted into a

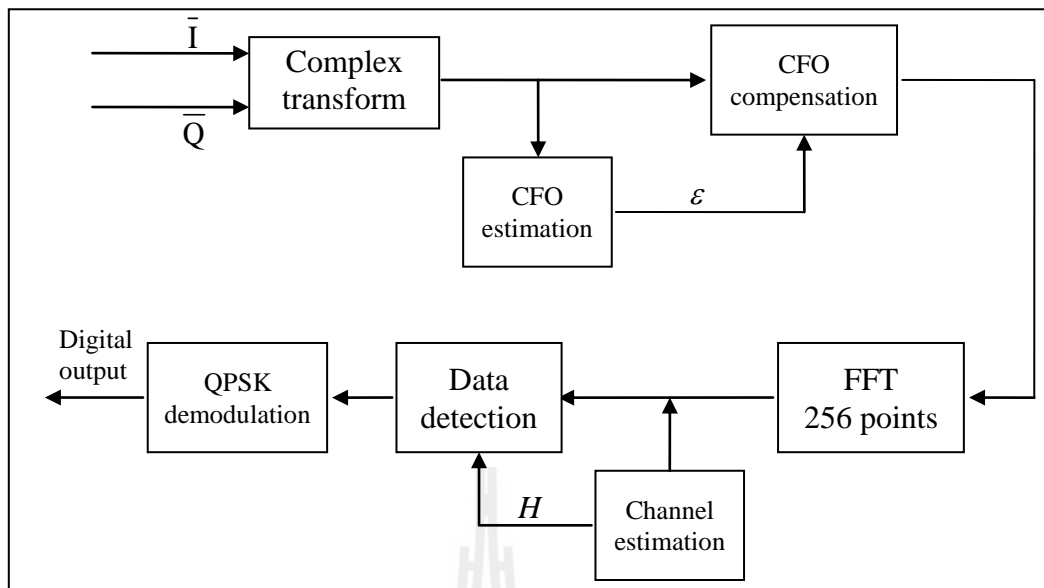


**Figure 6.19** Block diagram of Matlab programming.

complex signal. After that, this complex signal is used for CFO estimation and then compensation. The compensated signal is transformed into frequency domain signal by FFT operation with the same transformation size of transmitter where this frequency domain signal is used for both channel estimation and data detection. The entire estimated channels can be obtained by interpolation technique where the linear interpolation is used in this work. Finally, these detected data are mapped by QPSK demodulation in order to provide digital output signal. However, even if transmitter continuous sends OFDM symbols of fixed data but receiver can carry out with only one OFDM symbol for each OFDM signal detection process. Thus during the detection process, another transmitted OFDM symbol should be discarded.

### 6.3.3 Measurement setup

At first, please note that the measurements of this work are based on a small scale environment due to the limitation of transmitted power. Therefore, the experimental results may be different from the real mobile broadband channel.

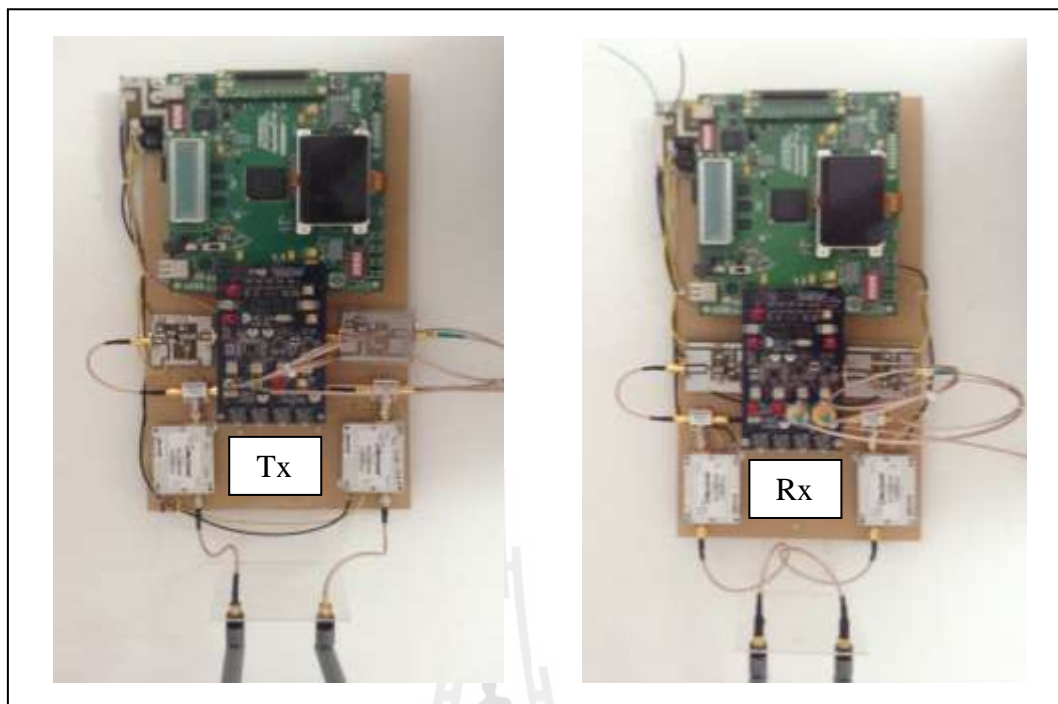


**Figure 6.20** Photograph of testbed.

However, the results from testbed can be used to predict the performance of the proposed technique in broadband channel in comparing with the conventional technique thus it can provide the same benefit even in mobile broadband channel.

The configuration of transmitter and receiver can be described in section 6.3.1 and 6.3.2 respectively. A photograph of transmitter and receiver can be shown in Figure 6.20. The guard time interval to prevent ISI is ignored in this work due to the consideration of small scale fading, and in order to reduce hardware complexity. The other testbed parameters are as follows:

- number of subcarriers ( $N$ ) = 256
- modulation = QPSK
- number of pilots ( $N_p$ ) = 43 (including  $N_{Null} = 14$  for null subcarrier technique)
- subcarrier spacing ( $\Delta f$ ) = 9.765 kHz

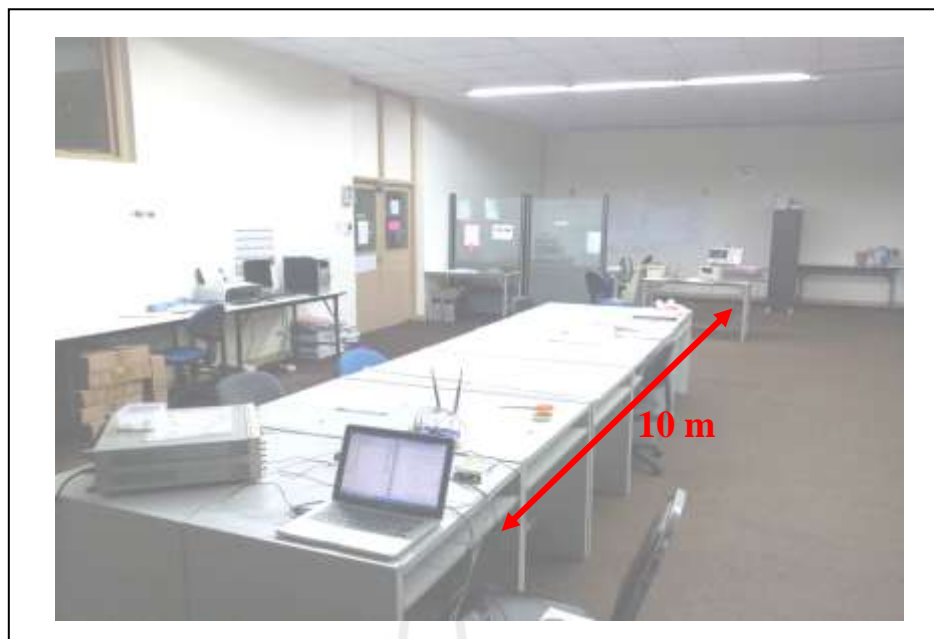


**Figure 6.21** A photograph of the measurement area.

- RF carrier frequency = 2.45 GHz
- step size of  $\varepsilon = 0.02$
- Interpolation technique = Linear interpolation

Where pilot subcarriers and null subcarriers for both techniques are placed by equi-space along the frequency axis. The proposed pilot scheme and the conventional pilot scheme for OFDM system have been described in section 5.2 where the conventional scheme is the combination between isolated pilot for channel estimation and null subcarriers for CFO estimation. Figure 6.21 shows a photograph of the measurement area where the distance between transmitter and receiver is about 10 meters. In this work, there is only one measurement location for the experimental setup because many cases of wireless channel can be happened in one measurement location. These cases are not the real mobile broadband channels, so one measurement location is sufficient for the experiment. In addition, it is impossible to know the exact CFO and

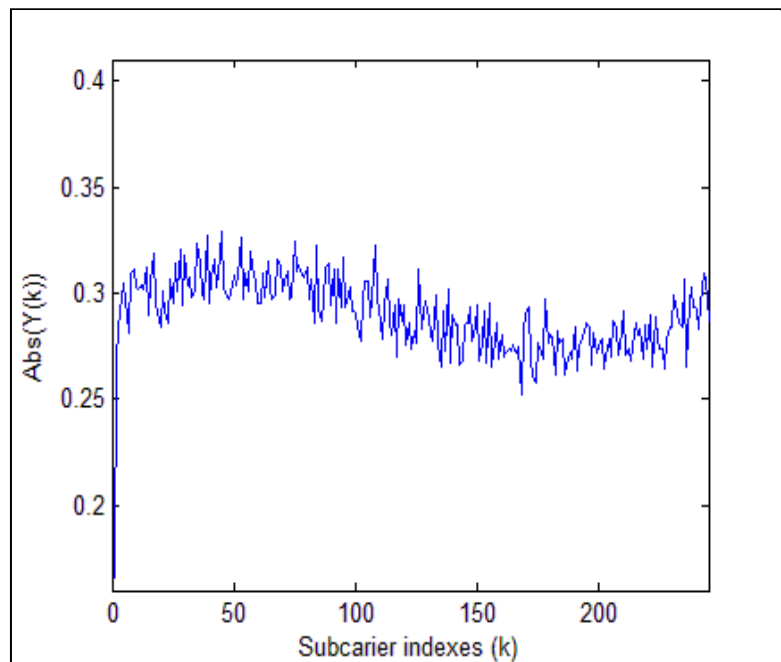
channel response that occurs in the practical system. Therefore, the error variance from estimation techniques cannot be calculated as same as the simulations presented in chapter 5. In order to make a performance comparison between the proposed technique and the conventional technique, BER performance is used instead where BER for each technique is calculated from 5,000 continuous OFDM symbols.

#### **6.4 Experimental results**

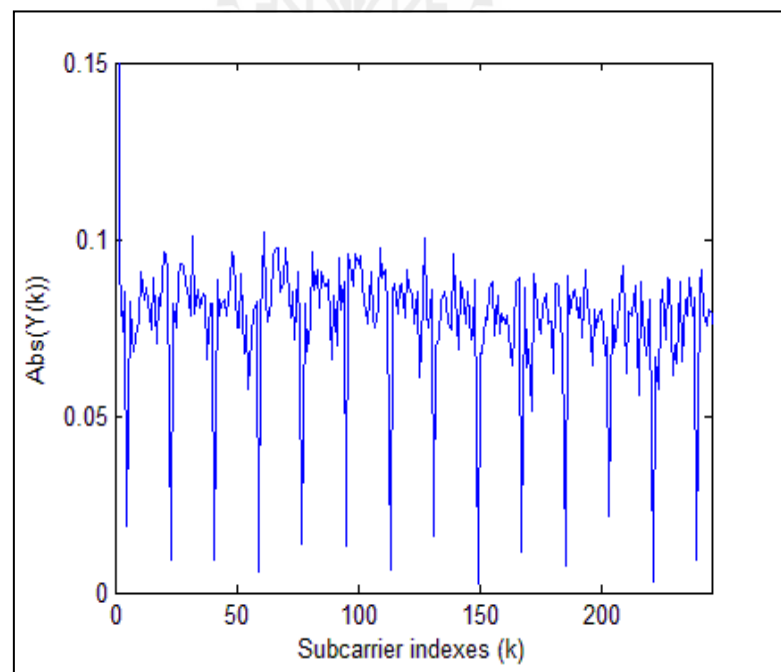
This section validates the performance of the proposed pilot scheme through the testbed testing as shown in last section. The performance is compared between the proposed clustered pilot scheme and the conventional pilot scheme. The BER performances are varied by adjusting the transmitted power. The transmitted power can be controlled easily by adjusting the RF carrier signal power at the signal generator. Note that, the transmitted power refers to RF carrier signal power for this section.

Figure 6.22 and 6.23 show examples of the received signal after performing FFT operation for the proposed clustered pilot technique and null subcarrier technique respectively. As seen in Figure 6.22 and 6.23, the spectrum of the proposed scheme differs from the spectrum of null subcarrier technique. There are low amplitude points which refer to null subcarriers in null subcarrier technique. These low amplitude points do not exist in the proposed scheme where these null subcarriers are placed by clustered pilot tones.

Figure 6.24, 6.25 and 6.26 show examples of the received signal constellation when the transmitted power is 0, 5 and -10 dBm respectively. As seen in these figures, the best performance of signal constellation is obtained when the transmitted power is 0 dBm. The groups of signals are clearly separated from each other when the



**Figure 6.22** The received signal in frequency domain of the proposed pilot scheme.



**Figure 6.23** The received signal in frequency domain of null subcarrier technique.

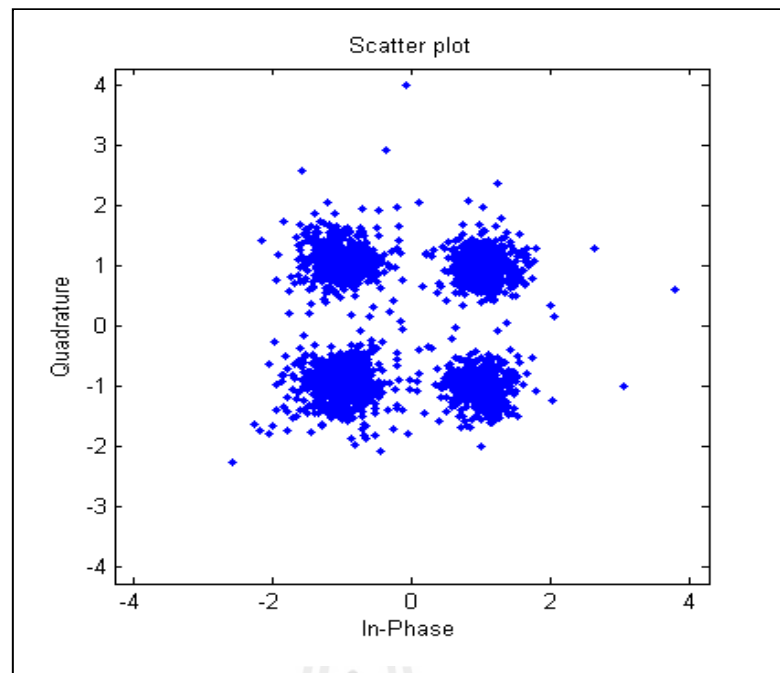


**Figure 6.24** The received signal constellation when transmitted power is 0 dBm.

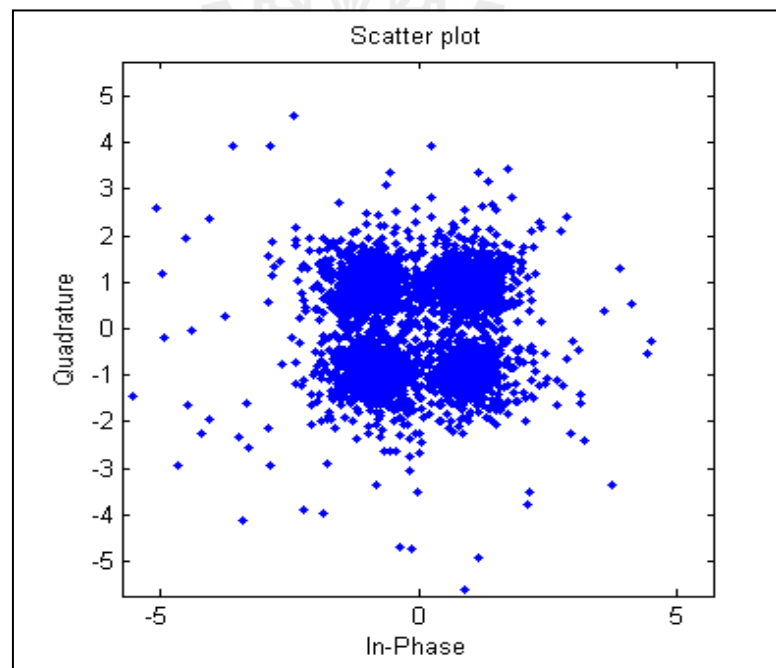


**Figure 6.25** The received signal constellation when transmitted power is -5 dBm.

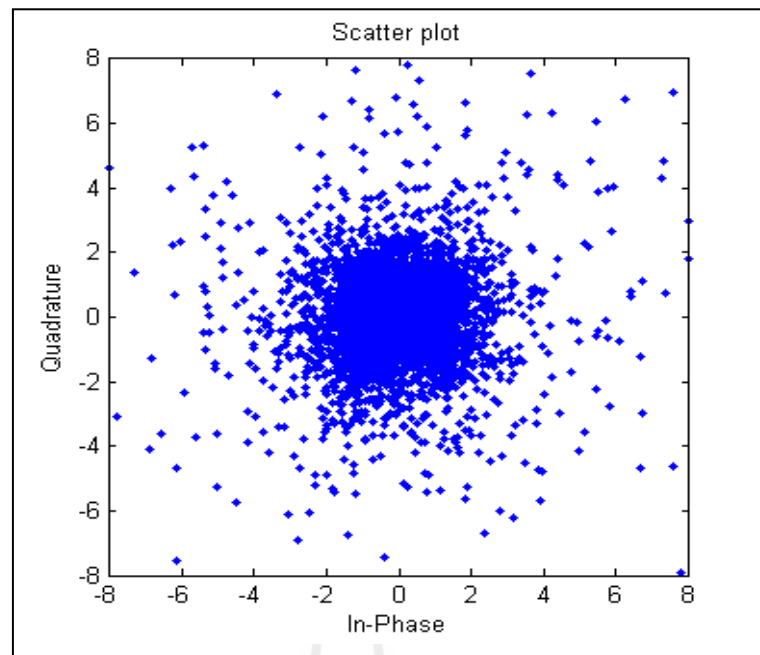


**Figure 6.26** The received signal constellation when transmitted power is -10 dBm.

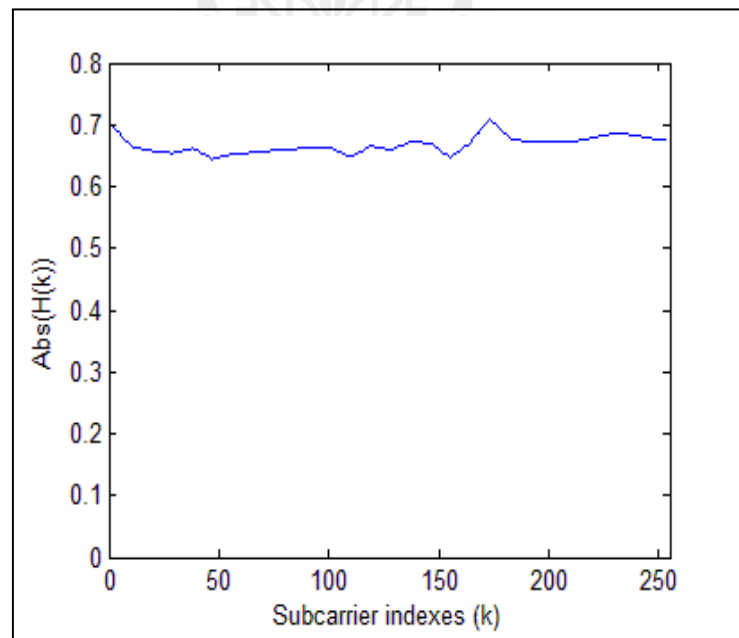


**Figure 6.27** The estimated channel response.

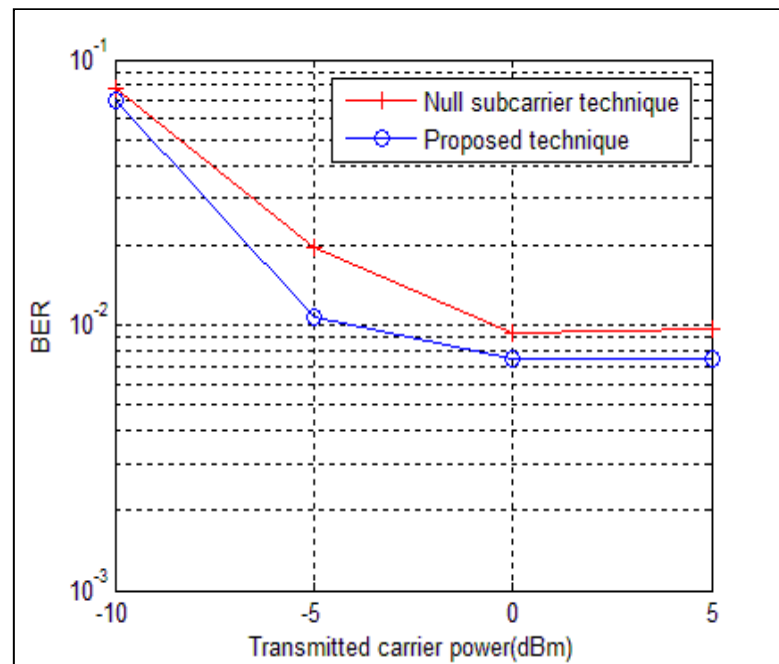


**Figure 6.28** BER versus Transmitted power.

transmitted power is 0 dBm. But groups of signals are mixed together when the transmitted power is -10 dBm, thus this case can provide a higher bit error rate.

Figure 6.27 shows an example of estimated channel. As seen in these figures, it must be noticed that the measured area is based on small scale fading environment which causes channel to act as flat in frequency response and there are few cases that frequency selective channel are occurred. It is the same result when the other measurement area (in the same room) is undertaken thus only one measurement area is sufficient for an analysis.

Figure 6.28 shows BER performance versus transmitted power where transmitted power range from -10 to 5 dBm. As seen in the figure, the proposed pilot scheme provides a better performance than the conventional pilot scheme for any value of transmitted power. Thus, this confirms that the proposed technique works well for practical system. However, BER performance for higher transmitted power

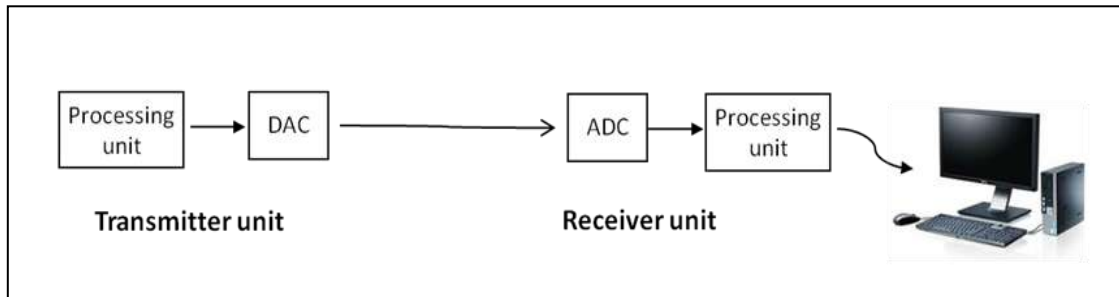


**Figure 6.29** Block diagram for testing IF signal.

from 0 to 5 dBm trends to reach a constant value which differs from simulation. The analysis of this effect is investigated and explained in the next section including performance comparison with simulation.

## 6.5 BER error floor analysis

### 6.5.1 IF signal analysis

In order to investigate BER floor from figure 6.28, IF signal to RF passband signal should be tested separately. Firstly, candidate start with IF signal test where the transmitter's DAC output of IQ modulation is connected directly with the ADC input at the receiver as shown in figure 6.29. The BER performance output of this configuration is 0 for every test. This BER value confirm that the processing unit, the data conversion unit and also algorithm in the Matlab's program work well for both transmitter and receiver thus BER error floor should come from another part in RF unit.

### 6.5.2 RF amplifier analysis

The case that RF amplifier can generate BER floor is when the input signal power is higher than the maximum rating of RF amplifier. If there is an OFDM signal point that exceeds this maximum threshold, it distorts the time domain

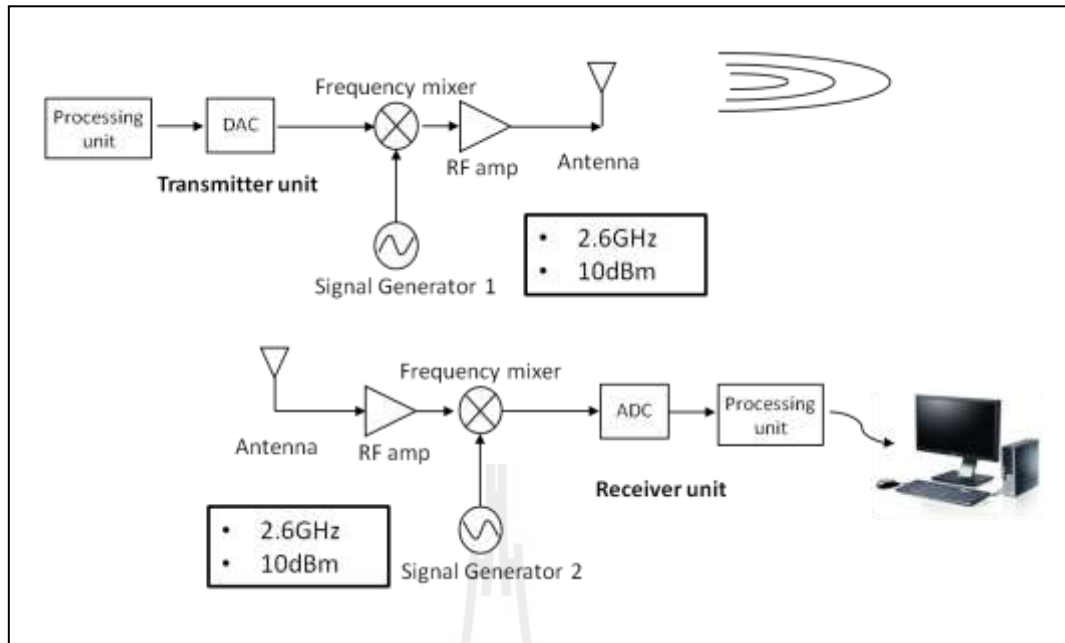


**Figure 6.30** Block diagram for testing RF amplifier.

OFDM signal which can produce more BER of system. To perform this analysis, the input power spectrum of RF amplifier is measured for both transmitter and receiver. However, IF amplifiers from both transmitter and receiver are neglected in this analysis (they are broken before doing BER error floor analysis), but this effect can be compensated by reducing the distance between the transmitter and the receiver. Figure 6.30 shows block diagram for testing RF amplifier. The transmitter and receiver carriers are set to be 2.6 GHz with the same signal power 10dBm (maximum transmitted carrier's power). The distance between transmitter and receiver is reduced to 3.5 meters which is about 65% distance reduction when comparing with figure 6.21. The input power of transmitted RF amplifier is about -35 dBm thus the possible maximum RF power input is about -25.5 dBm if IF amplifier is added (IF gain is 9.54 dB, see in 6.2.3). This power level cannot damage RF amplifier because the maximum input of RF amplifier ZQL-2700MLNW+ is 3dBm. It means that the transmitted

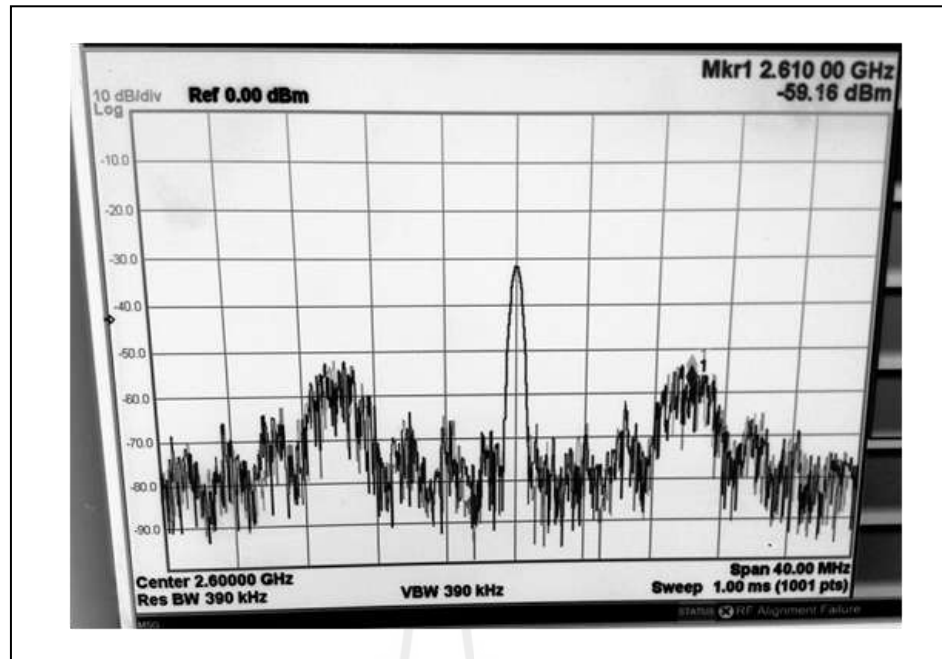


Figure 6.31 Received power spectrum.

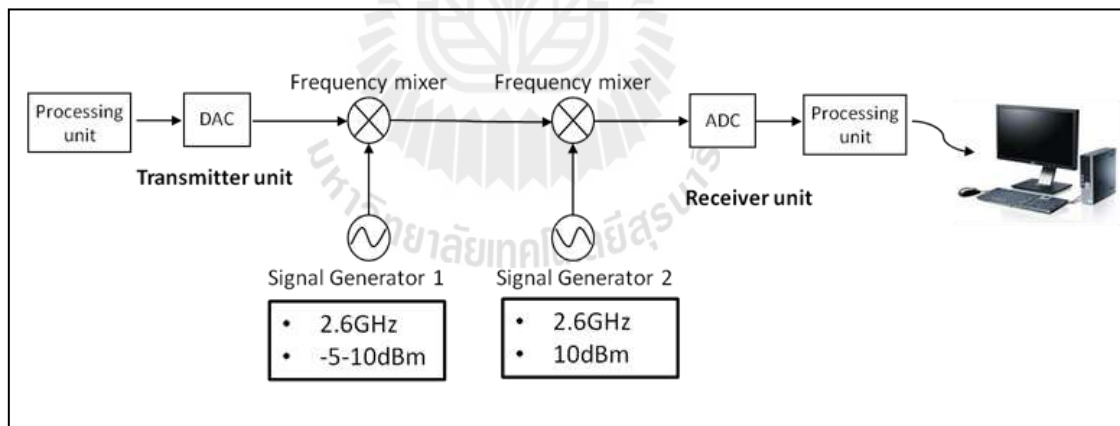
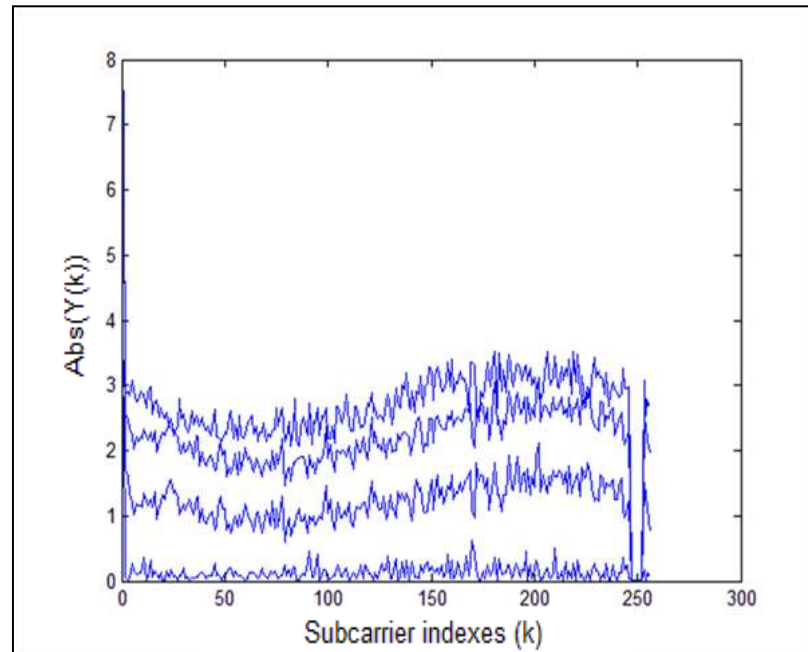


Figure 6.32 Block diagram for testing mixer.

RF amplifier operates in normal situations. Figure 6.31 shows the power spectrum of received signal where the power of OFDM signal is about -60 dBm and its carrier about -30 dBm. This signal also can not damage the received RF amplifier even if transmitted IF gain is included. The results from this analysis can conclude that



**Figure 6.33** FFT signal from receiver.

both RF amplifiers from transmitter and receiver normally operate.

### 6.5.3 Mixer analysis

Figure 6.32 shows block diagram for testing mixer. As seen in the figure, there is no RF amplifier for both transmitter and receiver where the output from transmitted mixer is directly connected with the input of received mixer. Thus wireless channel effect is not considered. The carrier signal power of transmitter varies from -5 to 10 dBm while received carrier signal power is fixed to 10 dBm. Figure 6.33 shows FFT output signals from the receiver by using 4 consecutive OFDM symbols and the transmitted carrier power is 10 dBm. As seen in figure 6.33, the FFT signals from receiver ripple between 3 and 0 where the lowest signal can produce bits error from 4 to 130 bits per OFDM symbol. The ripple in frequency domain signal occurs for any transmitted carrier power and it occurs only in the case that there is the difference between transmitted and received carrier frequencies.

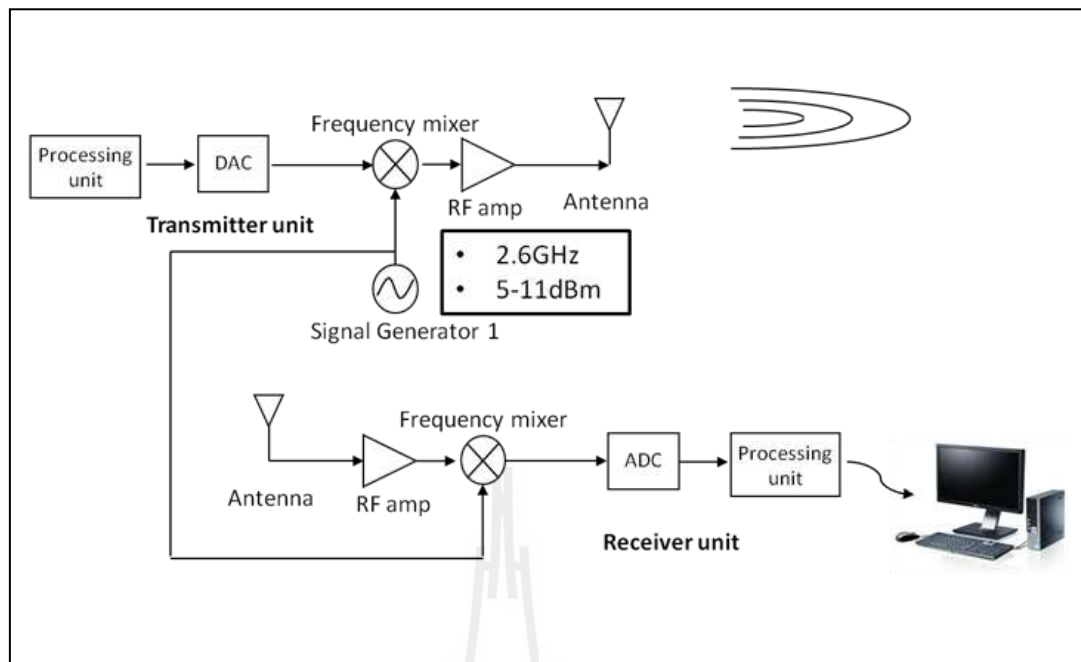


**Figure 6.34** The same source of signal generator test.

This frequency offset causes IF signals output from received mixer to be modulated with low frequency (frequency difference between transmitter and receiver). Thus it produces a slow ripple in received signal. The ripple in received signal causes directly to average received signal's SNR where it reduces SNR of the received signal even if transmitted carrier power is increased. At this point, candidate notices that the ripple in received signal due to the different carrier frequencies produces more BER from figure 6.28 and it also causes BER error floor for high transmitted carrier power.

In order to validate this assumption, the performance analysis when transmitter and receiver use the same source of carrier frequency is investigated. By using the same source of carrier frequency, it causes frequency offset from carrier signal to be 0. However, there might be frequency offset in the system even if the same carrier frequency is used. This is because the difference in IF frequency due to different clock's frequency from processing units and channel fading also produce

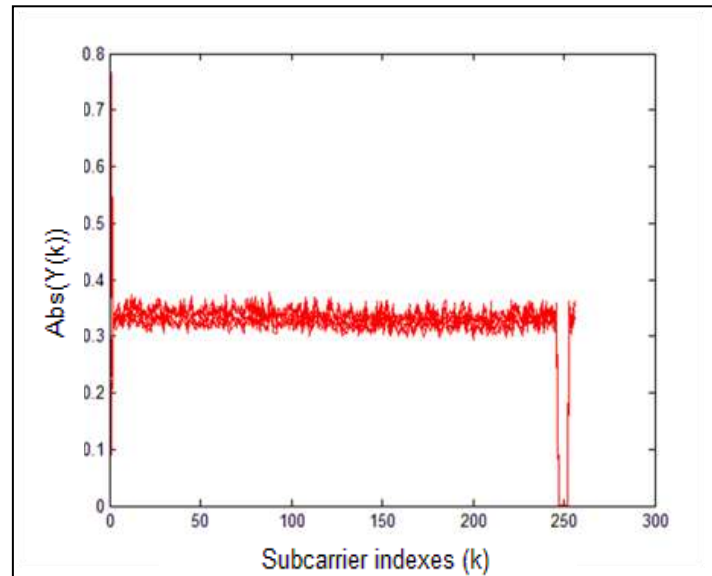
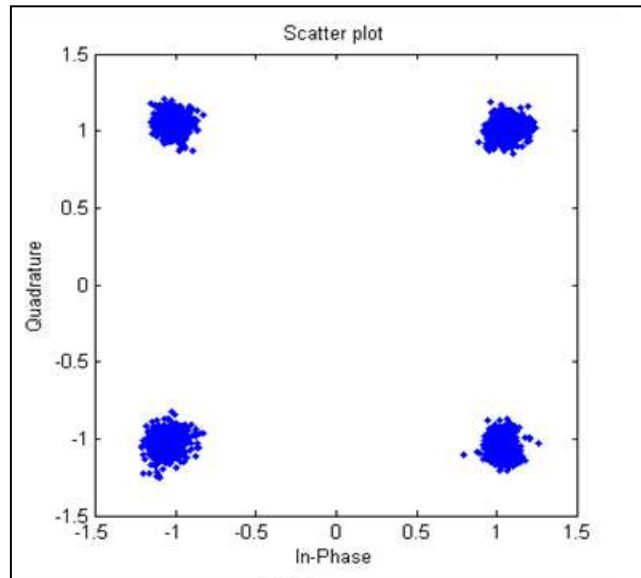


**Figure 6.35** FFT output of received signal.

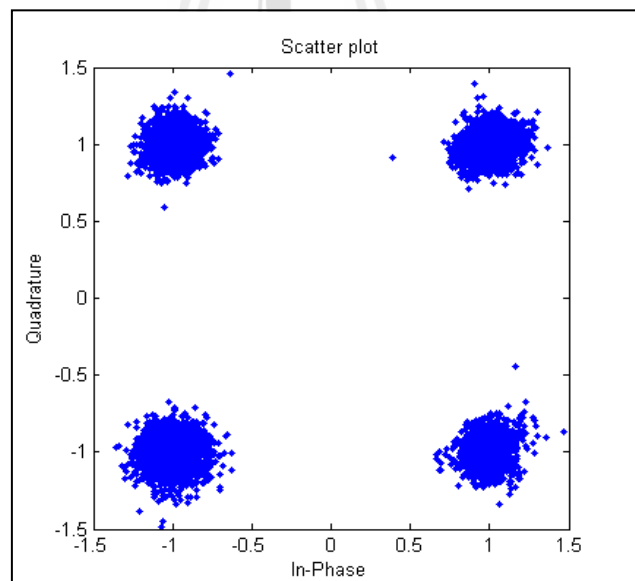
frequency offset. Figure 6.34 shows block diagram when the same carrier frequency is used. The distance between transmitter and receiver is 3.5 meters and the carrier power is 3 to 11 dBm.

Figure 6.35 shows FFT output of received signal when transmitted carrier power is 11 dBm and 50 consecutive OFDM symbols are undertaken. As seen in the figure, there is no ripple effect at received signal where there is a little change in FFT level which may be caused by fading channel. The result reveals that system can keep a constant SNR for every OFDM symbol when there is no ripple effect. Thus it not only improves BER performance from figure 6.28 but also provides possibility to compare experimental results with the simulation results.

Figure 6.36 and 6.37 show examples of received signal constellation when transmitted carrier powers are 9 and 7 dBm respectively. As seen in these figures, signals are separated into four groups where the signal dispersion becomes higher when transmitted carrier power is 7 dBm. The performances of these signal



**Figure 6.36** Signals constellation when carrier power is 9 dBm.



**Figure 6.37** Signals constellation when carrier power is 7 dBm.

constellations are better than prior test in figure 6.24 which is the case that there is a ripple effect due to the difference of carrier frequencies between transmitter and receiver.

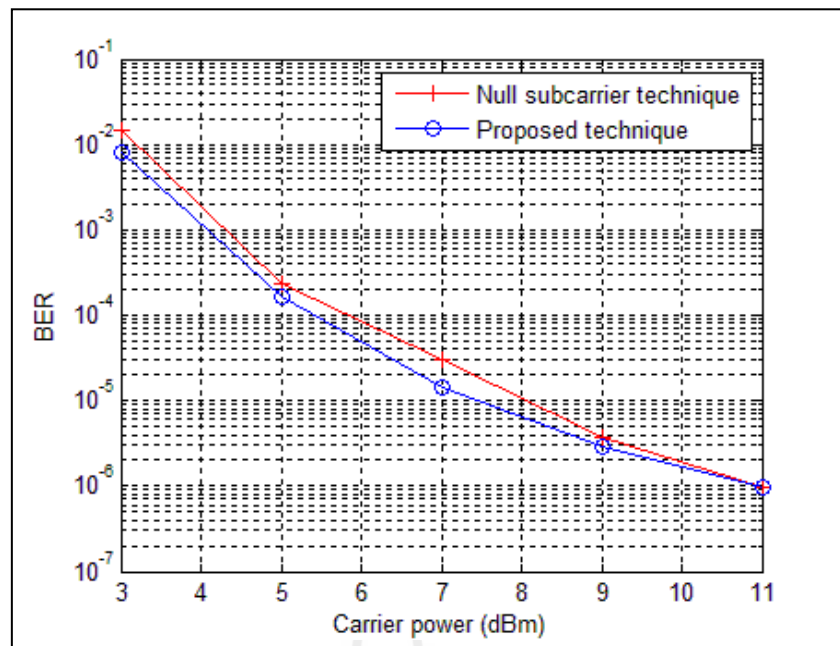


**Figure 6.38** BER versus carrier power.

Figure 6.38 shows BER performance versus transmitted carrier power when carrier power varies from 3 to 11 dBm. The result confirms that there is no BER error floor in the system. The performance looks better than figure 6.28 because there is no ripple effect in the received signal. Moreover, the proposed technique still provides a better performance than the null subcarrier technique and the performance gain is about 0.5 dB.

#### 6.5.4 Performance comparison between simulations and experiments

In order to compare the experimental BER with simulation, the carrier power axis has to be changed into  $E_b/N_0$ . The value of  $E_b/N_0$  is calculated by using received signals where these signals are compensated with the estimated channel, thus noise from channel estimation errors are also included. By assuming that, noise in system has zero mean then noise variance can be calculated by (Wireless Communications by Andrea Goldsmith)

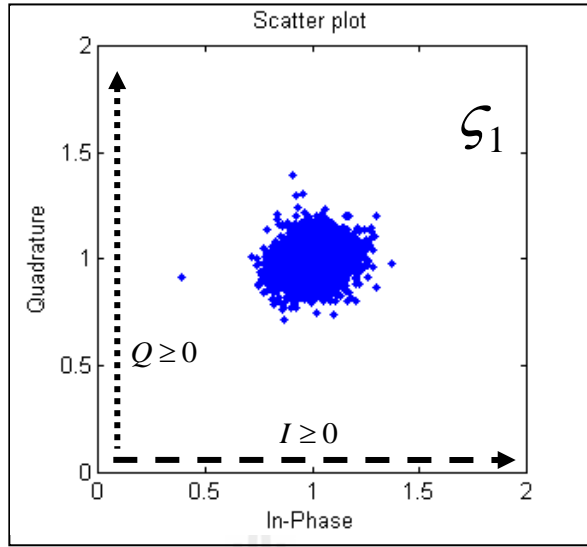


**Figure 6.39** Signals constellation of  $s_1$  when carrier power is 7dBm.

$$\sigma_q^2 = \frac{1}{N} \sum_{i=1}^N (z_i - s_q)(z_i - s_q)^* \quad z_i \in \zeta_q, \quad q = 1, 2, 3, 4 \quad (6.1)$$

where  $N$  is the number of signal samples,  $z_i$  is the received signal,  $\zeta_q$  is the decision region for each  $s_q$  and  $s_q$  is the QPSK signal. For QPSK modulation, there are four signals of  $s_q$  where candidate sets  $s_1$ ,  $s_2$ ,  $s_3$  and  $s_4$  are  $1+1j$ ,  $-1+1j$ ,  $-1-1j$  and  $1-1j$  respectively. Figure 6.39 shows an example of  $s_1$  noise variance calculation when 7 dBm of carrier power is investigated. As seen in the figure, the decision region can be given by  $\zeta_1 = Q \geq 0 \& I \geq 0$  and its variance can be written by

$$\sigma_1^2 = \frac{1}{N} \sum_{i=1}^N (z_i - (1+1j))(z_i - (1+1j))^* \quad z_i \in \zeta_1 \quad (6.2)$$

The average  $E_s/N_0$  can be given by

$$\frac{E_s}{N_0} (dB) = \frac{E_b}{N_0} (dB) + 3 = 10 \log \left( |s_q|^2 / \frac{1}{4} \sum_{i=1}^4 \sigma_i^2 \right) \quad (6.3)$$

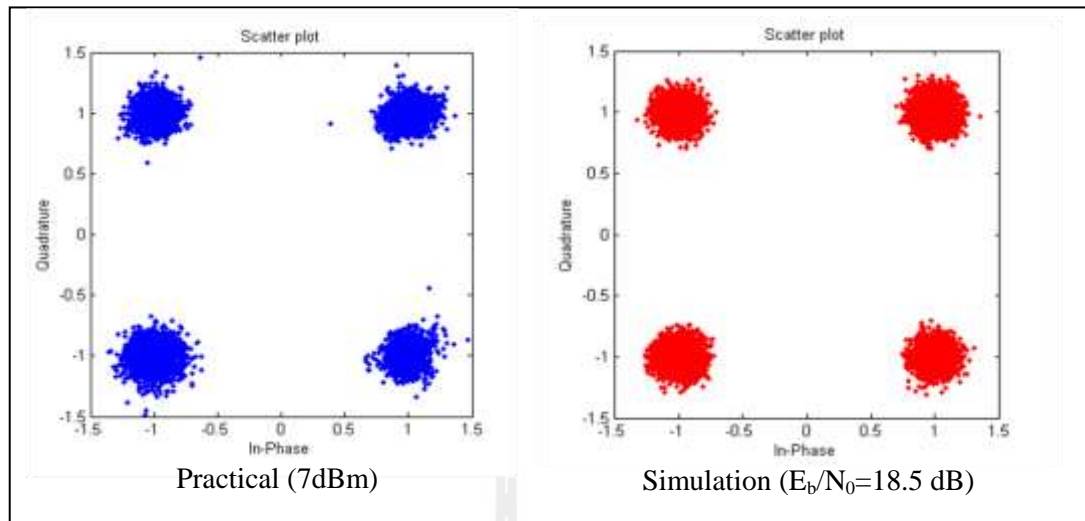


**Figure 6.40** Experimental results versus the calculated  $E_b/N_0$  from simulation.

Figure 6.40 shows the comparison of signals constellation between simulation and practical results where the simulation applied the calculated  $E_b/N_0$  to generate noise signals. As seen in the figure, these constellations are similar when they are put in the same scale of quadrature and in-phase axes. Therefore, the calculated  $E_b/N_0$  from the proposed method can be used to approximate  $E_b/N_0$ . However, CFO in the system is very low where there is no significant rotation in received signal constellation.

Figure 6.41 shows BER performance comparison between simulations and experimental results. Simulations for both the null subcarrier technique and the proposed technique are based on flat channel responses where CFO is set to be 0. As seen in the figure, the simulation results provide a better performance than experimental results for all  $E_b/N_0$ . The experimental results still provide a very low BER for high  $E_b/N_0$  while BER from simulations is 0 for both techniques. There is no surprise from this performance deviation between simulations and practical results. Simulations concern only CFO and channel problems where the other problems are

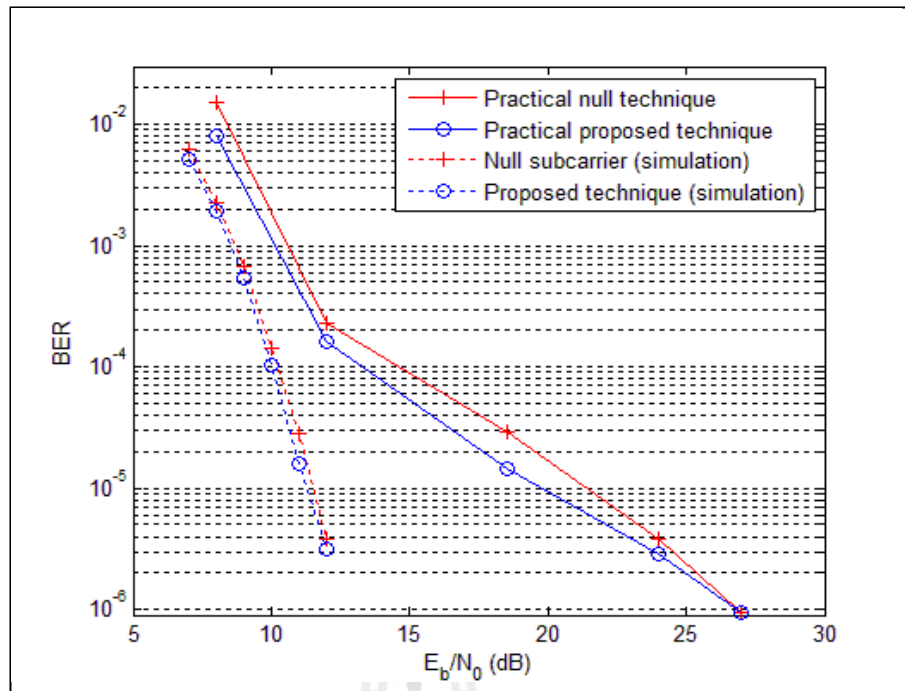


**Figure 6.41** BER performances for experimental and simulation results.

assumed to be perfect but in practical system there are many problems from literatures that can degrade BER performance such as IQ imbalance, phase synchronization at IQ demodulation, non-linearity of hardware components and signal errors from ADC and DAC. However, the performance of the proposed technique is better than the null subcarrier technique for both simulation and experimental results.

## 6.6 Chapter summary

This chapter has presented a testbed design in order to investigate the performance of the proposed pilot scheme for practical OFDM system. The performance of the proposed clustered pilot scheme is compared with the conventional scheme where the conventional scheme is the combination between isolated pilot tone for channel estimation and null subcarriers for CFO estimation. The results have

shown that the proposed scheme provides a better performance than the conventional scheme in term of BER performance. The practical BER has BER error floor which causes by ripple in received signal due to the difference between transmitted carrier frequency and the received carrier frequency. This ripple effect reduces received signal's SNR and thus it reduces BER performance. In fact, the proposed CFO estimation is used to solve this frequency offset but the proposed technique is based on digital domain likes the techniques which were proposed by Moose P., Fu X. and Zhang W. Therefore, the ripple effect is still existed if there is only CFO compensation in digital domain. In addition, the results are based on small scale fading environment which differs from mobile broadband channel. Thus, it may provide the different performance if mobile broadband channel is considered. However, these results can be used to be a guide line for the benefit of the proposed scheme over the conventional scheme even if mobile broadband channel is considered.

# CHAPTER VII

## THESIS CONCLUSION

### 7.1 Conclusion

The orthogonal frequency division multiplexing enables a high data rate transmission over multipath fading channels because of the transformation of entire frequency selective channel into a parallel set of frequency flat sub-channels. It has been widely adopted for standards such as DAB, DVB and WLAN. The quality of an OFDM system can be described by three basic parameters, namely the transmission rate, the transmission range and the transmission reliability. Conventionally, the transmission rate may be increased by reducing the transmission range and reliability. In turn, the transmission range may be extended at the cost of a lower transmission rate and reliability, while the transmission reliability may be improved by reducing the transmission rate and range. However, with the advent of MIMO assisted OFDM systems, the above-mentioned three parameters can be simultaneously improved. Thus MIMO-OFDM is a powerful technique for future wireless communications and it has been added into many wireless communication standards such as IEEE 802.11n, IEEE 802.16e and LTE.

Due to the growth of broadband communications, now broadband communication can support user's mobility where the standard is such as mobile WiMAX. However, user's mobility causes not only channel acting as time-varying channel but also frequency offset which causes transmitted carrier frequency to be

different from received carrier frequency. The OFDM signal is very sensitive to frequency offset where it causes a loss of BER performance. The channel and frequency offset are important parameters of a mobile broadband communication where both parameters can be changed every time due to mobility and surrounding environment. Thus, effective synchronization and tracking techniques for both channel estimation and frequency estimation have to be developed in order to improve the system performance. Recently, there are many works related to frequency offset estimation but they are based on measuring phase different between pilot symbols on consecutive OFDM symbols. Thus, these techniques may increase CFO estimation errors if channel is changed during sending two consecutive symbols. Therefore, in order to improve the CFO estimation performance, faster estimation algorithm should be more suitable for mobile broadband communications.

In this work, I present pilot scheme for channel estimation and CFO estimation for both OFDM system and MIMO-OFDM system where  $2 \times 2$  MIMO configuration is considered. The proposed pilot scheme was designed based on null subcarriers for CFO estimation. The estimation process of null subcarrier technique can be carried out with only one OFDM symbol, thus it is an effective technique especially for mobile broadband communications and it can be applied in both OFDM and MIMO-OFDM systems. In addition, the complexity of  $2 \times 2$  MIMO-OFDM's channel estimation can be reduced by the proposed pilot scheme and its estimation process can be successful with one OFDM symbol (as same as null subcarrier for CFO estimation). Thus, the proposed pilot scheme should be more suitable for mobile broadband communications.

The results have shown the performance comparison between the proposed scheme and the conventional scheme where the conventional scheme is the combination between null subcarriers for CFO estimation and isolated pilot tones for channel estimation. The results from simulation and experiment have shown that the proposed scheme provides better performance than the conventional scheme for both channel estimation and CFO estimation which leads to BER reduction. In addition, the experimental results are based on an OFDM system and small scale fading consideration. Therefore, in order to investigate the performance in the real mobile broadband channel for both OFDM and MIMO-OFDM systems, some future works based on these considerations should be tested and validated. However, the experimental results and simulation results from this thesis can be used as a guide line for the performance of the proposed scheme in practical mobile broadband channel, where the benefit of the proposed scheme is still better than the conventional scheme.

## REFERENCES

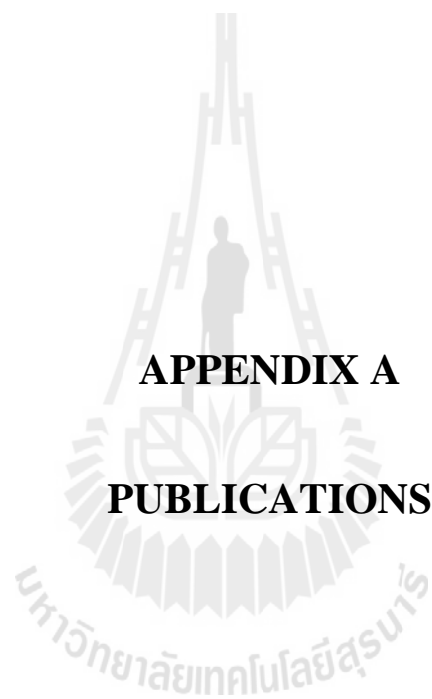
- Li, Y. and Stüber, G. (2006). **Orthogonal Frequency Division Multiplexing for Wireless Communications**. New York: Springer-Verlag.
- Digital Video Broadcasting (DVB); Framing Structure, Channel Coding and Modulation for Digital Terrestrial Television**. ETSI EN300 744, 1.4.1, Jan. 2001.
- Radio Broadcasting Systems; Digital Audio Broadcasting (DAB) to Mobile, Portable and Fixed Receivers**. ETSI EN 300 401, 1.3.3, May 2001.
- Telatar, I.E. (1995). Capacity of multiantenna Gaussian channels. **AT&T Bell Laboratories**. Tech. Memo.
- Sampath, H., Talwar, S., Tellado, J., Erceg, V. and Paulraj, A. (2002). A fourth generation MIMO-OFDM broadband wireless system: design, performance and field trial results. **IEEE Communications Magazine**. (9): 143-149.
- Zelst, A.v. and Schenk, Tim C.W. (2004). Implementation of a MIMO OFDM based wireless LAN system. **IEEE Transaction on Signal Processing**. 52(2).
- Hou, X., Zhao, C., Yin and Yue, G. (2005). Unified view of channel estimation in MIMO OFDM systems. **International Conference on Wireless Communication, Networking and Mobile Computing**. 54-58.
- Edfors, O., Sandell, M., van de Beek, J. J., Wilson, S. K. and Borjesson, P. O. (1998). OFDM channel estimation by singular value decomposition. **IEEE Transactions on Communications**. 46(7): 931-939.

- Rinne, J. and Renfors, M. (1996). Pilot spacing in orthogonal frequency division multiplexing system on practical channels. **IEEE Transactions on Consumer Electronics**. Vol. 42, No. 4, pp. 959-1343.
- Cho, Y.S. (2010). **MIMO-OFDM Wireless Communications with MATLAB**. John Wiley & Sons.
- He Zhong Tang and Cen Zi Li (2005). Simplified Channel Estimation Using Special Training Sequence for MIMO-OFDM Systems. **In Proc. IEEE Int. Conf. Wireless Communications, Networking and Mobile Computing**. 1: 19-23.
- Delestre, F. and Sun, Y. (2010). MIMO-OFDM with Pilot-Aided Channel Estimation for WiMax Systems. **In Proc. IEEE Int. Conf. Wireless and Mobile Computing, Networking and Communications**. 586-590.
- Bahumi, I., Leus, G. and Moonen, M. (2003). Optimal Training Design for MIMO OFDM Systems in Mobile Wireless Channels. **IEEE Transaction on Signal Processing**. 51(6): 1615-1624.
- Wang, D., Zhu, G. and Hu, G. (2004). Optimal Pilots in Frequency Domain for Channel Estimation in MIMO-OFDM Systems in Mobile Wireless Channels. **IEEE Vehicular Technology Conference**. 2: 608-612.
- Qiao, Y., Yu, S., Su, P. and Zhang, L. (2004). Research on an Iterative Algorithm of LS Channel Estimation in MIMO OFDM Systems. **IEEE CAS Symposium on Engineering Technologies; Mobile and Wireless Communication**.
- Zhao, Y. and Haggman, S. G. (1996). Sensitivity to Doppler shift and carrier frequency errors in OFDM systems—The consequences and solutions. **IEEE 46th Vehicular Technology Conference**. 1564–1568.

- Gudmundson, M. and Anderson, P. O. (1996). Adjacent channel interference in an OFDM system. **IEEE 46th Vehicular Technology Conference**. 918–922.
- Moose, P. (1994). A technique for orthogonal frequency division multiplexing frequency offset correction. **IEEE Transactions on Communications**. 42: 2908–2914.
- Van de Beek, J. J., Sandell, M. and Borjesson, P. O. (1997). ML estimation of time and frequency offset in OFDM systems. **IEEE Transactions on Signal Processing**. 45: 1800–1805.
- Morelli, M. and Mengali, U. (1999). An improved frequency offset estimator for OFDM applications. **IEEE Communications Letter**. 3(3): 75–77.
- Schmidl, T. M. and Cox, D. C. (1997). Robust frequency and timing synchronization for OFDM. **IEEE Transactions on Communications**. 45: 1613–1621.
- Shim, E. S., Kim, S. T., Song, H. K. and You, Y. H. (2007). OFDM Carrier Frequency Offset Estimation Methods With Improved Performance. **IEEE Transactions on Broadcasting**. 53(2): 567-573.
- Fu, X. and Minn, H. (2007). Modified Data-Pilot-Multiplexed Schemes for OFDM Systems. **IEEE Transactions on Wireless Communications**. 6(2): 730-737.
- Zhang, W., Xia, X. G. and Ching, P.C. (2007). Clustered Pilot Tones for Carrier Frequency Offset Estimation in OFDM Systems. **IEEE Transactions on Wireless Communications**. 6(1): 101-109.
- Yang, F., Li, K.H. and The, K.C. (2005). Adaptive LMS-LIKE Algorithm for Carrier Frequency Offset Estimation in OFDM Systems. **IEEE International Symposium on Signal processing and Its Applications**. 1: 131-134.

- Jian, X. and Chunni, Z. (2009). Frequency Offset Estimation of OFDM System Based on Kalman Filtering. **Communication Technology**. 42(1): 62-65.
- Liu, H. and Tureli, U. (1998). A high-efficiency carrier estimator for OFDM communications. **IEEE Communications Letter**. 2(4): 104–106.
- Ma, X., Tepedelenlioglu, C., Giannakis, G. B. and Barbarossa, S. (2001). Non-data-aided carrier offset estimators for OFDM with null subcarriers: Identifiability, algorithms, and performance. **IEEE J. Sel. Areas Commun.** 19(12): 2504–2515.
- Huang, D. and Letaef, K.B. (2006). Carrier Frequency Offset Estimation for OFDM Systems Using Null Subcarriers. **IEEE Transactions on Communications**. 54(5): 813-823.
- Lin, H., Nakao, T., Lu, W. and Yamashita, K. (2007). Subspace-based OFDM Carrier Frequency Offset Estimation in the presence of DC Offset. **IEEE proc. ICC 2007**. 2884-2887.
- Zhen, L. and Jianhua, G. (2006). Carrier Frequency Offset and Channel Estimation for MIMO OFDM Systems. **IEEE IET Conference on Wireless, Mobile and Sensor Networks**. 536-539.
- He, L. M. (2008). Carrier Frequency Offset Estimation in MIMO OFDM Systems. **IEEE Int. Conf. Wireless Communications, Networking and Mobile Computing**. 1-4.
- Simon, E. P., Ross, L., Hijazi, H., Jin, F., Gaillot, D. P. and Berbineau, M. (2011). Joint Carrier Frequency Offset and Fast Time-Varying Channel Estimation for MIMO-OFDM Systems. **IEEE Transactions on Vehicular Technology**. 60(3): 955-965.

- Hung, N.L., Tho, L.,N. and Chi, C. K. (2007). Vector RLS-Based Joint Estimation of Channel Response and Frequency Offsets for MIMO-OFDM. **Proc. IEEE Globecom 2007.**
- Wu, Y., Samir, A. and Bergmans, J.W.M. (2007). Efficient Training Sequence for Joint Carrier Frequency Offset and Channel Estimation for MIMO-OFDM Systems. **Proc. IEEE ICC.** 2604-2609.
- Chang, R.W. (1996). Synthesis of band- limited orthogonal signals for multichannel data transmission. **Bell Sys. Tech. Journal.** Vol. 45.
- ITU-R M.1225 International Telecommunication Union. (1997). **Guidelines for evaluation of radio transmission technologies for IMT-2000.**
- Sameer, S. M. and Raja Kumar, R. V. (2008). An efficient maximum likelihood CFO estimation scheme for MIMO-OFDM systems. **IEEE conference TENCON2008.** 1-5.
- D'Andrea, N. A., Mengali, U. and Reggiannini, R. (1994). The modified Cramer Rao bound and its application to synchronization problems. **IEEE Trans. Commun.** 42: 1391-1399.



**APPENDIX A**  
**PUBLICATIONS**

## List of Publications

### International Journal Paper

Uthansakul, P., Attakitmongkol, K., Promsuvana, N. and Uthansakul M. (2010).

MIMO Antenna Selections using CSI from Reciprocal Channel. **World Academy of Science, Engineering and Technology (WASET)**. 44: 587-596.

(Scopus)

Uthansakul, P., Promsuvana, N. and Uthansakul, M. (2011). Performance of Antenna

Selection in MIMO System Using Channel Reciprocity with Measured Data.

**International Journal of Antennas and Propagation (IJAP)**. 2011. (ISI

Impact factor 0.49)

### International Conference Paper

Promsuwanna, N., Uthansakul, P. and Uthansakul, M (2011). Modified Orthogonal

Pilot Scheme for Carrier Frequency Offset Estimation in 2x2 MIMO System.

**Asia-Pacific Microwave Conference (APMC)**.

Promsuwanna, N., Uthansakul, P. and Uthansakul, M (2013). A Novel Pilot Scheme

for Frequency Offset and Channel Estimation in 2x2 MIMO-OFDM.

**International Conference on Electrical, Computer and Communication**

**Engineering (ICECCE)**.

# MIMO Antenna Selections using CSI from Reciprocal Channel

P. Uthansakul, K. Attakitmongkol, N. Promsuvana and M. Uthansakul

**Abstract**—It is well known that the channel capacity of Multiple-Input-Multiple-Output (MIMO) system increases as the number of antenna pairs between transmitter and receiver increases but it suffers from multiple expensive RF chains. To reduce the cost of RF chains, Antenna Selection (AS) method can offer a good tradeoff between expense and performance. In a transmitting AS system, Channel State Information (CSI) feedback is necessarily required to choose the best subset of antennas in which the effects of delays and errors occurred in feedback channels are the most dominant factors degrading the performance of the AS method. This paper presents the concept of AS method using CSI from channel reciprocity instead of feedback method. Reciprocity technique can easily archive CSI by utilizing a reverse channel where the forward and reverse channels are symmetrically considered in time, frequency and location. In this work, the capacity performance of MIMO system when using AS method at transmitter with reciprocity channels is investigated by own developing Testbed. The obtained results show that reciprocity technique offers capacity close to a system with a perfect CSI and gains a higher capacity than a system without AS method from 0.9 to 2.2 bps/Hz at SNR 10 dB.

**Keywords**—Antenna Selection, Capacity, Channel, Measurement, MIMO, Reciprocity.

## I. INTRODUCTION

Multiple-Input-Multiple-Output (MIMO) system recently becomes one of the most attractive techniques for the future use because it proposes an extensive improvement over conventional smart antenna systems in both Quality of Service (QoS) and the transfer rate [1-4]. However, using multiple antennas require multiple radio frequency (RF) chains which consist of amplifiers, up and down converters, digital to analog converters, etc., that are typically very expensive. A promising approach for reducing cost while retaining a reasonably large fraction of the high potential data rate of a MIMO approach appears to be to employ some form of Antenna Selection (AS) [5-8]. The AS method employs a reduced number of RF chains at the receiver (or transmitter) and attempt to optimally allocate each chain to one of a larger number of receiving (transmitting) antennas which are usually cheaper elements. In this way, only the best set of antennas is

used, while the remaining antennas are not employed, thus reducing the number of required RF chains.

In literatures [9-17], the developments of AS method are classified into two main topics. At first, the algorithms to select the best subset of antennas are on focus. These algorithms may apply to either transmitter [9] or receiver [10]. The fast and precise selections are the required demand in practice. However, the success of these algorithms depends on the knowledge of CSI especially for the transmitting AS system that Channel State Information (CSI) feedback is necessarily required to be used for choosing the best subset of antennas [11-14]. Although the work presented in [15] tries to perform AS method without knowing CSI at transmitter for transmitting AS system, but the expense of many iterations degrades its attraction. For second topic, researchers pay attentions to the methods of Channel State Information (CSI) acquisitions. This is because the more exact CSI is realized, the more enhanced performance of AS method is obtained. Unfortunately, the CSI is usually not available at the transmitter so the method to realize CSI is still of important. In literatures, there are two approaches in order for the transmitter to obtain the CSI. The first approach utilizes CSI from feedback channel and the second approach is based on the reciprocity principle. In the first method, the forward channel is estimated at receiver and then it is sent back to the transmitter through the reverse channel. This method does not function properly if the channel is rapidly changed. In order to realize the correct CSI at transmitter, more frequent estimations and feedbacks are required. As a result, the overheads for the reverse channel become prohibitive. In turn, the second approach based on reciprocity does not have such a problem. Due to the reciprocity principle, it is well known that the radio propagation channel is reciprocal between two antennas. Ideally, the forward and reverse channels are assumed to be the same. Therefore, the transmitter can realize the forward CSI by estimating the reverse CSI instead. In Time-Division-Duplex (TDD) mode, the same carrier frequency is alternately used in forward and reverse channels. The propagation surrounding is not rapidly changed by time so the channel coefficients are able to be considered as similar for both directions. Based on TDD mode, the reciprocity approach is superior to any explicit feedbacks.

Recently there have been many researches concerning on channel reciprocity of a MIMO system which are based on the non-reciprocal effects between forward and reverse channel caused by any mismatches among RF components and

P. Uthansakul, N. Promsuvana and M. Uthansakul are with the School of Telecommunication Engineering, Suranaree University of Technology, Muang, Nakhon Ratchasima, Thailand 30000 (corresponding author phone: 66-44224351; fax: 66-44224603; e-mail: uthansakul@sut.ac.th).

K. Attakitmongkol is with the School of Electrical Engineering, Suranaree University of Technology, Muang, Nakhon Ratchasima, Thailand 30000.

interferences between transmitter and receiver [16-17]. However, from all works described in literatures [16-17], the system model is based on the assumption of that the forward and reverse channels are identical. This assumption is not practical because of the fact that fadings due to surroundings of transmitter and receiver are totally different. They cause the deviation of CSI between forward and reverse channel and it is wondered whether this deviation of non-reciprocal CSI would degrade the AS performance.

In this paper, the performances of adaptive MIMO system with AS method at transmitter based on channel reciprocity are investigated. The measured data are measured and tested by own developing Testbed based on FPGA board. In recent times, most researches move their experiments from simulations into real measurements. MIMO Testbed [18-23] is one the most comfortable platforms to realize the true performance of a proposed system under a real circumstance. For the work presented in [18-20], the performance investigations of MIMO system under indoor and outdoor have been reported through the Testbed. In [23], a transmitting AS system with an eigenbeam for MIMO-OFDM system is employed. This work achieves CSI via feedback technique and uses it to compute eigenvectors for selecting the best subset of transmitting antennas. In summary, all MIMO Testbeds presented in literatures utilize CSI from feedback channels. Moreover, some works [21-22] use a direct link to perform feedback channels which exclude any errors due to wireless operations. As far as the best survey of the authors, the issue of channel reciprocity for MIMO Testbed has never been reported in any publications. Hence, the contributions of this paper mainly fall into two issues. Firstly, the use of channel reciprocity for AS method in a MIMO system is originally demonstrated. The second contribution is on a proposed MIMO Testbed working by FPGA processors which is ready to be launched as commercial products. More importantly, it is interesting to delete the need of feedback channels by replacing reciprocity technique because this can save costs of system complexity and make the system more reliable.

In this work, the effect from the mismatches of RF components can be assumed to be neglected by using the exact same components at both transmitter and receiver. The CSI information between transmitter and receiver for using in AS method is acquired by channel emulator in which forward and reverse CSIs are measured from real propagation environments. The 2x4 MIMO channels are considered as 2x2 by AS method and then the channel capacity is calculated by computer to find the optimal subset of antennas. In addition, the comparison between feedback approach and reciprocity approach are also undertaken to provide the fair judgment with measured data. The results in this paper are helpful to realize the use of channel reciprocity in practice and its impact on channel capacity due to non-identical CSI between forward and reverse channels. The remainder of this paper is organized as follows. In Section II, the MIMO system model and two approaches estimating CSI are presented. Section III describes

the channel measurement and then the testing implementation is detailed in section IV. The MIMO channel capacities are presented in Section V. Finally, the paper conclusion is given in Section VI.

## II. MIMO SYSTEM MODEL

### A. MIMO Channel Capacity

Considering the MIMO system which has  $N_T$  transmitting antennas and  $N_R$  receiving antennas, the formula of MIMO channel capacity is given in (1) [4]. This expression presents the averaging capacity in bps/Hz by assuming the ergodic process for channel matrix  $\mathbf{H}$ .

$$C = E_H \left\{ \log_2 \det \left( \mathbf{I}_{N_T} + \frac{P_T}{P_N N_T} \mathbf{H} \mathbf{H}^* \right) \right\} \quad (1)$$

where  $\mathbf{I}_N$  is the  $N_R \times N_R$  identity matrix,  $P_T$  is the total transmit power,  $P_N$  is the noise power,  $N_T$  is the number of transmitting antennas,  $N_R$  is the number of receiving antennas,  $E_H\{\}$  is the expectation over  $\mathbf{H}$  and  $*$  denotes the conjugate and transpose operation.

When AS method is employed at the transmitter or the receiver, a subset of transmitting or receiving antenna elements is chosen. The channel seen by the subset is the sub-matrix,  $\mathbf{H}_{sub}$  that is obtained by selecting only the rows and columns of  $\mathbf{H}$  that correspond to the selected receiving and transmitting antenna elements. The optimal subset is one that leads to the largest mutual information between the antenna elements. The capacity of MIMO system with AS is given by

$$C_{sel} = \max_{S(\mathbf{H})} \log_2 \det \left( \mathbf{I}_{L_R} + \frac{P_T}{P_N L_T} \mathbf{H}_{sub} \mathbf{H}_{sub}^H \right) \quad (2)$$

where  $\mathbf{I}_{L_R}$  is the  $L_R \times L_R$  identity matrix,  $\mathbf{H}_{sub}$  is an  $L_R \times L_T$  matrix obtained by removing  $N_R - L_R$  rows and  $N_T - L_T$  columns from  $\mathbf{H}$  and  $S(\mathbf{H})$  denotes the set of all possible  $L_R \times L_T$  sub-matrices of  $\mathbf{H}$  that can be chosen.  $L_R$  and  $L_T$  represent the number of receiver RF chains and transmitter RF chains respectively. Please submit your manuscript electronically for review as e-mail attachments. When you submit your initial full paper version, prepare it in two-column format, including figures and tables.

### B. CSI at Transmitter

As seen in Section A, the system achieves the optimal capacity when the transmitter has knowledge of the forward channel. To obtain the CSI at transmitter, there are two approaches explained as follows.

#### 1. Feedback approach

For this approach, the receiver realizes a current CSI by channel estimation and then feeds it back to the transmitter through reverse channel. The configuration of feedback approach is shown in Figure 1.

In Figure 1, the receiver uses the estimated channel to extract the data and to generate the feedback CSI. The feedback CSI is sent back to the transmitter using the feedback control channel. It is assumed that CSI is perfectly known at the transmitter. The transmitter, in turn, uses this information to customize the transmitted signal for the channel.

In practice, errors from feedback link which influence to channel knowledge cannot be neglected. This effect can degrade the capacity performance and it is more pronounced when feedback link contain errors excessively, under this assumption the available CSI at transmitter can be expressed as

$$\mathbf{H}_T = \mathbf{H} + \varepsilon_E + \varepsilon_F \quad (3)$$

Or

$$\mathbf{H}_T = \mathbf{H}_{ES} + \varepsilon_F \quad (4)$$

where  $\mathbf{H}$  is the forward channel,  $\mathbf{H}_T$  is the available CSI at transmitter,  $\varepsilon_E$  and  $\varepsilon_F$  are  $N_R \times N_T$  errors matrix from estimation and error matrix from feedback link, respectively and  $\mathbf{H}_{ES}$  is the channel matrix which is achieved by channel estimation.

## 2. Reciprocity Approach

According to the principle of reciprocity, the forward and reverse channels are identical when the time, frequency and antenna locations are the same. Based on the principle, the transmitter may use the CSI obtained by the reverse link for the forward link. In practice, the forward and reverse channels are not truly identical because of the effect of channel fading, noises and environments. The CSI known at transmitter can be given by

$$\mathbf{H}_T = \mathbf{H} + \varepsilon_E + \varepsilon_R \quad (5)$$

where  $\varepsilon_R$  is the  $N_R \times N_T$  channel reciprocity error matrix realized by measurements.

## III. CHANNEL MEASUREMENT

The configuration of 2x4 MIMO system is shown in Figure 2, which network analyzer, power amplifier (PA) module, low-noise-amplifier module (LNA) and monopole antennas with 5 dBi gain are used. As seen in Figure 2, the PA module is used at transmitter to provide more transmitted power. As same as transmitter, the LNA module is used to increase the received signal level. The channel coefficients in both magnitude and phase are measured by network analyzer. The data was measured by 5 times per location. In each time, the 100 samples of channel data were recorded continuously within 1.5 seconds. However, we did not continue recording all 5 times in one round. The sequence of recording starts from Location 1 (100 samples) and then moves to Location 2 (100 samples) until Location 5 (100 samples). This sequence is called as one set. In the first day, we did two sets of measurements and the other three sets were done on the

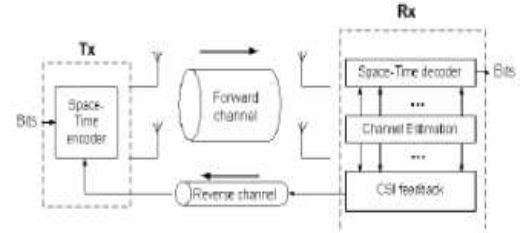


Fig. 1 MIMO model with a feedback channel.

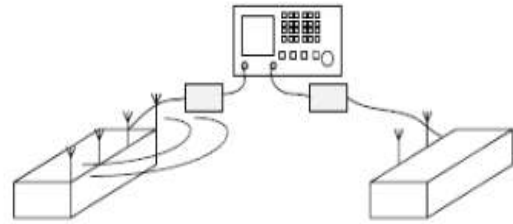


Fig. 2 Measurement set up.

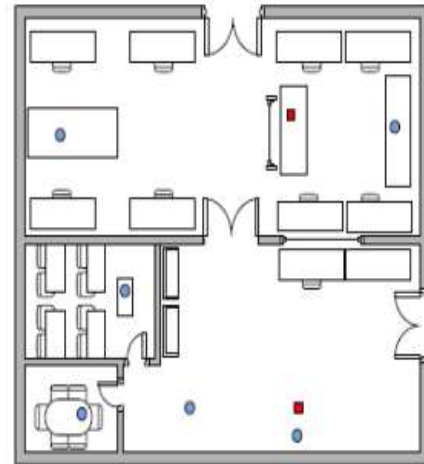


Fig. 3 Map of a measured area.

second day. In summary, 500 samples per location were collected over two days. In order to mitigate the effect of measurement noises, the function of network analyzer, called as smoothing command, is used to average the measured data over specific time. In this work, the specific time is the default operation at 10 ms. It means that each recorded sample is an averaging result over 10 ms.

For the measured area, we choose the large office room to provide many cases of study. Figure 3 shows the map of office room. The circular markers are referred to the locations where the measurement is undertaken. There are five measured locations. In each location transmitter and receiver are switched in order to measure the forward and reverse channel. Although, it is easier to measure both forward and reverse channels by switching transmitted port in network analyzer but the effect of non similarity of PA and LNA including feeding cables might differ the measured channel from the real

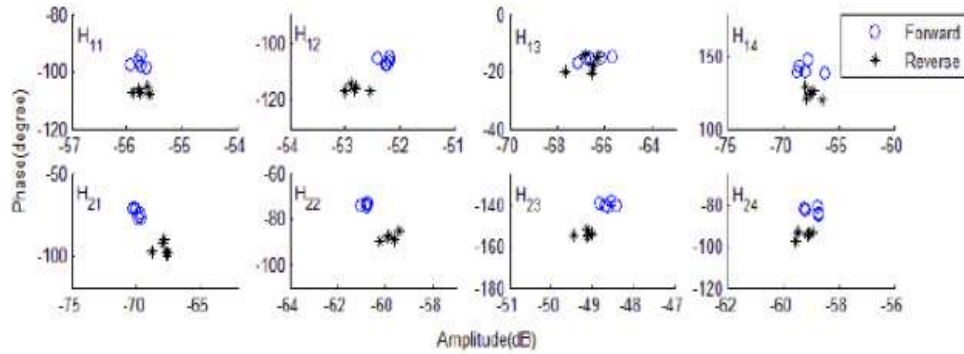


Fig. 4 Example of forward and reverse channels, measured at Location 4.

results. Therefore, we choose to switch all parts of transmitter and receiver in order to avoid any false outcomes. The switching time between transmitter and receiver is at least 20-30 seconds. In [24], the coherence time, which is the minimum interval that two signals are uncorrelated, is 21.2 ms. It means that the time interval between Tx frame and Rx frame of TDD mode must be longer than this coherence time. Hence, the measured forward and reverse channels are acceptably considered under the same criteria for TDD mode.

Figure 4 shows an example of each element of  $2 \times 4$  channel matrix at Location 4, where  $H_{ij}$  refers to the channel coefficient of  $i$ th receiving antenna and  $j$ th transmitting antenna. It can be observed that both forward and reverse channels are similar but not the same. The amplitude deviation is about  $\pm 2$  dB and the phase deviation is about  $\pm 15^\circ$ . These deviations were ignored in all works presented in literatures [16-17]. The result is important to realize how these deviations influence to the practical performance. As seen in Figure 4, the variation of measured data is very small because the environments seem to be a static channel. Hence, the results are grouped into two clusters, forward and reverse channels. However, the forward and reverse channels are not identical as expected because the surroundings of transmitter and receiver are different. For other locations, the deviations of amplitude and phase are similar to Location 4.

In addition, the correlation coefficients evaluated from measurements are 0.62, 0.325, 0.9, 0.52 and 0.73 for Location 1, Location 2, Location 3, Location 4 and Location 5, respectively. These values conclude that Location 2 is the most suitable area for MIMO operation because it has the lowest correlation coefficient in comparison with other locations. Then it is expected that Location 2 should offer more capacity than other locations as well. In turn, the capacity performance of Location 3 is expected to be poor due to its high correlation.

#### IV. TESTBED IMPLEMENTATION

##### A. Antenna Selection (AS) Technique

The capacity of MIMO system employing AS technique is described in (2), however this work concerns only the case of AS known at the transmitter. In order to find the optimal subset from knowing of only CSI at transmitter modeled in (3)

and (5) for feedback and reciprocity approaches respectively, the conventional technique is applied by searching all possible subsets of antennas and then select the best subset providing the highest capacity. As a result, the formula of MIMO channel capacity with AS technique at transmitter can be given by

$$C_{sel} = \max_{S \subseteq \{1, \dots, N_T\}} \log_2 \left[ \det \left( I_{L_R} + \frac{P}{L_T} \mathbf{H}_{T,sub} \mathbf{H}_{T,sub}^H \right) \right] \quad (6)$$

Where  $\mathbf{H}_{T,sub}$  is the  $N_R \times L_T$  sub-matrix (AS at transmitter) of CSI ( $\mathbf{H}_T$ ) obtained by feedback or reciprocity approaches.

It must be noticed that by using CSI in (6) to find the optimal subset of antenna, the differences between  $\mathbf{H}_T$  and  $\mathbf{H}$  ( $\mathbf{H}_T \neq \mathbf{H}$ ) cause directly to the capacity performance in (2) due to implementing errors from either feedback or reciprocity channels. In this work, the exhaustive search is applied to find the best antenna subset from all possible cases. Although there are many algorithms proposed in literature to select the antenna subset but the best solution is still the same as exhaustive search. Only fast processing and low complexity are the benefits of other algorithms. The purpose in this work is to investigate the performance of reciprocity channels in comparison with feedback channels so the same conclusion should be found for any AS methods.

##### B. Design of Developing Testbed

This work chooses Field Programmable Gate Array (FPGA) technology to implement  $2 \times 4$  MIMO Testbed because FPGAs processing were introduced as promising alternative to custom ICs for implementing entire system on one chip and to provide flexibility of re-program ability to the user. All functions are constructed inside FPGA boards including the AS method at transmitter where 2 transmitting antennas are selected. Hence, the system requires only 2 transmit and 2 receive components such as Analog to Digital Converter (ADC), Digital to Analog Converter (DAC). The block diagram of FPGA boards can be shown in Figure 5. As seen in Figure 5, RF components of transmitter and receiver have been replaced by using channel emulator. The concept of channel emulator has been adopted in many publications [21-22] in order to simulate the various

conditions of channel collected by real measurements. Another point of using channel emulator is to save cost of RF components because the boards can be functionally tested before passing through the production line.

In this work, we use Spartan 3An starter kit boards from Xilinx Company to implement transmitter and receiver which is explained as follows. Note that both transmitter and receiver boards shown in Figure 5 have the same components of transmitter and receiver to perform full duplex communication. However, we name the direction from transmitter board to receiver board as forward channel and the other direction as reverse channel.

### 1. Transmitter

The configuration of transmit system is shown in Figure 6. The series of bit information are generated and then it is fed to the de-multiplexer to convert from series to parallel bit information. After that it is modulated by BPSK modulation with frequency 12.5 kHz, bit 1 and bit 0 are represented by phase  $0^\circ$  and  $180^\circ$  respectively. The BPSK signal is fed to the channel emulator which acts as wireless communication channel. Finally, the signals from channel emulator are converted to analog signals which are sent to receiver board.

### 2. Receiver

The received analog signals from transmitter are fed to the channel estimation block to estimate the CSI which is used to select the optimum subset of antennas in AS method. The estimated CSI is shown via chip scope pro software on PC which is connected to the receiver board.

### C. Channel Estimation Methods

To obtain CSI at both transmitter and receiver, we develop the simple technique to estimate CSI and it can reduce the complexity of hardware implementation. Considering MIMO system which has 4 transmitting antennas and 2 receiving antennas, the set of training sequence is specified in Figure 7. To understand the principle of channel estimation, first we have to understand the layout of communication in 2x4 MIMO which can be written as

$$\begin{bmatrix} y_1 \\ y_2 \end{bmatrix} = \begin{bmatrix} h_{1,1} & h_{1,2} & h_{1,3} & h_{1,4} \\ h_{2,1} & h_{2,2} & h_{2,3} & h_{2,4} \end{bmatrix} \begin{bmatrix} x_1 \\ x_2 \\ x_3 \\ x_4 \end{bmatrix} \quad (7)$$

As seen in Figure 7, then the received signal at each receiving antenna at  $t$  time duration can be shown as

$$y_1(t) = h_{1,1}x_1(t) + h_{1,2}x_2(t) + h_{1,3}x_3(t) + h_{1,4}x_4(t)$$

and

$$y_2(t) = h_{2,1}x_1(t) + h_{2,2}x_2(t) + h_{2,3}x_3(t) + h_{2,4}x_4(t)$$

Let  $S_0$  and  $S_1$  are defined by BPSK signals representing 0 and 1 bit modulation respectively, then the channel coefficient can be calculated by

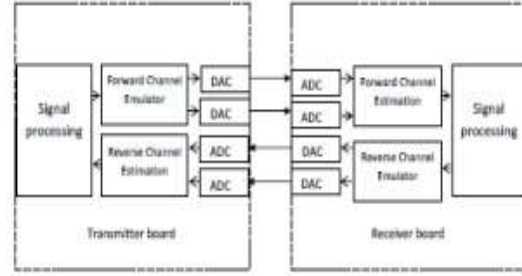


Fig. 5 System diagrams of transmitter and receiver.

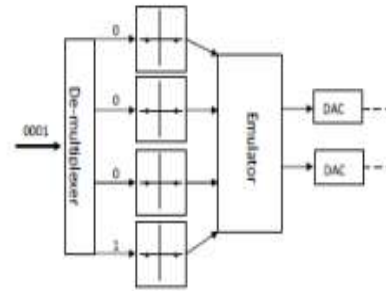


Fig. 6 Configuration of a transmitting system.

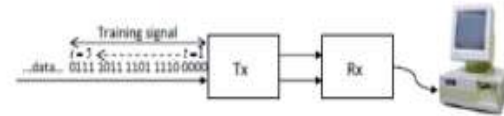


Fig. 7 Pattern of a training signal.

$$h_{k,l-1} = \frac{y_k(t=1) + y_k(t)}{2|S_0|} \quad (8)$$

In this work, eq. (8) is used to implement on FPGA and it is help to estimate both forward and reverse CSI. Accordingly, these estimated CSIs are used in AS algorithm mentioned earlier.

### D. Test Results

To complete testing system, channel emulators are operated for both forward and reverse channels. These channel information are determined by real measured data and programmed on FPGA boards. The obtained results are collected for the case of AS method, which is employed at only transmitter. Personal computers are connected to the transmitter and receiver to provide programmable interface and capture all concurrence data. Moreover, the oscilloscope is used to capture a real signal coming from any concerned ports in order to compare signal from both forward and reverse channels.

To implement channel emulators for both forward and reverse channels, the measured data described in Section 3 is used. However, channel information matrices from

measurements have to be multiplied and divided with a constant value in order to adjust a suitable level for ADC and DAC specifications. This is to avoid the unwanted effect due to low sensitivity of ADC or DAC, which it causes a signal error at receiver. Also, by multiplying or dividing channel information matrices with a constant value, it does not change the property of channel characteristics.

Figure 8 shows an example of channel information of forward channel at Location 1 which is obtained by channel estimation and it is shown by Chip scope pro software. As seen in Figure,  $a_{Hij}$  and  $p_{Hij}$  refer to estimated amplitude and phase of channel coefficient of  $i$  th row and  $j$  th column respectively (Each amplitude are in ADC's based values and these values must be convert to the actual value before use). The estimated forward and reverse channels have the similar channel responses and there are some phase and amplitude errors between forward and reverse channel for any locations. These errors are occurred by non-identical property of forward and reverse channels. However the other errors due to hardware such as DAC and ADC have been already considered and included in the results. After capturing by both Chip scope pro software as well as real oscilloscope, the channel emulators implemented on FPGA boards properly provide the correct forward and reverse channels realized by measurements. Figure 9 shows an example of comparison in complex form between forward and estimated forward channel matrix by using one sample of channel data at Location 1. The estimated forward and forward channels are similar in terms of real and imaginary parts. Although the deviations are still valid, these are very little in comparison with the errors between forward and reverse channels depicted in Figure 4. Therefore, the channel estimation implemented in the Testbed works very well and ensures the correct achievement of CSI from available sources, either feedback or reciprocity approaches.

## V. RESULTS AND DISCUSSION

All capacity results in this section are off-line produced on computer by using real AS outcomes from Testbed selections mentioned in the previous section. Therefore, these capacities can be compared with various system conditions including Rayleigh propagation channel and perfect CSI system which are hardly measured in real scenarios. The MIMO channel capacities are computed by MATLAB programming when AS methods are employed by using (2) and (6). Note that  $\mathbf{H}_T$  of forward and reverse channels are obtained by Testbed system. For feedback approach, at first we assume that there is no feedback error in feedback channel and then at the end of this section the effect of this error will be illustrated. The simulations disregard the mismatches of RF circuits in transmit/receive components as well as mutual coupling effects because they are included in one part of channel measurements.

The capacity performances are base on Cumulative Distribution Function (CDF) at SNR=10dB by using 500 samples of the collected channel data and they are illustrated into five cases, Rayleigh channel, AS with feedback channel, AS with perfect CSI, AS with reciprocity channel and no use

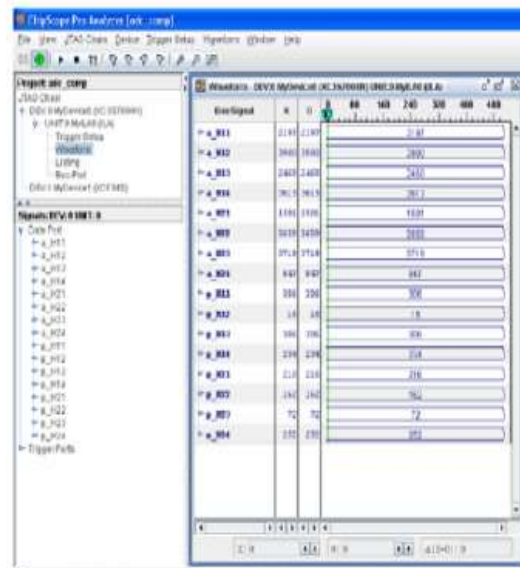


Fig. 8 Example of channel information obtained by own developing channel estimation.

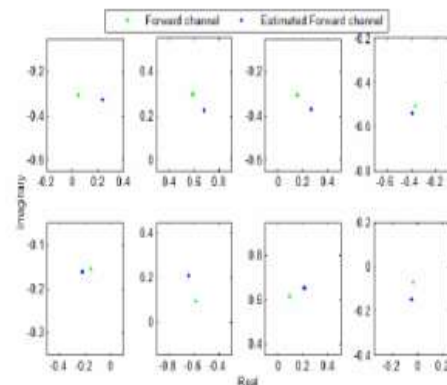


Fig. 9 The comparison example between forward and estimated forward channels at Location 1.

of AS method. In case of no antenna selection, the first and second transmitting antennas are used to transmit signals for any locations. For sake of comparison, the channels are normalized to provide a comparable discussion by  $\sum |H_{ij}|^2 = N_T N_R$  which limits total channel energy to one constant value. This normalization is done in order to compare channel properties between various conditions by neglecting the effect of path loss. All details of five cases are explained as follows.

- *Rayleigh channel* : this case represents the capacity of 2x2 MIMO system when wireless channel acts as Rayleigh fading channel which is random channels over 10,000 times.
- *No Antenna Selection* : this case represents capacity of 2x2 MIMO system when there is no selection at transmitter where the first and second antenna elements are used to transmit signals.

- *AS with Feedback* : this case represents the capacity when the CSI from feedback approach is used to select transmitting antennas in AS technique. Two of four transmitting antennas are optimally chosen to offer the best capacity.
- *AS with perfect CSI* : this case represents the capacity when the CSI is assumed to be perfectly known at transmitter. Hence, the selected transmitting antennas in AS technique are ideally optimal corresponding with the wireless channels. There is no error taken into account so the capacity is computed by using (2).
- *AS with Reciprocity* : this case represents the capacity when the CSI from reciprocity approach is used to select transmitting antennas in AS technique.

As mentioned in Section III, there are five measured locations in which the channels are collected. The surrounding of each location is so different that the capacity results are considerably separated into each location to make a fair judgment on all approaches.

*Location 1* As seen in Figure 10, the cumulative distribution function of capacity for AS methods with reciprocity and feedback approaches are close to a perfect CSI case where a feedback case is slightly better than a reciprocity case. The results of reciprocity case provide a performance gain 1 bps/Hz higher than Rayleigh at 50% probability. For this reason, it can be explained that the measured channels at Location 1 might be captured in the area above 50% probability of Rayleigh distribution. However, at 95% probability, the AS methods based either feedback or reciprocity reach the same performance as Rayleigh. In addition, AS method with reciprocity give a performance gain 1.15 bps/Hz higher than a system without AS method at 50% probability.

*Location 2* In Figure 11, the cumulative distribution function of capacity for no AS method, AS methods with reciprocity and feedback cases are close to a perfect CSI case and they provide a performance gain up to 1.3 bps/Hz higher than a case of Rayleigh at 50% probability. It is interesting to observe that no AS method provides a performance close to a perfect CSI case at this location. The reason is that no AS method always fixes the first and second transmitting antennas to operate a 2x2 MIMO system which is the best subset of antenna selections.

*Location 3* Figure 12 shows the cumulative distribution function of capacity at Location 3. In this location, the interesting point is that a Rayleigh case gives the highest capacity at 50% probability while a Rayleigh case is lower than a perfect CSI case for the other locations. It is also noticed that the performance of a reciprocity case seems to fail on selecting the best subset because the difference of reciprocity and feedback approaches is very large. In this response, the authors generate the other cases with the fixed transmitting antennas to closely investigate this outcome. The presented dot line with (x,y) is defined as a system with no AS method which always use xth and yth transmitting antennas to perform 2x2 MIMO operation. The results indicate that a reciprocity case still offers a higher capacity than all cases of no AS method. It is implied that the AS method still works

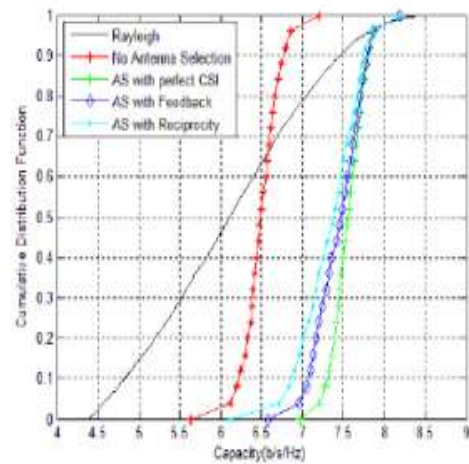


Fig. 10 The cumulative distribution function of capacity at Location 1.

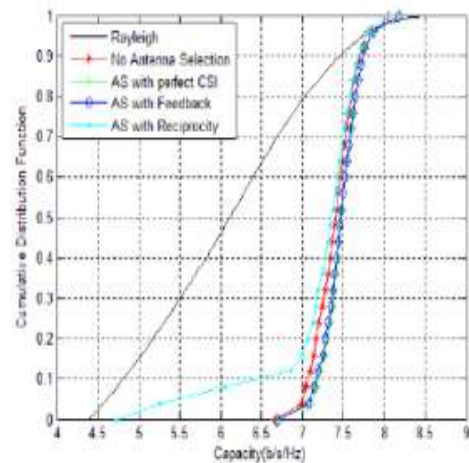


Fig. 11 The cumulative distribution function of capacity at Location 2.

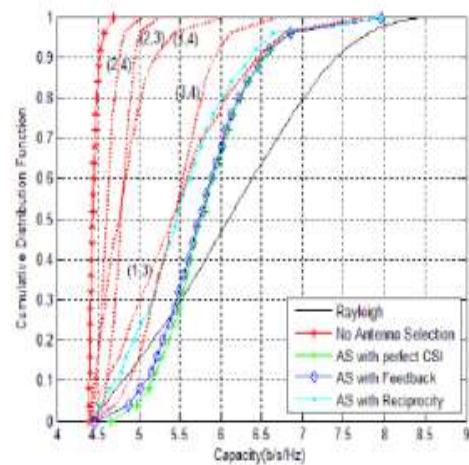


Fig. 12 The cumulative distribution function of capacity at Location 3.

well based on a reciprocity channel. Hence, the poor performance of a reciprocity case in this location is due to only the property of channel which is a direct LOS communication illustrated in Figure 3. The results confirm the well known conclusion that a MIMO capacity in a dominant LOS signal is less than in a Rayleigh channel.

*Location 4* The aim of measuring at this location is to investigate the channel property when there are obstructions between transmitter and receiver, in comparison with Location 3. As shown in Figure 13, the cumulative distribution functions of capacity for AS methods with reciprocity and feedback cases are similar and close to a perfect CSI case after 50% probability. The capacity results of AS methods in this location are higher than the results at Location 3 which confirms the conclusion mentioned in Location 3. For Location 4, the use of AS method with reciprocity can provide 2.2 bps/Hz higher than a case of No AS method at 50% probability.

*Location 5* As noticed in Figure 14, the results of AS method with reciprocity seem to fail on selecting the best subset of antennas as same as in Location 3. However, the authors did the other cases of fixed transmitting antennas and achieved the same conclusion that AS method with reciprocity still provide a higher capacity than all cases of no AS methods. However, the difference of reciprocity cases between Location 3 and Location 5 is that the capacity of Location 5 is higher than a Rayleigh channel. This can be described by the surrounding around transmitter and receiver are very different and its cause more scattering than Location 3.

In summary, a system using AS method with reciprocity always gives the performance better than a system without AS method while it is slightly less than feedback and perfect CSI cases. However, for AS method with feedback, the presented results are based on the exclusion of any errors in a feedback channel in which these errors are compulsorily occurred in practice due to channel delays and feedback noises. As a result, it is also necessary to examine the effect of feedback errors on capacity performances.

In order to investigate feedback errors included in feedback channel, this work assumes that the model of feedback error ( $\varepsilon_F$  from (3)) is given by

$$\varepsilon_F = \sigma \mathbf{H}_{i.i.d.} \quad (9)$$

where  $\mathbf{H}_{i.i.d.}$  is i.i.d. (Independent Identically Distributed) channel matrix with zero mean and unit variance,  $\sigma^2$  is the variance of feedback errors  $\varepsilon_F$ .

Figure 15 shows the effect of feedback errors on capacity performance of AS method at Location 5. It is obviously seen that errors degrade the capacity performance as a function of error variance. Also seen in the figure, the capacity performance of AS method with feedback is worse than a reciprocity case when the error variance in a feedback channel is more than 0.4. The results indicate the tradeoffs between using reciprocity and feedback approaches. If the variance of

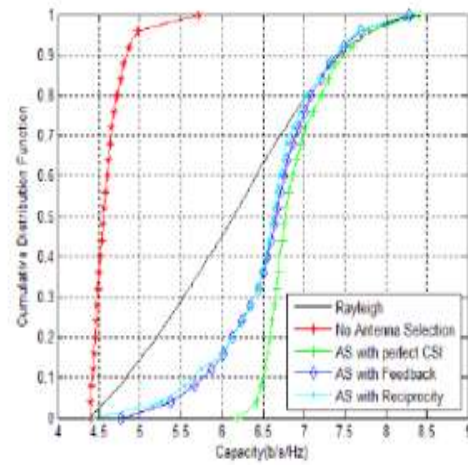


Fig. 13 The cumulative distribution function of capacity at Location 4.

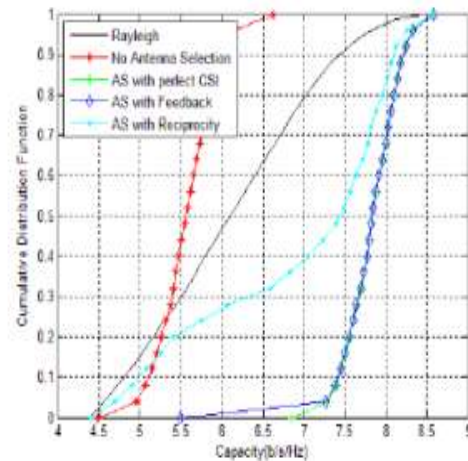


Fig. 14 The cumulative distribution function of capacity at Location 5.

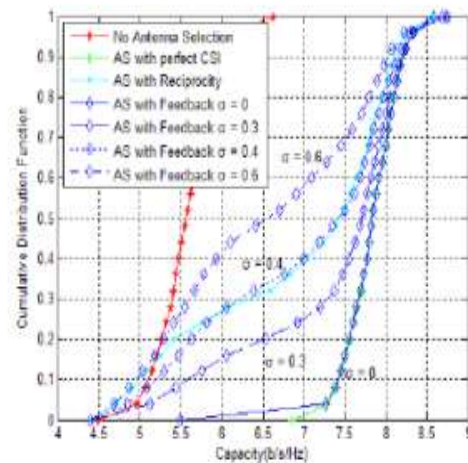


Fig. 15 The cumulative distribution function of capacity with the present of feedback error at Location 5.

feedback errors is higher than 0.4, the reciprocity approach might be more attractive than feedback with the benefit of low complexity.

## VI. CONCLUSION

This paper presents the performance of adaptive 2x4 MIMO system when AS technique is employed at transmitter using channel reciprocity realized by the measured data. The experimental results reveal that antenna selection using channel reciprocity provides the capacity performance slightly less than perfectly knowing CSI at transmitter. In addition, the system using AS method with reciprocity approach offers higher capacity than system without antenna selection for all locations. Instead of feedback approach, the reciprocity does not require any information sent back to the other side. Therefore, the proposed system can properly be an attractive choice to replace the feedback system with the less complexity.

## ACKNOWLEDGMENT

This work is financially supported by Grant MRG 5180344. The authors are also thankful to TRIDI as one of authors received NTC scholarship funded by TRIDI.

## REFERENCES

- [1] Murch R.D., Letiaief K.B., Antenna systems for broadband wireless access, *IEEE Communications Magazine* 2002; 40(4) : 76-83.
  - [2] Wong K.K., Murch R.D., Letiaief K.B., Performance enhancement of multiuser MIMO wireless communications systems, *IEEE Transactions on Communications* 2002; 50(12) : 1960-1970.
  - [3] Foschini G.J., Gans M.J., On limits of wireless communications in a fading environment when using multiple antennas, *Wireless Personal Communications* 1998; 6(3) : 311-335.
  - [4] Telatar I.E., Capacity of multi-antenna Gaussian channels, *AT&T Bell Laboratories*, Tech. Memo. 1995.
  - [5] Kong N., Milstein L.B., Combined average SNR of a generalized diversity selection combining scheme, *IEEE International Conference on Communications* 1998; 3 : 1556-1560.
  - [6] Win M.Z., Winters J.H., Analysis of hybrid selection/maximal-ratio combining in Rayleigh fading, *IEEE Transactions on Communications* 1999; 47 : 1773-1776.
  - [7] Win M.Z., Winters J.H., Analysis of hybrid selection/maximal-ratio combining of diversity branches with unequal SNR in Rayleigh fading, *IEEE Vehicular Technology Conference Proceedings* 1999; 215-220.
  - [8] Win M. Z., Beaulieu N. C., Shepp L. A., Logan B. F., Winters J. H., On the SNR penalty of MPSK with hybrid selection/maximal ratio combining over IID Rayleigh fading channels, *IEEE Transactions on Communications* 2003; 51(6) : 1012-1023.
  - [9] Molisch A., Win M.Z., Winters J.H., Capacity of MIMO systems with antenna selection, *IEEE International Conference on Communications* 2001; 570-574.
  - [10] Nabar R., Gore D., Paulraj A., Optimal selection and use of transmit antennas in wireless systems, *IEEE International Conference on Telecommunications* 2000.
  - [11] Blum R.S., Winters J.H., On optimum MIMO with antenna selection, *Communications Letters* 2002; 6(8) : 322-324.
  - [12] Dai L., Sfar S., Letiaief K.B., Optimal antenna selection based on capacity maximization for MIMO systems in correlated channels, *IEEE Transactions on Communications* 2006; 54(3) : 563-573.
  - [13] Heath R.W., Jr., Paulraj A.J., Antenna selection for spatial multiplexing systems based on minimum error rate, *IEEE International Conference on Communications*; 2276-2280.
  - [14] Ghayeb A., Duman T.M., Performance analysis of MIMO systems with antenna selection over quasi-static fading channels, *IEEE Transactions on Vehicular Technology* 2003; 52(2) : 281-288.
  - [15] Yangyang Zhang, Gan Zheng, Chunlin Ji, Kai-Kit Wong, Edwards D.J., Tiejun Cui, Near-optimal joint antenna selection for amplify-and-forward relay networks, *IEEE Wireless Communications & Signal Processing* 2009: 1-5
  - [16] Jiann G., Ching G., Larsson L. D., Modeling and evaluation of MIMO systems exploiting channel reciprocity in TDD mode, *IEEE Vehicular Technology Conference Proceedings* 2004; 6: 4265-4269.
  - [17] Tolli A., Codreanu M., Compensation of interference non-reciprocity in adaptive TDD MIMO-OFDM systems, *International Symposium on Personal, Indoor, and Mobile Radio Communications* 2004; 2: 859-863.
  - [18] Kim D., Torlak M., Rapid prototyping of a cost effective and flexible 4x4 mimo testbed, *IEEE Sensor Array and Multichannel Signal Processing Workshop* 2008: 5-8.
  - [19] Nishimori K., Kudo R., Honma N., Takatori Y., Ohta Atsushi, Okada K., Experimental evaluation using 16 x 16 multiuser MIMO testbed in an actual indoor scenario, *IEEE Antennas and Propagation Society International Symposium* 2008: 1-4.
  - [20] Azami F., Ghorssi A., Hemesi H., Mohammadi A., Abdipour A., Design and implementation of a flexible 4x4 MIMO testbed, *International Symposium on Telecommunications* 2008: 268-272.
  - [21] Chen S., Jun C., Ohira T., Handbook on Advancements in Smart Antenna Technologies for Wireless Networks, *Information Science Reference* 2009: 474-499.
  - [22] Uthansakul P., Bialkowski K., Bialkowski M., Postula A., Assessing an FPGA Implemented MIMO Testbed with the Use of Channel Emulator, *International Conference on Microwaves, Radar and Wireless Communications* 2006: 410-413.
  - [23] Onizawa T., Ohta A., Asai Y., Experiments on FPGA-Implemented Eigenbeam MIMO-OFDM With Transmit Antenna Selection, *IEEE Transactions on Vehicular Technology* 2009: 1281-1291.
  - [24] Heather MacLeod, Chris Loadman, Zhizhang (David) Chen, Experimental Studies of the 2.4-GHz ISM Wireless Indoor Channel, 3rd Annual Communication Networks and Services Research Conference, 2005, 63-68.
- P. Uthansakul (M'07) received B.Eng and M.Eng degrees from Chulalongkorn University, Thailand in 1996 and 1998, respectively. In 1998-2000, he worked as Telecommunication Engineer with Telephone Organization of Thailand (TOT) and then he has joined Suranaree University of Technology since 2000. During 2003-2007, he studied PhD at University of Queensland, Australia, in the area of wireless communications especially MIMO technology.
- He currently works as Assistant Professor in school of Telecommunication Engineering, Faculty of Engineering, Suranaree University of Technology, Thailand. He wrote 1 book entitled Adaptive MIMO Systems: Explorations for Indoor Wireless Communications (also available on amazon.com) and he has published more than 60 refereed journal and conference papers. His current research interests include MIMO, OFDM, WiMAX and Wireless Mesh Network.
- Dr. Uthansakul received 2005 Best Student Presentation Prize winner at the 9th Australian Symposium on Antennas, Sydney, 16-17 February 2005, Australia and 2004 Young Scientist Travel Grant winner at the 2004 International Symposium on Antenna and Propagation, 17-21 August 2004, Japan.
- K. Attakitmongkol received B.Eng degree from King Mongkut's Institute of Technology Ladkrabang, Bangkok, Thailand in 1994. In 1996 and 1999, he received M. Eng and Ph.D degrees in Electrical Engineering, Vanderbilt University, Nashville, TN, USA.
- He currently works as Associate Professor in school of Electrical Engineering, Faculty of Engineering, Suranaree University of Technology, Thailand. He wrote 2 books and he has published more than 40 refereed journal and conference papers. His current research interests include Digital Signal Processing, Wavelet and multiwavelet theories, Digital signal processing and image processing.
- N. Promsuvana received B.Eng and M.Eng degrees from Suranaree University of Technology, Thailand, in 2007 and 2009, respectively. Currently

he is pursuing his Ph.D degree at the school of Telecommunication Engineering, Faculty of Engineering, Suranaree University of Technology, Thailand. His current research interests include WMAX, MIMO system and channel estimation.

M. Uthansakul (M'07) received B.Eng degree from Suranaree University of Technology, Thailand, in 1997 and M.Eng degrees from Chulalongkorn University, Thailand in 1999. She has joined Suranaree University of Technology since 1999. During 2003-2007, she studied Ph.D at University of Queensland, Australia, in the area of smart antenna especially wideband beamforming.

She currently works as Assistant Professor in school of Telecommunication Engineering, Faculty of Engineering, Suranaree University of Technology, Thailand. She wrote 1 book chapter entitled Wideband smart antenna avoiding tapped-delay lines and filters in Handbook on Advancements in Smart Antenna Technologies for Wireless Networks, Idea Group Publishing, USA, 2008 and she has published more than 50 referee journal and conference papers. Her current research interests include antenna array processing, compact switched beam antenna and body communications.

Dr. Uthansakul received Young Scientist Contest 2nd Prize at 16th International Conference on Microwaves, Radar and Wireless Communications, Krakow, Poland, 22-24 May 2006

*Research Article***Performance of Antenna Selection in MIMO System Using Channel Reciprocity with Measured Data****Peerapong Uthansakul, Nattaphat Promsuwanna, and Monthippa Uthansakul***School of Telecommunication Engineering, Suranaree University of Technology, Muang, Nakhon Ratchasima 30000, Thailand*

Correspondence should be addressed to Nattaphat Promsuwanna, jame\_maxwell@hotmail.com

Received 15 February 2011; Revised 1 April 2011; Accepted 5 April 2011

Academic Editor: Byungje Lee

Copyright © 2011 Peerapong Uthansakul et al. This is an open access article distributed under the Creative Commons Attribution License, which permits unrestricted use, distribution, and reproduction in any medium, provided the original work is properly cited.

The channel capacity of MIMO system increases as a function of antenna pairs between transmitter and receiver but it suffers from multiple expensive RF chains. To reduce cost of RF chains, antenna selection (AS) method can offer a good tradeoff between expense and performance. For a transmitting AS system, channel state information (CSI) feedback is required to choose the best subset of available antennas. However, the delay and error in feedback channel are the most dominant factors to degrade performances. In this paper, the concept of AS method using reciprocal CSI instead of feedback channel is proposed. The capacity performance of proposed system is investigated by own developing Testbed. The obtained results indicate that the reciprocity technique offers a capacity close to a system with perfect CSI and gains a higher capacity than a system without AS method. This benefit is from 0.9 to 2.2 bps/Hz at SNR 10 dB.

**1. Introduction**

A multiple-input-multiple-output (MIMO) system recently becomes one of the most attractive techniques for the future use because it proposes an extensive improvement over conventional smart antenna systems in both quality of service (QoS) and the transfer rate [1–4]. However, using multiple antennas requires multiple radio frequency (RF) chains which consist of amplifiers, up and down converters, digital to analog converters, and so forth. Those are typically very expensive. A promising approach for reducing cost while retaining a reasonably large fraction of the high potential data rate of an MIMO approach is to employ some form of antenna selection (AS) [5–8]. The AS method employs a reduced number of RF chains at the receiver (or transmitter) and attempts to optimally allocate each chain to one of a large number of receiving (transmitting) antennas which are usually cheap elements. In this way, only the best set of antennas is used while the remaining antennas are not employed, thus reducing the number of required RF chains. It can be noted that water-filling technique always provides the optimal performance which is better than antenna selection only if the numbers of RF chain of

both systems are the same. However, water-filling technique requires the full equipped RF modules for each branch of MIMO antennas which affect the price of manufacturing considerably. To reduce RF hardware by using antenna selection technique is more economic. Thus, somewhere in the middle, an effective MIMO antenna selection can achieve a good tradeoff between performance and cost.

In literatures [9–17], the developments of AS method are classified into two main topics. At first, the algorithms to select the best subset of antennas are on focus. These algorithms can be applied to either transmitter [9] or receiver [10]. The fast and precise selections are the required demand in practice. However, the success of these algorithms depends on the knowledge of channel state information (CSI) especially for the transmitting AS system that CSI feedback is necessarily required to choose the best subset of antennas [11–14]. Although the work presented in [15] tries to perform AS method without knowing CSI at transmitter for transmitting AS system, the expense of many iterations degrades its attraction.

For second topic, researchers pay attention to the methods of CSI acquisitions. This is because the more exact CSI is realized, the more enhanced performance of AS method

is obtained. Unfortunately, the CSI is usually not available at the transmitter. So the method to realize CSI is still important. In literatures, there are two approaches in order for the transmitter to obtain the CSI. The first approach utilizes CSI from feedback channel and the second approach is based on the reciprocity principle. In the first method, the forward channel is estimated at receiver and then it is sent back to the transmitter through the reverse channel. This method does not function properly if the channel is rapidly changed. In order to realize the correct CSI at transmitter, more frequent estimations and feedbacks are required. As a result, the overheads for the reverse channel become prohibitive. In turn, the second approach based on reciprocity does not have such a problem. Due to the reciprocity principle, it is well known that the radio propagation channel is reciprocal between two antennas. Ideally, the forward and reverse channels are assumed to be the same. Therefore, the transmitter can realize the forward CSI by estimating the reverse CSI instead. In time-division-duplex (TDD) mode, the same carrier frequency is alternately used in forward and reverse channels. The propagation surrounding is not rapidly changed by time. So the channel coefficients are able to be considered as similar for both directions. Based on TDD mode, the reciprocity approach is superior to any explicit feedbacks.

Recently, there have been many researches concerning channel reciprocity of an MIMO system which is based on the nonreciprocal effects between forward and reverse channels caused by any mismatches among RF components and interferences between transmitter and receiver [16, 17]. However, from all works described in literatures [16, 17], the system model is based on the assumption that the forward and reverse channels are exactly identical. This assumption is not valid in practice because the transmitter realizes the reciprocal channel after the time that signals used for estimating channel completely passes through it. Also the time-varying noises on forward and reverse channels are not identical. Therefore, apart from component mismatches and interferences, the time delays and noises between expected and actual channels cause the nonreciprocal effect in practice. As a result, it is interesting to examine whether AS method still works under such a deviation of nonreciprocal CSI.

In this paper, the performances of adaptive MIMO system with AS method at transmitter based on channel reciprocity are investigated. The data are measured and tested by our developing Testbed based on FPGA board. In recent times, most researchers move their experiments from simulations into real measurements. MIMO Testbed [18–23] is one the most comfortable platforms to realize the true performance of a proposed system under a real circumstance. For the work presented in [18–20], the performance investigations of MIMO system under indoor and outdoor have been reported through the Testbed. In [23], a transmitting AS system with an eigenbeam for MIMO-OFDM system is employed. This work achieves CSI via feedback technique and uses it to compute eigenvectors for selecting the best subset of transmitting antennas. In summary, all MIMO Testbeds presented in literatures utilize

CSI from feedback channels. Moreover, some works [21, 22] use a direct link to perform feedback channels which exclude any errors due to wireless operations. As far as the survey of the authors is concerned, the issue of channel reciprocity for MIMO Testbed has never been reported in any publications. Hence, the contributions of this paper mainly fall into two issues. Firstly, the use of channel reciprocity for AS method in a MIMO system is originally demonstrated. The second contribution is on a proposed MIMO Testbed working by FPGA processors which is ready to be launched as commercial products. More importantly, it is interesting to delete the need of feedback channels by replacing reciprocity technique because this can save costs of system complexity and make the system more reliable.

In this work, the effect of the mismatches of RF components can be assumed to be neglected by using the same components at both transmitter and receiver. The CSI information between transmitter and receiver used in AS method is acquired by channel emulator in which forward and reverse CSIs are measured from real propagation environments. The  $2 \times 4$  MIMO channels are considered as  $2 \times 2$  by AS method and then the channel capacity is calculated by computer to find the optimal subset of antennas. In addition, the comparison between feedback approach and reciprocity approach are also undertaken to provide the fair judgment with measured data. In [24], the authors performed the initial study to confirm the reciprocity approach. However, many data details are missing and have been fulfilled in this paper. More data measurements have been undertaken. In particular, the new discussion on measured coherent time is added to practically prove the use of reciprocity. The results in this paper are helpful to realize the use of channel reciprocity in practice and its impact on channel capacity due to nonidentical CSI between forward and reverse channels. The remainder of this paper is organized as follows. In Section 2, the MIMO system model and two approaches estimating CSI are presented. Section 3 describes the channel measurement and then the testing implementation is detailed in Section 4. The MIMO channel capacities are discussed in Section 5. Finally, the paper conclusion is given in Section 6.

## 2. MIMO System Model

**2.1. MIMO Channel Capacity.** Consider the MIMO system which has  $N_T$  transmitting antennas and  $N_R$  receiving antennas. The formula of MIMO channel capacity is given in (1) [4]. This expression presents the averaging capacity in bps/Hz by assuming the ergodic process for channel matrix  $\mathbf{H}$ ;

$$C = E_H \left\{ \log_2 \det \left( \mathbf{I}_{N_R} + \frac{P_T}{P_N N_T} \mathbf{H} \mathbf{H}^* \right) \right\}, \quad (1)$$

where  $\mathbf{I}_{N_R}$  is the  $N_R \times N_R$  identity matrix,  $P_T$  is the total transmit power,  $P_N$  is the noise power,  $N_T$  is the number of transmitting antennas,  $N_R$  is the number of receiving antennas,  $E_H \{ \cdot \}$  is the expectation over  $\mathbf{H}$ , and  $*$  denotes the conjugate and transpose operation.

When AS method is employed at the transmitter or the receiver, a subset of transmitting or receiving antenna elements is chosen. The channel seen by the subset is the sub-matrix  $\mathbf{H}_{\text{sub}}$  which is obtained by selecting only the rows and columns of  $\mathbf{H}$  that correspond to the selected receiving and transmitting antenna elements. The optimal subset is the one that leads to the largest mutual information between the antenna elements. The capacity of MIMO system with AS is given by

$$C_{\text{sel}} = \max_{S(\mathbf{H})} \log_2 \det \left( \mathbf{I}_{L_R} + \frac{P_T}{P_N L_T} \mathbf{H}_{\text{sub}} \mathbf{H}_{\text{sub}}^H \right), \quad (2)$$

where  $\mathbf{I}_{L_R}$  is the  $L_R \times L_R$  identity matrix,  $\mathbf{H}_{\text{sub}}$  is a  $L_R \times L_T$  matrix obtained by removing  $N_R - L_R$  rows and  $N_T - L_T$  columns from  $\mathbf{H}$ , and  $S(\mathbf{H})$  denotes the set of all possible  $L_R \times L_T$  sub-matrices of  $\mathbf{H}$  that can be chosen.  $L_R$  and  $L_T$  represent the number of receiver RF chains and transmitter RF chains, respectively.

**2.2. CSI Realization at Transmitter.** As seen in Section 2.1, the system can achieve the optimal selection by employing the knowledge of the forward channel if there is no error of knowledged channel (perfect CSI). To obtain the CSI at transmitter, there are two approaches explained as follows.

**2.2.1. Feedback Approach.** For this approach, the receiver realizes a current CSI by channel estimation and uses the estimated channel to extract the data and to generate the feedback CSI. The feedback CSI is sent back to the transmitter using the feedback control channel. The transmitter, in turn, uses this information to customize the transmitted signal for the channel.

In practice, errors from feedback link which influence channel knowledge can degrade the capacity performance which is more pronounced when feedback link contains errors excessively. Under this assumption, the available CSI at transmitter can be expressed as

$$\mathbf{H}_T = \mathbf{H}_F + \varepsilon_E + \varepsilon_F, \quad (3)$$

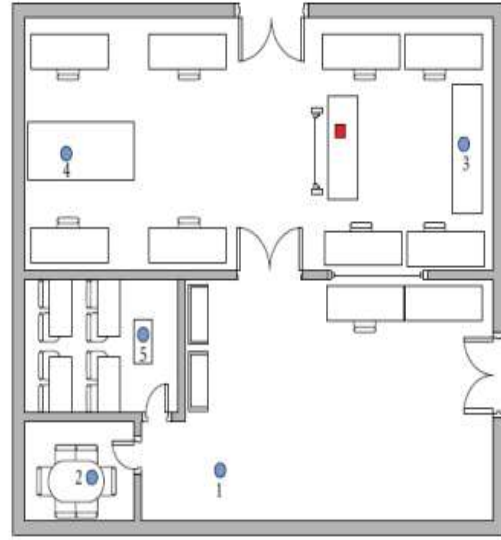
or

$$\mathbf{H}_T = \mathbf{H}_{\text{ES}} + \varepsilon_F, \quad (4)$$

where  $\mathbf{H}_F$  is the forward channel,  $\mathbf{H}_T$  is the available CSI at transmitter,  $\varepsilon_E$  and  $\varepsilon_F$  are  $N_R \times N_T$  error matrix from estimation and error matrix from feedback link, respectively, and  $\mathbf{H}_{\text{ES}}$  is the channel matrix which is achieved by channel estimation.

**2.2.2. Reciprocity Approach.** According to the principle of reciprocity, the forward and reverse channels are identical when the time, frequency, and antenna locations are the same. Based on this principle, the transmitter may use the CSI obtained by the reverse link for the forward link. In practice, the forward and reverse channels are not truly identical because of the effect of channel fading, noises, and environments. The CSI known at transmitter can be given by

$$\mathbf{H}_T = \mathbf{H}_R^T + \varepsilon_E + \varepsilon_R, \quad (5)$$



- Network analyzer
- Test point

FIGURE 1: Map of a measured area.

where  $\mathbf{H}_R^T$  is the transpose of reverse channel matrix [25] and  $\varepsilon_R$  is the  $N_R \times N_T$  channel reciprocity error matrix realized by measurements.

### 3. Channel Measurement

The configuration of  $2 \times 4$  MIMO system consists of network analyzer, power amplifier (PA) module, low-noise-amplifier module (LNA), and monopole antennas with 5 dBi gain. The PA module is used at transmitter to increase transmitted power. The LNA module is used to increase received signal level. The channel coefficients in both magnitude and phase are measured by network analyzer. The center frequency is 2.45 GHz and its bandwidth is 100 MHz. The data was measured by 5 times per location. In each time, 100 samples of channel data were recorded continuously within 1.5 seconds. However, we did not continue recording all 5 times in one round. The sequence of recording starts from Location 1 (100 samples) and then moves to Location 2 (100 samples) until Location 5 (100 samples). This sequence is called one set. In the first day, we performed two sets of measurements and the other three sets were done on the second day. In summary, 500 samples per location were collected over two days. In order to mitigate the effect of measurement noises, the function of network analyzer, called smoothing command, is used to average the measured data over specific time. In this work, the specific time is the default operation at 10 ms. It means that each recorded sample is an averaging result over 10 ms.

For the measured area, we choose large office room to provide many cases of study. Figure 1 shows the map of an office room. The circular markers refer to the locations where the measurement is undertaken. There are five measured

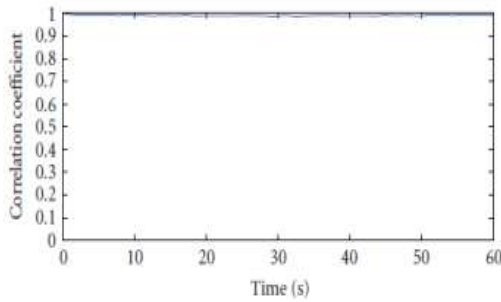


FIGURE 2: Correlation coefficients as a function of time in measured environment.

locations. For channel coefficient measurement, the forward channel and reverse channel are made by switching all modules (PA and LNA) but not including the cables. This is because all phase shifts and amplitude attenuations of cables are calibrated before measuring. While modules are being switched, all cables are placed at the same positions as they are started. Hence, by keeping the same configuration of cables for both forward and reverse channels and switching only PA and LNA modules, we believe that the measured results might reflect the true forward and reverse comparison. For PA and LNA modules, they are put in the same small boxes covered by absorbers and placed on fixed locations behind antennas array to reduce their fading effects.

The switching time between transmitter and receiver is at least 20–30 seconds. In order to confirm whether reciprocity channel is still valid for our measurements, the authors have calculated the correlation coefficient from the measured data as the same method as presented in [26]. The result of correlation coefficient as a function of time is shown in Figure 2. It is noticed that our result is similar to the result illustrated by static channel in [26]. In literatures, the coherent time achieved by experiments is defined as the duration from start to the time that correlation coefficient is lower than 0.5. Therefore, it can be concluded that our measurements are performed under a static channel with a very large coherent time (over 20–30 s). Accordingly, the coherence time in our experiments is large enough to hold on the property of channel reciprocity.

Figure 3 shows an example of each element of  $2 \times 4$  channel matrix at Location 4, where  $H_{ij}$  refers to the channel coefficient of  $i$ th receiving antenna and  $j$ th transmitting antenna. For the sake of illustration, it is noted that the symbol of  $H_{ij}$  is referred as an entry element of only forward channel matrix while it is also referred as the transpose element of reverse channel matrix [25]. It can be observed that both forward and reverse channels are quite similar but not exactly the same. The amplitude deviation is about  $\pm 2$  dB and the phase deviation is about  $\pm 15^\circ$ . These deviations were ignored in all works presented in literatures [16, 17]. The result is important to realize how these deviations influence the practical performance. As seen in Figure 3, the variation of measured data is very small because the environments seem to be a static channel. Hence, the results are grouped into two clusters, forward and reverse channels. However, the

forward and reverse channels are not identical as expected because the measured data are collected in different time. For other locations, the deviations of amplitude and phase are similar to Location 4.

In addition, the correlation coefficients evaluated from measurements are 0.62, 0.33, 0.90, 0.52, and 0.73 for Locations 1, 2, 3, 4, and 5, respectively. Assuming all channel matrices of each location have the equally received SNR, thus it can be concluded that Location 2 is the most suitable area for MIMO operation because it yields the lowest correlation coefficient in comparison with other locations. Then, it is expected that Location 2 should offer more capacity than other locations as well. In turn, the capacity performance of Location 3 is expected to be poor due to its high correlation.

## 4. Testbed Implementation

**4.1. Antenna Selection (AS) Technique.** The capacity of MIMO system employing AS technique is described in (2); however this work concerns only the case of AS known at the transmitter. In order to find the optimal subset from knowing only CSI at transmitter modeled in (3) and (5) for feedback and reciprocity approaches, respectively, the conventional technique is applied by searching all possible subsets of antennas and then selecting the best subset providing the highest capacity. As a result, the formula of MIMO channel capacity with AS technique at transmitter can be given by

$$C_{\text{sel}} = \max_{S(H_T)} \log_2 \left[ \det \left( I_{L_R} + \frac{P}{L_T} \mathbf{H}_{T,\text{sub}} \mathbf{H}_{T,\text{sub}}^H \right) \right]. \quad (6)$$

where  $\mathbf{H}_{T,\text{sub}}$  is the  $N_R \times L_T$  sub-matrix (AS at transmitter) of CSI ( $\mathbf{H}_T$ ) obtained by feedback or reciprocity approaches.

It must be noticed that by using CSI in (6) to find the optimal subset of antenna, the differences between  $\mathbf{H}_T$  and  $\mathbf{H}$  ( $\mathbf{H}_T \neq \mathbf{H}$ ) cause direct effect to the capacity performance in (2) due to implementing errors from either feedback or reciprocity channels. In this work, the exhaustive search is applied to find the best antenna subset from all possible cases. Although there are many algorithms proposed in the literature to select the antenna subset, the best solution is still the same as the one obtained from exhaustive search. The only benefits of other algorithms are fast processing and low complexity. The purpose of this work is to investigate the performance of reciprocity channels in comparison with feedback channels. So the same conclusion should be found for any AS methods.

**4.2. Design of Developing Testbed.** This work chooses field programmable gate array (FPGA) technology to implement  $2 \times 4$  MIMO Testbed because FPGAs processing is introduced as promising alternative to custom ICs for implementing entire system on one chip and to provide flexibility of reprogram ability to the user. All functions are constructed inside FPGA boards including the AS method at transmitter where 2 transmitting antennas are selected. Hence, the system requires only 2 transmitting and 2 receiving components such as analog-to-digital converter

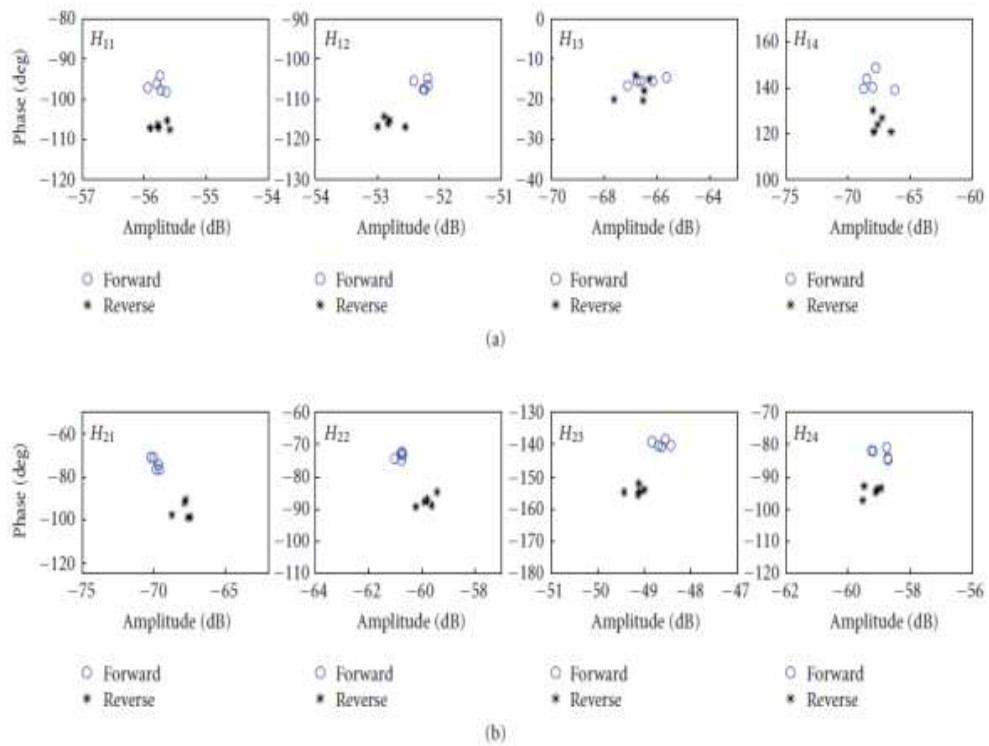


FIGURE 3: Example of forward and reverse channels measured at Location 4.

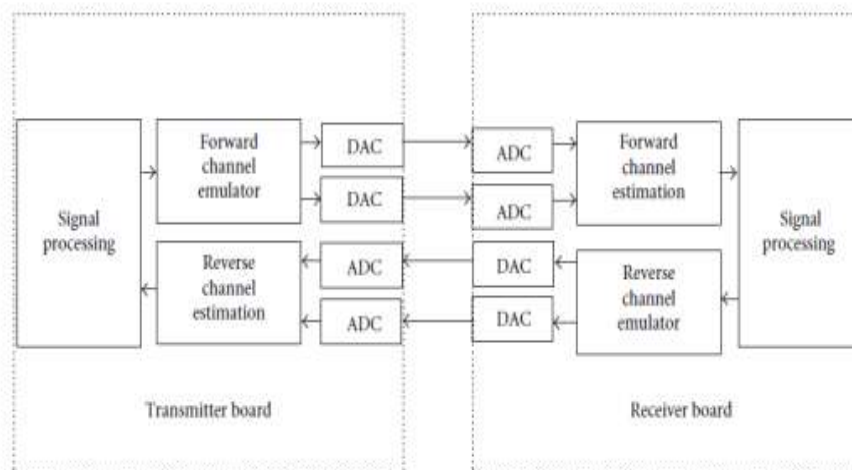


FIGURE 4: System diagrams of transmitter and receiver.

(ADC) and digital to analog converter (DAC). The block diagram of FPGA boards can be shown in Figure 4. As seen in Figure 4, RF components of transmitter and receiver have been replaced by using channel emulator. The concept of channel emulator has been adopted in many publications [21, 22] in order to simulate the various conditions of channel collected by real measurements. Another point of using channel emulator is to save cost of RF components

because the boards can be functionally tested before passing through the production line.

In this work, we use Spartan 3An starter kit boards from Xilinx Company to implement transmitter and receiver which is explained as follows. Note that both transmitter and receiver boards shown in Figure 4 have the same components as transmitter and receiver to perform full duplex communication. However, we name the direction

from transmitter board to receiver board as forward channel and the other direction as reverse channel.

**4.2.1. Transmitter.** The series of bit information (4 bits) are generated and then it is converted from series to parallel bit information. After that, it is modulated by BPSK modulation with frequency 12.5 kHz in which bit 1 and bit 0 are represented by phase  $0^\circ$  and  $180^\circ$ , respectively. The BPSK signal is fed to the channel emulator which acts as wireless communication channel. Finally, the signals from channel emulator are transformed to analog signals which are sent to receiver board.

**4.2.2. Receiver.** The received analog signals from transmitter are fed to the channel estimation block to estimate the CSI which is used to select the optimum subset of antennas in AS method. The estimated CSI is shown via chip scope pro software on PC which is connected to the receiver board.

**4.3. Channel Estimation Method.** To obtain CSI at both transmitter and receiver, we develop a simple technique to estimate CSI and it can reduce the complexity of hardware implementation. Consider MIMO system which has 4 transmitting antennas and 2 receiving antennas. The set of training sequence is specified by 5 times of four bit transmissions. These are  $0111_{t-5}$ ,  $1011_{t-4}$ ,  $1101_{t-3}$ ,  $1110_{t-2}$ , and  $0000_{t-1}$  where  $t$  indicates the order sequence. To understand the principle of channel estimation, first we have to understand the layout of communication in  $2 \times 4$  MIMO which can be written as

$$\begin{bmatrix} y_1 \\ y_2 \end{bmatrix} = \begin{bmatrix} h_{1,1} & h_{1,2} & h_{1,3} & h_{1,4} \\ h_{2,1} & h_{2,2} & h_{2,3} & h_{2,4} \end{bmatrix} \begin{bmatrix} x_1 \\ x_2 \\ x_3 \\ x_4 \end{bmatrix}. \quad (7)$$

Then the received signal at each receiving antenna at  $t$  time duration can be shown as

$$\begin{aligned} y_1(t) &= h_{1,1}x_1(t) + h_{1,2}x_2(t) + h_{1,3}x_3(t) + h_{1,4}x_4(t), \\ y_2(t) &= h_{2,1}x_1(t) + h_{2,2}x_2(t) + h_{2,3}x_3(t) + h_{2,4}x_4(t). \end{aligned} \quad (8)$$

Let  $S_0$  and  $S_1$  be defined as BPSK signals representing 0 and 1 bit modulation, respectively. Then, the channel coefficient can be calculated by

$$h_{k,t-1} = \frac{y_k(t-1) + y_k(t)}{2|S_0|}. \quad (9)$$

In this work, (9) is implemented on FPGA to estimate both forward and reverse CSI. Accordingly, these estimated CSI are used in AS algorithm mentioned earlier.

**4.4. Test Results.** To complete testing system, channel emulators are operated for both forward and reverse channels. The channel information is determined by real measured data and programmed on FPGA boards. The obtained results

are collected for the case of AS method, which is employed at the transmitter only. Personal computers are connected to the transmitter and receiver to provide programmable interface and capture all concurrence data. Moreover, the oscilloscope is used to capture a real signal coming from any concerned ports in order to compare signals between forward and reverse channels.

To implement channel emulators for both forward and reverse channels, the measured data described in Section 3 are used. However, channel information matrices from measurements have to be multiplied and divided by a constant value in order to adjust a suitable level for ADC and DAC specifications. This is to avoid the unwanted effect due to low sensitivity of ADC or DAC, which causes a signal error at receiver. It is noted that multiplying or dividing channel information matrices with a constant value does not change the property of channel characteristics.

Figure 5 shows an example of comparison in complex form between forward and estimated forward channel matrix using one sample of channel data at Location 1. The estimated forward and forward channels are similar in terms of real and imaginary parts. Although the deviations are still valid, these errors are very small when compared with errors between forward and reverse channels depicted in Figure 3. Therefore, the channel estimation implemented in the Testbed works very well and ensures the correct achievement of CSI from available sources, either feedback or reciprocity approaches.

## 5. Results and Discussions

**5.1. Simulation Results.** All capacity results in this section are off-line produced on computer by using real AS outcomes from Testbed selections mentioned in the previous section. Therefore, these capacities can be compared with various system conditions including Rayleigh propagation channel and perfect CSI system which are hardly measured in real scenarios. The MIMO channel capacities are computed by MATLAB programming when AS methods are employed by using (2) and (6). Note that  $H_T$  of forward and reverse channels are obtained by Testbed system. For feedback approach, at first we assume that there is no feedback error in feedback channel and then at the end of this section, the effect of this error will be illustrated. The simulations disregard the mismatches of RF circuits in transmitting/receiving components as well as mutual coupling effects because they are included in one part of channel measurements.

The capacity performances are based on cumulative distribution function (CDF) at SNR = 10 dB by using 500 samples of the collected channel data and they are illustrated into five cases, Rayleigh channel, AS with feedback channel, AS with perfect CSI, AS with reciprocity channel, and fixed antennas. In case of fixed antennas, the first and second transmitting antennas are used to transmit signals for any locations. For the sake of comparison, the channels are normalized to provide a comparable discussion by  $\sum |H_{ij}|^2 = N_T N_R$  which limits total channel energy to one constant value. This normalization is done in order to compare channel properties between various conditions by

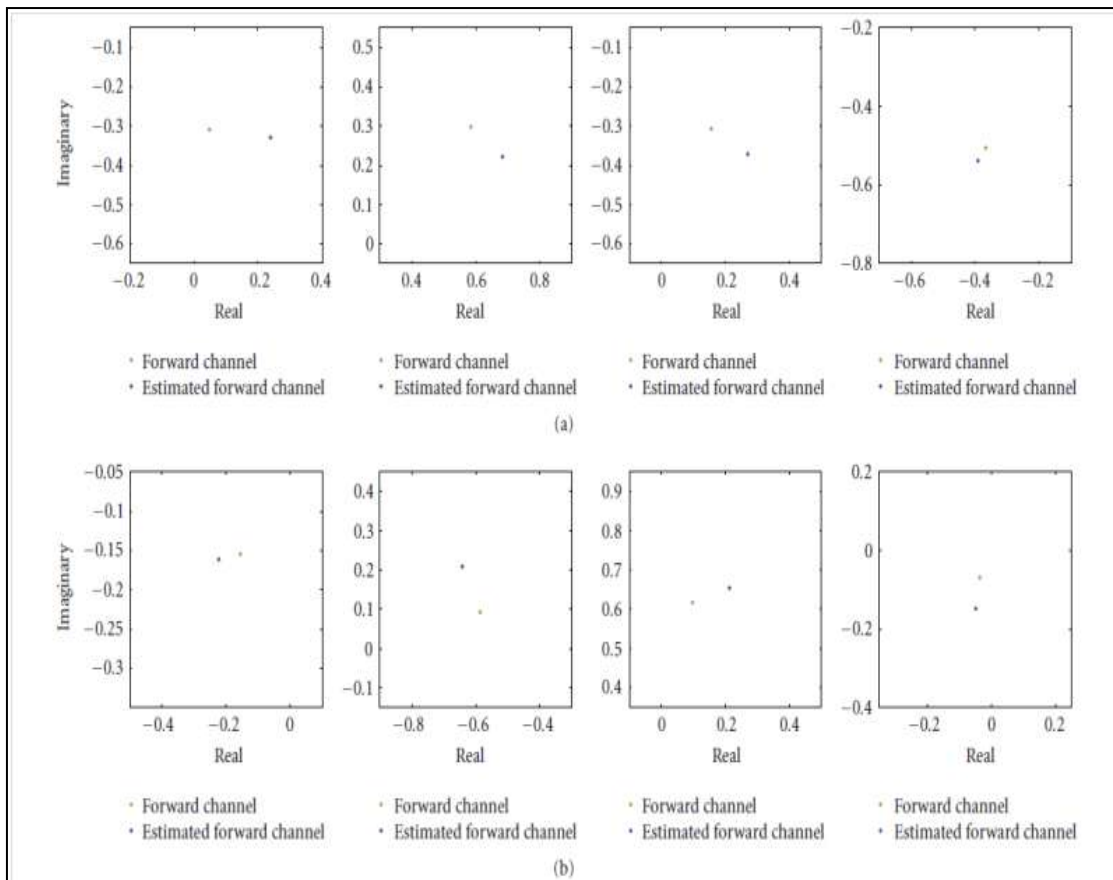


FIGURE 5: Comparison example between forward and estimated forward channels at Location 1.

neglecting the effect of path loss. All details of five cases are explained as follows.

- (i) Rayleigh Channel: this case represents the capacity of  $2 \times 2$  MIMO system when wireless channel acts as Rayleigh fading channel which is random over 10,000 times.
- (ii) Fixed Antennas: this case represents capacity of  $2 \times 2$  MIMO system where the first and second antenna elements are used to transmit signals.
- (iii) AS with feedback: this case represents the capacity when the CSI from feedback approach is used to select transmitting antennas in AS technique. Two of four transmitting antennas are optimally chosen to offer the best capacity.
- (iv) AS with Perfect CSI: this case represents the capacity when the CSI is assumed to be perfectly known at transmitter. Hence, the selected transmitting antennas in AS technique are ideally optimal corresponding with the wireless channels. There is no error taken into account so that the capacity is computed by using (2).
- (v) AS with reciprocity: this case represents the capacity when the CSI from reciprocity approach is used to select transmitting antennas in AS technique.

As mentioned in Section 3, there are five measured locations in which the channels are collected. The surrounding of each location is so different that the capacity results are considerably separated into each location to make a fair judgment on all approaches.

*Location 1.* As seen in Figure 6, the cumulative distribution function of capacity for AS methods with reciprocity and feedback approaches are close to a perfect CSI case where a feedback case is slightly better than a reciprocity case. In addition, AS method with reciprocity gives a performance gain 1.15 bps/Hz higher than a case of fixed antennas at 50% probability. However, AS method provides the capacity performance at 50% probability equal to a case of Rayleigh at 92% probability. This is because the channels at Location 1 offer AS method to select the antenna subset that causes a very low channel correlation.

*Location 2.* In Figure 7, the cumulative distribution function of capacity for fixed antennas, AS methods with reciprocity, and feedback are close to perfect CSI and they provide capacity at 50% probability equal to a case of Rayleigh at 90% probability. It is interesting to observe that fixed antennas method provides a performance close to a perfect CSI case at this location. The reason is that fixed antennas method

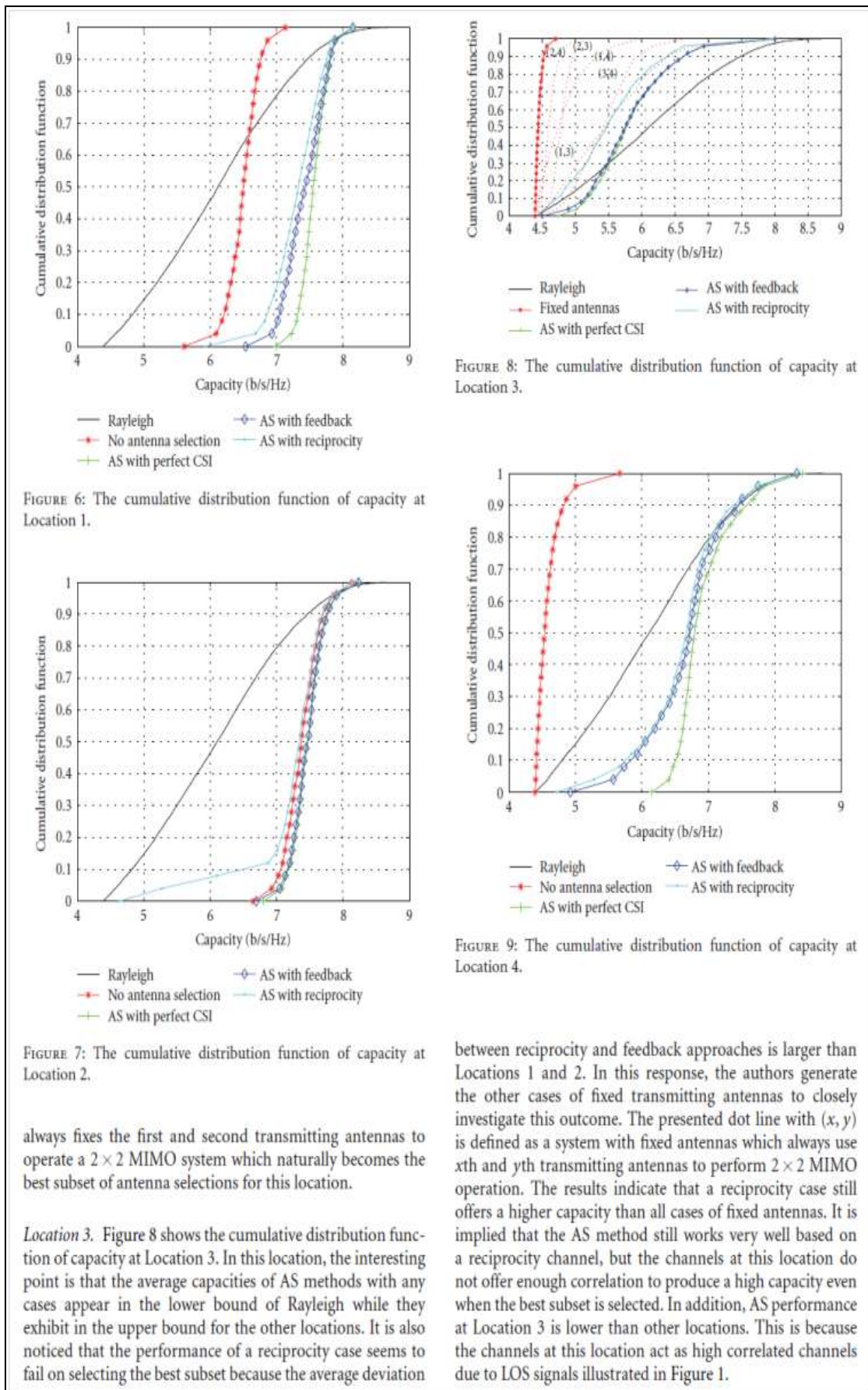


FIGURE 6: The cumulative distribution function of capacity at Location 1.

FIGURE 7: The cumulative distribution function of capacity at Location 2.

always fixes the first and second transmitting antennas to operate a  $2 \times 2$  MIMO system which naturally becomes the best subset of antenna selections for this location.

*Location 3.* Figure 8 shows the cumulative distribution function of capacity at Location 3. In this location, the interesting point is that the average capacities of AS methods with any cases appear in the lower bound of Rayleigh while they exhibit in the upper bound for the other locations. It is also noticed that the performance of a reciprocity case seems to fail on selecting the best subset because the average deviation

FIGURE 8: The cumulative distribution function of capacity at Location 3.

FIGURE 9: The cumulative distribution function of capacity at Location 4.

between reciprocity and feedback approaches is larger than Locations 1 and 2. In this response, the authors generate the other cases of fixed transmitting antennas to closely investigate this outcome. The presented dot line with  $(x, y)$  is defined as a system with fixed antennas which always use  $x$ th and  $y$ th transmitting antennas to perform  $2 \times 2$  MIMO operation. The results indicate that a reciprocity case still offers a higher capacity than all cases of fixed antennas. It is implied that the AS method still works very well based on a reciprocity channel, but the channels at this location do not offer enough correlation to produce a high capacity even when the best subset is selected. In addition, AS performance at Location 3 is lower than other locations. This is because the channels at this location act as high correlated channels due to LOS signals illustrated in Figure 1.

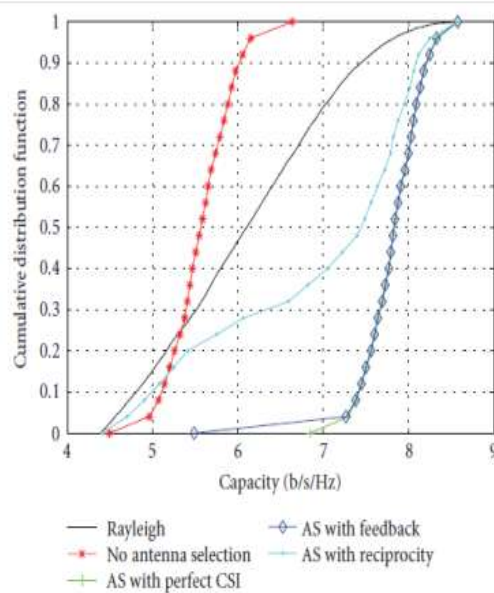


FIGURE 10: The cumulative distribution function of capacity at Location 5.

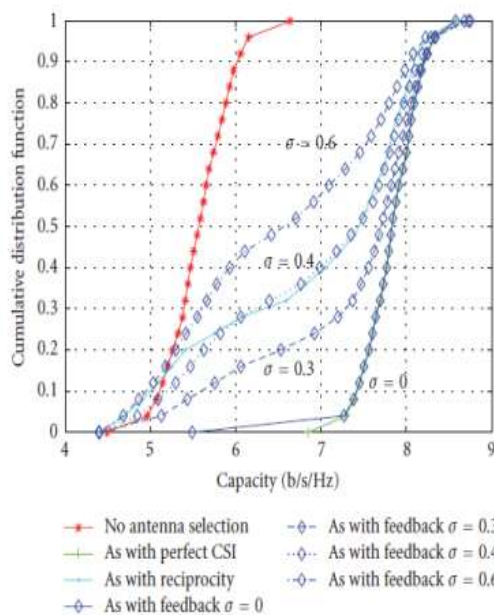


FIGURE 11: The cumulative distribution function of capacity with the presence of feedback error at Location 5.

*Location 4.* The aim of measuring at this location is to investigate the channel property when there are obstructions between transmitter and receiver, in comparison with Location 3. As shown in Figure 9, the cumulative distribution functions of capacity for AS methods with reciprocity and feedback cases are similar and close to a perfect CSI case after 50% probability. The capacity results of AS methods in this location are higher than the results at Location 3. For Location 4, the use of AS method with reciprocity can provide 2.2 bps/Hz higher than a case of fixed antennas method at 50% probability.

*Location 5.* As noticed in Figure 10, the results of AS method with reciprocity seem to fail on selecting the best subset of antennas. However, the authors did the other cases of fixed transmitting antennas and achieved the same conclusion that AS method with reciprocity still provides the highest capacity over all cases of fixed antennas.

In summary, a system using AS method with reciprocity always gives better performance better than fixed antennas while the feedback and perfect CSI cases slightly outperform this method. However, for AS method with feedback, the presented results are based on the exclusion of any errors in a feedback channel in which these errors are compulsorily occurred in practice due to channel delays and feedback noises. As a result, it is also necessary to examine the effect of feedback errors on capacity performances.

In order to investigate feedback errors included in feedback channel, this work assumes that the model of feedback error ( $\epsilon_F$  from (3)) is given by

$$\epsilon_F = \sigma \mathbf{H}_{\text{i.i.d.}}, \quad (10)$$

where  $\mathbf{H}_{\text{i.i.d.}}$  is i.i.d. (independent identically distributed) channel matrix with zero mean and unit variance  $\sigma^2$  is the variance of feedback errors  $\epsilon_F$ .

Figure 11 shows the effect of feedback errors on capacity performance of AS method at Location 5. It is obviously seen that errors degrade the capacity performance as a function of error variance. Also seen in this figure, the capacity performance of AS method with feedback is worse than a reciprocity case when the error variance in a feedback channel is more than 0.4. The results indicate the tradeoffs between using reciprocity and feedback approaches. If the variance of feedback errors is higher than 0.4, the reciprocity approach might be more attractive than feedback with the benefit of low complexity.

## 6. Conclusion

This paper presents the performance of an adaptive  $2 \times 4$  MIMO system when AS technique is employed at transmitter using channel reciprocity realized by the measured data. The experimental results reveal that antenna selection using channel reciprocity provides the capacity performance slightly worse than perfectly knowing CSI at transmitter. Furthermore, the system using AS method with reciprocity approach offers higher capacity than system with fixed antennas for all locations. Instead of feedback approach, the reciprocity does not require any information sent back to the other side. Therefore, the proposed system can properly be an attractive choice to replace the feedback system with the less complexity.

## Acknowledgments

This work is financially supported by Thailand Research Fund (Grant no. MRG 5180344). The authors are also thankful to TRIDI as one of the authors received NTC scholarship funded by TRIDI.

## References

- [1] R. D. Murch and K. Ben Letaief, "Antenna systems for broadband wireless access," *IEEE Communications Magazine*, vol. 40, no. 4, pp. 76–83, 2002.
- [2] K. K. Wong, R. D. Murch, and K. B. Letaief, "Performance enhancement of multiuser MIMO wireless communication systems," *IEEE Transactions on Communications*, vol. 50, no. 12, pp. 1960–1970, 2002.
- [3] G. J. Foschini and M. J. Gans, "On limits of wireless communications in a fading environment when using multiple antennas," *Wireless Personal Communications*, vol. 6, no. 3, pp. 311–335, 1998.
- [4] I. E. Telatar, *Capacity of Multiantenna Gaussian Channels*, AT&T Bell Laboratories, Technical Memorandum, 1995.
- [5] N. Kong and L. B. Milstein, "Combined average SNR of a generalized diversity selection combining scheme," in *Proceedings of the IEEE International Conference on Communications (ICC '98)*, vol. 3, pp. 1556–1560, June 1998.
- [6] M. Z. Win and J. H. Winters, "Analysis of hybrid selection/maximal-ratio combining in rayleigh fading," *IEEE Transactions on Communications*, vol. 47, no. 12, pp. 1773–1776, 1999.
- [7] M. Z. Win and J. H. Winters, "Analysis of hybrid selection/maximal-ratio combining of diversity branches with unequal SNR in Rayleigh fading," in *Proceedings of the 49th IEEE Vehicular Technology Conference*, pp. 215–220, May 1999.
- [8] M. Z. Win, N. C. Beaulieu, L. A. Shepp, B. F. Logan, and J. H. Winters, "On the SNR penalty of MPSK with hybrid selection/maximal ratio combining over IID Rayleigh fading channels," *IEEE Transactions on Communications*, vol. 51, no. 6, pp. 1012–1023, 2003.
- [9] A. F. Molisch, M. Z. Win, and J. H. Winters, "Capacity of MIMO systems with antenna selection," in *Proceedings of the IEEE International Conference on Communications (ICC '01)*, pp. 570–574, June 2001.
- [10] R. Nabar, D. Gore, and A. Paulraj, "Optimal selection and use of transmit antennas in wireless systems," in *IEEE International Conference on Telecommunications*, 2000.
- [11] R. S. Blum and J. H. Winters, "On optimum MIMO with antenna selection," *IEEE Communications Letters*, vol. 6, no. 8, pp. 322–324, 2002.
- [12] L. Dai, S. Sfar, and K. B. Letaief, "Optimal antenna selection based on capacity maximization for MIMO systems in correlated channels," *IEEE Transactions on Communications*, vol. 54, no. 3, pp. 563–573, 2006.
- [13] R. W. Heath and A. Paulraj, "Antenna selection for spatial multiplexing systems based on minimum error rate," in *Proceedings of the IEEE International Conference on Communications (ICC '00)*, pp. 2276–2280, June 2000.
- [14] A. Ghayeb and T. M. Duman, "Performance analysis of MIMO systems with antenna selection over quasi-static fading channels," *IEEE Transactions on Vehicular Technology*, vol. 52, no. 2, pp. 281–288, 2003.
- [15] Y. Zhang, G. Zheng, C. Ji, K. K. Wong, D. J. Edwards, and T. Cui, "Near-optimal joint antenna selection for amplify-and-forward relay networks," in *Proceedings of the International Conference on Wireless Communications and Signal Processing*, pp. 1–5, November 2009.
- [16] J. C. Guey and L. D. Larsson, "Modeling and evaluation of MIMO systems exploiting channel reciprocity in TDD mode," in *Proceedings of the 60th IEEE Vehicular Technology Conference*, vol. 6, pp. 4265–4269, September 2004.
- [17] A. Tölli and M. Codreanu, "Compensation of interference non-reciprocity in adaptive TDD MIMO-OFDM systems," in *Proceedings of the 15th IEEE International Symposium on Personal, Indoor and Mobile Radio Communications*, vol. 2, pp. 859–863, September 2004.
- [18] D. Kim and M. Torlak, "Rapid prototyping of a cost effective and flexible 4X4 MIMO testbed," in *Proceedings of the 5th IEEE Sensor Array and Multichannel Signal Processing Workshop*, pp. 5–8, July 2008.
- [19] K. Nishimori, R. Kudo, N. Honma, Y. Takatori, O. Atsushi, and K. Okada, "Experimental evaluation using  $16 \times 16$  Multiuser MIMO testbed in an actual indoor scenario," in *Proceedings of the IEEE International Symposium on Antennas and Propagation*, pp. 1–4, July 2008.
- [20] F. Azami, A. Ghorssi, H. Hemesi, A. Mohammadi, and A. Abdipour, "Design and implementation of a flexible  $4 \times 4$  MIMO testbed," in *Proceedings of the International Symposium on Telecommunications*, pp. 268–272, August 2008.
- [21] S. Chen, C. Jun, and T. Ohira, *Handbook on Advancements in Smart Antenna Technologies for Wireless Networks*, Information Science Reference, 2009.
- [22] P. Uthansakul, K. Bialkowski, M. Bialkowski, and A. Postula, "Assessing an FPGA implemented mimo testbed with the use of channel emulator," in *Proceedings of the 16th International Conference on Microwaves, Radar and Wireless Communications*, pp. 410–413, May 2006.
- [23] T. Onizawa, A. Ohta, and Y. Asai, "Experiments on FPGA-implemented eigenbeam MIMO-OFDM with transmit antenna selection," *IEEE Transactions on Vehicular Technology*, vol. 58, no. 3, pp. 1281–1291, 2009.
- [24] P. Uthansakul, K. Attakitmongkol, N. Promsuvana, and M. Uthansakul, "MIMO antenna selections using CSI from reciprocal channel," *WASET International Journal of Electrical and Information Engineering*, vol. 5, pp. 349–358, 2010.
- [25] J. Jose, A. Ashikhmin, P. Whiting, and S. Vishwanath, "Scheduling and pre-conditioning in multi-user MIMO TDD systems," in *Proceedings of the IEEE International Conference on Communications (ICC '98)*, pp. 4100–4105, May 2008.
- [26] A. J. Johansson, J. Karedal, E. Tufvesson, and A. F. Molisch, "MIMO channel measurements for personal area networks," in *Proceedings of the 61st IEEE Vehicular Technology Conference*, pp. 171–176, June 2005.

# Modified Orthogonal Pilot Scheme for Carrier Frequency Offset Estimation in 2x2 MIMO System

N.Promsuwanna<sup>#1</sup>, P.Uthansakul<sup>#2</sup>, M.Uthansakul<sup>#3</sup>

<sup>#</sup> School of Telecommunication Engineering, Suranaree University of Technology,  
Nakhonratchasima, Thailand 30000

<sup>1</sup>n\_promsuwanna@hotmail.co.uk

<sup>2</sup>uthansakul@sut.ac.th

<sup>3</sup>mtp@sut.ac.th

**Abstract** — The emerging of OFDM technique applied on MIMO systems to improve signal quality and capacity has recently gained a lot of attention. The Carrier Frequency Offset (CFO) due to time-varying fading channel is the main cause of the loss of orthogonality among OFDM subcarriers which is linked to inter-carrier interference (ICI). Hence, it is necessary to precisely estimate and compensate the CFO. Especially for data-aid transmission, CFO also has to be correctly estimated in order to track the channel and frequency synchronization. In this paper, we present the new pilot scheme which reduces the effect of data-interference to pilot tone by modifying the orthogonal pilot pattern. The results show that our proposed scheme provides better system performance by reducing the variance of CFO error.

**Index Terms** — CFO, MIMO, OFDM, channel estimation, orthogonal pilot.

## I. INTRODUCTION

Orthogonal Frequency Division Multiplexing (OFDM) enables a high data rate transmission over multipath fading channels because of the transformation of entire frequency selective channel into a parallel set of frequency flat sub-channels. However, OFDM signal is very sensitive to carrier frequency offset (CFO) due to the frequency difference between transmitter and receiver's local oscillator and time varying fading channel. CFO results in the severe degradation on the performance of reception by producing inter-carrier interference (ICI) and it causes a loss of bit error rate (BER) performance [1] so CFO is needed to be estimated and compensated in order to maintain a good system performance.

In recent year, there have been several works that are related to single input single output (SISO) CFO estimation. In [2], the authors proposed the frequency domain maximum likelihood CFO estimation by using the repeat data symbol. The estimation length of this technique is  $\pm 0.5$  of sub-carrier spacing. Based on training symbol, there are many works using the repeat data symbol such as [3] and [4] which are designed for burst transfer mode and suitable for slow fading channel. In broadcasting applications, the pilot schemes are usually employed by inserting the pre defined data in every OFDM symbol in order to track the variations of channel and CFO. Then CFO is able to be estimated by using various techniques such as the method described in [1] or [5]. However, the effect of data-interference to pilots causes the

degradation of estimation performance. Due to this issue, the work in [6] proposes data-pilot multiplex schemes to reduce the effect of data-interference to pilot and the authors in [7] proposes a cluster pilot to provide higher signal to ICI power ratio in order to improve CFO estimation.

So far in literature, the concept of data-pilot scheme has not been applied to MIMO system. In this paper, the new design of data adjacent pilot tone is proposed to reduce the result of data-interference to pilot. The proposed scheme can correct the estimated CFO where pilot tones are used for both channel and CFO estimations. Moreover, the pilot scheme in this work is based on an orthogonal pilot scheme which converts the complexity of multiple antenna channel estimation into simple single antenna system [8]. Consequently, the proposed scheme is complete within only one OFDM symbol.

The remainder of this paper is organized as follows. The system models of SISO and MIMO OFDM with the effect of CFO are described in Section II. The new data adjacent pilot is designed and described in Section III. In section IV, the simulation results of proposed pilot scheme for 2x2 MIMO system are presented and finally the conclusion is given in Section V.

## II. SYSTEM MODELS

In an SISO OFDM system, the N-point inverse fast Fourier transform (IFFT) of transmitted OFDM symbol is given by

$$x(k) = \frac{1}{\sqrt{N}} \sum_{n=0}^{N-1} S(n) e^{j \frac{2\pi n k}{N}} \quad (1)$$

Where  $S(n)$  is the information symbol on sub-carrier  $n$ .

After  $x(k)$  enters a wireless channel, due to the effect of time and frequency selective fading channel and CFO caused by Doppler and inherent instabilities of the transmitter and receiver local oscillators, the received signal is given by

$$y(k) = \frac{1}{\sqrt{N}} \sum_{n=0}^{N-1} H(n) S(n) e^{j \frac{2\pi n (k+\epsilon)}{N}} + W(n) \quad (2)$$

Where  $H(n)$  and  $\varepsilon$  are the complex channel gain in frequency domain at sub-carrier  $n$  and normalized CFO (the ratio of the actual frequency offset to the intercarrier spacing) respectively. According to [2], frequency domain of (2) can be expressed as given in (3).

$$Y(n) = (S(n)H(n)) \left\{ \frac{\sin(\pi\varepsilon)}{N \sin(\pi\varepsilon/N)} \right\} \cdot e^{j \frac{\pi\varepsilon(N-1)}{N}} + I(n) + W(n) \quad (3)$$

where  $I(n)$  is the ICI caused by frequency offset.

In MIMO-OFDM system with  $N_t$  transmit antennas and  $N_r$  receive antennas, the received signal vector in frequency domain on the  $v^{\text{th}}$  antenna can be described by the summation of  $N_t$  SISOs system that related to  $v^{\text{th}}$  received antenna and it is given by [9]

$$Y_v = \sum_{u=1}^{N_t} K_{v,u} H_{v,u} S_u + W_v \quad (4)$$

where  $S_u$ ,  $Y_v$  and  $W_v$  are the  $N \times 1$  vector of data symbol at  $u^{\text{th}}$  transmitted antenna, received data at  $v^{\text{th}}$  antenna and additive white Gaussian noise (AWGN). The channel matrix  $H_{v,u}$  is  $N \times N$  diagonal matrix of  $[H_{v,u}(0), H_{v,u}(1), \dots, H_{v,u}(N-1)]$  which corresponds to  $u^{\text{th}}$  transmitted antenna and  $v^{\text{th}}$  received antenna.  $K_{v,u}$  is the  $N \times N$  ICI coefficients which is described by

$$K_{v,u} = \begin{bmatrix} K_{v,u}(0) & K_{v,u}(1) & \dots & K_{v,u}(N-1) \\ K_{v,u}(-1) & K_{v,u}(0) & \dots & K_{v,u}(N-2) \\ \vdots & \vdots & \ddots & \vdots \\ K_{v,u}(1-N) & K_{v,u}(2-N) & \dots & K_{v,u}(0) \end{bmatrix}$$

where the coefficients  $K_{v,u}(i-m)$  at  $m^{\text{th}}$  row  $i^{\text{th}}$  column is given by

$$K_{v,u}(i-m) = \frac{\sin(\pi[i-m+\varepsilon_{v,u}]) e^{j\pi(i-n+\varepsilon_{v,u})(N-1)/N}}{N \sin(\pi[i-m+\varepsilon_{v,u}]/N)}$$

### III. DATA ADJACENT PILOT DESIGN

In this paper, we aim to design a new data adjacent pilot tone in 2x2 MIMO system in order to reduce the effect of data-interference to pilot which cause the performance degradation of frequency offset estimation and channel estimation. Pilot tones in this work are used in both frequency offset and channel estimations where the orthogonal pilot pattern [8] is considered. Orthogonal pilot pattern reduces the

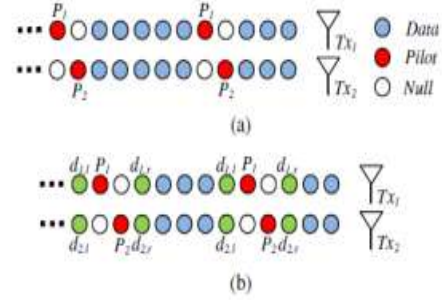


Fig. 1. (a) Orthogonal pilot pattern, (b) Modified orthogonal pilot pattern by adding data adjacent pilot tones (proposed scheme).

complexity of multiple antennas system to single antenna system (without the need of matrix inversion in channel estimation) and it is able to track channel variations by symbol per symbol.

Let's consider 2x2 MIMO system, the orthogonal pilot pattern can be shown in Fig. 1a. The new design of data adjacent pilot tone is determined by inserting the unknown data tones at left and right of pilot tone which are defined by  $d_{1,l}$ ,  $d_{1,r}$ ,  $d_{2,l}$  and  $d_{2,r}$  where 1 and 2 refer to the first and second antenna,  $l$  and  $r$  are the position of designing data on left and right of pilot tone as shown in Fig. 1b.

In order to design data on the left and right of pilot tone, firstly the authors assume that there is only data adjacent pilot interfere to pilot tone and it acts as the dominant interference where another are neglected. By using this assumption, the received signal of each pilot group based on (4) can be given by

$$\begin{aligned} Y_1^{\text{pilot}} &= K_{1,1}^{\text{pilot}} H_{1,1}^{\text{pilot}} X_1 + K_{1,2}^{\text{pilot}} H_{1,2}^{\text{pilot}} X_2 + W_1 \\ Y_2^{\text{pilot}} &= K_{2,1}^{\text{pilot}} H_{2,1}^{\text{pilot}} X_1 + K_{2,2}^{\text{pilot}} H_{2,2}^{\text{pilot}} X_2 + W_2 \end{aligned} \quad (5)$$

where  $(\cdot)^{\text{pilot}}$  denote sub-matrix or sub-vector,  $X_1$  and  $X_2$  are group of pilot at 1<sup>st</sup> and 2<sup>nd</sup> transmitted antenna, respectively and they are consisted of orthogonal pilot tone and adjacent data tone which are defined by (as seen in Fig. 1b)

$$X_1 = [d_{1,l} \ P_1 \ 0 \ d_{1,r}]^T, X_2 = [d_{2,l} \ 0 \ P_2 \ d_{2,r}]^T$$

Hence, the received signal on pilot  $P_1$  and  $P_2$  can be written as

$$Y_{1,P_1} = H_{1,1}(n_{P_1}) K_{1,1}(0) P_1 + \{ H_{1,1}(n_{P_1}-1) K_{1,1}(-1) d_{1,l} + H_{1,2}(n_{P_1}-1) K_{1,2}(-1) d_{2,l} + H_{1,2}(n_{P_1}+1) K_{1,2}(1) P_2 \} \quad (6)$$

$$Y_{2,P_2} = H_{2,2}(n_{P_2}) K_{2,2}(0) P_2 + \{ H_{2,2}(n_{P_2}+1) K_{2,2}(1) d_{2,r} + H_{2,1}(n_{P_2}-1) K_{2,1}(-1) P_1 + H_{2,1}(n_{P_2}+1) K_{2,1}(1) d_{1,r} \} \quad (7)$$

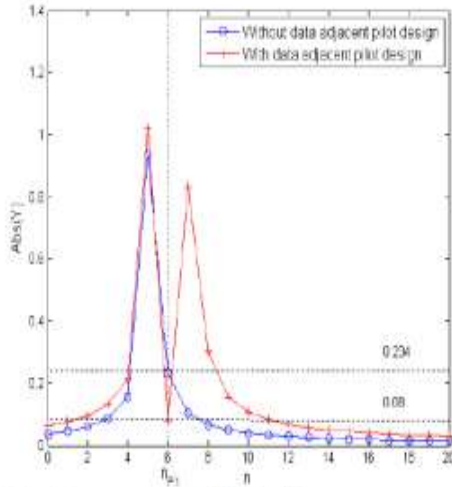


Fig. 2. Frequency response of ICI on  $P_1$

The second term in (6) and (7) are referred to ICI which is caused by CFO of data adjacent pilot tone and these data tones have to be compensated in order to reduce ICI on pilot tone. To design data tones in (6) and (7), we assume that, the channel responses on adjacent tone are equal ( $H(n) \approx H(n+1) \approx H(n-1) = H(n)$ ). By using superposition theorem, data tones on each antenna from (6) are given by

Consider ICI from 1<sup>st</sup> transmit antenna

$$d_{1,j} = 0 \quad (8)$$

Consider ICI from 2<sup>nd</sup> transmit antenna

$$d_{2,j} = -K_{1,2}(1)P_2/K_{1,2}(-1) \quad (9)$$

As same as the consideration in (8) and (9), data tones on each antenna in (7) are given by

$$d_{1,e} = 0 \quad (10)$$

$$d_{2,e} = -K_{2,1}(-1)P_1/K_{2,1}(1) \quad (11)$$

From (8), (9), (10) and (11), now we can assign data adjacent pilot symbols that result in none dominant ICI on pilot tone thus CFO estimation performance can be improved. However, according to (9) and (11), it is necessary to know CFO of each path and it is possible that the designed data requires more symbol power than another in order to complete dominant ICI cancellation at pilot tone. Thus, this leads to increase the average OFDM symbol power.

Due to these issues, to design data adjacent pilot tone in (9) where the designed data  $d_{2,j}$  is used to reduce ICI from  $P_2$  on  $P_1$ , in the special case if we let  $d_{2,j} = P_2$  then the amplitude of frequency response of  $d_{2,j}$  and  $P_2$  can be shown by Fig. 2. The simulation parameters for Fig. 2 are as following. A symbol modulation scheme is QAM,  $n_p = 6$ ,  $N = 256$ ,  $H(n) = 1$ ,  $d_{2,j} = P_2 = 0.707 + j0.707$  and  $\varepsilon$  is 0.2. The simulation reveals that ICI from  $P_2$  is reduced when using  $d_{2,j} = P_2$ . There is no  $d_{2,j}$  where the performance is 65.8% reduction and it can be up to 86% reduction when  $\varepsilon = 0.1$ . As same as the method in Fig. 2, the group of pilots is given by

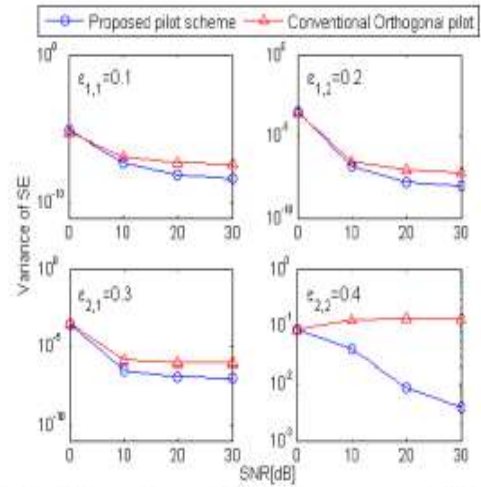


Fig. 3. Variance of square CFO estimation errors versus SNR

$$X_1 = [0 \ P_1 \ 0 \ P_{1,e}]^T, X_2 = [P_{2,e} \ 0 \ P_2 \ 0]^T \quad (12)$$

where this pilot group is inserted in frequency domain in order to track multipath channel gains and to estimate frequency offset.

In order to estimate CFO, the maximum likelihood estimator which is proposed by Moose [2] is used in this work. With the use of orthogonal pilot pattern and designed data adjacent pilot, this method can estimate and exact all  $N_s \times N_f$  CFOs. In 2x2 MIMO system, the estimated CFO can be given by

$$\hat{\varepsilon}_{v,u} = (1/2\pi) \tan^{-1} \left\{ \frac{\left( \sum_{n \in n_p} \text{Im} [Y_{v,u}^{*2} Y_{v,u}^{n1}] \right)}{\left( \sum_{n \in n_p} \text{Re} [Y_{v,u}^{*2} Y_{v,u}^{n1}] \right)} \right\} \quad (13)$$

where  $(\cdot)^*$  denote complex conjugate,  $n_p$  is the set of all pilots index on  $u^{\text{th}}$  transmit antenna and  $(\cdot)^{n1}$ ,  $(\cdot)^{n2}$  are signal of 1<sup>st</sup> and 2<sup>nd</sup> OFDM symbol respectively.

#### IV. SIMULATION RESULTS

In this paper, the simulations are undertaken by using MATLAB programming. The simulation parameters are as follow. The OFDM system has  $N = 256$  subcarriers, the channel frequency response is assumed to be flat and slow fading and we let  $H(0), H(1), \dots, H(N-1) = 1$ . Therefore, it is not necessary to concern the guard time in simulations.

Fig. 3 shows the comparison of variance of square CFO estimation errors between proposed pilot in (12) and conventional orthogonal pilot where there are four different  $\varepsilon$  which are 0.1, 0.2, 0.3 and 0.4. In order to make the simulations comparable, data information on the left and

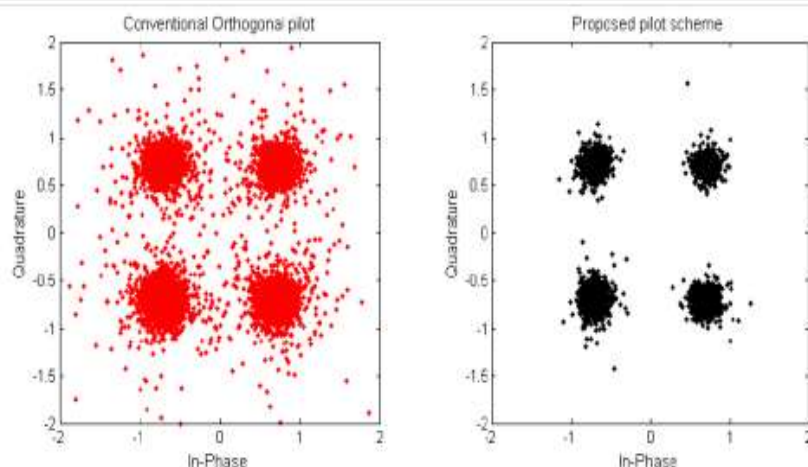


Fig. 4. The data constellation of detected symbols for conventional orthogonal pilot scheme (left) and proposed scheme (right)

right of pilot in both methods are the same. However, the pilots in (12) are designed when there is only dominant ICI from adjacent tone since this idea may cause frequency offset estimation performance failed where the ICI from all subcarriers should be considered. Therefore, the performance evaluations in Fig. 3 are achieved by averaging the 5000 times of random data symbols.

As can be seen from the figure, the proposed pilot scheme provides more estimation efficiency than conventional orthogonal pilot scheme by reducing variance of square errors. The average variance reduction is 90% for  $\varepsilon_{s,1}$ ,  $\varepsilon_{s,2}$  and  $\varepsilon_{s,3}$ , except  $\varepsilon_{s,4}$  which has the most of variance reduction (the performance of these reduction is shown in Fig. 4). However, variance of  $\varepsilon_{s,4}$  is the worst due to the ICI caused by  $\varepsilon_{s,4}$  is higher than others.

Fig. 4 shows the constellation plot of detected symbols where noiseless channel is assumed and the simulation is performed in 500 OFDM symbols. We set  $\varepsilon$  for the same received antenna to be equal but it is not equal for the different received antenna ( $\varepsilon_{s,1} = \varepsilon_{s,2} = 0.1$ ,  $\varepsilon_{s,3} = \varepsilon_{s,4} = 0.2$ ) in order to reduce the complexity of detection. As seen in figure, it is clearly seen that the reduction of variance in Fig. 4 provides more system reliable and it thus leads to the improvement of BER performance.

#### IV. CONCLUSION

This paper proposes the modified orthogonal pilot scheme in order to correctly estimate CFO by reducing data-interference to pilot based on dominant ICI reduction. The results reveal that the proposed pilot scheme can improve frequency offset estimation performance via the reduction of variance of estimation error and also it leads to the BER improvement.

#### ACKNOWLEDGEMENT

The authors thank the financial support from Telecommunications Research and Industrial Development Institute (TRIDI).

#### REFERENCES

- [1] W. Hwang, H. Kang, and K. Kim, "Sensitivity of SNR degradation of OFDM to carrier frequency offset in shadowed two-path channels," *IEICE Trans. Commun.*, vol. E86-B, pp. 3630-3633, Dec. 2003.
- [2] P. H. Moose, "A technique for orthogonal frequency division multiplexing frequency offset correction," *IEEE Trans. Commun.*, vol. 42, pp. 2908-2914, Oct. 1994.
- [3] Z. Zhang, J. Liu, C. Wang, K. Sohraby and Y. Liu, "Joint frame synchronization and carrier frequency offset estimation in OFDM systems," *2005 IEEE EIT Int. conf.*, pp. 1-5, May 2005.
- [4] J. van de Beek, M. Sandell, and P. O. Borjesson, "ML estimation of time and frequency offset in OFDM systems," *IEEE Trans. Signal Processing*, vol. 45, pp. 1800-1805, July 1997.
- [5] F. Classen and H. Meyr, "Frequency synchronization algorithms for OFDM systems suitable for communication over frequency selective fading channels," in *Proc. IEEE VTC'94*, pp. 1655-1659, Jun. 1994.
- [6] X. Fu and H. Minn, "Modified data-pilot-multiplexed schemes for OFDM systems," *IEEE Trans. Wireless Commun.*, vol. 6, pp. 730-737, Feb. 2007.
- [7] W. Zhang, X. Xia and P.C. Ching, "Clustered pilot tones for carrier frequency offset estimation in OFDM systems," *IEEE Trans. Wireless Commun.*, vol. 6, pp. 101-109, Jan. 2007.
- [8] Y. Qiao, S. Yu, P. Su and L. Zhang, "Research on an iterative algorithm of LS channel estimation in MIMO OFDM systems," in *Proc. IEEE CASSET 2004*, pp. 729-732, May 2004.
- [9] P. Tan, N.C. Beaulieu, "ICI Mitigation in MIMO OFDM Systems," *IEEE WCNC 2007*, pp. 847-851, March 2007.

# A Novel Pilot Scheme for Frequency Offset and Channel Estimation in 2x2 MIMO-OFDM

N. Promsuwanna, P. Uthansakul and M. Uthansakul

**Abstract**—The Carrier Frequency Offset (CFO) due to time-varying fading channel is the main cause of the loss of orthogonality among OFDM subcarriers which is linked to inter-carrier interference (ICI). Hence, it is necessary to precisely estimate and compensate the CFO. Especially for mobile broadband communications, CFO and channel gain also have to be estimated and tracked to maintain the system performance. Thus, synchronization pilots are embedded in every OFDM symbol to track the variations. In this paper, we present the pilot scheme for both channel and CFO estimation where channel estimation process can be carried out with only one OFDM symbol. Additional, the proposed pilot scheme also provides better performance in CFO estimation comparing with the conventional orthogonal pilot scheme due to the increasing of signal-to-interference ratio.

**Keywords**—MIMO, OFDM, carrier frequency offset, channel, estimation

## I. INTRODUCTION

Orthogonal Frequency Division Multiplexing (OFDM) has enables a high data rate transmission over multipath fading channels because of the transformation of entire frequency selective channel into a parallel set of frequency flat sub-channels. It has been widely adopted for standards such as DAB, DVB and WLAN [1]. However, OFDM signal is very sensitive to carrier frequency offset (CFO) which cause a loss of BER performance. Thus CFO is needed to be estimated and compensated in order to maintain a good system performance.

There have been several works that are related to CFO estimation. In [2], the authors proposed the frequency domain maximum likelihood CFO estimation by using the repeat data symbol. The estimation length of this technique is 0.5 of subcarrier spacing. Based on training symbol, there are many works using the repeat data symbol such as [3] and [4] which are designed for burst transfer mode and suitable for slow fading channel. In broadcasting applications, the pilot schemes are usually employed by inserting the pre defined data in every OFDM symbol in order to track the variations of channel and CFO. Then CFO is able to be estimated by using various techniques such as the method described in [1] or [5]. However, the effect of data-interference to pilots causes the degradation of estimation performance. Due to this issue, the work in [6] proposes data-pilot multiplex schemes to reduce

the effect of data-interference to pilot and the authors in [7] proposes a cluster pilot to provide higher signal to ICI power ratio in order to improve CFO estimation. However, the work in [6] and [7] is based on single input single output OFDM system.

In this paper, we proposed pilot scheme for both CFO and channel estimation for mobile broadband MIMO-OFDM system. Where channel estimation process of the proposed scheme can be carried out with only one OFDM symbol. This provides the same benefit as the orthogonal pilot scheme proposed in [8]. But the proposed scheme can improve the CFO estimation performance by the increasing of signal-to-interference ratio (SIR). Thus, better CFO estimation leading to better in channel estimation.

The remainder of this paper is organized as follows. The system models of MIMO-OFDM with the effect of CFO are described in section II. The performance investigation of the conventional pilot scheme and the proposed pilot scheme are described in section III and IV respectively. In section V, the simulation results of proposed pilot scheme for 2x2 MIMO system are presented and finally the conclusion is given in Section VI.

## II. SYSTEM MODEL

In the MIMO-OFDM system with  $N_t$  transmitted antennas,  $M_r$  received antennas and  $N$  subcarriers, we denote  $\mathbf{X}_i^n = [X_i^n(1) \ X_i^n(2) \ \dots \ X_i^n(N)]^T$  is transmitted signal vector in the frequency domain of  $n$ th transmitted antenna on  $i$ th OFDM symbol,  $\mathbf{z}_i$  is an AWGN and  $N_{cp}$  is the cyclic prefix (CP) length to prevent intersymbol interference. The received signal vector in time domain of  $m$ th received antenna is effect by normalized CFO ( $\varepsilon$ ) which is given by

$$\mathbf{y}_i^n = \sum_{n=1}^{N_t} \mathbf{D}_\varepsilon e^{j\theta} \mathbf{V} \mathbf{H}^{n,c} \mathbf{X}_i^n + \mathbf{z}_i \quad (1)$$

where  $\mathbf{V}$  is the inverse DFT matrix  $\mathbf{V} = [\mathbf{v}_1 \ \mathbf{v}_2 \ \dots \ \mathbf{v}_N]$

$$\mathbf{v}_k = (1/\sqrt{N}) [1 \ e^{j2\pi k/N} \ e^{j2\pi(2k)/N} \ \dots \ e^{j2\pi((N-1)k)/N}]^T$$

$$\mathbf{D}_\varepsilon = \text{diag} [1, e^{j2\pi\varepsilon/N}, \dots, e^{j2\pi(N-1)\varepsilon/N}]$$

$$\theta = 2\pi\varepsilon i (N + N_{cp}) / N$$

The authors are with School of Telecommunication Engineering, Suranaree University of Technology, Nakhon Ratchasima, 30000 Thailand (phone: 66-4422-4351; fax: 66-4422-4603; e-mail: n.promsuwanna@hotmail.co.uk, uthansakul@sut.ac.th, mtp@sut.ac.th).

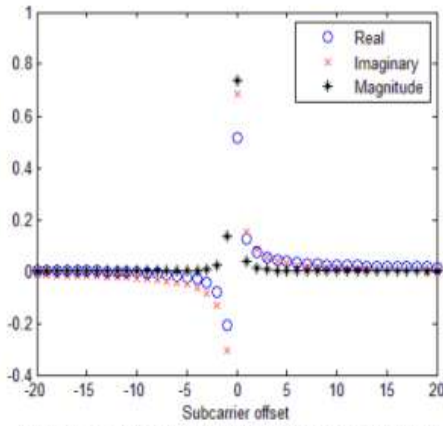


Fig. 1 Real part, imaginary part and magnitude of the ICI coefficients.

and  $\mathbf{H}^{m,n} = \text{diag}[H^{m,n}(1), H^{m,n}(2), \dots, H^{m,n}(N)]$  where  $H^{m,n}(k)$  is channel frequency response on  $k$ th subcarrier of  $m$ th received antenna and  $n$ th transmitted antenna. Then the received signal in frequency domain on  $k$ th subcarrier after using DFT can be shown by

$$Y_i^m(k) = \sum_{n=1}^{N_t} \mathbf{v}_i^H \mathbf{D}_\varepsilon e^{j\theta} \mathbf{V} \mathbf{H}^{m,n} \mathbf{X}_i^n(k) + Z_i(k) \quad (2)$$

$$= e^{j\theta} \sum_{n=1}^{N_t} \left\{ \begin{array}{l} \alpha_0 H^{m,n}(k) X_i^n(k) + \\ \sum_{l=0, l \neq k}^{N-1} \alpha_{l-k} H^{m,n}(l) X_i^n(l) \end{array} \right\} + Z_i(k)$$

where  $^H$  represents hermitian, ICI coefficient ( $\alpha$ ) is given by

$$\alpha_{l-k} = \frac{1}{N} \sum_{n=0}^{N-1} e^{j \frac{2\pi n(l-k+s)}{N}} \quad (3)$$

Fig.1 shows the complex weighting coefficients for the case of  $\varepsilon = 0.3$  and  $N = 64$ . It reveals that both the real and the imaginary parts of the ICI coefficients are slightly changing for each subcarrier except for several coefficients around the zero subcarrier. This effect can be stronger when  $\varepsilon$  is higher.

### III. CONVENTIONAL PILOT SCHEME

In this paper, we use the orthogonal pilot scheme in [8] be the conventional pilot scheme. This pilot scheme converts the complexity of multiple antenna channel estimation into simple single antenna system where the channel estimation process can be completed with only one OFDM symbol. Thus, it is a useful technique especially for mobile broadband communication. This pilot scheme can be shown in Fig. 2.

#### A. CFO estimation

Based on the orthogonal pilot scheme in Fig. 2, CFO can be estimated by measuring the phase shift of pilot symbols in two consecutive OFDM symbols. By giving  $a$  is the pilot symbol

and  $\Gamma$  is the set of pilot tone indexes. By ignoring the effect of noise from (6), we can write received signal of pilot tone on  $i$ th and  $i+1$ th OFDM symbol by

$$Y_i^m(k)_{k \in \Gamma} = e^{j\theta} (\alpha_0 H^{m,n}(k)a + I_i^{m,1}(k) + I_i^{m,2}(k)) \quad (4)$$

$$Y_{i+1}^m(k)_{k \in \Gamma} = e^{j\theta_{i+1}} (\alpha_0 H^{m,n}(k)a + I_{i+1}^{m,1}(k) + I_{i+1}^{m,2}(k)) \quad (5)$$

where ICI term can be given by

$$I_i^{m,n}(k) = \sum_{l=0, l \neq k}^{N-1} \alpha_{l-k} H^{m,n}(l) X_i^n(l) \quad (6)$$

Based on [2], the estimated phase can be given by

$$\hat{\phi}_{i+1} - \hat{\phi}_i \approx \hat{\phi}_\Delta = \frac{\text{Im} \left( Y_i^m(k)_{k \in \Gamma}^* Y_{i+1}^m(k)_{k \in \Gamma} \right)}{\text{Re} \left( Y_i^m(k)_{k \in \Gamma}^* Y_{i+1}^m(k)_{k \in \Gamma} \right)} \quad (7)$$

where  $*$  stand for conjugate,  $\text{Re}(\cdot)$  and  $\text{Im}(\cdot)$  denote real and imaginary part respectively. Then the estimated normalized CFO can be given by

$$\hat{\varepsilon} = \frac{\hat{\phi}_\Delta}{2\pi(N + N_{CP})/N} \quad (8)$$

By assuming that, transmitted signals on each transmitted antenna are uncorrelated,  $|X_i^n(k)|^2 = |X_i^n|^2$ ,  $E\{X_i^n(k)} = 0$  and  $\text{Cov}(X_i^n(k), X_i^n(m))_{m \neq k} = 0$ . Then SIR of pilot tone based on (4) can be given by

$$\text{SIR} = \frac{|\alpha_0 H^{m,n} a|^2}{|I_i^{m,1}(k)|^2 + |I_i^{m,2}(k)|^2} \quad (9)$$

$$|I_i^{m,n}(k)|^2 = \sum_{l=0, l \neq k}^{N-1} |\alpha_{l-k}|^2 |H^{m,n}(l) X_i^n(l)|^2 \quad (10)$$

The work in [9] indicated that the performance of CFO estimation on (7) can be improved with the increasing of SIR. Thus, it is interest of designing pilot scheme that can improve SIR to provide more accurate estimated CFO.

#### B. Channel estimation

After estimating and compensating the CFO, channel estimation of the orthogonal pilot scheme can be achieved easily as in SISO-OFDM system by

$$H^{m,n} = Y_i^m(k; k \in \Gamma^n) / a \quad (11)$$

where  $\Gamma^n$  is the set of pilot indexes from  $n$ th antenna.

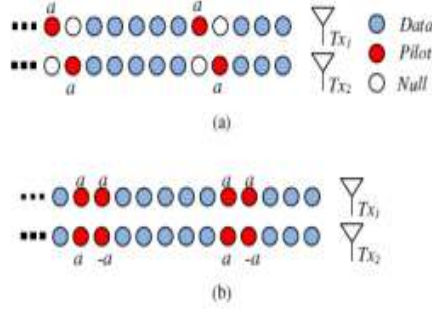


Fig. 2 (a) orthogonal pilot scheme (b) proposed pilot scheme

#### IV. PROPOSED PILOT SCHEME

The proposed pilot scheme can be shown in Fig. 2. We cluster two adjacent pilot tones as group for each antenna. We set pilot tones in each group of the first antenna are identical while pilot tones in each group of the second antenna are antipodal.

##### A. CFO estimation

Assuming that  $\Gamma_l$  is the set containing the left pilot tone indexes and channel response is assumed to be flat in the preliminary study where  $H^{m,n}(k) = H^{m,n}$ . The received signal in frequency domain of the left pilot tone and the right pilot tone in each pilot group based on (2) without noise can be given by

$$Y_l^m(k)_{k \in \Gamma_l} = e^{j\theta} a \left[ \alpha_0 H^{m,2} + \alpha_0 H^{m,2} + \alpha_l H^{m,1} - \alpha_l H^{m,2} + I_l^{m,1}(k) + I_l^{m,2}(k) \right] \quad (12)$$

$$Y_r^m(k+1)_{k \in \Gamma_r} = e^{j\theta} a \left[ \alpha_0 H^{m,1} - \alpha_0 H^{m,2} + \alpha_{-l} H^{m,1} + \alpha_{-l} H^{m,2} + I_r^{m,1}(k+1) + I_r^{m,2}(k+1) \right] \quad (13)$$

Equation (12) and (13) represent the received signal of the left and the right pilot tone at  $m$ th received antenna respectively. From (12) and (13),  $\alpha_l H^{m,1}$ ,  $\alpha_l H^{m,2}$ ,  $\alpha_{-l} H^{m,1}$  and  $\alpha_{-l} H^{m,2}$  represent the ICI from the adjacent pilot tone. Then the clustered pilot tones can be given by

$$\begin{aligned} (12)-(13) &= Y_l^m(k)_{k \in \Gamma_l} - Y_r^m(k+1)_{k \in \Gamma_r} \\ &= e^{j\theta} a \left[ 2\alpha_0 H^{m,2} + \alpha_l H^{m,1} - \alpha_{-l} H^{m,1} - \alpha_l H^{m,2} - \alpha_{-l} H^{m,2} \right. \\ &\quad \left. + I_l^{m,1}(k) - I_r^{m,1}(k+1) + I_l^{m,2}(k) - I_r^{m,2}(k+1) \right] \\ &= e^{j\theta} a \left[ H^{m,2} (2\alpha_0 - \alpha_l - \alpha_{-l}) + H^{m,1} (\alpha_l - \alpha_{-l}) + I_{\Delta}^{m,1} + I_{\Delta}^{m,2} \right] \end{aligned} \quad (14)$$

where

$$I_{\Delta}^{m,n} = I_l^{m,n}(k) - I_r^{m,n}(k+1) = \sum_{\substack{l=0 \\ l \neq k, k+1}}^N (\alpha_{l-k} - \alpha_{l-k-1}) H^{m,n} X_l^*(l) \quad (15)$$

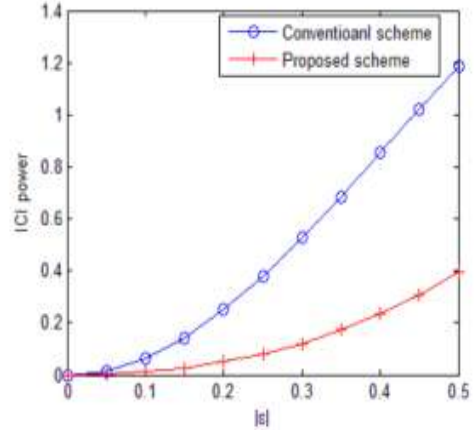


Fig. 3 ICI power comparison

As same as (9), we can write SIR of the propose pilot scheme by

$$SIR = \frac{|a|^2 |H^{m,2} (2\alpha_0 - \alpha_l - \alpha_{-l}) + H^{m,1} (\alpha_l - \alpha_{-l})|^2}{|I_{\Delta}^{m,1}(k)|^2 + |I_{\Delta}^{m,2}(k)|^2} \quad (16)$$

$$|I_{\Delta}^{m,n}(k)|^2 = |H^{m,n}|^2 |X|^2 \sum_{\substack{l=0 \\ l \neq k, k+1}}^N |(\alpha_{l-k} - \alpha_{l-k-1})|^2 \quad (17)$$

Based on (17) and (10), we can show the performance of ICI reduction by the proposed scheme in Fig. 3. Where  $|H^{m,2}|^2$  and  $|X|^2$  are assumed to be 1. As seen in Fig. 3, the proposed scheme provides less ICI power than the conventional scheme for any  $\epsilon$  where the reduction is about 6 dB on the average.

In addition, the proposed scheme can improve signal power of pilot as shows in (16). However signal power from (16) is based on  $H^{m,2}$  and  $H^{m,1}$  thus the performance of several case of  $H^{m,2}$  and  $H^{m,1}$  should be investigated. Fig. 4 shows the average performance of signal power where  $H^{m,2}$  and  $H^{m,1}$  are random from 5000 Gaussian channels. We categorize case of  $H^{m,2}$  and  $H^{m,1}$  into 5 events which are  $|H^{m,2}|_{\text{dB}}^2 - |H^{m,1}|_{\text{dB}}^2 = 7, 3, 0, -3, -7$  and  $-13$  dB and we normalize channel by  $|H^{m,2}|^2 + |H^{m,1}|^2 = 2$ . As seen in Fig. 4, the proposed scheme can enhance signal power of pilot tone for above  $|H^{m,2}|_{\text{dB}}^2 - |H^{m,1}|_{\text{dB}}^2 \geq -3$  dB while  $|H^{m,2}|_{\text{dB}}^2 - |H^{m,1}|_{\text{dB}}^2 \leq -7$  dB provide better performance in signal power when  $|\epsilon| \geq 0.25$ .

However, the deviation of  $|H^{m,2}|_{\text{dB}}^2 - |H^{m,1}|_{\text{dB}}^2 \leq -7$  dB is very limit situations in a broadband channel where it should occur when there is rich of multipath like an indoor channel. Thus the proposed scheme still provides better average performance than the conventional scheme if a broadband channel is considered.

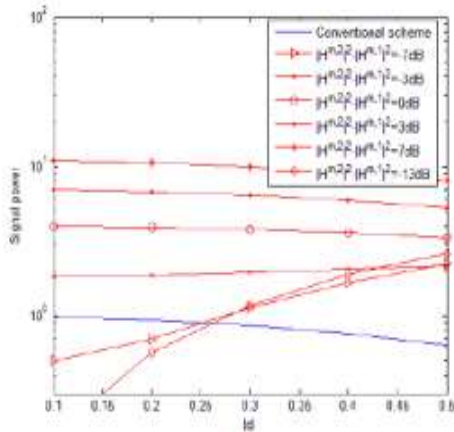


Fig. 4 Signal power comparison

The estimated CFO of the proposed scheme based on (7) can be given by

$$\hat{\phi}_\Delta = \frac{\text{Im}\left(K_l^n(k)_{\text{est}}^* K_{l+i}^n(k)_{\text{est}}\right)}{\text{Re}\left(K_l^n(k)_{\text{est}}^* K_{l+i}^n(k)_{\text{est}}\right)} \quad (18)$$

where  $K_l^n(k)_{\text{est}} = Y_l^n(k)_{\text{est}} - Y_l^n(k+1)_{\text{est}}$ .

In addition, we also combine estimated phase from (7) with (18) in order to improve the performance of phase estimation.

### B. Channel estimation

The proposed pilot scheme can estimate MIMO channel by using only one OFDM symbol as same as the orthogonal pilot scheme. This based on the assumption that even if channel response of a broadband channel is selective but channel gain between adjacent subcarrier can be assumed to be the same  $H^{m,n}(k) \approx H^{m,n}(k+1)$ . Thus we can use adjacent subcarrier to complete channel estimation process of MIMO-OFDM system. The estimated channel of the proposed pilot scheme based on least square Estimation (LSE) can be given by

$$\hat{\mathbf{H}}(k) = \mathbf{Y}(k) \mathbf{X}^\dagger \quad (18)$$

where  $\dagger$  represent pseudo-inverse,

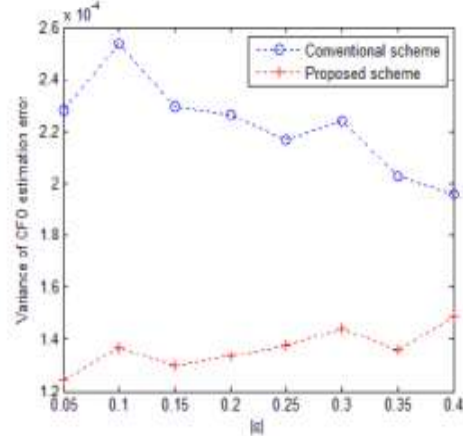
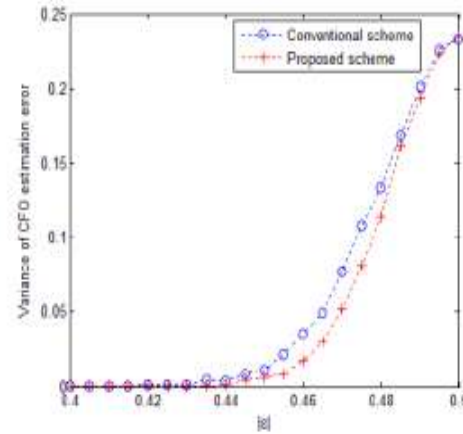
$$\mathbf{Y}(k) = \begin{bmatrix} Y^1(k) & Y^1(k+1) \\ Y^2(k) & Y^2(k+1) \end{bmatrix} \quad (19)$$

$$\mathbf{X} = \begin{bmatrix} a & a \\ a & -a \end{bmatrix} \quad (20)$$

The channel responses of remain subcarriers can be achieved by interpolation between estimated subcarrier.

## V. SIMULATION RESULTS

In this section, the simulation experiments will be presented to investigate the performance of the proposed technique for

Fig. 5 Variance of estimation errors versus  $\epsilon$  ( $0 < \epsilon \leq 0.4$ )Fig. 6 Variance of estimation errors versus  $\epsilon$  ( $0.4 \leq \epsilon \leq 0.5$ )

frequency selective channels. Pilots are placed by equi-space along the subcarrier axis and the performance was averaged for 5,000 random Gaussian channels. The number of pilot subcarriers for each technique is equal in order to make a peer comparison. The other simulation parameters are as follows:

- number of subcarriers ( $N$ ) = 256
- modulation = QPSK
- number of pilots = 32
- subcarrier spacing = 10.93kHz
- cyclic prefix length =  $N/8$

In order to investigate the estimation performance in frequency selective channel, this paper adopts the ITU vehicular A to be a channel model where this model has been adopted in the WiMAX forum. The relative multipath delay ( $\tau$ ) and the normalized path gain ( $\rho$ ) can be given by

$$\tau = [0 \ 0.31 \ 0.71 \ 1.09 \ 1.73 \ 2.51] \mu\text{s}$$

$$\rho = [0 \ -1 \ -9 \ -10 \ -15 \ -20] \text{dB}$$

Fig. 5 shows the estimation performance in terms of variance of estimation errors versus  $\epsilon$  ( $0 < \epsilon \leq 0.4$ ) when OFDM symbol's SNR is 5dB. As seen in Fig. 5, the proposed scheme provides better CFO estimation performance than the conventional scheme which is about 80% in an error variance reduction. For other values of SNR, the proposed scheme still

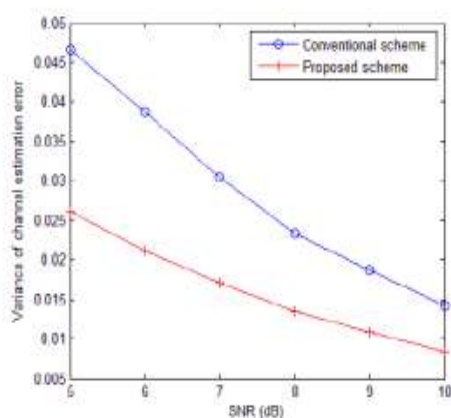


Fig. 7 Variance of channel estimation errors versus SNR

provides similar benefit over the conventional scheme as shown in Fig. 5. Fig. 6 shows the estimation performance where  $0.4 \leq \varepsilon \leq 0.5$ . As seen in Fig. 6, the proposed scheme still provides better CFO estimation performance but the error variance become larger than Fig. 5. This is because the interference from data subcarriers becomes larger when there is high value of  $\varepsilon$ .

Fig. 7 shows variance of channel estimation error of  $H^{1/1}$  versus OFDM symbol's SNR for both the proposed scheme and the conventional scheme when  $\varepsilon = 0.3$ . The whole channel frequency responses of both schemes are achieved by channel estimation and linear interpolation. Channel estimation for both techniques are performed after compensates the CFO for received signal. As seen in Fig. 7, the proposed scheme provides better performance by reducing channel estimation errors. This is because the proposed scheme provides better performance in CFO estimation thus it causes less CFO effect from the compensated received signal. For other values of  $\varepsilon$ , the proposed technique still provides similar benefits over the conventional scheme where variance of estimation error become larger when  $\varepsilon$  is higher.

## VI. CONCLUSION

This paper proposes pilot scheme for both channel and CFO estimation for mobile broadband MIMO-OFDM system. Orthogonal pilot scheme is a useful technique especially for MIMO-OFDM channel estimation where the estimation process can be carried out with only one OFDM symbol. However using null subcarriers in orthogonal pilot scheme cause information on these subcarriers is wasteful. The proposed pilot scheme converts these null subcarriers into pilot tone where the information on pilot tones are carefully design in order to improve CFO estimation performance. In addition, the proposed scheme still provides the same benefit of channel estimation as the conventional orthogonal pilot scheme.

## ACKNOWLEDGMENT

The authors thank the financial support from Telecommunications Research and Industrial Development Institute (TRIDI).

## REFERENCES

- [1] W. Hwang, H. Kang, and K. Kim, "Sensitivity of SNR degradation of OFDM to carrier frequency offset in shadowed two-path channels," *IEICE Trans. Commun.*, vol. E86-B, pp. 3630-3633, Dec. 2003.
- [2] P. H. Moose, "A technique for orthogonal frequency division multiplexing frequency offset correction," *IEEE Trans. Commun.*, vol. 42, pp. 2908-2914, Oct. 1994.
- [3] Z. Zhang, J. Liu, C. Wang, K. Sohraby and Y. Liu, "Joint frame synchronization and carrier frequency offset estimation in OFDM systems," 2005 IEEE EIT Int. conf., pp. 1-5, May 2005.
- [4] J. van de Beek, M. Sandell, and P. O. Borjesson, "ML estimation of timeand frequency offset in OFDM systems," *IEEE Trans. Signal Processing*, vol. 45, pp. 1800-1805, July 1997.
- [5] F. Classen and H. Meyr, "Frequency synchronization algorithms for OFDM systems suitable for communication over frequency selective fading channels," in *Proc. IEEE VTC'94*, pp. 1655-1659, Jun. 1994.
- [6] X. Fu and H. Minn, "Modified data-pilot-multiplexed schemes for OFDM systems," *IEEE Trans. Wireless Comm.*, vol. 6, pp. 730-737, Feb. 2007.
- [7] W. Zhang, X. Xia and P.C. Ching, "Clustered pilot tones for carrier frequency offset estimation in OFDM systems," *IEEE Trans. Wireless Comm.*, vol. 6, pp. 101-109, Jan. 2007.
- [8] Y. Qiao, S. Yu, P. Su and L. Zhang, "Research on an iterative algorithm of LS channel estimation in MIMO OFDM systems," in *Proc. IEEE CASSET 2004*, pp. 729-732, May 2004.
- [9] Z. Wang and S. S. Abeysekera, "Frequency estimation using the pulsepair method in different fading environments," in *Proc. IEEE ICASSP 2003*, vol. 4, pp. 517-520.

## **BIOGRAPHY**

Mister Nattaphat Promsuwanna was born in Phuket, Thailand, in 1983. He graduated with the Bachelor Degree and Master Degree of Engineering in Telecommunication Engineering in 2006 and 2009 respectively from Suranaree University of Technology, Nakorn Ratchasima, Thailand. Then he is currently pursuing his Ph.D program in Telecommunication Engineering, School of Telecommunication Engineering, Suranaree University of Technology. His research interests are wireless communication system, mobile broadband communication, channel estimation and frequency synchronization.

